FEEDING ECOLOGY AND THE TRABECULAR STRUCTURE OF THE MANDIBULAR CONDYLE IN EXTANT PRIMATES

by

Susan F. Coiner-Collier

A dissertation submitted to the

Graduate School-New Brunswick

Rutgers, The State University of New Jersey

In partial fulfillment of the requirements

For the degree of

Doctor of Philosophy

Graduate Program of Anthropology

Written under the direction of

Dr. Robert S. Scott

And approved by

_____

_____

_____

_____

New Brunswick, NJ
October, 2015

ABSTRACT OF THE DISSERTATION

Feeding ecology and the trabecular structure of the mandibular condyle in extant primates

by SUSAN F. COINER-COLLIER

Dissertation Director:

Dr. Robert S. Scott

No straightforward functional relationship has been established between jaw morphology and diet in extant primates despite much research devoted to this issue. Food preparation and ingestion serve to load the mandible, and because of known remodeling responses to increased mandibular strain, the expectation is that higher mechanical loads generated by mechanically challenging foods and/or repetitive loading cycles should produce changes in mandibular morphology.

This dissertation examines the relationship between primate mandibular morphology —specifically, the internal trabecular structure of the mandibular condyle—and two aspects of feeding ecology: food mechanical properties (FMPs) and time spent feeding. Because dietary FMPs influence chewing behavior, more mechanically challenging foods and/or increased repetitive loading cycles are expected to produce denser and/or more anisotropic trabecular bone within the mandibular condyle. I used high-resolution X-ray computed tomography (HRXCT) to image 28 anthropoid primate mandibles, and compared the results of trabecular analyses to data on FMPs and feeding time.

My results demonstrated a strong relationship between dietary toughness and

trabecular anisotropy. As toughness increases, trabecular bone within the mandibular condyle becomes more anisotropic. Toughness is associated with fiber content, and fiber requires greater durations of oral processing; tougher foods may thus require a greater total number of chewing cycles, and this increased overall load appears to be associated with a functional response within the condyle. Similarly, average daily time spent feeding is associated with trabecular thickness and trabecular number, although these relationships are not as strong as that between anisotropy and toughness and are modulated by changes in body size.

In accordance with previous studies of the mammalian mandibular condyle, my results showed that trabecular bone within the mandibular condyle is oriented to maximally resist the compressive forces associated with mastication. Taken together, these results support a functional dietary signal in the trabecular structure of the primate mandibular condyle. FMPs and feeding time are associated with changes in trabecular orientation and volume fraction.

While the skull is the creation of God, the jaw is the work of the devil.
– attributed to William Straus

One can always extract oneself from a failed biomechanical prediction by invoking the mantra of conflicting functional demands.
– Daegling & McGraw, 2001

Acknowledgments

I am grateful first and foremost to my advisor, Dr. Rob Scott, for many years of friendship, wisdom, and advice. He refused to give up on me, even when he probably should have, and refused to let me give up on myself, even when I really wanted to. I look forward to many years of attempting to insert the word “nexus” into all of my papers. Dr. Erin Vogel has gone above and beyond as a mentor and friend, and I cannot thank her enough for taking me under her wing. Many thanks to Dr. Susan Cachel for helpful discussions and insight, and to Dr. Tim Ryan, head honcho of Team Trabeculae, for kindly providing advice and guidance in the face of research crises large and small.

Dr. Jessie Maisano and Dr. Matt Colbert coordinated and conducted the scanning of my skeletal sample with astounding efficiency. I am also grateful to Linda Gordon and Darrin Lunde at the National Museum of Natural History for loaning specimens and providing access to the collections. I am grateful to the many co-authors of Chapter 2 for providing FMP data and input, particularly Dr. Nate Dominy, Halszka Glowacka, Dr. Kerry Ossi-Lupo, Dr. Andrea Taylor, Dr. Chris Vinyard, and Dr. Nayuta Yamashita. Dr. Matt Ravosa encouraged me to think about ontogeny.

My fellow graduate students, past and present, have been a constant source of moral support and encouragement. Special thanks go to Darcy Shapiro, my partner in trabecular crime, and to Fred Foster, for doing the math. I am grateful to Penny Burness, Ginny Caputo, Marilyn Reyes, and Maydelle Romero for administrative support over the years.

My parents, Mary Coiner and Lou Collier, first took me to the National Museum of Natural History at age five, and are thus more or less responsible for this whole ordeal. Thank you for finally sending me to “a hard college.”

And, finally, to Dr. (!) John Mioduszewski, who performed the artificial image degradation in Matlab, tirelessly helped me with statistics, and is in general my favorite primate: thank you.

Table of Contents

List of Tables

List of Figures

Chapter 1. Introduction

1.1 Background

The relationship between jaw form and diet is of great interest to primatologists and paleoanthropologists, and considerable research has been dedicated to establishing the exact nature of morphological variation related to diet and feeding behavior. Hylander's classic work on primate masticatory function (1979a, 1979b, 1979c, 1984, 1985) provides the theoretical framework for most subsequent anthropological research into mandibular morphology. His work provided an experimental test of Greaves' lever-system model (Greaves, 1978), which established the mandible not as a simple third-class lever but instead a more complex system involving reaction forces at the working side temporomandibular joint (TMJ), balancing side TMJ, and bite point. This "triangle of support" model, while simple, has subsequently been verified by experimental data (Hylander, 1979c; Brehnan et al., 1981; Mongini et al., 1981; Herring and Liu, 2001; Naeije and Hofman, 2003).

Mastication subjects the mandible to various bending and twisting stresses (Hylander, 1979b); consequently, the shape of the mandible is designed to resist these stresses. For instance, shearing is best resisted by a thicker cross-sectional area of stress-absorbing cortical bone (Hylander, 1985; Daegling, 1993), and a transversely thick corpus is most effective for resisting twisting and wishboning (Hylander, 1988). Cortical thickness and distribution are directly related to the ability to withstand stress (Daegling, 1993; Schwartz and Conroy, 1996). The primate mandible, being roughly U-shaped, can be modeled as a curved beam (Hylander, 1984, 1985), with an associated uneven

distribution of masticatory stresses. Cortical bone in the mandible is likewise unevenly distributed: it is thicker lingually in the symphysis (Hylander, 1984; Ukase and Fukase, 2007) and thicker bucally in the postcanine corpus (Daegling and Hotzman, 2003). This suggests a functional relationship between masticatory loading and cortical bone within the mandible.

These relationships between jaw morphology and masticatory loading suggest additional relationships between jaw morphology and diet, which have been born out to some extent by developmental and comparative research. Developmental studies of primates and other mammals show a general relationship between diet properties and mandibular morphology. Animals raised on "hard" diets have, overall, more robust mandibles with thicker cortical bone than do animals raised on "soft" diets (Bouvier and Hylander, 1981, 1984; Corruccini and Beecher, 1982, 1984; Yamada and Kimmel, 1991; Teng and Herring, 1995; Ravosa et al., 2007, 2008; Scott et al., 2014). Likewise, morphological evidence from extant primates suggests functional relationships between load resistance and mandibular robusticity (Daegling, 1992; Ravosa, 1996; Daegling and McGraw, 2001, 2007; Taylor, 2002, 2005, 2006a, 2006b; Vogel et al., 2014).

But attempts to establish finer-grained relationships between diet and mandibular morphology have yielded inconsistent results, and the overall relationship between jaw form and diet can be charitably described as "complex." Although studies within taxa have demonstrated links between diet and certain aspects of jaw form (Smith, 1983; Smith et al., 1983; Bouvier, 1986a, 1986b; Daegling, 1992; Taylor, 2006a, 2006b; Vogel et al., 2014), these relationships are inconsistent and do not always fulfill functional predictions (Smith, 1983; Daegling and McGraw, 2001; Taylor, 2002, 2005; Meloro et

al., in press) and cannot be considered diagnostic of particular diets across primates. Even higher-level efforts to characterize a diet are not always successful; the recent reimagining of the diet of *Paranthropus boisei* demonstrates the ambiguity of morphological features used to distinguish tough versus hard diets (Ungar et al., 2008; Cerling et al., 2011; Smith et al., 2015).

This lack of an expected relationship between jaw form and diet in primates does not necessarily mean that the jaw is not subject to selective pressures related to feeding, or that anthropologists have been misguided in their efforts to discern a dietary signal. In other mammalian taxa, such as carnivorans, feeding behavior (specifically killing) is more clearly linked to variation in mandibular morphology (Biknevicius and Ruff, 1992). Moreover, tooth crest morphology among primates is clearly linked with diet (Kay 1975; Kay et al., 1978), and there is also some evidence that enamel thickness is associated with differences in diet (Molnar and Gantt, 1977; Martin et al., 2003; Lucas et al., 2008; Vogel et al., 2008). It is thus possible that a consistent mandibular morphological signal of dietary or feeding variation does exist in primates but has not yet been established by comparative research.

Different diets are expected to present different loading regimes because of differences in food mechanical properties (FMPs), which describe how food items defend themselves against consumption (Lucas et al., 2000). These properties have been shown to influence jaw movements and chewing patterns during mastication (Agrawal et al., 1997, 1998, 2000; Agrawal and Lucas, 2003; Williams et al., 2005; Chen, 2009), and have long been hypothesized to influence primate craniomandibular morphology (Hylander, 1979a; Bouvier and Hylander, 1984; Bouvier, 1986a, 1986b; Yamada and

Kimmel, 1991; Daegling, 1992; Taylor et al., 2008; Koyabu and Endo, 2009). Primatologists have recently begun to quantify dietary FMPs (Darvell et al., 1996; Lucas et al., 2001) and to consider how FMPs influence jaw form (Taylor et al., 2008; Vogel et al., 2013, 2014) and chewing (Wright et al., 2008; Ross et al., 2009b), but much is still unknown about the ways FMPs relate to mandibular morphology.

It is also possible that FMPs have less of an influence on jaw form than do variations in feeding behavior. Hylander (1979b) noted that the need to resist repetitive masticatory loading may have an equal or even greater influence on mandibular morphology than does the need to exert high masticatory forces to process mechanically challenging foods. Both magnitude and frequency of masticatory loading have been shown to produce epigenetic changes in bone morphology (Turner, 1998; Giesen et al., 2003; Judex et al., 2007; Ravosa et al., 2007). However, FMPs (specifically toughness) may increase chewing time within species (Tanton, 1962; Hylander, 1979a; Wright et al., 2008; Ross et al., 2009b), which complicates efforts to pinpoint specific influences on jaw form. It is likely that both duration and magnitude of loading work in tandem to shape mandibular morphology.

This dissertation focuses on the internal structure of the mandibular condyle (hereafter "condyle"), which articulates with the temporal bone to form the temporomandibular joint. The TMJ is synovial joint with an articular disc, or meniscus, placed between the mandibular fossa and the condyle. The condyle is loaded during incision and mastication (Hylander, 1979c; Brehnan et al., 1981; Wall, 1999; Herring and Liu, 2001), and its morphology should thus be influenced by differences in diet and feeding. Comparative research has investigated variations in the size and shape of the

condyle in relation to diet in non-human primates (Smith et al., 1983; Taylor, 2005; Terhune, 2011, 2013), and the internal (trabecular) structure of the condyle has been studied in humans (Giesen and van Eijden, 2000; Giesen et al., 2001, 2003; van Ruijven et al., 2002; van Eijden et al., 2006) and other mammals (Teng and Herring, 1995; Cornish et al., 2006; Mulder et al., 2007; Willems et al., 2007). This research has established that the trabecular bone of the mandibular condyle is in general plate-like, highly anisotropic, and oriented perpendicular to the articular surface of the condyle. Only one study, however, has examined the trabecular structure of the condyle in non-human primates (Ryan et al., 2010).

Studying the internal architecture of the condyle may be informative due to the nature of trabecular remodeling. Bone responds to changes in the loading environment (Goldstein et al., 1991; Ma et al., 2002; Giesen et al., 2004; Pontzer et al., 2006; Ruff et al., 2006), and different magnitudes or durations of masticatory stresses should thus produce an epigenetic signal within the condyle that is indicative of variations in loading. Based on evidence from developmental and experimental studies, it is expected that the volume fraction and/or anisotropy of trabecular bone should increase in response to increased masticatory loading.

Temporomandibular disorder

Edentate humans show reduced bone volume fraction in the mandibular condyle, suggesting that a reduction in loading leads to bone resorption (Giesen et al., 2004). While no research has addressed the relationship between TMJ disorder and internal changes in condylar morphology, if TMJ pain leads to a reduction in chewing, I would

expect a similar response of reduction in volume fraction.

Mandibular symphysis

Anthropoid primates have a fused mandibular symphysis, which serves to strengthen the symphysis and reduce strain in the corpus during mastication (Hylander, 1979a). No research has addressed the relationship between symphyseal fusion and the trabecular structure of the mandibular condyle, and my sample contains no strepsirrhines, which have unfused symphyses. However, I would expect that the higher corpus strains associated with unfused symphyses would translate to increased loading of the mandibular condyle, and as such would generate more anisotropic trabecular bone and/or higher bone volume fraction.

1.2 Data and Methodology

My research investigates the nature of trabecular variation within the non-human primate mandibular condyle in relation to feeding behavior and FMPs. Variation in FMPs has been hypothesized to influence jaw form. But how much variation is required to produce a morphological signature? Do only very tough or resistant foods generate a signal, or do relatively minor variations in FMPs influence jaw morphology? What types of food properties are most influential? What role do fallback foods play? How do FMPs interact with other feeding behaviors, like pre-ingestive oral processing? Are FMPs more or less important than other aspects of feeding, like time spent chewing? Do the repetitive loading cycles produced by tough or fibrous foods obscure the signal of the food items themselves?

This dissertation attempts to answer some of these questions. I used high-resolution X-ray computed tomography (HRXCT) to image the mandibles of 16 primate species, and here compare variation in the trabecular architecture of the condyle to data on average daily time spent feeding and FMPs. I also test the relationship between FMPs and several aspects of dietary ecology, including dietary quality and body mass. Previously, most analyses of the relationship between diet and jaw form among primates have sought to establish links between mandibular variation and broad, descriptive dietary categories (frugivore, folivore). Researchers have long criticized these categories as insufficient because of the great variety of feeding behaviors and diets included within each category (Kay, 1975; Rosenberger and Kinzey, 1976; Smith, 1983; Yamashita, 1996), but better data did not exist. The recent availability of dietary FMP data for multiple primate species enables finer-grained assessments of feeding ecology.

The mechanical properties considered here are toughness (*R*) and Young's modulus (*E*). The toughness of an object is, in the most basic terms, the work of fracture: the amount of energy that breaks a cross-sectional area of a given material (Gordon, 1978). McGowan (1999: 77) defines toughness as the "ability to tolerate cracks without failing," that is, the ability to resist crack growth. Toughness is related to the critical crack length, which represents the point at which a crack leaves equilibrium and rapid crack propagation begins. As such, toughness has been described as the energy required to grow a crack (Lucas and Pereira, 1990; Lucas et al., 2000; Taylor et al., 2008). Young's modulus, also called the elastic modulus, is the ratio of stress to strain, and is widely used to represent stiffness, or the ability of an object to resist deformation. If stress and strain are plotted as a graph, the slope of the resultant line is the Young's modulus. The higher

the Young's modulus, the more resistant the object to deformation (Williams et al., 2005); the lower, the more flexible (Gordon, 1978). Because these properties quantify the mechanical challenges that food items present to consumption, they provide a more precise understanding of diet-related selective pressures on mandibular morphology than do descriptive dietary categories. Primate diets are complex, and a folivorous diet, for example, often includes considerable amounts of non-leaf food items (Fossey and Harcourt, 1977; Watts, 1984). Consequently, investigating the relationship between FMPs and jaw form may yield a more consistent morphological signature of dietary variation.

HRXCT scanning was chosen as the primary methodology of this study because of its widespread application to both fossil and extant organisms (Schwartz and Conroy, 1996; Fajardo et al., 2002, 2007; Ryan and Ketcham, 2005; Ryan and van Rietbergen, 2005; Parga et al., 2006; Silcox et al., 2009; Ryan et al., 2010). HRXCT also allows for the imaging of full mandibles, unlike μCT, which is typically limited to smaller or partial specimens.

Finally, data on feeding time were drawn from estimates of daily activity budgets and used as a rough proxy for time spent chewing. Repetitive loading is hypothesized to influence mandibular morphology (Hylander, 1979b), and longer durations of chewing should entail more loading cycles, although primates do chew at different rates (Ross et al., 2009a). Feeding time is thus not a perfect approximation of chewing time, but more precise data are very limited in the literature (Williams et al., 2008; Ross et al., 2009b; Thompson et al., 2011; Vinyard et al., 2012). Feeding time data from activity budgets are thus the best data currently available for interspecific comparison.

1.3 Dissertation Organization

Chapter 2 presents the first large-scale comparative sample of FMPs in extant primates, and explores how FMPs vary in relation to different aspects of feeding ecology, including body mass, traditional dietary categories, dietary quality, and feeding time. This chapter also examines how FMPs vary across food items and with ripeness or maturity within food items. FMP data were collected in the field by co-authors using the Darvell HKU tester (Darvell et al., 1996). Dietary quality was calculated from published data on dietary composition, and data on body mass and time spent feeding were taken from the literature or provided by co-authors. This chapter has been submitted to the *Journal of Human Evolution*.

In Chapter 3, I compare data on FMPs with fabric density and anisotropy variables calculated from the HRXCT scans of 19 primate mandibles. The trabecular bone within the mandibular condyle was isolated for analysis, and architectural variables were calculated using BoneJ and Quant3D. Phylogenetic generalized least squares analysis was utilized to account for potential effects related to phylogeny.

Chapter 4 uses a slightly larger sample of primate mandibles (n = 28) to explore the relationship between the trabecular structure of the mandibular condyle and estimates of average daily time spent feeding. Again, feeding times were drawn from the literature, and trabecular variables were calculated with BoneJ and Quant3D.

Finally, Chapter 5 provides a brief overview of the general structure of the trabecular bone within the mandibular condyle and compares these results to previous research on human, pig, and primate condylar trabecular bone. This chapter also tests for any right/left asymmetries in condyle morphology, and examines relationships with body

mass and mandibular length.

References

Agrawal, K.R., Lucas, P.W., 2003. The mechanics of the first bite. Proceedings of the Royal Society of London: Biology. 270, 1277–1282.

Agrawal, K.R., Lucas, P.W., Bruce, I., Prinz, J., 1998. Food properties that influence neuromuscular activity during human mastication. Journal of Dental Research. 77, 1931–1938.

Agrawal, K.R., Lucas, P.W., Bruce, I.C., 2000. The effects of food fragmentation index on mandibular closing angle in human mastication. Archives of Oral Biology. 45, 577–584.

Agrawal, K.R., Lucas, P.W., Prinz, J., Bruce, I., 1997. Mechanical properties of foods responsible for resisting food breakdown in the human mouth. Archives of Oral Biology. 42, 1–9.

Biknevicius, A.R., Ruff, C.B., 1992. The structure of the mandibular corpus and its relationship to feeding behaviours in extant carnivorans. Journal of Zoology. 228, 479–507.

Bouvier, M., 1986a. Biomechanical scaling of mandibular dimensions in New World monkeys. International Journal of Primatology. 7, 551–567.

Bouvier, M., 1986b. A biomechanical analysis of mandibular scaling in Old World monkeys. American Journal of Physical Anthropology. 69, 473–482.

Bouvier, M., Hylander, W.L., 1981. Effect of bone strain on cortical bone structure in macaques (*Macaca mulatta*). Journal of Morphology. 167, 1–12.

Bouvier, M., Hylander, W.L., 1984. The effect of dietary consistency on gross and histologic morphology in the craniofacial region of young rats. American Journal of Anatomy. 170, 117–126.

Brehnan, K., Boyd, R.L., Laskin, J., Gibbs, C.H., Mahan, P., 1981. Direct measurement of loads at the temporomandibular joint in *Macaca arctoides*. Journal of Dental Research. 60, 1820–1824.

Cerling, T.E., Mbua, E., Kirera, F.M., Manthi, F.K., Grine, F.E., Leakey, M.G., Sponheimer, M., Uno, K.T., Kyalo, F., 2011. Diet of *Paranthropus boisei* in the early Pleistocene of East Africa. Proceedings of the National Academy of Sciences of the United States of America. 108, 9337–41.

Chen, J., 2009. Food oral processing—A review. Food Hydrocolloids. 23, 1–25.

Cornish, R.J., Wilson, D.F., Logan, R.M., Wiebkin, O.W., 2006. Trabecular structure of the condyle of the jaw joint in young and mature sheep: A comparative histomorphometric reference. Archives of Oral Biology. 51, 29–36.

Corruccini, R., Beecher, R., 1982. Occlusal variation related to soft diet in a nonhuman primate. Science. 218, 74–6.

Corruccini, R., Beecher, R., 1984. Occlusofacial morphological integration lowered in baboons raised on soft diet. Journal of Craniofacial Genetics and Developmental Biology. 4, 135–142.

Daegling, D.J., 1992. Mandibular morphology and diet in the genus Cebus. International Journal of Primatology. 13, 545–570.

Daegling, D.J., 1993. The relationship of in vivo bone strain to mandibular corpus morphology in *Macaca fascicularis*. Journal of Human Evolution. 25, 247–269.

Daegling, D.J., Hotzman, J.L., 2003. Functional significance of cortical bone distribution

in anthropoid mandibles: An in vitro assessment of bone strain under combined loads. American Journal of Physical Anthropology. 122, 38–50.
Daegling, D.J., McGraw, W.S., 2001. Feeding, diet, and jaw form in West African *Colobus* and *Procolobus*. International Journal of Primatology. 22, 1033–1055.
Daegling, D.J., McGraw, W.S., 2007. Functional morphology of the mangabey mandibular corpus: Relationship to dietary specializations and feeding behavior. American Journal of Physical Anthropology. 134, 50–62.
Darvell, B.W., Lee, P.K.D., Yuen, T.D.B., Lucas, P.W., 1996. A portable fracture toughness tester for biological materials. Measurement Science and Technology. 7, 954–962.
Fajardo, R.J., Müller, R., Ketcham, R.A., Colbert, M., 2007. Nonhuman anthropoid primate femoral neck trabecular architecture and its relationship to locomotor mode. Anatomical Record. 290, 422–36.
Fajardo, R.J., Ryan, T.M., Kappelman, J., 2002. Assessing the accuracy of high-resolution X-ray computed tomography of primate trabecular bone by comparisons with histological sections. American Journal of Physical Anthropology. 118, 1–10.
Fossey, D., Harcourt, A.H., 1977. Feeding ecology of free ranging mountain gorillas. In: Clutton-Brock, T. (Ed.), Primate Ecology: Studies of Feeding and Ranging Behavior in Lemurs, Monkeys and Apes. Academic Press, London, pp. 415-447.
Giesen, E., Ding, M., Dalstra, M., van Eijden, T., 2001. Mechanical properties of cancellous bone in the human mandibular condyle are anisotropic. Journal of Biomechanics. 34, 799–803.
Giesen, E., Ding, M., Dalstra, M., van Eijden, T., 2003. Reduced mechanical load decreases the density, stiffness, and strength of cancellous bone of the mandibular condyle. Clinical Biomechanics. 18, 358–363.
Giesen, E., Ding, M., Dalstra, M., van Eijden, T., 2004. Changed morphology and mechanical properties of cancellous bone in the mandibular condyles of edentate people. Journal of Dental Research. 83, 255–259.
Giesen, E., van Eijden, T., 2000. The three-dimensional cancellous bone architecture of the human mandibular condyle. Journal of Dental Research. 79, 957–963.
Goldstein, S.A., Matthews, L.S., Kuhn, J.L., Hollister, S.J., 1991. Trabecular bone remodeling: An experimental model. Journal of Biomechanics. 24, 135–150.
Gordon, J., 1978. Structures, or, Why Things Don't Fall Down. Penguin, London.
Greaves, W., 1978. The jaw lever system in ungulates: A new model. Journal of Zoology. 184, 271–283.
Herring, S.W., Liu, Z., 2001. Loading of the temporomandibular joint: anatomical and in vivo evidence from the bones. Cells, Tissues, Organs. 169, 193–200.
Hylander, W.L., 1979a. Mandibular function in *Galago crassicaudatus* and *Macaca fascicularis*: An in vivo approach to stress analysis of the mandible. Journal of Morphology. 159, 253–296.
Hylander, W.L., 1979b. The functional significance of primate mandibular form. Journal of Morphology. 160, 223–239.
Hylander, W.L., 1979c. An experimental analysis of temporomandibular joint reaction force in macaques. American Journal of Physical Anthropology. 51, 433–456.
Hylander, W.L., 1984. Stress and strain in the mandibular symphysis of primates: A test of competing hypotheses. American Journal of Physical Anthropology. 64, 1–46.

Hylander, W.L., 1985. Mandibular function and biomechanical stress and scaling. American Zoologist. 25, 315–330.

Hylander, W.L., 1988. Implications of in vivo experiments for interpreting the functional significance of "robust" australopithecine jaws. In: Grine, F.E. (Ed.), Evolutionary History of the "Robust" Australopithecines. Transaction, New Brunswick, NJ, pp. 55–80.

Judex, S., Lei, X., Han, D., Rubin, C., 2007. Low-magnitude mechanical signals that stimulate bone formation in the ovariectomized rat are dependent on the applied frequency but not on the strain magnitude. Journal of Biomechanics. 40, 1333–1339.

Kay, R.F., 1975. The functional adaptations of primate molar teeth. American Journal of Physical Anthropology. 43, 195–216.

Kay, R.F., Sussman, R.W., Tattersal, I., 1978. Dietary and dental variations in the genus *Lemur*, with comments concerning dietary-dental correlations among Malagasy primates. American Journal of Physical Anthropology. 49, 119-127.

Koyabu, D.B., Endo, H., 2009. Craniofacial variation and dietary adaptations of African colobines. Journal of Human Evolution. 56, 525–536.

Lucas, P.W., Beta, T., Darvell, B.W., Dominy, N.J., Essackjee, H.C., Lee, P.K.D., Osorio, D., Ramsden, L., Yamashita, N., Yuen, T.D., 2001. Field kit to characterize physical, chemical and spatial aspects of potential primate foods. Folia Primatologica. 72, 11–25.

Lucas, P.W., Pereira, B., 1990. Estimation of the fracture toughness of leaves. Functional Ecology. 4, 819–822.

Lucas, P.W., Turner, I.M., Dominy, N.J., Yamashita, N., 2000. Mechanical defences to herbivory. Annals of Botany. 86, 913–920.

Lucas, P.W., Constantino, P.J., Wood, B.A., Lawn, B., 2008. Dental enamel as a dietary indicator in mammals. BioEssays : news and reviews in molecular, cellular and developmental biology. 30, 374–85.

Ma, B., Sampson, W., Wilson, D., Wiebkin, O., Fazzalari, N., 2002. A histomorphometric study of adaptive responses of cancellous bone in different regions in the sheep mandibular condyle following experimental forward mandibular displacement. Science. 47, 519–527.

Martin, L.B., Olejniczak, A.J., Maas, M.C., 2003. Enamel thickness and microstructure in pitheciin primates, with comments on dietary adaptations of the middle Miocene hominoid *Kenyapithecus*. Journal of Human Evolution. 45, 351–367.

Meloro, C., Cáceres, N.C., Carotenuto, F., Sponchiado, J., Melo, G.L., Passaro, F., Raiai, P., in press. Chewing on the trees: Constraints and adaptation in the evolution of the primate mandible. Evolution. 1–29.

Molnar, S., Gantt, D.G., 1977. Functional implications of primate enamel thickness. American Journal of Physical Anthropology. 46, 447-454.

Mongini, F., Preti, G., Calderale, P.M., Barberi, G., 1981. Experimental strain analysis on the mandibular condyle under various conditions. Medical & Biological Engineering & Computing. 19, 521–523.

Mulder, L., van Ruijven, L.J., Koolstra, J.H., van Eijden, T., 2007. Biomechanical consequences of developmental changes in trabecular architecture and mineralization of the pig mandibular condyle. Journal of Biomechanics. 40, 1575–82.

Naeije, M., Hofman, N., 2003. Biomechanics of the human temporomandibular joint during chewing. Journal of Dental Research. 82, 528–531.

Parga, J.A., Maga, M., Overdorff, D.J., 2006. High-resolution X-ray computed tomography scanning of primate copulatory plugs. American Journal of Physical Anthropology. 129, 567–576.

Pontzer, H., Lieberman, D.E., Momin, E., Devlin, M.J., Polk, J.D., Hallgrímsson, B., Cooper, D.M.L., 2006. Trabecular bone in the bird knee responds with high sensitivity to changes in load orientation. The Journal of Experimental Biology. 209, 57–65.

Ravosa, M.J., 1996. Jaw morphology and function in living and fossil Old World monkeys. International Journal of Primatology. 17, 909–932.

Ravosa, M.J., Kunwar, R., Stock, S.R., Stack, M.S., 2007. Pushing the limit: masticatory stress and adaptive plasticity in mammalian craniomandibular joints. Journal of Experimental Biology. 210, 628–41.

Ravosa, M.J., Lopez, E.K., Menegaz, R.A., Stock, S.R., Stack, M.S., Hamrick, M.W., 2008. Adaptive Plasticity in the Mammalian Masticatory Complex: You Are What, and How, You Eat. In: Vinyard, C., Ravosa, M.J., Wall, C. (Eds.), Primate Craniofacial Function and Biology. Springer US, Boston, MA, pp. 293–328.

Rosenberger, A.L., Kinzey, W.G., 1976. Functional patterns of molar occlusion in platyrrhine primates. American Journal of Physical Anthropology. 45, 281–98.

Ross, C.F., Reed, D.A., Washington, R.L., Eckhardt, A., Anapol, F., Shahnoor, N., 2009a. Scaling of chew cycle duration in primates. American Journal of Physical Anthropology. 138, 30–44.

Ross, C.F., Washington, R.L., Eckhardt, A., Reed, D.A., Vogel, E.R., Dominy, N.J., Machanda, Z.P., 2009b. Ecological consequences of scaling of chew cycle duration and daily feeding time in primates. Journal of Human Evolution. 56, 570–85.

Ruff, C.B., Holt, B., Trinkaus, E., 2006. Who's afraid of the Big Bad Wolff?: "Wolff's Law" and bone functional adaptation. American Journal of Physical Anthropology. 129, 484–498.

Ryan, T.M., Colbert, M., Ketcham, R.A., Vinyard, C.J., 2010. Trabecular bone structure in the mandibular condyles of gouging and nongouging platyrrhine primates. American Journal of Physical Anthropology. 141, 583–93.

Ryan, T.M., Ketcham, R. a, 2005. Angular orientation of trabecular bone in the femoral head and its relationship to hip joint loads in leaping primates. Journal of Morphology. 265, 249–63.

Ryan, T.M., van Rietbergen, B., 2005. Mechanical significance of femoral head trabecular bone structure in *Loris* and *Galago* evaluated using micromechanical finite element models. American Journal of Physical Anthropology. 126, 82–96.

Schwartz, G.T., Conroy, G.C., 1996. Cross-sectional geometric properties of the *Otavipithecus* mandible. American Journal of Physical Anthropology. 99, 613–623.

Scott, J.E., McAbee, K.R., Eastman, M.M., Ravosa, M.J., 2014. Experimental perspective on fallback foods and dietary adaptations in early hominins. Biology Letters.

Silcox, M.T., Bloch, J.I., Boyer, D.M., Godinot, M., Ryan, T.M., Spoor, F., Walker, A., 2009. Semicircular canal system in early primates. Journal of Human Evolution. 56, 315–327.

Smith, A.L., Benazzi, S., Ledogar, J.A, Tamvada, K., Pryor Smith, L.C., Weber, G.W., Spencer, M.A., Lucas, P.W., Michael, S., Shekeban, A., Al-Fadhalah, K., Almusallam, A.S., Dechow, P.C., Grosse, I.R., Ross, C.F., Madden, R.H., Richmond, B.G., Wright, B.W., Wang, Q., Byron, C., Slice, D.E., Wood, S., Dzialo, C., Berthaume, M.A., van Casteren, A., Strait, D.S., 2015. The feeding biomechanics and dietary ecology of *Paranthropus boisei*. The Anatomical Record. 298, 145–67.

Smith, R.J., 1983. The mandibular corpus of female primates: Taxonomic, dietary, and allometric correlates of interspecific variations in size and shape. American Journal of Physical Anthropology. 61, 315–330.

Smith, R.J., Petersen, C.E., Gipe, D.P., 1983. Size and shape of the mandibular condyle in primates. Journal of morphology. 177, 59–68.

Tanton, M., 1962. The effect of leaf "toughness" on the feeding of larvae of the mustard beetle *Phaedon cochleariae Fab*. Entomologia Experimentalis et Applicata. 5, 74–78.

Taylor, A.B., 2002. Masticatory form and function in the African apes. American Journal of Physical Anthropology. 117, 133–156.

Taylor, A.B., 2005. A comparative analysis of temporomandibular joint morphology in the African apes. Journal of Human Evolution. 48, 555–74.

Taylor, A.B., 2006a. Feeding behavior, diet, and the functional consequences of jaw form in orangutans, with implications for the evolution of *Pongo*. Journal of Human Evolution. 50, 377–93.

Taylor, A.B., 2006b. Diet and mandibular morphology in African apes. International Journal of Primatology. 27, 181–201.

Taylor, A.B., Vogel, E.R., Dominy, N.J., 2008. Food material properties and mandibular load resistance abilities in large-bodied hominoids. Journal of Human Evolution. 55, 604–16.

Teng, S., Herring, S.W., 1995. A stereological study of trabecular architecture in the mandibular condyle of the pig. Archives of Oral Biology. 40, 299–310.

Terhune, C.E., 2011. Dietary correlates of temporomandibular joint morphology in New World primates. Journal of Human Evolution. 61, 583–596.

Terhune, C.E., 2013. Dietary correlates of temporomandibular joint morphology in the great apes. American Journal of Physical Anthropology. 150, 260–72.

Thompson, C.L., Donley, E.M., Stimpson, C.D., Horne, W.I., Vinyard, C.J., 2011. The influence of experimental manipulations on chewing speed during in vivo laboratory research in tufted capuchins (*Cebus apella*). American Journal of Physical Anthropology. 145, 402–14.

Turner, C.H., 1998. Three rules for bone adaptation to mechanical stimuli. Bone. 23, 399–407.

Ukase, H.F., Fukase, H., 2007. Functional significance of bone distribution in the human mandibular symphysis. Anthropological Science. 115, 55–62.

Ungar, P.S., Grine, F.E., Teaford, M.F., 2008. Dental microwear and diet of the Plio-Pleistocene hominin *Paranthropus boisei*. PloS one. 3, e2044.

Van Eijden, T., van Der Helm, P.N., van Ruijven, L., Mulder, L., 2006. Structural and mechanical properties of mandibular condylar bone. Journal of Dental Research. 85, 33–37.

Van Ruijven, L.L.J., Giesen, E., van Eijden, T., 2002. Mechanical significance of the

trabecular microstructure of the human mandibular condyle. Journal of Dental Research. 81, 706–710.

Vinyard, C.J., Glander, K.E., Teaford, M.F., Thompson, C.L., Deffenbaugh, M., Williams, S.H., 2012. Methods for studying the ecological physiology of feeding in free-ranging howlers (*Alouatta palliata*) at La Pacifica, Costa Rica. International Journal of Primatology. 33, 611–631.

Vogel, E.R., van Woerden, J.T., Lucas, P.W., Utami Atmoko, S.S., van Schaik, C.P., Dominy, N.J., 2008. Functional ecology and evolution of hominoid molar enamel thickness: *Pan troglodytes schweinfurthii* and *Pongo pygmaeus wurmbii*. Journal of Human Evolution. 55, 60–74.

Vogel, E.R., Coiner-Collier, S., Chalk, J., Constantino, P.J., Glowacka, H., Raguet-Schofield, M., Talebi, M.G., Vinyard, C.J., Wright, B.W., Yamashita, N., Dominy, N.J., Lucas, P.W., Scott, R.S., 2013. Do food material properties predict jaw and tooth morphology in primates? American Journal of Physical Anthropology. 150, 217.

Vogel, E.R., Zulfa, A., Hardus, M.E., Wich, S.A., Dominy, N.J., Taylor, A.B., 2014. Food mechanical properties, feeding ecology, and the mandibular morphology of wild orangutans. Journal of Human Evolution.

Wall, C.E., 1999. A model of temporomandibular joint function in anthropoid primates based on condylar movements during mastication. American Journal of Physical Anthropology. 109, 67–88.

Watts, D.P., 1984. Composition and variability of mountain gorilla diets in the central Virungas. American Journal of Primatology. 7, 323–356.

Willems, N.M.B.K., Mulder, L., Langenbach, G.E.J., Grünheid, T., Zentner, A., van Eijden, T.M.G.J., 2007. Age-related changes in microarchitecture and mineralization of cancellous bone in the porcine mandibular condyle. Journal of Structural Biology. 158, 421–427.

Williams, S.H., Vinyard, C.J., Glander, K.E., Deffenbaugh, M., Teaford, M.F., Thompson, C.L., 2008. Telemetry system for assessing jaw-muscle function in free-ranging primates. International Journal of Primatology. 29, 1441–1453.

Williams, S.H., Wright, B.W., Truong, V., Daubert, C.R., Vinyard, C.J., 2005. Mechanical properties of foods used in experimental studies of primate masticatory function. American Journal of Primatology. 67, 329–346.

Wright, B.W., Ulibarri, L., O'Brien, J., Sadler, B., Prodhan, R., Covert, H.H., Nadler, T., 2008. It's tough out there: Variation in the toughness of ingested leaves and feeding behavior among four Colobinae in Vietnam. International Journal of Primatology. 29, 1455–1466.

Yamada, K., Kimmel, D., 1991. The effect of dietary consistency on bone mass and turnover in the growing rat mandible. Archives of Oral Biology. 36, 129–138.

Yamashita, N., 1996. Seasonally and site specificity of mechanical dietary patterns in two Malagasy lemur families (Lemuridae and Indriidae). International Journal of Primatology. 17, 355–387.

Chapter 2. Primate dietary ecology in the context of food mechanical properties

2.1 Abstract

Recent studies have shown that the mechanical properties of foods consumed by a primate species may vary substantially, even within a single food type. The mechanical properties of plant items have been shown to influence food selection and ingestion in non-human primates. To date, no large-scale comparative study has examined the relationships between these properties and the feeding strategies of primates. Here we present comparative data on Young's modulus and toughness of foods consumed by 31 species of wild primates. We use these data to examine the relationships between food mechanical properties and body mass, dietary quality, and feeding time. We also examine the relationship between food mechanical properties and dietary categories that have been used to infer food properties. We found a complex relationship between body mass, feeding time, and food mechanical properties, with interactions between body mass and mechanical properties. Feeding time appears to scale with body mass such that smaller primates increase their feeding time in response to an increase in median dietary toughness, whereas this trend is less evident in larger primates, which may even decrease their feeding time as toughness increases. Traditional dietary categories, such as folivory and frugivory, did not separate out according to food mechanical properties, and dietary quality also had no relationship with either toughness or Young's modulus. Our results emphasize the need for additional studies quantifying the mechanical and chemical properties of primate diets so that they may be meaningfully compared to research on feeding behavior and jaw morphology.

2.2 Introduction

Primates feed on a diverse array of plant items and animal tissues to meet their nutritional needs. Variation in the mechanical properties of these items has been hypothesized to play a fundamental role in the evolution of primate dental and craniomandibular morphology and feeding behavior (Jolly, 1970; Kinzey, 1974, 1992; Hylander, 1975; Kay, 1975; Rosenberger and Kinzey, 1976; Bouvier, 1986 a, 1986 b; Daegling, 1992; Rosenberger, 1992; Silverman et al., 2001; Taylor, 2002; Lucas, 2004; Daegling and McGraw, 2007; Koyabu and Endo, 2009). These properties influence how primates select (Kinzey and Norconk, 1990; Hill and Lucas, 1996; Yamashita, 1996; Teaford et al., 2006), prepare and process (Ungar, 1995; Fragaszy et al., 2004; Yamashita et al., 2009), and ingest, chew, and swallow (Ungar, 1995; Hill and Lucas, 1996; Reed and Ross, 2010; Yamashita et al., 2012) food items, as well as how these items pass through the gut (Milton, 1981; Milton, 1984; Milton and McBee, 1983; Lambert, 1998). Thus, accurate measurement of food mechanical properties (FMPs) may improve our understanding of observed variation in diet selection among primates (Milton, 1981; Chapman, 1987; Kinzey and Norconk, 1990; Maisels et al., 1994; Ungar, 1995; Palombit, 1997; Wich et al., 2002; Knogge and Heymann, 2003; Lambert et al., 2004; Yamashita et al., 2009; Tombak et al., 2012).

FMPs were originally considered by anthropologists in an effort to understand variation in tooth morphology in primates and early hominins (Wolfpoff, 1973; Kinzey, 1974, 1992; Kay, 1975, 1981; Rosenberger and Kinzey, 1976; Lucas et al., 1986). To our knowledge, there has never been any broad synthesis of the influence of FMPs on the dietary choices of animals in any ecological context. Here, we provide the most

comprehensive comparative analysis of dietary FMPs in primates to date and use an innovative approach that considers the influence of FMPs on non-dental aspects of feeding ecology. We consider how FMPs relate to feeding time, body mass, and dietary quality (Sailer et al., 1985) in a sample of 31 species of free-ranging primates. Understanding the relationship among FMPs, dietary ecology, and feeding behavior is essential for informing hypotheses about primate adaptations to diet, and may help to untangle the complex relationship between FMPs and skull morphology (Ross et al., 2012; Ross and Iriarte-Diaz, 2014). We also investigate the extent to which traditional dietary categories (e.g., frugivory, insectivory, folivory) accurately map onto the mechanical properties of primate diets.

Predictions

Many factors influence diet selection and feeding behavior in primates (Kay, 1984; Milton, 1984; Janson, 1988; van Schaik et al., 1993; Hill and Lucas, 1996; Lambert, 1998; Rothman et al., 2011). In this study, we focus on the relationships between FMPs and time spent feeding, dietary quality, dietary categories, and body mass. Data on feeding time and body mass were widely available in the literature for most primate species for which FMP data were available. Dietary quality (DQ) roughly describes the available nutrients within a primate's diet (Sailer et al., 1985), and can be calculated from dietary composition data available in the literature. Because data on the nutritional composition of food items are limited for primates (Chapman et al., 2003; Norconk et al., 2009; Rothman et al., 2011; Rothman et al., 2012; Rothman et al., 2013; Raubenheimer et al., 2015), we used DQ as a proxy for nutritional quality.

Prediction 1. Dietary categories and FMPs. If dietary categories are useful descriptors of mechanical variation in primate diets, then FMPs should closely map onto traditional dietary categories (e.g., folivory, frugivory, insectivory). Traditionally, frugivores are predicted to experience relatively smaller masticatory loads, as fruits are often assumed to be soft and present fewer challenges to oral processing (Peters, 1987; Anapol and Lee, 1994; Ravosa, 1996; Taylor, 2006). Frugivory, therefore, and particularly the consumption of ripe pulp, should be associated with low values for toughness and/or Young's modulus, in contrast to the presumably more mechanically challenging diets of folivores.

Prediction 2. Dietary quality and FMPs. According to the Jarman-Bell Principle (Bell, 1971; Jarman, 1974; Gaulin, 1979), large-bodied animals are expected to eat large quantities of nutrient-poor (i.e. low-quality) foods while small-bodied animals are expected to eat small quantities of nutrient-rich (i.e. high-quality) foods. In this model, a low value for dietary quality indicates reliance on abundant and relatively nutrient-poor foods such as leaves, while a high value indicates a diet comprised of readily available energy such as fruit or insects. Tough foods are expected to have greater defensive mechanisms, specifically in the form of fiber, which is difficult to digest (Van Soest, 1994; Lambert, 1998; Rothman et al., 2013). Some researchers have equated "low-quality" with "tough" (e.g., Remis, 2003; Constantino et al., 2009; Pontzer et al., 2011; Scott, 2011), although the relationship between food toughness and nutrition has received little attention (but see Choong et al., 1992; Hill and Lucas, 1996; Lucas et al., 2000; Huang et al., 2010). Thus, we predict a negative relationship between DQ and toughness if toughness is an adequate measure of nutritional content. The relationship between DQ

and Young's modulus is less clear. However, if the historical assumption is made that fruits tend to be soft (Peters, 1987; Anapol and Lee, 1994; Ravosa, 1996; Taylor, 2006), then one would also expect a negative relationship between DQ and Young's modulus.

Prediction 3. Food items and FMPs. We predict that broad categories of food items (e.g., fruits, leaves, bark) will separate out by FMPs. If traditional assumptions about the mechanical properties of food items are correct, then leaves should have the highest values for toughness. Likewise, we expect that young leaves will be less tough than mature leaves, and that ripe fruit will be less tough than unripe fruit. We predict that ripe fruit will have lower measures of Young's modulus than does unripe fruit.

Prediction 4. Body mass and FMPs. If larger-bodied primates consume lower quality foods more frequently than do smaller primates (Bell, 1971; Jarman, 1974; Gaulin, 1979), then we expect FMPs to positively scale with body mass. If FMPs can be used to infer nutritional quality, then, all else being equal, we expect smaller primates with higher metabolic rates to rely on foods with lower toughness and Young's modulus while larger primates will exploit foods with higher values for toughness and Young's modulus.

Prediction 5. Feeding time and body mass. As body mass is related to metabolic rate (Kleiber, 1947; Elgar and Harvey, 1987; McNab, 2008) and dietary nutrient density (Clutton-Brock and Harvey, 1977; Gaulin, 1979; Sailer et al., 1985), we expect that feeding time may also scale positively with body mass to allow primates to meet their metabolic needs. Previous studies have found a weak relationship between feeding time and body mass with a strong phylogenetic component (Ross et al., 2009 b; Organ et al., 2011). Here, we re-test this relationship with a different data set including different species and different values for time spent feeding.

Prediction 6. Feeding time and FMPs. Experimental observations that jaw movements and chewing patterns vary with mechanical properties within species (Agrawal et al., 1998, 2000; Vinyard et al., 2006; Wright et al., 2008; Thompson et al., 2011), and that the ratio of toughness to Young's modulus determines the rate at which a food is broken down (Agrawal et al., 1997), lead to our prediction that FMPs might modulate feeding time across primates. Leaf toughness has been found to scale positively with feeding time in insects (Williams, 1954; Tanton, 1962). Tough foods, which can be higher in fiber, may therefore require more time to break down both orally and within the gut (Van Soest, 1994; Milton, 1984; Lambert, 1998). Thus, a diet reliant on these tough foods may ultimately increase the proportion of the daily activity budget devoted to feeding time and/or the number of masticatory cycles (i.e. repetitive loading of the mandible). While data are not available to test the latter, we can use feeding time to explore the relationship between dietary toughness and time devoted to feeding, quantified as time spent orally processing food items. Thus, we predict that primates with tougher diets will devote more time to feeding.

2.3 Materials and Methods

Study species

Our study sample comprises 31 wild primate species, including both haplorhines and strepsirrhines from a variety of habitats (Table 2.1). These species represent the majority of primate species for which FMP data have been collected using equivalent mechanical testing protocols and equipment (Darvell et al., 1996; Lucas et al., 2001).

Mechanical properties

For each primate species, we collected FMP data on food items consumed using the Darvell HKU tester. This tester allows for testing of food items in the field and has become the standard means of measuring FMPs in primates (Williams et al., 2005; Wright, 2005; Teaford et al., 2006; Dominy et al., 2008; Taylor et al., 2008; Vogel et al., 2008; Yamashita et al., 2009; Chalk et al., in review). All samples were collected during focal feeding bouts or consisted of food items that are known to comprise a primate species' diet, and were tested on the same day as collection when possible. For some primate species (e.g. *Pongo pygmaeus wurmbii*) we were unable to test the most mechanically challenging items due to limitations of our load cell and our inability to reduce the size of certain seeds (see Vogel et al., 2008, 2014 for details).

Measurements of toughness (*R*) were recorded for foods, including food parts, eaten by all species, while measurements of Young's modulus (*E*) were recorded for foods eaten by 21 species (see Supplement). Although fragmentation indices have been hypothesized as a potential driver of feeding adaptations in primates (Agrawal et al., 1997; Lucas et al., 2002; Williams et al., 2005), our limited data on Young's modulus prevented us from including these indices in our analyses.

Toughness Toughness (in J m^{-2}) is estimated here as the energy required to extend a unit area of a crack (Gordon, 1978; Lucas and Pereira, 1990; Vincent, 1992; Lucas et al., 2000, 2011). We performed scissors tests for sheet-like items such as leaves (Lucas and Pereira, 1990; Vincent, 1992), and employed wedge tests for thicker items (e.g. >2 mm). In both cases, the blade(s) move progressively through the material being tested to

determine the work done (force x displacement) to force a crack in a specified direction (Lucas et al., 2001).

Young's modulus Young's modulus (in MPa), also termed the elastic modulus, is the ratio of stress to strain throughout elastic deformation, and is defined as an object's ability to resist elastic deformation. The higher the Young's modulus, the more resistant the object is to such deformation (Gordon, 1978; Williams et al., 2005). We measured modulus with both bending and compression tests. Three-point bending was used to measure modulus in food items that could be prepared into the beam-shaped format needed for this type of testing (Vincent, 1992; Yamashita et al., 2009), such as bark or branches (whenever possible length to width ratios of 10:1 or greater were maintained). Compression tests entail the extraction of a cuboid or cylindrical sample (Agrawal et al., 1997), which is then placed under compression to measure the associated stress and strain during elastic deformation (Agrawal and Lucas, 2003).

It is unknown whether the mechanical properties of the most common food items in a primate's diet exert greater selective pressures on primate feeding ecology than do the most challenging items (Rosenberger, 1992; Yamashita, 1998; Lambert et al., 2004; Taylor et al., 2008; Wright et al., 2013; Vogel et al., 2014). Consequently, we used estimates designed to quantify both of these aspects of a primate's diet. To estimate the FMPs of a diet at its most challenging, we used maximum estimates of the toughness (R) and Young's modulus (E) of the toughest and most resistant item in the diet, respectively. For example, a fruit may have toughness data available for the exocarp, mesocarp, and endosperm. If all of these were eaten, the maximum R and E of these measures were used to represent that food item. In turn, the maximum of these values for all foods eaten by a

given primate species was used as the maximum *R* or *E* for that species, resulting in the variables *MaximumR* and *MaximumE.*

We also generated two estimates—a weighted mean and a median measure—to approximate the typical or usual dietary mechanical demand for each species. A mean *R* or *E* calculated for all of the food items in a species' diet makes the implicit assumption that an item eaten infrequently is weighted equally with an item eaten frequently. Certain barks and piths, for example, are extremely tough, but represent only a very small portion of the annual diet composition (Vogel et al., 2008). A robust estimate of the FMPs that are typically encountered by a primate requires weighting data on the FMPs of each item in the diet by the frequency of consumption, but these data were not available for every food item. Thus, we weighted FMP data by composition of a species' diet based on food category to avoid over- or under-representing the importance of specific food items. For example, if the proportions of leaves, seeds, flowers, and fruit (pericarp and whole fruit) in a species' diet were available, we calculated the mean *R* and *E* of all foods eaten for each of those categories. These category means were then weighted by the proportion of each category in a primate species' diet. The denominator was equal to the total proportion of a primate's diet for which some FMP data were available. Thus, if a primate ate 50% leaves, 20% seeds, 10% pericarp or whole fruit, and 10% insects, the weighted mean *R* for that species was:

(0.5 * mean *R* for leaves + 0.2 * mean *R* for seeds + 0.1 * mean *R* for pericarp or whole fruit) / 0.8

The above equation does not include insects because FMP data were not available for insects in our sample. This process resulted in the variables *WeightedR* and *WeightedE.*

As the median is minimally influenced by extreme outliers, we also computed medians for *R* and median *E* for each food item eaten by a species. We first calculated a

mean *R* and *E* of each food item. If a food item comprised multiple parts, we computed the mean across those parts. For example, for a fruit item, we first computed the mean *R* and *E* for exocarp, mesocarp, and endosperm. The median *R* and *E* values of all food items in a species' diet resulted in the variables *MedianR* and *MedianE,* respectively.

Feeding time

Following Ross *et al.* (2009 b), we define feeding time as the percentage of the daily activity budget spent ingesting and orally processing foods. Gut digestion time is known to play an important role in primate diet selection (Milton, 1981; Milton, 1984; Lambert, 1998), but because these data were not available for many species in our sample, we did not consider this variable in our analyses. Whenever possible, feeding times used here were drawn from the same study populations as those from which FMP data were collected (n = 18). When unavailable, we drew on feeding times from the literature (Table 2.1). For two species (*Chiropotes satanas* and *Piliocolobus rufomitratus*), multiple feeding times were available, and none was specific to the sites where FMPs were measured. In these cases, we used the average of the available measures. We preferentially used feeding time data that did not include time spent foraging, as determined by the methodology of each paper (e.g., feeding and foraging were defined and measured separately). Chewing, feeding, and foraging are separate activities, and are not always clearly distinguished out in the literature. Ideally, data on feeding times would include an estimate of time spent chewing, but these data are only available for a limited number of captive species (Ross et al., 2009 a; Ross et al., 2009 b).

We specifically excluded any papers that did not clearly define feeding or did not

distinguish between feeding and foraging. Excluding foraging time likely underestimates time spent feeding for insectivorous primates, which tend to feed continuously while foraging (e.g., Terborgh, 1983; Robinson, 1986). However, in the absence of fine-grained data that separate out insect feeding and foraging, we chose the more conservative approach of excluding foraging time.

Body mass

Body mass data specific to the populations in our sample were used whenever possible (n = 7), while the remaining body mass estimates were taken from the literature (Table 2.1). We used species averages that included both males and females. When body mass estimates were presented separately for males and females, we averaged these estimates to achieve a species mean.

Dietary quality

Dietary quality (DQ) was calculated by using coefficients to weight the percentages of plant structural parts, plant reproductive parts, and animal material consumed by a primate species (Sailer et al., 1985). Coefficients for dietary quality were taken from Sailer *et al.* (1985): 1 for structural parts, 2 for reproductive parts, and 3.5 for animal matter and exudates. DQ was calculated as $DQ = 1s+2r+3.5a$. For this study, we also included exudates as animal matter, because principal components analysis showed that insects and exudates were co-related (Janson pers. comm. to ERV). We calculated the DQ index for each primate species using data on dietary composition (Table 1). Food items were assigned to categories as outlined in Figure 2.1 (e.g., pith and shoots were

structural; seeds were reproductive). These data included either time spent feeding on different food items or percentage of feeding records devoted to different food items. Data reporting diet as a percentage of total items consumed were excluded. When possible, data on dietary composition were taken from the same populations as FMP data (n = 29). All other data were drawn from the available literature (Table 2.1). If the reported dietary composition did not add up to 100%, we adjusted the numbers to maintain relative proportions, using the equation:

% structural (or reproductive, animal, exudate) * 100 / total recorded diet composition

For example, as dietary composition for *Cebus libidinosus* was only recorded for 86% of its diet, and 51% of its diet was reproductive matter, we calculated an adjusted figure for reproductive matter as: (0.51 *100) / 0.86

Dietary categories

We established two dietary categories. Our *general* dietary classification identifies primate species as folivorous, frugivorous, or insectivorous based on dietary composition (Table 2.1). Following Muchlinski (2010), a species is frugivorous if at least 60% of its diet (as measured by records of dietary composition taken from time spent feeding on different food items) is comprised of fruit. The distinction between folivory and insectivory was determined by whether the non-fruit portion of the diet consists of more leaves or more insects. We classified *Callithrix jacchus* as a gummivore (Sussman and Kinzey, 1984).

We also considered a *specific* classification system, following Plavcan and van Schaik (1992), to ensure that the *general*, higher-level categories do not obscure

meaningful biological differences in food properties. This *specific* classification identified taxa as frugivorous, folivorous, insectivorous, gummivorous, frugivorous-folivorous, frugivorous-insectivorous, or frugivorous-gummivorous (Table 2.1). Frugivores were given a mixed classification if the secondary component of their diet comprised more than 15% (for leaves) or 25% (for insects and exudates) of the total diet.

Food items

Food items were classified by type (Figure 2.1) to examine FMP variation across food types. For analyses testing the relationship between FMPs and food items, we set a threshold of $n \geq 15$ individual FMP tests for inclusion. Thus, we included the food items highlighted in bold (*R*: bamboo, bark, flower, pericarp and whole fruit, leaf, seed, stem/stalk; *E:* bamboo, fruit, leaf, seed) and excluded those that fell below the threshold (cambium, grass, pith, root/tuber/bulb part, shoot). After analyzing variation in FMPs for food categories, we performed additional analyses to test for differences in FMPs based on food ripeness or maturity. We separated pericarp and whole fruit based on ripeness (ripe and unripe) and leaves based on maturity (young and mature). We categorized seeds separately from pericarp and whole fruit because these items were frequently measured separately, and because seeds and whole fruits often differ in mechanical properties (Lucas et al., 1991; Vogel et al., 2008, 2014; Daegling et al., 2011; Chalk et al., in review). We used values for *R* and *E* that represented either single tests of individual food items or an average of multiple tests of the same plant species or category of food item, according to how these data were reported.

Analyses

We applied phylogenetic generalized least squares (PGLS) to evaluate our predictions relating FMPs to body mass, feeding time, and dietary quality. We used the GenBank consensus tree from 10kTrees (http://10ktrees.nunn-lab.org/) (Arnold et al., 2010) to estimate phylogenetic relationships and divergence dates for primate species (Figure 2.2). Because not all of the species in our sample are included in the 10kTrees database, we relied on published phylogenetic positions and divergence estimates for the missing species. For *Cebus libidinosus* and *Cebus apella,* we used a divergence date of 400,000 years (Lynch Alfaro et al., 2012). For *Pongo pygmaeus wurmbii* and *Pongo pygmaeus morio*, we used a divergence date of 178,000 years (Nater et al., 2011).

To test our hypothesis about feeding time and FMPs, and given our expectations about this relationship, we ran PGLS regression models incorporating an interaction between FMPs and body mass. If the interaction was not significant and did not trend toward significance, we then ran the models without the interaction. We used Kruskal-Wallis rank sum tests (Kruskal and Wallis, 1952) to examine the relationship between FMPs and diet categories and between FMPs and food items. We performed pairwise comparisons using a Wilcoxon rank sum test (Wilcoxon, 1945) for post-hoc analysis of FMPs and food items. For all analyses, the natural log of body mass averages and FMP values were used, and feeding times were logit transformed before analysis. We set the significance level for all tests at $\alpha < 0.05$, and noted trends toward significance at $0.05 < p < 0.1$. We used a Bonferroni-Holm correction for multiple comparisons (Holm, 1979) to control for family-wise error rate, applied separately for models of *R* and *E*. All analyses were performed using the R Statistical Programming Language version 3.1.0

(http://www.R-project.org/). Packages APE (Paradis et al., 2004) and caper (Orme et al., 2013) were used for PGLS.

2.4 Results

Dietary categories and FMPs

When we grouped primate species into *general* and *specific* traditional dietary categories, we found no significant differences in FMPs across categories (Table 2.2; Figure 2.3).

Dietary quality and FMPs

There were no significant relationships between our measure of dietary quality and the three measures of FMPs (Table 2.3). However, there was a negative trend between *MaximumE* and dietary quality.

Food items and FMPs

Toughness varied significantly among food items across primates (K-W test $\chi^2 = 171.23$, $p < 0.001$) (Figure 2.4A). Post-hoc pairwise comparisons yielded several significant differences among food items; however, fruits, seeds, and leaves showed no differences in toughness (Table 2.4A). Bark and bamboo were not significantly different from each other, but were tougher than all other food items except for stems, which were less tough than bamboo but not bark. Flowers approached but did not achieve significance relative to seeds.

We also observed a significant difference in Young's modulus across food items (K-

W test $\chi^2 = 66.59$, $p < 0.001$) (Figure 2.4B). Here, all food items were significantly different from each other (Table 2.4B). Bamboo had higher modulus values than fruits or seeds, and fruits had higher values than seeds.

Variation was found in maturity stage in both leaves and fruits (K-W test $\chi^2 = 17.8$, $p < 0.001$) (Figure 2.4C). The toughness of young leaves did not differ from that of mature leaves, ripe fruit, or unripe fruit (Table 2.4C). Ripe fruit was less tough than unripe fruit and mature leaves. Unripe fruit and mature leaves did not differ.

There was no significant difference in Young's modulus between ripe and unripe fruit (K-W test $\chi^2 = 3.01$, $p = 0.08$).

Body mass and FMPs

There was no relationship between body mass and any of our three estimates of toughness (Table 2.5; Figure 2.5A-C), although *MedianR* and body mass showed a negative trend. In contrast, all measures of Young's modulus were significantly inversely correlated with body mass (Table 2.5; Figure 2.5D-F).

Feeding time and body mass

PGLS analysis of feeding time versus body mass was significant ($F(1, 29) = 5.18$, $p = 0.03$, $R^2 = 0.12$) (Figure 2.6). This model resulted in a maximum-likelihood estimate of 0 for λ (C.I = NA, 0.8), suggesting no phylogenetic signal.

Feeding time and FMPs

We found a complex relationship between feeding time and all measures of toughness (Table 2.6). For *MaximumR* and *WeightedR*, the interaction term was not

significant, and we then ran models excluding the interaction. *WeightedR* and feeding time were positively correlated (Figure 2.7A), but the overall significance of the model including *MaximumR* was driven by body mass (Table 2.6C), and *MaximumR* was not correlated with feeding time. For *MedianR*, inclusion of the interaction with body mass (Table 2.6B) resulted in a positive relationship with feeding time at small body sizes and a negative one at large body sizes (Figure 2.7B).

For the relationship between Young's modulus and feeding time, none of the overall models was significant (Table 2.6). Body mass was significant for the models including *WeightedE* and *MaximumE* (Table 2.6D, E).

2.5 Discussion

Dietary categories, dietary quality, and FMPs

We found no significant differences among traditional dietary categories, either *general* or *specific*, and any measures of toughness or Young's modulus. The lack of significant differences suggests that these categorical descriptions of primate diets do not sufficiently describe a potential relationship between FMPs and primate diets. Categorizing a primate as "folivorous," for example, may fail to fully characterize the range of mechanical variation within folivory: folivores eat leaves with a wide range of values for toughness and Young's modulus, as well as a variety of non-leaf foods. Our results support a continued move away from reliance on descriptive dietary categories as proxies for the mechanical properties of food items (Kay, 1975; Rosenberger and Kinzey, 1976; Lucas et al., 1985; Rosenberger, 1992; Yamashita, 1996, 1998; Wright and Willis, 2012).

Likewise, we found no relationship between dietary quality and FMPs. Foods classified as low quality are typically those with higher fiber content, and fiber contributes to toughness (Hill and Lucas, 1996; Lucas et al., 2000, 2011). However, the relationship between food toughness and nutrition has received minimal attention (but see Choong et al., 1992; Hill and Lucas, 1996; Lucas et al., 2000; Huang et al., 2010). It is likely that certain mechanically challenging foods may be preferentially selected by primates because of their nutritional value (Vogel et al., 2008, 2009, 2014; Daegling et al., 2011; Chalk et al., in review). Moreover, manual and oral processing of foods, as well as gut adaptations related to digestion, may allow primates to extract resources from foods that would otherwise be considered low-quality. The more simplistic DQ index used in this study and others (Sailer et al., 1985; Jaeggi and Van Schaik, 2011) assumes that all primates receive similar energetic benefits from all food items and ignores that different primate species have variable gut morphology and gut passage times. Thus, what may be considered a high quality diet for one species can be considered a low quality diet for another (Milton, 1981; Milton, 1993). Furthermore, recent studies have highlighted the important role of nutritional balancing of macronutrients in primate diet selection (Rothman et al., 2011; Rothman, 2015). Thus, it is conceivable that a mechanically challenging diet may also be characterized as nutritionally high-quality (Daegling et al., 2011). While dietary quality may reflect caloric or nutritive aspects of primate food choice, the mechanical properties associated with different food items are not described by measures of DQ.

Differences in the mechanical properties of food items themselves suggest that ranked, descriptive categories cannot accurately describe variation in FMPs. Our results

showed that the fruits, leaves, and seeds eaten by the primates in our sample are overall indistinguishable in terms of toughness. On average, a primate that exclusively consumes leaves does not ingest tougher foods than does a frugivore. However, maturity stage influences FMPs to some extent, such that ripe fruits are less tough than are unripe fruits. Contrary to our expectations, there was no difference in toughness between young and mature leaves in our dataset. Because our data examine relationships across primates, our results may overlook variation that exists within species. For example, the leaf lamina of mature leaves consumed by Bornean orangutans is tougher than immature leaf lamina (Vogel et al., 2008).

Primates do appear to make decisions about food consumption based on detectable properties of foods (Milton, 1984; Kinzey and Norconk, 1990; Hill and Lucas, 1996; Yamashita, 1996; Teaford et al., 2006; Vogel et al., 2008), including toughness; it is not unreasonable to expect that leaves as a whole are tougher than are fruits. Our results simply indicate that the species of leaves selected for consumption by primates have, on average, similar mechanical properties to fruits similarly selected. FMPs may in part determine the range of foods eaten by primates: extremely tough foods, whether leaves or fruits, may be avoided because of their mechanical challenges.

Body mass, feeding time, and FMPs

Food mechanical properties exhibit complex, likely clade-specific relationships with feeding time and body mass. First, with respect to feeding time scaling with body mass, our results are similar to those of previous studies (Ross et al., 2009 b; Organ et al., 2011), and suggest a weak relationship between body mass and feeding time. It may be

the case that feeding time is too simplistic of a measure and obscures a meaningful relationship between body mass and food intake. Our measures of feeding time were drawn from daily activity budgets, which are recorded and reported differently across studies. Alternatively, time spent ingesting and chewing may be more relevant. Similarly, the relationship between chewing rate and feeding time may be informative. Experimental research has examined this relationship (Ross et al., 2009 a, 2009 b; Thompson et al., 2011), but data remain too limited to enable large-scale, interspecific analysis (but see Williams et al., 2008; Vinyard et al., 2012). Thus, feeding time as drawn from data on daily activity budgets represents the best current measure for comparative study.

Our expectation that larger primates would eat more mechanically challenging foods was not supported, as we found no relationship between toughness and body mass, while dietary Young's modulus actually decreases in larger primates (Figure 2.5D-F). This latter result may be a consequence of a sampling bias. We found that bamboo has, on average, higher values for Young's modulus than do fruits and seeds (Figure 2.4). In our sample, bamboo was almost exclusively consumed by the relatively small-bodied bamboo lemurs, with the exception of *Trachypithecus phayrei.* Further sampling of Young's modulus on food items is critical for drawing conclusions about these relationships. Toughness is not significantly related to body mass after Bonferroni-Holm correction. However, as seen in Figure 2.5B and reflected by a significant result prior to Bonferroni-Holm correction (Table 2.5) the possibility of a weak effect whereby smaller primates consume tougher foods may be worth further investigation. Such an effect might imply that, to meet their daily caloric needs, smaller primates may turn to more

mechanically challenging—yet nutrient-rich—food items that are avoided by larger primates with slower metabolisms. The key point is that this result underscores the need to quantify the complete range of food properties from mechanical to chemical to nutritional.

Evaluating whether species with more mechanically challenging diets invest more time in feeding seems to depend in part on the way FMPs are quantified. First, there is clearly no relationship between feeding time and maximum toughness. This result is what we would expect if the toughest items in a primate's diet represent fallback foods that are important primarily during periods of low availability of preferred food items (Lambert et al., 2004; Laden and Wrangham, 2005; Marshall and Wrangham, 2007; Constantino et al., 2009).

Analysis of median toughness suggests the possibility that the relationship between median toughness and feeding time is modulated by an interaction with body mass (although Table 2.6 implies a complex web of weak effects). Feeding time and median toughness appear to scale differently for smaller primates than for larger primates. For small primates, as median toughness increases, feeding time increases as well. However, for larger primates, feeding time and toughness have a negative relationship (Figure 2.7B). In other words, large primates do not respond to increased dietary toughness by increasing the proportion of their activity budget devoted to feeding as much as do smaller primates. This result may be a consequence of larger primates' hypothesized increased capacity for masticatory force production (Greaves, 1978, 1988; Demes and Creel, 1988; Wroe et al., 2005), or of their slower metabolic rates and thus relatively lower energetic demands (Kleiber, 1947; Gaulin, 1979; Elgar and Harvey,

1987; Lambert, 1998; McNab, 2008). Differences in oral processing and digestion may also play a role. Mountain gorillas (*G. beringei*) excrete long, fibrous strings of minimally processed food (Elgart-Berry, 2000) and are commonly observed to use coprophagy as a method to maximize available energy from fibrous foods (Harcourt et al., 1978; Mahaney et al., 1990).

In contrast, when we examined feeding time and weighted mean toughness, we found a more straightforward relationship with no interaction. As weighted mean toughness increases, feeding time increases as well (Figure 2.7A). Although we elected to use a weighted mean to avoid over-representing items with high FMP values that are eaten relatively infrequently, this method may serve to obscure an interaction similar to that seen among feeding time, body mass, and median toughness, and may account for the different slopes seen in Figures 2.7A and 2.7B. The dietary composition data used to calculate the weighted mean did not always reflect 100% of the diet, and the food items for which FMPs were measured comprise only a portion of the total diet for each species. Consequently, further research is needed to establish whether median or weighted mean toughness more accurately represents the true relationship with feeding time.

Our results with median toughness suggest a possible upper limit on feeding time. Even highly insectivorous tarsiers spend no more than 60% of their time foraging and feeding (Gursky, 2000). The demands of social behavior and social grooming may serve to constrain the amount of time primates can dedicate to other behaviors (Aiello and Dunbar, 1993), including feeding. Assuming this upper limit, primates likely cannot rely solely on increased chewing time to process tough diets. Jaw and tooth morphology may be of vital importance, as a limit on feeding time would place an adaptive premium on

dental morphology. The lack of a significant relationship between feeding time and maximum toughness may result from selection pressure of fallback foods on tooth morphology. We would then expect to see strong functional relationships between FMPs and cranial and dental morphology.

2.6 Conclusion

Our results deviated from traditional evaluations of primate diets based on the assumed mechanical properties of food items or dietary categories. We found no significant differences in average FMPs between, for example, foods eaten by frugivorous and folivorous primates. Dietary quality also failed to yield a relationship with FMPs. Moreover, the food items that form the bulk of most anthropoid primates' diets—leaves, fruits, and seeds—are indistinguishable in terms of average toughness.

The patterning of FMPs, feeding time, and body mass demonstrate that size influences primate feeding ecology in complex ways that have not been fully characterized by current research. Further study of this relationship is warranted and will benefit from improved sampling and the integration of nutritional analyses. Thus, primate feeding ecology would benefit from FMPs collected in tandem with detailed measurements of feeding behavior and non-mechanical food properties. In addition to detailed activity budgets differentiating time spent feeding from time spent foraging, other desirable data include measurements of time and frequency of feeding on specific food items, time spent ingesting versus chewing, oral processing versus chewing times and rates, seasonal or even monthly variations in FMPs and feeding behavior, food intake, bite counts, food weight, and nutritional and chemical properties of individual

food items. The variation in behavioral data collection across sites (Schuelke et al., 2006) and the lack of site-specific data for all primates in our sample underscore the need for greater consistency in data collection and more detailed fieldwork on the populations in which FMPs were collected.

Finally, we recommend that FMPs be utilized for further investigation of the relationship between diet and jaw and tooth morphology. While some research has addressed the question of possible relationships between FMPs and craniodental morphology (Taylor et al., 2008; Norconk et al., 2009; Vogel et al., 2014), a large-scale comparison of FMPs and craniodental morphology may uncover meaningful form-function interactions that will provide new insight into primate mastication.

Table 2.1. Species included in the study sample, with body mass, feeding time, dietary quality, and dietary categories.

Species	Source of FMPs[1]	Body mass average (kg)	Feeding time (%)	Dietary quality (%A, R, S, E)[2]	Diet category (specific)[3]	Diet category (simple)[3]
Alouatta clamitans	Carlos Botelho State Park, Brazil (MT & ES)	4.84[a]	18[l]	130.3 (0, 30, 69, 0)[jj]	FO	FO
Alouatta paliatta	Ometepe, Nicaragua (MRS)	6.25[b]	**11.47**[m]	**145.34 (0, 44.72, 53.92, 0)**[m]	FO	FO
Alouatta seniculus	Iwokrama, Guyana (BW)	5.95[b]	12.7[n]	**165.85 (0, 65.86, 34.15, 0)**	FL	FR
Ateles paniscus	Iwokrama, Guyana (BW)	8.78[b]	18.9[o]	**194.92 (0, 94.92, 5.08, 0)**	FR	FR
Brachyteles arachnoides	Carlos Botelho State Park, Brazil (MT & ES)	**9.25**[c]	**22.2**[p]	**177.62 (0, 74.9, 21.6, 0)**[kk]	FL	FR
Callithrix jacchus	Pernambuco, Brazil (CV)	0.35[d]	35[q]	317.45 (18.9, 21.7, 0, 59.4)[ll]	G	G
Cebus apella	Iwokrama, Guyana (BW)	3.09[b]	16[r]	**180.23 (0, 80.23, 19.77, 0)**	FL	FR
Cebus libidinosus	Fazenda Boa Vista, Brazil (JC)	2.44[e]	17[s]	**249.42 (31, 51, 4, 0)**[mm]	FI	I
Cebus olivaceus	Iwokrama, Guyana (BW)	2.91[b]	34.2[t]	**196.43 (0, 96.42, 3.57, 0)**	FR	FR
Cercopithecus ascanius	Kibale, Uganda (ND)	3.31[b]	**25**	**171.91 (8, 48, 41, 0.5)**[nn]	FL	FO
Chiropotes satanas	Iwokrama, Guyana (BW)	2.88[b]	22.3 [u–w]	**200 (0, 100, 0, 0)**	FG	FR
Colobus guereza	Kibale, Uganda (ND)	11.35[b]	**31**	**109 (0, 9, 91, 0)**[nn]	FO	FO
Colobus vellerosus	Boabeng-Fiema, Ghana (AE)	9.1[f]	**23.7**[x]	**123.71 (0, 23, 74,**	FO	FO

				0)[x]		
Gorilla beringei	Karisoke, Rwanda (HG)	130[b]	**55.4**[y]	**101.18** (**0, 1.13, 94.4, 0**)[oo]	FO	FO
Hapalemur aureus	Ranomafana, Madagascar (NY)	**1.46**[g]	**34.4**[z]	**104.21** (**0, 4, 91, 0**)[pp]	FO	FO
Hapalemur griseus	Ranomafana, Madagascar (NY)	**0.93**[g]	**37.42**[z]	**105.15** (**0, 5, 92, 0**)[pp]	FO	FO
Hylobates albibarbis	Sabangau, Indonesia (SC)	5.85[b]	**29**[aa]	**176.5** (**1, 74, 25, 0**)[aa]	FL	FR
Lemur catta	Beza Mahafaly, Madagascar (NY)	**2.1**[h]	**25.77**	**151.73** (**0, 51.73, 48.27, 0**)	FL	FO
Pan troglodytes schweinfurthii	Kibale, Uganda (ND)	38.2[b]	**27.7**	**196.43** (**0, 84, 14, 3**)[nn]	FR	FR
Papio ursinus	Giant's Castle and Royal Natal, South Africa (PC)	22.3[b]	**56.6**[bb]	**110.01** (**0, 10, 89.9, 0**)[qq]	FO	FO
Piliocolobus badius	Kibale, Uganda (ND)	8.29[b]	**39.9**	**114.9** (**0, 13, 86, 0.5**)[nn]	FO	FO
Piliocolobus rufomitratus	Tana River, Kenya (PS)	8.44[b]	27.97[cc,dd]	140.45 (0, 39.5, 58.16, 0)[cc]	FO	FO
Pithecia pithecia	Iwokrama, Guyana (BW)	1.76[b]	19[ee]	**200** (**0, 100, 0, 0**)	FG	FR
Pongo abelii	Ketambe, Indonesia (EV)	56.75[b]	**53.9**[ff]	**194.03** (**8.8, 71, 19.1, 0**)[ff]	FL	FR
Pongo pygmaeus morio	Kutai, Indonesia (LL)	57.15[b]	**45.9**[gg]	**158** (**0.8, 56, 43.2, 0**)[gg]	FL	FO
Pongo pygmaeus wurmbii	Tuanan, Indonesia (EV)	57.15[b]	56[ff]	**191.16** (**6.3, 74.5, 18.2, 0**)[ff]	FL	FR
Prolemur simus	Ranomafana, Madagascar (NY)	**2.57**[g]	**41.2**[z]	**100** (**0, 0, 98, 0**)[pp]	FO	FO

Propithecus verreauxi	Beza Mahafaly, Madagascar (NY)	**2.8**[i]	**46.83**	**128.32** (**0, 28.32, 71.68, 0**)	FO	FO
Pygathrix nigripes	Ni Chua, Vietnam (BW)	**8.46**[j]	27.1[hh]	**144.57** (**0, 43.9, 54.6, 0**)[rr]	FO	FO
Rhinopithecus avunculus	Tonkin Snub-Nosed Monkey Species/Conservation Area, Vietnam (BW)	11.25[k]	14.78[ii]	**162.87** (**0, 61.09, 36.08, 0**)[ss]	FL	FR
Trachypithecus phayrei	Phu Khieo, Thailand (KO)	7.09[b]	**27.9**	**158.1** (**3.6, 48.4, 46.8, 0**)[tt]	FL	FO

Note: Any data without a citation were provided by one of the authors. Data in bold font were taken from the same site where FMP data were collected.
[1]Site name with initials of contributing author.
[2]Dietary quality was calculated from coefficients; see discussion in text. Numbers in parentheses are the percentage of the diet consisting of animal matter (A), reproductive parts (R), structural parts (S), and exudates (G), with the source given for dietary composition. The dietary composition data are the raw figures not adjusted to equal 100%; DQ indices were calculated based on adjusted figures.
[3]See discussion in text. FO = folivore, FR = frugivore, G = gummivore, I = insectivore, FL = frugivore-folivore, FI = frugivore-insectivore, FG = frugivore-gummivore.

[a]Chagas *et al.* 2010. [b]Smith and Jungers 1997. [c]Talebi 2005. [d]Araujo *et al.* 2000. [e]Ford and Davis 1992. [f]Oates *et al.* 1994. [g]Vinyard *et al.* 2008. [h]Gould *et al.* 2003. [i]Richard *et al.* 2006. [j]Wright and Willis 2012. [k]Ratajszczak *et al.* 1992. [l]Chiarello 1993. [m]Raguet-Schofield 2010. [n]Gaulin and Gaulin 1982. [o]Wallace 2001. [p]Talebi and Lee 2010. [q]Digby *et al.* 2006. [r]Terborgh 1983. [s]Sabbatini *et al.* 2008. [t]cited in Rímoli *et al.* 2008. [u]Boyle and Smith 2010. [v]Silva and Ferrari 2009. [w]Port-Carvalho and Ferrari 2004. [x]Teichroeb *et al.* 2003. [y]Watts 1988. [z]Tan 2000. [aa]Cheyne 2010. [bb]Dunbar 1992. [cc]Decker 1994. [dd]Marsh 1981. [ee]Vié 2001. [ff]Morrogh-Bernard 2007. [gg]Rodman 1977. [hh]Rawson 2009. [ii]Hai 2007. [jj]Agostini 2010. [kk]Talebi *et al.* 2005. [ll]Correa *et al.* 2000. [mm]Izar *et al.* 2012. [nn]Dominy and Lucas 2004. [oo]Watts 1984. [pp]Tan *et al.* submitted. [qq]Whiten *et al.* 1987. [rr]Duc *et al.*

Table 2.2. The relationship between FMPs and dietary categories using Kruskal-Wallis rank sum tests, where dietary categories are the independent variables and FMPs are the dependent variables. The simple diet classification included four categories (folivore, frugivore, insectivore, and gummivore); the specific classification included seven (folivore, frugivore, insectivore, gummivore, frugivore-folivore, frugivore-gummivore, and frugivore-insectivore).

Dependent variable	**Independent variable**	χ^2	**df**	***p***
WeightedR	specific diet category	6.75	5	0.239
WeightedR	simple diet category	3.86	3	0.277
MedianR	specific diet category	4.5	5	0.479
MedianR	simple diet category	3.49	3	0.321
MaximumR	specific diet category	0.86	5	0.973
MaximumR	simple diet category	1.25	3	0.742
WeightedE	specific diet category	3.66	5	0.596
WeightedE	simple diet category	2.82	3	0.421
MedianE	specific diet category	4.53	5	0.476
MedianE	simple diet category	3.69	3	0.297
MaximumE	specific diet category	3.62	5	0.605
MaximumE	simple diet category	2.48	3	0.479

Table 2.3. The relationship between dietary quality and FMPs using PGLS, where dietary quality is the independent variable. $\lambda = 0$ for all results. After Bonferroni-Holm corrections, no results are significant.

Dependent variable	***F***	**df**	**slope**	**Adjusted R^2**	***p***
WeightedR	1.12	29	-0.002	0.004	0.298
MedianR	0.07	29	-0.001	-0.032	0.788
MaximumR	0.13	29	-0.001	-0.029	0.721
WeightedE	2.85	19	-0.007	0.084	0.108
MedianE	2.27	19	-0.007	0.059	0.149
MaximumE	4.57	19	-0.009	0.152	0.046

Table 2.4. The relationship between FMPs and categories of food items using a Wilcoxon rank sum test for post-hoc analysis of a Kruskal-Wallis rank sum test, where food items are the independent variables and FMPs are the dependent variables. Significant results are highlighted in bold. Results of Kruskal-Wallis tests were significant for both toughness ($\chi^2 = 122.48$, $p < 0.001$) and Young's modulus ($\chi^2 = 66.59$, $p < 0.001$), and for toughness by maturity level ($\chi^2 = 17.8$, $p < 0.001$).

A. Toughness.

	bark	flower	fruit	leaf	seed	stem
bamboo	0.223	**<0.0001**	**<0.0001**	**<0.0001**	**<0.0001**	**0.005**
bark		**<0.0001**	**<0.0001**	**<0.0001**	**0.002**	0.486
flower			**0.031**	**0.005**	0.095	**<0.001**
fruit				1[1]	1	**0.049**
leaf					1	0.068
seed						1

B. Young's modulus.

	fruit	seed
bamboo	**<0.0001**	**<0.0001**
fruit		**<0.01**

C. Toughness by maturity level.

	unripe fruit	ripe fruit	mature leaf
young leaf	0.086	1	0.061
unripe fruit		**0.023**	1
ripe fruit			**0.003**

[1]Exact *p*-value cannot be computed for ties.

Table 2.5. The relationship between body mass and measures of food mechanical properties using PGLS analyses, with body mass as the independent variable. Significant results after performing a Bonferroni-Holm correction for multiple comparisons are indicated in bold. $\lambda = 0$ for all results.

Dependent variable	***F***	**df**	**slope**	**Adjusted R^2**	***p***
WeightedR	1.76	1, 29	-0.13	0.025	0.195
MedianR	4.73	1, 29	-0.209	0.11	0.038
MaximumR	<0.01	1, 29	-0.002	-0.034	0.989
WeightedE	22.94	1, 19	-0.572	0.523	**0.0001**
MedianE	28.12	1, 19	-0.645	0.576	**<0.0001**
MaximumE	10.75	1, 19	-0.48	0.327	**0.004**

Table 2.6. PGLS results for models where feeding time is the dependent variable and body mass and different food material properties are the independent variables. Models including interactions were run first; if the interaction term did not trend toward significance ($0.05 < p < 0.1$), the result without the interaction is presented.

A. Feeding time vs body mass and *WeightedR*, no interaction (F(2,28) = 5.57, λ = 0.242, R^2 = 0.23, ***p* = 0.009**)			
Independent variable	*t*	slope	*p*
body mass	2.66	0.09	**0.013**
WeightedR	2.62	0.162	**0.014**

B. Feeding time vs body mass and *MedianR* (F(3,27) = 3.51, λ = 0.085, R^2 = 0.2, ***p* = 0.029**)			
Independent variable	*t*	slope	*p*
body mass	2.19	0.827	**0.037**
MedianR	2.13	0.986	**0.043**
body mass * MedianR	-1.96	-0.109	0.061

C. Feeding time vs body mass and *MaximumR*, no interaction (F(2,28) = 4.96, λ = 0, R^2 = 0.21, ***p* = 0.014**)			
Independent variable	*t*	slope	*p*
body mass	2.43	0.086	**0.022**
MaximumR	2.01	0.125	0.055
D. Feeding time vs body mass and *WeightedE* (F(3,17) = 2.09, λ = 0.12, R^2 = 0.14, *p* = 0.139)			
Independent variable	*t*	slope	*p*
body mass	2.27	0.212	**0.036**
WeightedE	1.94	0.954	0.071
body mass * WeightedE	-1.9	-0.115	0.074

E. Feeding time vs body mass and *MedianE* (F(3,17) = 2.24, λ = 0.09, R^2 = 0.16, *p* = 0.12)			
Independent variable	*t*	slope	*p*
body mass	2.29	0.195	**0.035**
MedianE	1.96	0.843	0.065
body mass * MedianE	-1.93	-0.1	0.07

F. Feeding time vs body mass and *MaximumE*, no interaction ($F(2,18) = 1.61$, $\lambda = 0.64$, $R^2 = 0.06$, $p = 0.228$)			
Independent variable	*t*	slope	*p*
body mass	1.74	0.095	0.099
MaximumE	0.71	0.048	0.488

Figure 2.1. Categorization of food items used for this study. Food items were grouped by type according to the second nested level (e.g. leaf, shoot). Sample sizes and min/max ranges for toughness (*R*) and Young's modulus (*E*) are provided in parentheses. Each sample corresponds to a specific test of a food item. In some cases, this represents an average of all food items of a particular type for a given species (e.g. the average of all tests for mature leaves eaten by *A. clamitans*) because of how data were reported. In other cases, the sample is a single measurement for a particular plant species. Items in bold are those which were analyzed for variations in FMPs (Table 4).

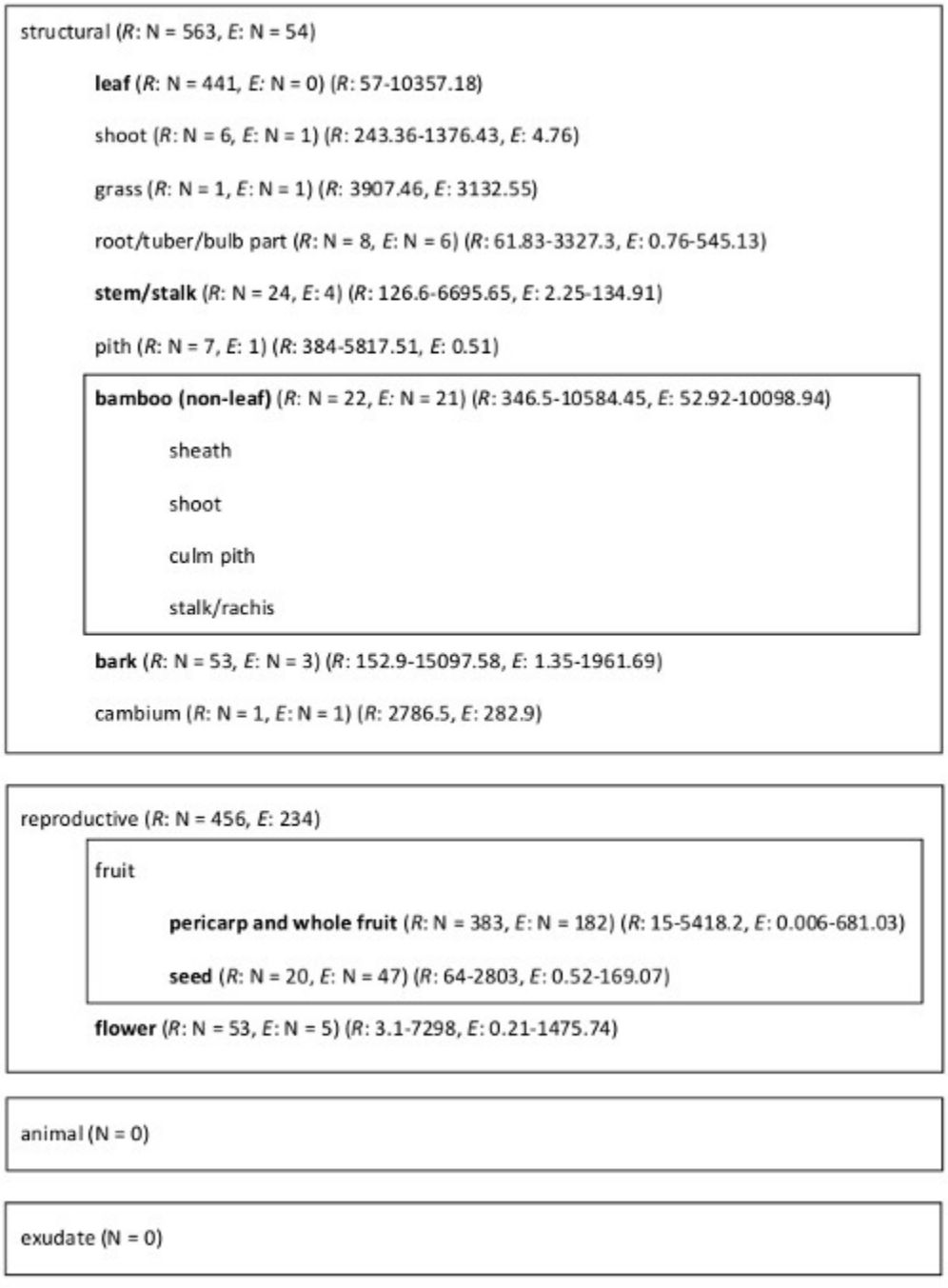

Figure 2.2. Phylogenetic tree used for PGLS. The consensus tree was taken from the 10kTrees website (Arnold et al., 2010) and pruned to fit our sample.

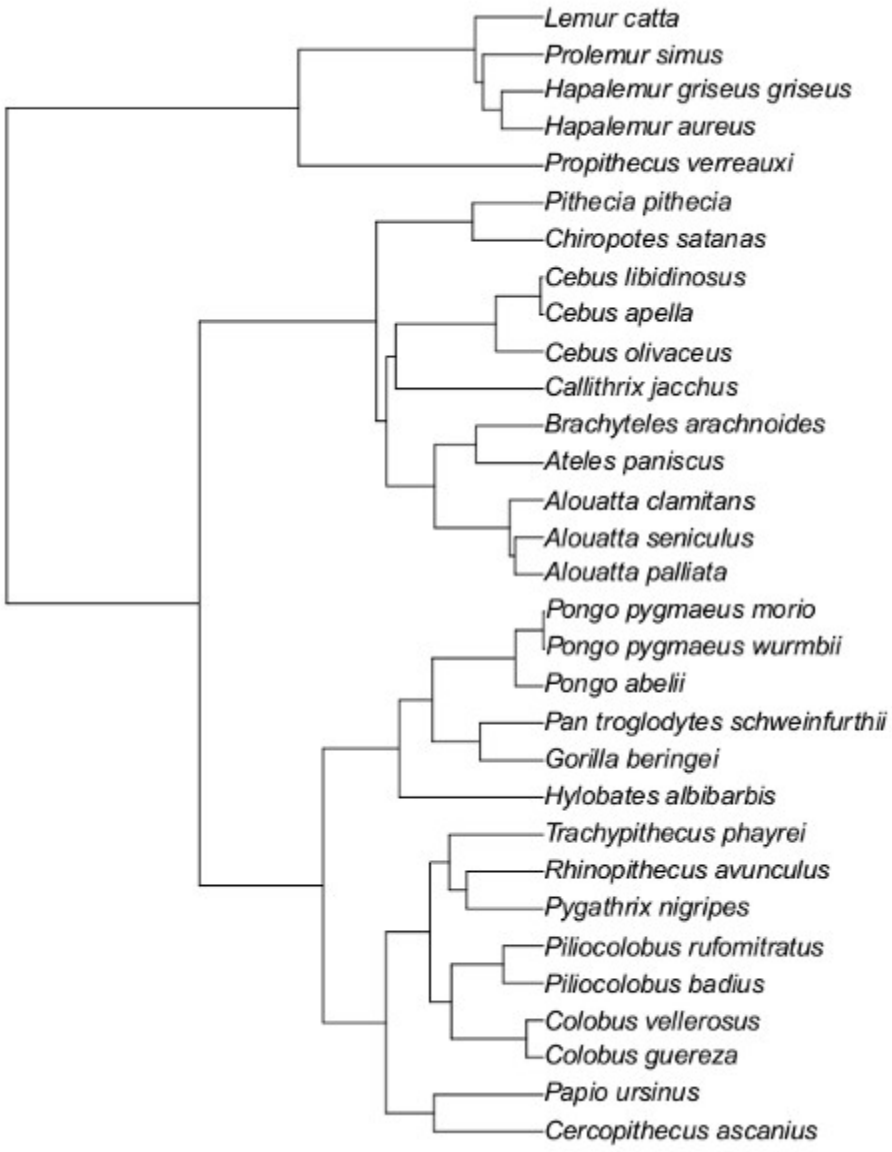

Figure 2.3. Plots by specific dietary category showing distributions of median FMPs. A is toughness and B is Young's modulus. FG = frugivore-gummivore, FI = frugivore-insectivore, FL = frugivore-folivore, FO = folivore, FR = frugivore, and G = gummivore. Species designations are listed in Table 1. No significant results were found.

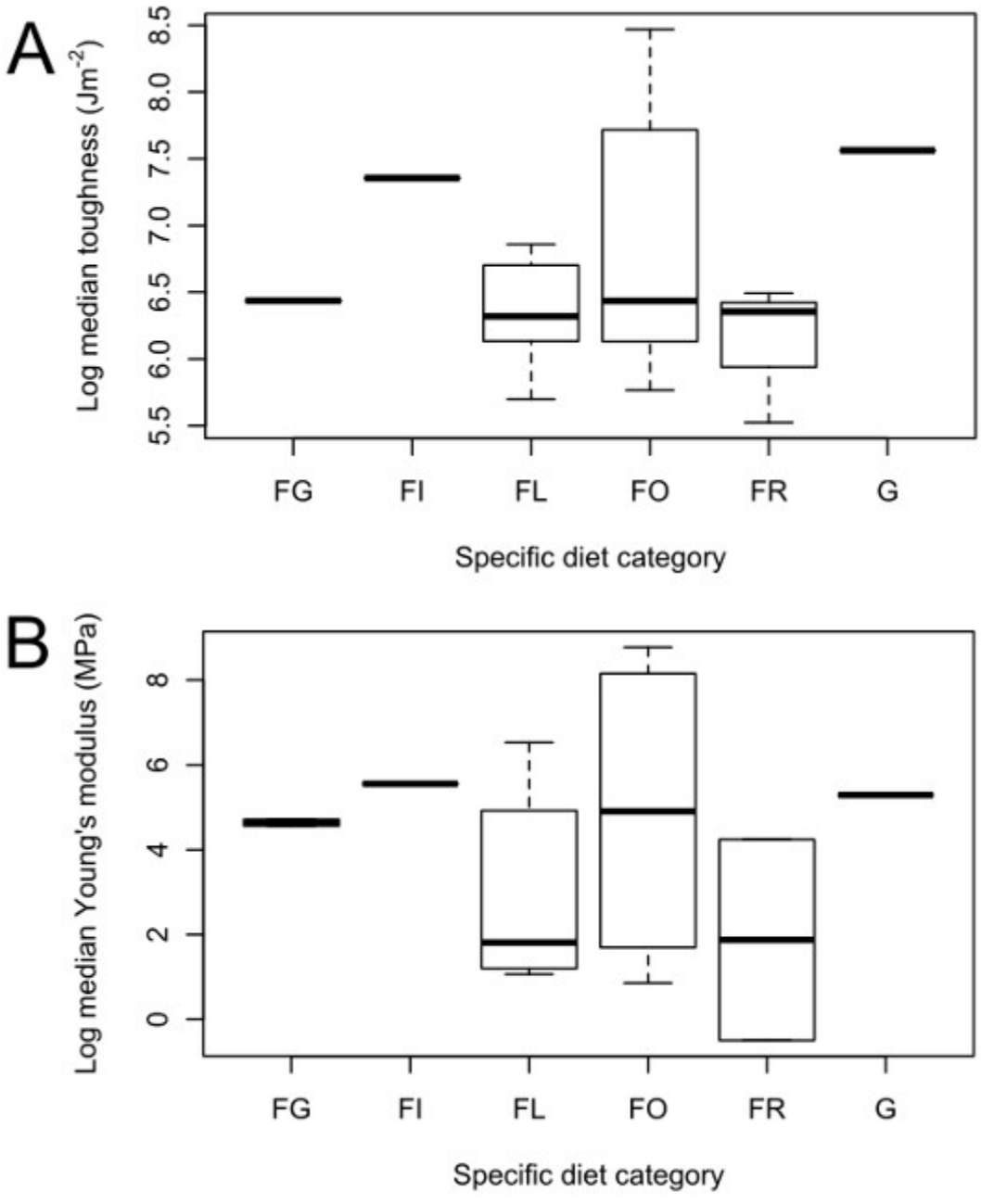

Figure 2.4. Plots by food item showing distributions of FMPs. A is toughness and B is Young's modulus. C is toughness by ripeness/maturity. FMP values are not logged, so as to demonstrate clustering of FMPs. Names of food items are different than those used elsewhere in the paper. Here, we use "bamboo" to refer to "bamboo (non-leaf)," "fruit" for "pericarp and whole fruit," and "stem" for "stem/stalk." The carrot icon in 4C provides context.

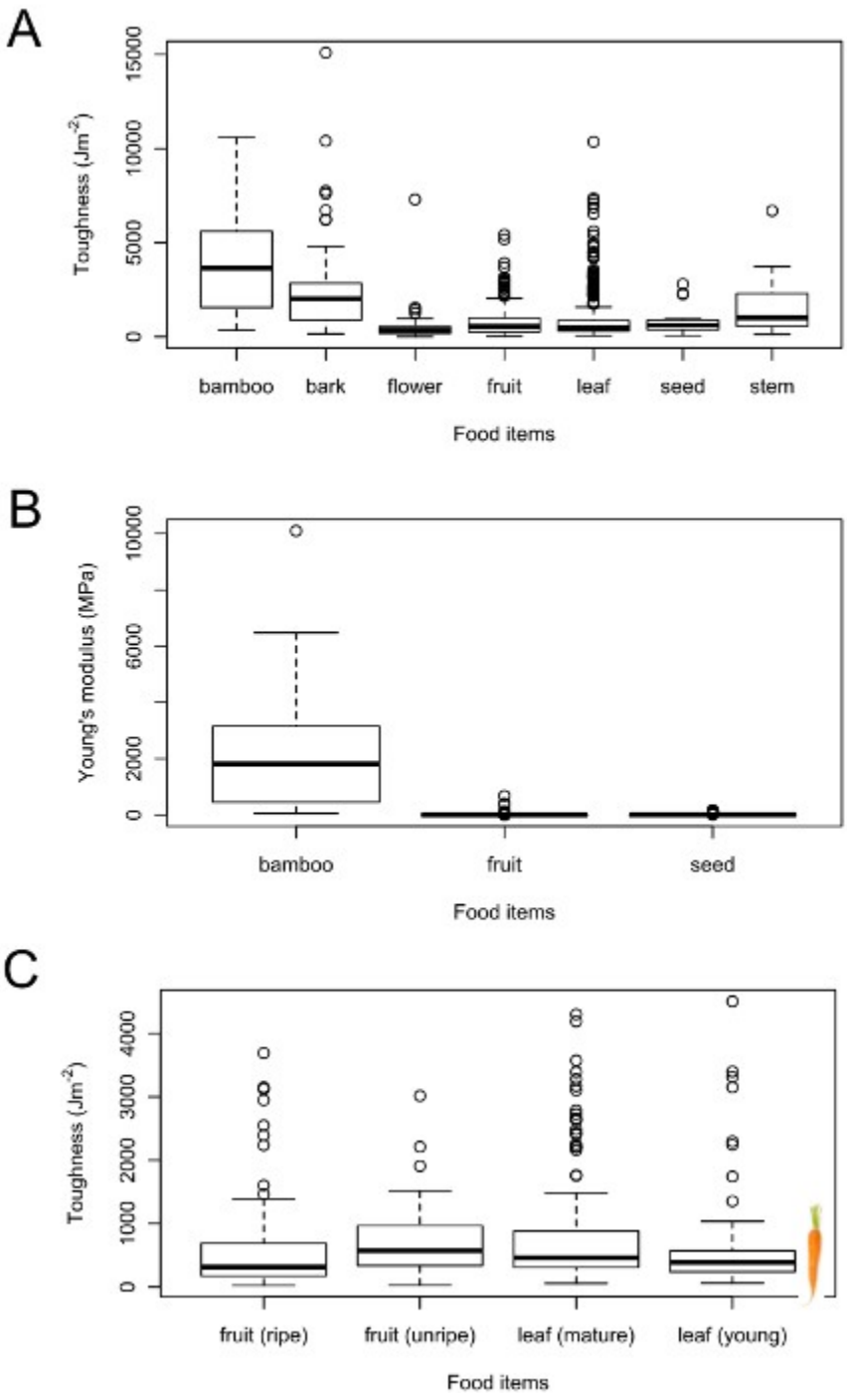

Figure 2.5. Plots of FMPs (log) against body mass (log). OLS regression lines are shown. A-C represent toughness (A: *WeightedR*, B: *MedianR*, C: *MaximumR*), and D-F represent Young's modulus (D: *WeightedE*, E: *MedianE*, F: *MaximumE*). A-C are not significant, but D-F are significant ($p < 0.01$). Data points are separated by taxon (open red triangles = hominoids, shaded teal triangles = cercopithecoids, purple squares = platyrrhines, blue circles = strepsirrhines). The carrot and almond icons are provided for context.

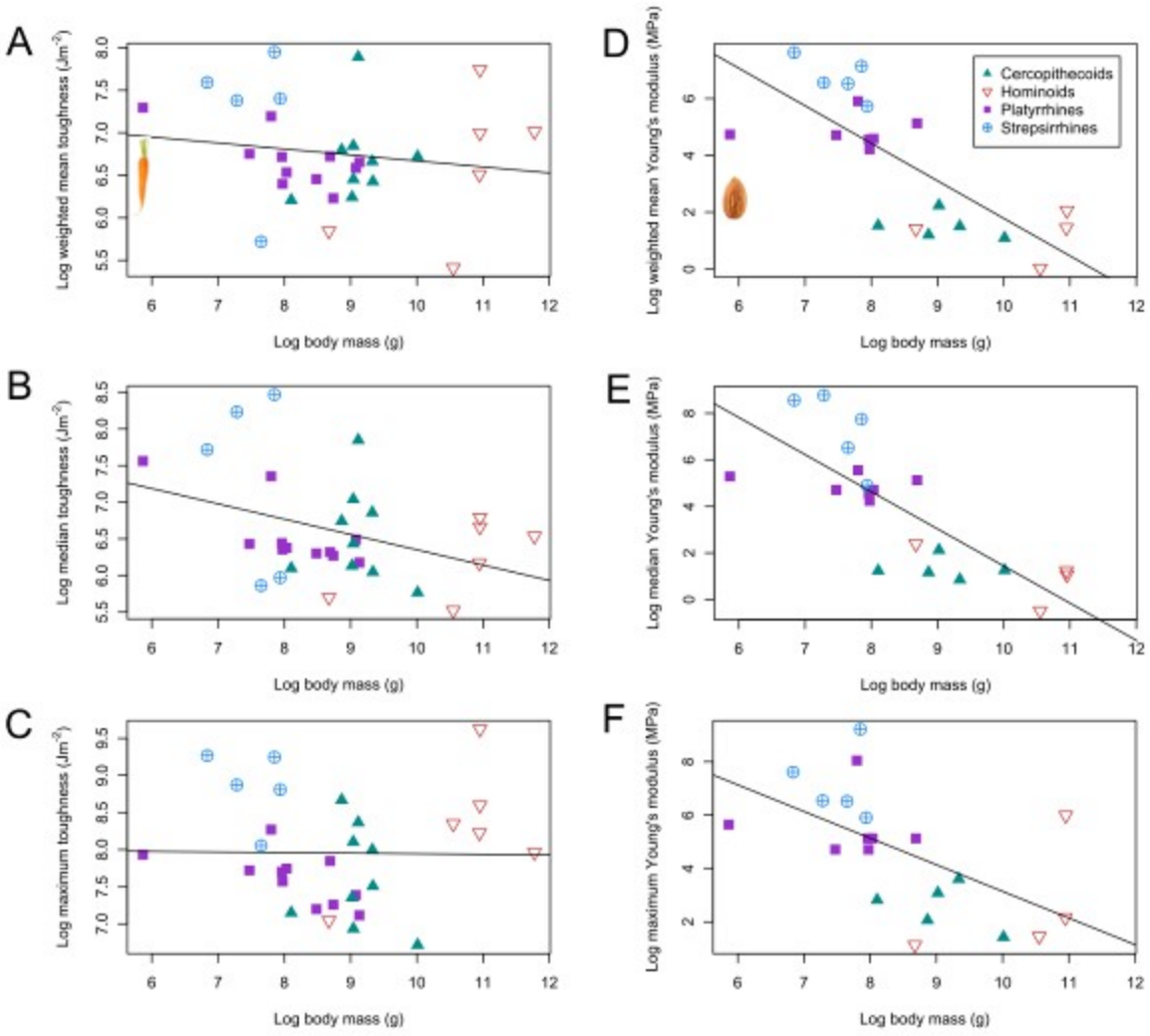

Figure 2.6. Plot of feeding time (logit) versus body mass (log). The OLS regression line is shown ($p = 0.03$, $R^2 = 0.12$) as PGLS analysis resulted in $\lambda = 0$. Data points are separated by taxon (open red triangles = hominoids, shaded teal triangles = cercopithecoids, purple squares = platyrrhines, blue circles = strepsirrhines).

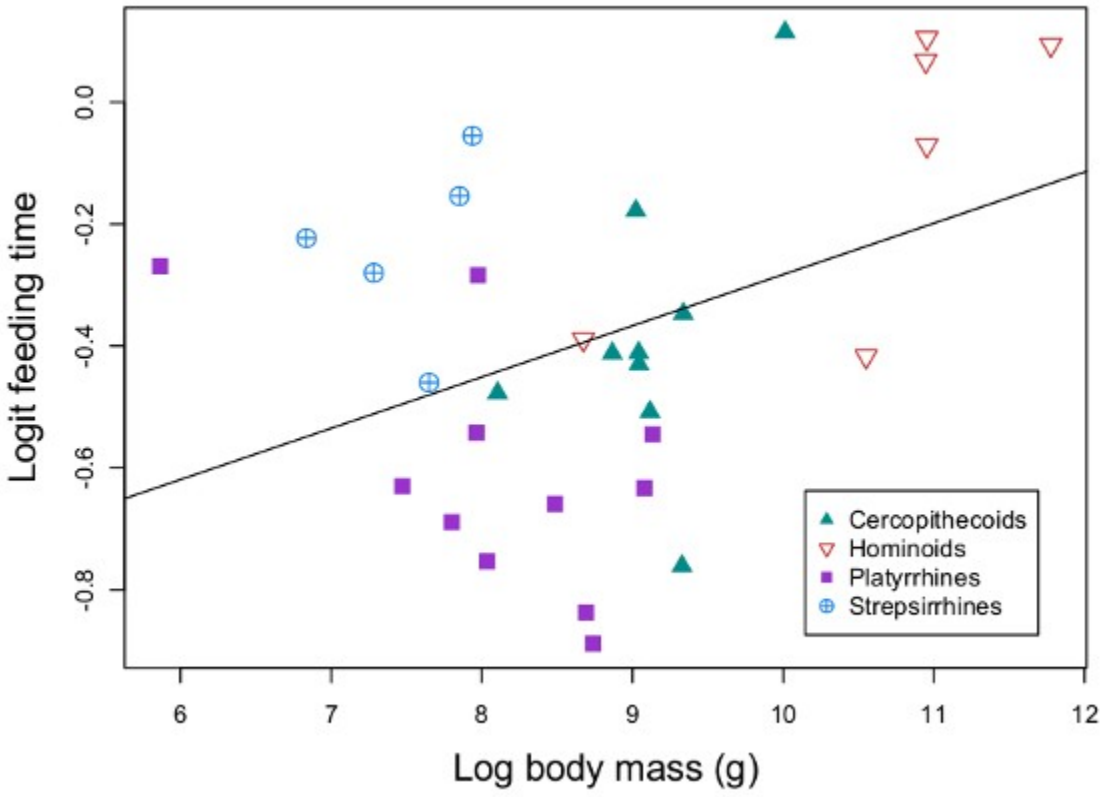

Figure 2.7. Plot of feeding time versus *WeightedR* (A) and *MedianR* (B) with trend lines representing the interaction between toughness and body mass. The area of each data point is scaled to body mass (unlogged). (Red = hominoids, green = cercopithecoids, purple = platyrrhines, blue = strepsirrhines.) The dashed trendlines correspond to the trend expected based on the PGLS model shown in Table 3 for a primate the size of the largest species (*Gorilla beringei*) in the sample (in black) and for a primate the size of the smallest species (*Callithrix jacchus*) in the sample (in grey). The solid trendlines are based on an OLS model. For A, the trendline shows an increase in feeding time as weighted mean toughness increases. For B, the trendlines describe the nature of the interaction between body mass and median toughness as correlates of feeding time. At smaller body sizes, feeding time increases as toughness increases, but at larger body sizes, the reverse is true.

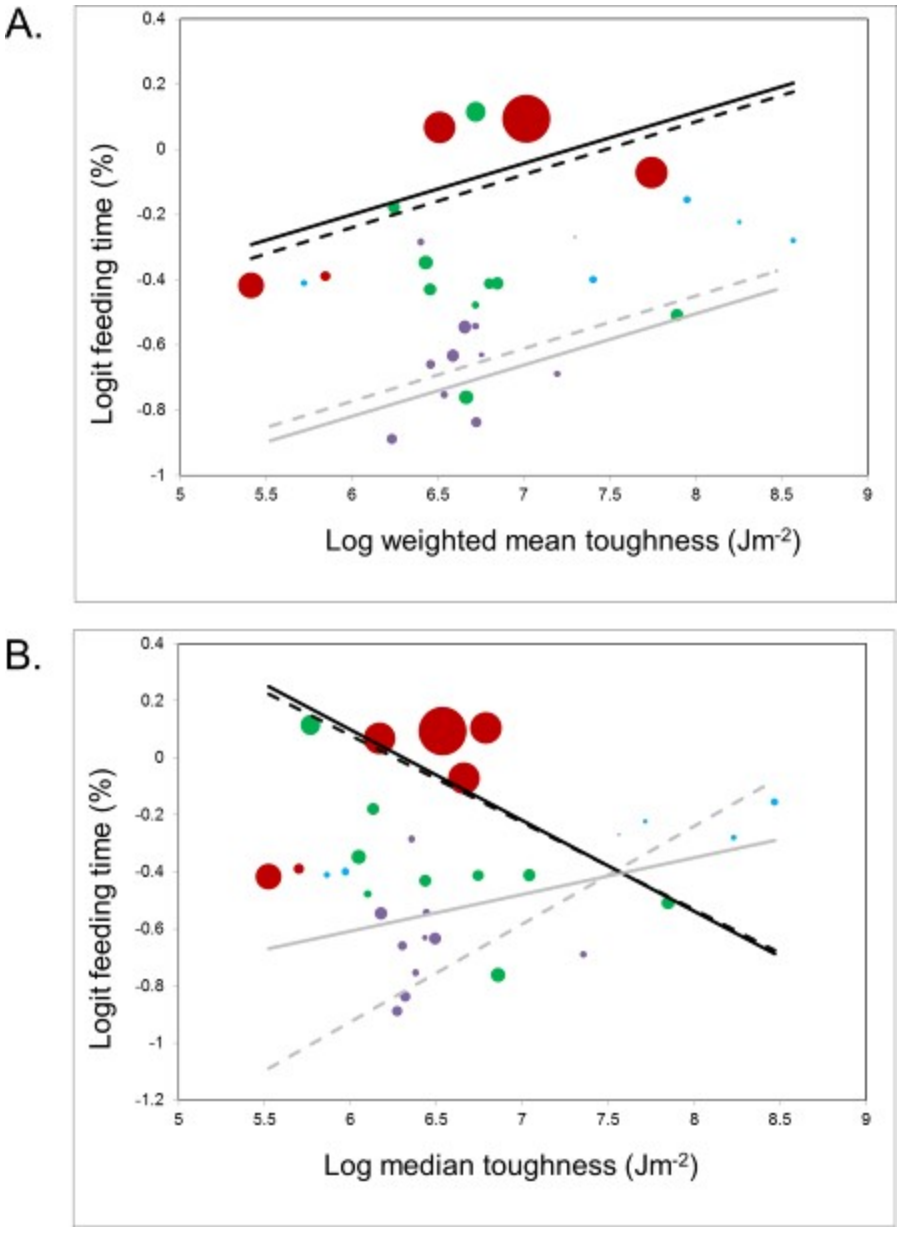

References

Agostini, I., Holzmann, I., Di Bitetti, M.S., 2010. Are howler monkey species ecologically equivalent?
Trophic niche overlap in syntopic *Alouatta guariba clamitans* and *Alouatta caraya*. Am. J. Primatol. 72, 173–86.

Agrawal, K.R., Lucas, P.W., 2003. The mechanics of the first bite. Proc. R. Soc. Lond. [Biol]. 270, 1277–1282.

Agrawal, K.R., Lucas, P.W., Bruce, I.C., Prinz, J., 1998. Food properties that influence neuromuscular activity during human mastication. J. Dent. Res. 77, 1931–1938.

Agrawal, K.R., Lucas, P.W., Bruce, I.C., 2000. The effects of food fragmentation index on mandibular closing angle in human mastication. Arch. Oral. Biol. 45, 577–584.

Agrawal, K.R., Lucas, P.W., Prinz, J., Bruce, I.C., 1997. Mechanical properties of foods responsible for resisting food breakdown in the human mouth. Arch. Oral. Biol. 42, 1–9.

Aiello, L.C., Dunbar, R., 1993. Neocortex size, group size, and the evolution of language. Curr. Anthropol. 34, 184–193.

Anapol, F., Lee, S., 1994. Morphological adaptation to diet in platyrrhine primates. Am. J. Phys. Anthropol. 94, 239–261.

Araujo, A., Arruda, M.F., Alencar, A.I., Albuquerque, F., Nascimento, M.C., Yamamoto, M.E., 2000. Body weight of wild and captive common marmosets (*Callithrix jacchus*). Int. J. Primatol. 21, 317–324.

Arnold, C., Matthews, L.J., Nunn, C.L., 2010. The 10kTrees website: A new online resource for primate phylogeny. Evol. Anthropol. 19, 114–118.

Bell, R., 1971. A grazing ecosystem in the Serengeti. Sci. Am. 225, 86–93.

Bouvier, M., 1986a. A biomechanical analysis of mandibular scaling in Old World monkeys. Am. J. Phys. Anthropol. 69, 473–482.

Bouvier, M., 1986b. Biomechanical scaling of mandibular dimensions in New World Monkeys. Int. J. Primatol. 7, 551–567.

Boyle, S.A., Smith, A.T., 2010. Behavioral modifications in northern bearded saki monkeys (*Chiropotes satanas chiropotes*) in forest fragments of central Amazonia. Primates. 51, 43–51.

Chagas, J.A.B., Oleskovicz, N., Moraes, A.N. De, Flôres, F.N., Corrêa, A.L., Souza Júnior, J.C., Soares, A.V., Costa, Á., 2010. Associação de cetamina S(+) e midazolam pelo método convencional de cálculo e pela extrapolação alométrica em bugios-ruivo (*Alouatta guariba clamitans*): resposta clínica e cardiorrespiratória. Ciênc. Rural. 40, 109–114.

Chalk, J., Wright, B.W., Lucas, P.W., Schuhmacher, K.D., Vogel, E.R., Fragaszy, D., Visalberghi, E., Izar, P., and Richmond, B.G., in review. Age-related variation in the mechanical properties of foods processed by *Sapajus libidinosus*. Am. J. Phys. Anthropol.

Chapman, C.A., 1987. Flexibility in diets of three species of Costa Rican primates. Folia Primatol. 49, 90–105.

Chapman, C.A., Chapman, L.J., Rode, K.D., Hauck, E.M., McDowell, L.R., 2003. Variation in the nutritional value of primate foods: Among trees, time periods, and areas. Int. J. Primatol. 24, 317–333.

Cheyne, S., 2010. Behavioural ecology of gibbons (*Hylobates albibarbis*) in a degraded peat-swamp forest. In: Gursky-Doyen, S., Supriatna, J. (Eds.), Indonesian Primates. Springer, New York, pp. 121–156.

Chiarello, A., 1993. Activity pattern of the brown howler monkey *Alouatta fusca*, Geoffroy 1812, in a forest fragment of southeastern Brazil. Primates. 34, 289–293.

Choong, M., Lucas, P.W., Ong, J., Pereira, B., Tan, H., Turner, I.M., 1992. Leaf fracture toughness and sclerophylly: Their correlations and ecological implications. New Phytol. 121, 597–610.

Clutton-Brock, T., Harvey, P., 1977. Species differences in feeding and ranging behavior in primates. In: Clutton-Brock, T. (Ed.), Primate Ecology: Studies of Feeding and Ranging Behavior in Lemurs, Monkeys and Apes. Academic Press, London, pp. 557–584.

Constantino, P.J., Lucas, P.W., Lee, J.J.-W., Lawn, B.R., George, T., 2009. The influence of fallback foods on great ape tooth enamel. Am. J. Phys. Anthropol. 140, 653–60.

Correa, H., Coutinho, P.E.G., Ferrari, S.F., 2000. Between-year differences in the feeding ecology of highland marmosets (*Callithrix aurita* and *Callithrix flaviceps*) in south-eastern Brazil. J. Zool. 252, 421–427.

Daegling, D.J., 1989. Biomechanics of cross-sectional size and shape in the hominoid mandibular corpus. Am. J. Phys. Anthropol. 80, 91–106.

Daegling, D.J., 1992. Mandibular morphology and diet in the genus *Cebus*. Int. J. Primatol. 13, 545–570.

Daegling, D.J., McGraw, W.S., 2007. Functional morphology of the mangabey mandibular corpus: Relationship to dietary specializations and feeding behavior. Am. J. Phys. Anthropol. 134, 50-62.

Daegling, D.J., McGraw, W.S., Ungar, P.S., Pampush, J.D., Vick, A.E., Anderson, E., Bitty, E.A., 2011. Hard-object feeding in sooty mangabeys (*Cercocebus atys*) and interpretation of early hominin feeding ecology. PloS one. 6, e23095.

Darvell, B.W., Lee, P.K.D., Yuen, T.D.B., Lucas, P.W., 1996. A portable fracture toughness tester for biological materials. Meas. Sci. Technol. 7, 954–962.

Decker, B., 1994. Effects of habitat disturbance on the behavioral ecology and demographics of the Tana River red colobus (*Colobus badius rufomitratus*). Int. J. Primatol. 15, 703–737.

Demes, B., Creel, N., 1988. Bite force, diet, and cranial morphology of fossil hominids. J. Hum. Evol. 17, 657–670.

Digby, L., Ferrari, S., Saltzman, W., 2006. Callitrichines: The role of competition in cooperatively breeding species. In: Campbell, C., Fuentes, A., Mackinnon, K., Panger, M., Bearder, S. (Eds.), Primates in Perspective. Oxford University Press, Oxford, pp. 85–106.

Dominy, N.J., Lucas, P.W., 2004. Significance of color, calories, and climate to the visual ecology of catarrhines. Am. J. Primatol. 62, 189–207.

Dominy, N.J., Vogel, E.R., Yeakel, J.D., Constantino, P.J., Lucas, P.W., 2008. Mechanical properties of plant underground storage organs and implications for dietary models of early hominins. Evol. Biol. 35, 159–175.

Duc, H.M., Baxter, G.S., Page, M.J., 2009. Diet of *Pygathrix nigripes* in Southern Vietnam. Int. J. Primatol. 30, 15–28.

Dunbar, R., 1992. Time: A hidden constraint on the behavioural ecology of baboons.

Behav. Ecol. Sociobiol. 31, 35–49.
Elgar, M., Harvey, P., 1987. Basal metabolic rates in mammals: Allometry, phylogeny and ecology. Funct. Ecol. 1, 25–36.
Elgart-Berry, A., 2000. The Relationship of Fracture Toughness of Plants to the Morphology and Durability of Gorilla (Gorilla Gorilla) Mandibles and Teeth. Ph.D. Dissertation, Cornell University.
Ford, S., Davis, L., 1992. Systematics and body size: implications for feeding adaptations in New World monkeys. Am. J. Phys. Anthropol. 88, 415–468.
Fragaszy, D., Izar, P., Visalberghi, E., Ottoni, E.B., de Oliveira, M.G., 2004. Wild capuchin monkeys (*Cebus libidinosus*) use anvils and stone pounding tools. Am. J. Primatol. 366, 359–366.
Gaulin, S.J., 1979. A Jarman/Bell model of primate feeding niches. Hum. Ecol. 7, 1–20.
Gaulin, S.J., Gaulin, C.K., 1982. Behavioral ecology of *Alouatta seniculus* in Andean cloud forest. Int. J. Primatol. 3, 1–32.
Gordon, J., 1978. Structures, or, Why Things Don't Fall Down. Penguin, London.
Gould, L., Sussman, R.W., Sauther, M.L., 2003. Demographic and life-history patterns in a population of ring-tailed lemurs (*Lemur catta*) at Beza Mahafaly Reserve, Madagascar: A 15-year perspective. Am. J. Phys. Anthropol. 120, 182–94.
Greaves, W., 1978. The jaw lever system in ungulates: A new model. J. Zool. 184, 271–285.
Greaves, W., 1988. The maximum average bite force for a given jaw length. J. Zool. 214, 295–306.
Gursky, S., 2000. Effect of seasonality on the behavior of an insectivorous primate, *Tarsius spectrum*. Int. J. Primatol. 21, 477–495.
Hai, T.D., 2007. Behavioural ecology and conservation of *Rhinopithecus avunculus* in Vietnam. The Australian National University.
Harcourt, A.H., Stewart, K.J., 1978. Coprophagy by wild mountain gorillas. Afr. J. Ecol. 16, 223-225.
Hill, D.A., Lucas, P.W., 1996. Toughness and fiber content of major leaf foods of Japanese macaques (*Macaca fuscata yakui*) in Yakushima. Am. J. Primatol. 38, 221–231.
Holm, S., 1979. A simple sequentially rejective multiple test procedure. Scand. J. Stat. 6, 65–70.
Huang, Z., Huo, S., Yang, S., Cui, L., Xiao, W. 2010. Leaf choice in black-and-white snub-nosed monkeys *Rhinopithecus bieti* is related to the physical and chemical properties of leaves. Curr. Zool. 56, 643-649.
Hylander, W.L., 1975. Incisor size and diet in anthropoids with special reference to Cercopithecidae. Science. 189, 1095–1098.
Hylander, W.L., 1979a. An experimental analysis of temporomandibular joint reaction force in macaques. Am. J. Phys. Anthropol. 51, 433–456.
Hylander, W.L., 1979b. The functional significance of primate mandibular form. J. Morphol. 160, 223–239.Am. J. Phys. Anthropol
Izar, P., Verderane, M.P., Peternelli-Dos-Santos, L., Mendonça-Furtado, O., Presotto, A., Tokuda, M., Visalberghi, E., Fragaszy, D., 2012. Flexible and conservative features of social systems in tufted capuchin monkeys: comparing the socioecology of *Sapajus libidinosus* and *Sapajus nigritus*. Am. J. Primatol. 74, 315–331.

Jaeggi, A., Van Schaik, C., 2011. The evolution of food sharing in primates. Behav. Ecol. Sociobiol. 65, 2125-2140.
Janson, C.H., 1988. Food competition in brown capuchin monkeys (*Cebus apella*): Quantitative effects of group size and tree productivity. Behaviour. 105, 53-76.
Jarman, P., 1974. The social organisation of antelope in relation to their ecology. Behaviour. 48, 215–267.
Jolly, A., 1985. The evolution of primate behavior. Amer. Sci. 73, 230-239.
Jolly, C.J., 1970. The seed-eaters: A new model of hominid differentiation based on a baboon analogy. Man. 5, 5–26.
Kay, R.F., 1975. The functional adaptations of primate molar teeth. Am. J. Phys. Anthropol. 43, 195–216.
Kay, R.F., 1981. The nut-crackers—A new theory of the adaptations of the Ramapithecinae. Am. J. Phys. Anthropol. 55, 141–151.
Kinzey, W., 1974. Ceboid models for the evolution of hominoid dentition. J. Hum. Evol. 3, 193–203.
Kinzey, W.G., Norconk, M.A., 1990. Hardness as a basis of fruit choice in two sympatric primates. Am. J. Phys. Anthropol. 81, 5–15.
Kleiber, M., 1947. Body size and metabolic rate. Physiol. Rev. 27.
Knogge, C., Heymann, E.W., 2003. Seed dispersal by sympatric tamarins, *Saguinus mystax* and *Saguinus fuscicollis*: Diversity and characteristics of plant species. Folia Primatol. 74, 33–47.
Koyabu, D.B., Endo, H., 2009. Craniofacial variation and dietary adaptations of African colobines. J. Hum. Evol. 56, 525-536.
Kruskal, W., Wallis, W., 1952. Use of ranks in one-criterion variance analysis. JASA. 47, 583–621.
Laden, G., Wrangham, R.W., 2005. The rise of the hominids as an adaptive shift in fallback foods: Plant underground storage organs (USOs) and australopith origins. J. Hum. Evol. 49, 482–98.
Lambert, J.E., 1998. Primate digestion: Interactions among anatomy, physiology, and feeding ecology. Evol. Anthropol. 7, 8–20.
Lambert, J.E., Chapman, C.A., Wrangham, R.W., Conklin-Brittain, N.L., 2004. Hardness of cercopithecine foods: Implications for the critical function of enamel thickness in exploiting fallback foods. Am. J. Phys. Anthropol. 125, 363–368.
Le, Q.K., Nguyen, D.A., Vu, T.A., Wright, B.W., Covert, H.H., 2007. Diet of the Tonkin snub-nosed monkey (*Rhinopithecus avunculus*) in the Khau Ca area, Ha Giang Province, Northeastern Vietnam. Vietnamese Journal of Primatology. 1, 75–83.
Lucas, P., Corlett, R., Luke, D., 1986. Postcanine tooth size and diet in anthropoid primates. Z. Morphol. Anthropol. 76, 253–276.
Lucas, P.W., 2004. Dental Functional Morphology: How Teeth Work. Cambridge University Press, Cambridge.
Lucas, P.W., Beta, T., Darvell, B.W., Dominy, N.J., Essackjee, H.C., Lee, P.K.D., Osorio, D., Ramsden, L., Yamashita, N., Yuen, T.D., 2001. Field kit to characterize physical, chemical and spatial aspects of potential primate foods. Folia Primatol. 72, 11–25.
Lucas, P.W., Copes, L., Constantino, P.J., Vogel, E.R., Chalk, J., Talebi, M.G., Landis, M., Wagner, M., 2011. Measuring the toughness of primate foods and its ecological value. Int. J. Primatol. 33, 598–610.

Lucas, P.W., Corlett, R., Luke, D., 1985. Plio-Pleistocene hominid diets: An approach combining masticatory and ecological analysis. J. Hum. Evol. 14, 187–202.
Lucas, P.W., Lowreytt, T.K., Pereira, B.P., Sarafjsw, V., 1991. The ecology of *Mezzettia leptopoda* (Hk. f. et Thoms.) Oliv. (Annonaceae) seeds as viewed from a mechanical perspective. Funct. Ecol. 5, 545–553.
Lucas, P.W., Pereira, B., 1990. Estimation of the fracture toughness of leaves. Funct. Ecol. 4, 819–822.
Lucas, P.W., Prinz, J., Agrawal, K.R., Bruce, I., 2002. Food physics and oral physiology. Food Qual. Prefer. 13, 203–213.
Lucas, P.W., Turner, I.M., Dominy, N.J., Yamashita, N., 2000. Mechanical defences to herbivory. Annal. Bot. 86, 913–920.
Lynch Alfaro, J.W., Boubli, J.P., Olson, L.E., Di Fiore, A., Wilson, B., Gutiérrez-Espeleta, G. a., Chiou, K.L., Schulte, M., Neitzel, S., Ross, V., Schwochow, D., Nguyen, M.T.T., Farias, I., Janson, C.H., Alfaro, M.E., 2012. Explosive Pleistocene range expansion leads to widespread Amazonian sympatry between robust and gracile capuchin monkeys. J. Biogeogr. 39, 272–288.
Mahaney, W.C., Watts, D.P., Hancock, R.G.V., 1990. Geophagia by mountain gorillas (*Gorilla gorilla beringei*) in the Virunga Mountains. Rwanda Primates. 31, 113-120.
Maisels, F., Gautier-Hion, A., Gautier, J., 1994. Diets of two sympatric colobines in Zaire: More evidence on seed-eating in forests on poor soils. Int. J. Primatol. 15, 681–701.
Marsh, C., 1981. Time budget of Tana River red colobus. Folia Primatol. 35, 30–50.
Marshall, A.J., Wrangham, R.W., 2007. Evolutionary consequences of fallback foods. Int. J. Primatol. 28, 1219–1235.
McNab, B.K., 2008. An analysis of the factors that influence the level and scaling of mammalian BMR. Comp. Biochem. Phys. A. 151, 5–28.
Milton, K., 1981. Food choice and digestive strategies of two sympatric primate species. Am. Nat. 117, 496–505.
Milton, K., 1984. The role of food-processing factors in primate food choice. In: Rodman, P., Cant, J. (Eds.), Adaptations for Foraging in Nonhuman Primates. pp. 249–279.
Milton, K., 1993. Diet and primate evolution. Sci. Am. 269, 86-93.
Milton, K., McBee, R.H., 1983. Rates of fermentative digestion in the howler monkey, *Alouatta paliatta* (Primates: Ceboidea). Comp. Biochem. Phys. 74A, 29–31.
Morrogh-Bernard, H.C., Husson, S.J., Knott, C.D., Wich, S.A., Schaik, C.P. Van, Noordwijk, M.A. Van, Lackman-ancrenaz, I., Marshall, A.J., Kuze, N., Sakong, R., 2007. Orangutan activity budgets and diet: A comparison between species, populations and habitats. In: Wich, S.A., Utami Atmoko, S.S., Mitra Setia, T., van Schaik, C.P. (Eds.), Orangutans: Geographic Variation in Behavioral Ecology and Conservation. Oxford University Press, Oxford, pp. 119–133.
Muchlinski, M.N., 2010. Ecological correlates of infraorbital foramen area in primates. Am. J. Phys. Anthropol. 141, 131–141.
Nater, A., Nietlisbach, P., Arora, N., van Schaik, C.P., van Noordwijk, M.A., Willems, E.P., Singleton, I., Wich, S.A., Goossens, B., Warren, K.S., Verschoor, E.J., Perwitasari-Farajallah, D., Pamungkas, J., Krützen, M., 2011. Sex-biased dispersal and volcanic activities shaped phylogeographic patterns of extant Orangutans

(genus: *Pongo*). Mol. Biol. Evol. 28, 2275–88.
Norconk, M.A., Wright, B.W., Conklin-Brittain, N.L. Vinyard, C.J., 2009. Mechanical and nutritional properties of food as factors in platyrrhine dietary adaptations. In: Garber, P., Estrada, A., Bicca-Marques, J., Heymann, E., Strier, K. (Eds.). South American Primates: Comparative Perspectives in the Study of Behavior, Ecology, and Conservation. Springer, New York, pp. 279-319.
Oates, J.F., Davies, A., Delson, E., 1994. The diversity of living colobines-the natural history of African colobines. In: Davies, A., Oates, J.F. (Eds.), Colobine Monkeys: Their Ecology, Behaviour, and Evolution. Cambridge University Press, Cambridge, pp. 45–75.
Organ, C., Nunn, C.L., Machanda, Z., Wrangham, R.W., 2011. Phylogenetic rate shifts in feeding time during the evolution of Homo. P. Natl. Acad. Sci. USA. 108, 14555–9.
Orme, D., Freckleton, R., Thomas, G., Petzoldt, T., Fritz, S., Isaac, N., Pearse, W., 2013. The caper package: Comparative analysis of phylogenetics and evolution in R. R package version 0.5. 1–36.
Palombit, R.R., 1997. Inter-and intraspecific variation in the diets of sympatric siamang (*Hylobates syndactylus*) and lar gibbons (*Hylobates lar*). Folia Primatol. 68, 321–337.
Paradis, E., Claude, J., Strimmer, K., 2004. APE: Analyses of Phylogenetics and Evolution in R language. Bioinformatics. 20, 289–290.
Peters, C., 1987. Nut-like oil seeds: Food for monkeys, chimpanzees, humans, and probably ape-men. Am. J. Phys. Anthropol. 73, 333–363.
Plavcan, J., van Schaik, C., 1992. Intrasexual competition and canine dimorphism in anthropoid primates. Am. J. Phys. Anthropol. 87, 461–477.
Pontzer, H., Scott, J.R., Lordkipanidze, D., Ungar, P.S., 2011. Dental microwear texture analysis and diet in the Dmanisi hominins. J. Hum. Evol. 61, 683–687.
Port-Carvalho, M., Ferrari, S., 2004. Occurrence and diet of the black bearded saki (*Chiropotes satanas satanas*) in the fragmented landscape of western Maranhão, Brazil. Neotrop. Primates. 12.
Raguet-Schofield, M., 2010. The ontogeny of feeding behavior of Nicaraguan mantled howler monkeys (*Alouatta palliata*). PhD Dissertation, University of Illinois at Urbana-Champaign.
Ratajszczak, R., Dang, N., Pham, N., 1992. A survey for Tonkin snub-nosed monkey (*Rhinopithecus avunculus*) in the North Vietnam, March 1992. FFPS, London and WWF, London.
Raubenheimer, D., Machovsky-Capuska, G.E., Chapman, C.A., Rothman, J.M., 2015. Geometry of nutrition in field studies: An illustration using wild primates. Oecologia. 177, 223-234.
Ravosa, M.J., 1996. Jaw morphology and function in living and fossil Old World monkeys. Int. J. Primatol. 17, 909–932.Folia Primatol.
Rawson, B.M., 2009. The Socio-Ecology of the Black-Shanked Douc (*Pygathrix nigripes*) in Mondulkiri Province, Cambodia. Ph.D. Dissertation, The Australian National University.
Reed, D.A., Ross, C.F., 2010. The influence of food material properties on jaw kinematics in the primate, *Cebus*. Arch. Oral. Biol. 55, 946–962.
Remis, M., 2003. Are gorillas vacuum cleaners of the forest floor? The roles of body size,

habitat, and food preferences on dietary flexibility and nutrition. In: Taylor, A.B., Goldsmith, M.L. (Eds.), Gorilla Biology: A Multidisciplinary Perspective. Cambridge University Press, Cambridge, pp. 385–404.

Richard, A.F., Dewar, R.E., Schwartz, M., Ratsirarson, J., 2006. Life in the slow lane? Demography and life histories of male and female sifaka (*Propithecus verreauxi verreauxi*). J. Zool. 256, 421–436.

Rímoli, J., Strier, K., Ferrari, S., 2008. Seasonal and longitudinal variation in the behavior of free-ranging black tufted capuchins *Cebus nigritus* (Goldfuss, 1809) in a fragment of Atlantic Forest in Southeastern Brazil. A Primatologia no Brasil. 9, 130–146.

Robinson, J.G., 1986. Seasonal variation in use of time and space by the wedge-capped capuchin monkey, *Cebus olivaceus*: implications for foraging theory. Smithsonian Institution Press, Washington, D.C.

Rodman, P., 1977. Feeding behaviour of orang-utans of the Kutai Nature Reserve, East Kalimantan. In: Clutton-Brock, T. (Ed.), Primate Ecology: Studies of Feeding and Ranging Behavior in Lemurs, Monkeys and Apes. Academic Press, London, pp. 383–413.

Rosenberger, A.L., 1992. Evolution of feeding niches in New World monkeys. Am. J. Phys. Anthropol. 88, 525–62.

Rosenberger, A.L., Kinzey, W.G., 1976. Functional patterns of molar occlusion in platyrrhine primates. Am. J. Phys. Anthropol. 45, 281–98.

Ross, C.F., Iriarte-Diaz, J., 2014. What does feeding system morphology tell us about feeding? Evol. Anthropol. 23, 105–120.

Ross, C.F., Iriarte-Diaz, J., Nunn, C.L., 2012. Innovative approaches to the relationship between diet and mandibular morphology in primates. Int. J. Primatol. 33, 632–660.

Ross, C.F., Reed, D.A., Washington, R.L., Eckhardt, A., Anapol, F., Shahnoor, N., 2009a. Scaling of chew cycle duration in primates. Am. J. Phys. Anthropol. 138, 30–44.

Ross, C.F., Washington, R.L., Eckhardt, A., Reed, D.A., Vogel, E.R., Dominy, N.J., Machanda, Z.P., 2009b. Ecological consequences of scaling of chew cycle duration and daily feeding time in primates. J. Hum. Evol. 56, 570–85.

Rothman, J.M., Raubenheimer, D., Chapman, C.A., 2011. Nutritional geometry: Gorillas prioritize non-protein energy while consuming surplus protein. Biol. Letters. 7, 1-3.

Rothman, J.M., Chapman, C.A., van Soest, P.J.P., 2012. Methods in primate nutritional ecology: A user's guide. Int. J. Primatol. 33, 542–566.

Rothman, J.M., Vogel, E.R., Blumenthal, S., 2013. Diet and nutrition. In: Sterling, E., Bynum, N., Blair, M. (Eds.), Primate Ecology and Conservation: A Handbook of Techniques. Oxford University Press, Oxford, pp. 195–212.

Rothman, J.M., 2015. Nutritional geometry provides new insights into the interaction between food quality and demography in endangered wildlife. Funct. Ecol. 29, 3-4.

Sabbatini, G., Stammati, M., Tavares, M., Visalberghi, E., 2008. Behavioral flexibility of a group of bearded capuchin monkeys (*Cebus libidinosus*) in the National Park of Brasília (Brazil): Consequences of cohabitation with visitors. Braz. J. Biol. 68, 685–693.

Sailer, L., Gaulin, S.J., Boster, J., Kurland, J., 1985. Measuring the relationship between dietary quality and body size in primates. Primates. 26, 14–27.

Scott, J.E., 2011. Folivory, frugivory, and postcanine size in the cercopithecoidea revisited. Am. J. Phys. Anthropol. 146, 20–7.

Schuelke, O., Chalise, M.K., Koenig, A., 2006. The importance of ingestion rates for estimating food quality and energy intake. Am. J. Primatol. 68, 951-965.
Silva, S.S.B., Ferrari, S.F., 2009. Behavior patterns of southern bearded sakis (*Chiropotes satanas*) in the fragmented landscape of eastern Brazilian Amazonia. Am. J. Primatol. 71, 1–7.
Silverman, N., Richmond, B.G., Wood, B.A., 2001. Testing the taxonomic integrity of *Paranthropus boisei sensu stricto*. Am. J. Phys. Anthropol. 115, 167–178.
Smith, R.J., Jungers, W.L., 1997. Body mass in comparative primatology. J. Hum. Evol. 32, 523–559.
Suarez, S.A., 2013. Diet of Phayre's leaf-monkey in the Phu Khieo Wildlife Sanctuary, Thailand. Asian Primates Journal. 3, 2–12.
Sussman, R.W., Kinzey, W.G., 1984. The ecological role of the Callitrichidae: A review. Am. J. Phys. Anthropol. 64, 419-449.
Talebi, M.G., 2005. Factors Affecting Food Choice of the Endangered Southern Muriquis (*Brachyteles arachnoides*, Primates, E. Geoffroy, 1806) in the Brazilian Atlantic Forest. Ph.D. Dissertation, University of Cambridge.
Talebi, M.G., Bastos, A., Lee, P.C., 2005. Diet of southern muriquis in continuous Brazilian Atlantic forest. Int. J. Primatol. 26, 1175–1187.
Talebi, M.G., Lee, P.C., 2010. Activity patterns of *Brachyteles arachnoides* in the largest remaining fragment of Brazilian Atlantic forest. Int. J. Primatol. 31, 571–583.
Tan, C.L., 2000. Behavior and Ecology of Three Sympatric Bamboo Lemur Species (genus *Hapalemur*) in Ranomafana National Park, Madagascar. Ph.D. Dissertation, Stony Brook: State University of New York.
Tan, C.L., Ganzhorn, J., Arrigo-Nelson, S., Eppley, T., Donati, G., Ballhorn, D., submitted. High protein or carbohydrate content in food as a possible offset for cost of cyanide detoxification in bamboo-eating gentle lemurs. Int. J. Primatol.
Tanton, M., 1962. The effect of leaf "toughness" on the feeding of larvae of the mustard beetle *Phaedon cochleariae* Fab. Entomol. Exp. Appl. 5, 74–78.
Taylor, A.B., 2002. Masticatory form and function in the African apes. Am. J. Phys. Anthropol. 117, 133-156.
Taylor, A.B., 2006. Diet and mandibular morphology in African apes. Int. J. Primatol. 27, 181–201.
Taylor, A.B., Vogel, E.R., Dominy, N.J., 2008. Food material properties and mandibular load resistance abilities in large-bodied hominoids. J. Hum. Evol. 55, 604–16.
Teaford, M.F., Lucas, P.W., Ungar, P.S., Glander, K.E., 2006. Mechanical defenses in leaves eaten by Costa Rican howling monkeys (*Alouatta palliata*). Am. J. Phys. Anthropol. 129, 99–104.
Team, R.C., 2014. R: A language and environment for statistical computing. R Foundation for Statistical Computing, Vienna.
Teichroeb, J.A., Saj, T.L., Paterson, J.D., Sicotte, P., 2003. Effect of group size on activity budgets of *Colobus vellerosus* in Ghana. Int. J. Primatol. 24, 743–758.
Terborgh, J., 1983. Five New World Primates: A Study in Comparative Ecology. Princeton University Press, Princeton, NJ.
Thompson, C.L., Donley, E.M., Stimpson, C.D., Horne, W.I., Vinyard, C.J., 2011. The influence of experimental manipulations on chewing speed during in vivo laboratory research in tufted capuchins (*Cebus apella*). Am. J. Phys. Anthropol. 145, 402–14.

Tombak, K.J., Reid, A.J., Chapman, C.A, Rothman, J.M., Johnson, C.A, Reyna-Hurtado, R., 2012. Patch depletion behavior differs between sympatric folivorous primates. Primates. 53, 57–64.

Ungar, P.S., 1995. Fruit preferences of four sympatric primate species at Ketambe, northern Sumatra, Indonesia. Int. J. Primatol. 16, 221–245.

Van Soest, P., 1994. Nutritional Ecology of the Ruminant. Cornell University Press, Ithaca.

Vié, J.C., Richard-Hansen, C., Fournier-Chambrillon, C., 2001. Abundance, use of space, and activity patterns of white-faced sakis (*Pithecia pithecia*) in French Guiana. Am. J. Primatol. 55, 203–21.

Vincent, J., 1992. Biomechanics–Materials: A Practical Approach, Oxford University Press, Oxford. Oxford University Press, Oxford.

Vinyard, C.J., Wall, C.E., Williams, S.H., Johnson, K.R., Hylander, W.L., 2006. Masseter electromyography during chewing in ring-tailed lemurs (*Lemur catta*). Am. J. Phys. Anthropol. 130, 85–95.

Vinyard, C.J., Yamashita, N., Tan, C., 2008. Linking laboratory and field approaches in studying the evolutionary physiology of biting in bamboo lemurs. Int. J. Primatol. 29, 1421–1439.

Vinyard, C.J., Glander, K.E., Teaford, M.F., Thompson, C.L., Deffenbaugh, M., Williams, S.H., 2012. Methods for studying the ecological physiology of feeding in free-ranging howlers (*Alouatta palliata*) at La Pacifica, Costa Rica. Int. J. Primatol. 33, 611-631.

Vogel, E.R., Haag, L., Mitra-Setia, T., van Schaik, C.P., Dominy, N.J., 2009. Foraging and ranging behavior during a fallback episode: *Hylobates albibarbis* and *Pongo pygmaeus wurmbii* compared. Am. J. Phys. Anthropol. 140, 716–26.

Vogel, E.R., Woerden, J.T. Van, Lucas, P.W., Utami, S.S., Schaik, C.P. Van, Dominy, N.J., van Woerden, J.T., Utami Atmoko, S.S., van Schaik, C.P., 2008. Funct. Ecol and evolution of hominoid molar enamel thickness: *Pan troglodytes schweinfurthii* and *Pongo pygmaeus wurmbii*. J. Hum. Evol. 55, 60–74.

Vogel, E.R., Zulfa, A., Hardus, M.E., Wich, S.A., Dominy, N.J., Taylor, A.B., 2014. Food mechanical properties, feeding ecology, and the mandibular morphology of wild orangutans. J. Hum. Evol.

Wallace, R.B., 2001. Diurnal activity budgets of black spider monkeys, *Ateles chamek*, in a southern Amazonian tropical forest. Neotrop. Primates. 9, 101–107.

Watts, D.P., 1984. Composition and variability of mountain gorilla diets in the central Virungas. Am. J. Primatol. 7, 323–356.

Watts, D.P., 1988. Environmental influences on mountain gorilla time budgets. Am. J. Primatol. 15, 195–211.

Whiten, A., Byrne, R., Henzi, S., 1987. The behavioral ecology of mountain baboons. Int. J. Primatol. 8, 367–388.

Wich, S.A., Fredriksson, G., Sterck, E.H.M., 2002. Measuring fruit patch size for three sympatric Indonesian primate species. Primates. 43, 19–27.

Wilcoxon, F., 1945. Individual comparisons by ranking methods. Biometrics Bull. 1, 80–83.

Williams, L., 1954. The feeding habits and food preferences of Acrididae and the factors which determine them. Trans. R. Entomol. Soc. Lond. 105, 423–454.

Williams, S.H., Wright, B.W., Truong, V., Daubert, C.R., Vinyard, C.J., 2005. Mechanical properties of foods used in experimental studies of primate masticatory function. Am. J. Primatol. 67, 329–346.

Williams, S.H., Vinyard, C.J., Glander, K.E., Deffenbaugh, M., Teaford, M.F., Thompson, C.L., 2008. Telemetry system for assessing jaw-muscle function in free-ranging primates. Int. J. Primatol. 29, 1441-1453.

Wolfpoff, M.H., 1973. Posterior tooth size, body size, and diet in South African gracile australopithecines. Am. J. Phys. Anthropol. 39, 375–394.

Wright, B.W., 2005. Craniodental biomechanics and dietary toughness in the genus *Cebus*. J. Hum. Evol. 48, 473–92.

Wright. B.W., Ulibarri, L., O'Brien, J., Sadler, B., Prodhan, R., Covert, H.H., Nadler, T., 2008. It's tough out there: Variation in the toughness of ingested leaves and feeding behavior among four Colobinae in Vietnam. Int. J. Primatol. 29, 1455-1466.

Wright, B.W., Vinyard, C.J., Yamashita, N., Vogel, E.R., 2013. Applying Extreme Value Analysis in assessing the material properties of the most challenging foods consumed by primates. Am. J. Phys. Anthropol. 150, 296.

Wright, B.W., Willis, M.S., 2012. Relationships between the diet and dentition of Asian leaf monkeys. Am. J. Phys. Anthropol. 148, 262–75.

Wroe, S., McHenry, C., Thomason, J., 2005. Bite club: Comparative bite force in big biting mammals and the prediction of predatory behaviour in fossil taxa. Proc. R. Soc. Lond. [Biol]. 272, 619–625.

Yamashita, N., 1996. Seasonally and site specificity of mechanical dietary patterns in two Malagasy lemur families (Lemuridae and Indriidae). Int. J. Primatol. 17, 355–387.

Yamashita, N., 1998. Functional dental correlates of food properties in five Malagasy lemur species. Am. J. Phys. Anthropol. 106, 169–88.

Yamashita, N., 2008. Food physical properties and their relationship to morphology: The curious case of kily. In: Vinyard, C., Ravosa, M.J., Wall, C. (Eds.), Primate Craniofacial Function and Biology. Springer US, Boston, MA, pp. 387–406.

Yamashita, N., Cuozzo, F.P., Sauther, M.L., 2012. Interpreting food processing through dietary mechanical properties: a *Lemur catta* case study. Am. J. Phys. Anthropol. 148, 205–14.

Yamashita, N., Vinyard, C.J., Tan, C.L., 2009. Food mechanical properties in three sympatric species of Hapalemur in Ranomafana National Park, Madagascar. Am. J. Phys. Anthropol. 139, 368–81.

Chapter 3. Trabecular orientation in the mandibular condyle is associated with dietary toughness.

3.1 Abstract

Past attempts to establish clear associations between mandibular morphology and different dietary categories (frugivore, folivore, insectivore) have had mixed results, likely because descriptive dietary categories are too broad and may obscure variation within primate diets. Recent emphasis on quantifying food mechanical properties (FMPs) has provided an alternative to reliance on dietary categories. I used data on FMPs to test for a relationship between dietary toughness and Young's modulus and the trabecular structure of the mandibular condyle, which is loaded during feeding and should reflect differences in masticatory strain associated with different dietary FMPs. Primate mandibles (n = 19) from 11 species were imaged using high-resolution X-ray computed tomography, and trabecular structure was analyzed with BoneJ and Quant3D to assess common three-dimensional trabecular parameters (BV/TV, Tb.Th, Tb.N, Tb.Sp, DA, E, Conn.D, SMI). Results of phylogenetic generalized least squares analysis demonstrated a strong relationship between degree of anisotropy and weighted mean and median toughness, and weaker relationships between FMPs and some other trabecular variables. Because degree of anisotropy contributes to the mechanical strength of bone, these results indicate a functional relationship between dietary toughness and trabecular orientation in the mandibular condyle.

3.2 Introduction

Several decades of research have attempted to establish a clear relationship between diet and jaw form in primates. Because the mandible is directly loaded during incision and mastication (Hylander, 1979a, 1979b, 1984, 1985; Hylander and Bays, 1979; Ross et al., 2007), the mechanical requirements of feeding should generate both bone remodeling and selective pressures on jaw and tooth morphology, and many researchers have sought to infer function from form (Robinson, 1954; Jolly, 1970; Hylander, 1979c; Kay, 1981, 1985; Demes and Creel, 1988; Verhaegen, 1992; Spencer and Demes, 1993; Daegling and Hylander, 2000; Lucas et al., 2008a; Teaford and Ungar, 2009; Strait et al., 2010; Constantino et al., 2011).

While differences in diet and dietary food mechanical properties (FMPs) are related to tooth morphology in non-human primates (Rosenberger and Kinzey, 1976; Kay, 1981; Martin, 1985; Dumont, 1995; Yamashita, 1998; Martin et al., 2003; Lucas, 2004; Olejniczak, 2006; Lucas et al., 2008b; Vogel et al., 2008; Berthaume, 2014), efforts to directly associate particular diets or loading regimes with particular aspects of mandibular morphology have been unsuccessful (Hylander, 1988; Daegling, 1993; Daegling and McGraw, 2001; Daegling et al., 2013). General trends exist among primate jaw form and dietary consistency, such that more mechanically challenging diets are associated with increased mandibular robusticity (Bouvier and Hylander, 1981; Corruccini and Beecher, 1982, 1984), but finer-grained resolution of specific dietary patterns is difficult to achieve. Relationships exist within taxa but not across all primates (Meloro et al., in press). Folivory, for example, is linked, among different species and taxonomic groups, with small condyles (Smith et al., 1983), large condyles (Taylor, 2005), wide corpora (Taylor, 2006a), and deep corpora (Bouvier, 1986a; Ravosa, 1996) of

the mandible. Moreover, these morphological traits overlap with other dietary adaptations, such that relatively large condyles are correlated with both folivory (Taylor, 2005) and durophagy (Smith et al., 1983). It is difficult, then, to argue that any one dietary niche necessitates a specific adaptive suite of jaw characteristics, or that jaw form can be used to infer details of feeding ecology. This issue is further complicated by the many factors unrelated to diet that may influence jaw morphology, such as canine size dimorphism (Lucas, 1981).

Nonetheless, FMPs likely present a selective pressure on primate dentognathic morphology. Developmental studies of primates and other mammals indicate a functional relationship between loading environment and mandibular morphology, such that more mechanically challenging diets produce larger condyles (Bouvier and Hylander, 1984; Ravosa et al., 2007, 2008), deeper mandibles (Bouvier and Hylander, 1981), broader mandibles (Corruccini and Beecher, 1982; Ravosa et al., 2007), thicker symphyseal cortical bone (Ravosa et al., 2007, 2008), and increased bone deposition and mineralization in the condyles (Dias et al., 2011). Mastication is likewise directly influenced by variations in FMPs (Thexton and Hiiemae, 1997; Agrawal et al., 1998, 2000; Chen, 2009). The lack of a consistent relationship between primate diets and mandibular morphology is therefore unexpected, and may indicate that previous studies of this relationship have failed to identify the aspect or aspects of mandibular morphology most relevant to establishing a clear link between jaw form and diet.

The internal structure of the non-human primate mandibular corpus has been extensively studied (Daegling, 1989, 1993; Daegling and Grine, 1991; Schwartz and Conroy, 1996; Vinyard and Ryan, 2006), but relatively little research has focused on the

internal structure of the mandibular condyle (Ryan et al., 2010). Trabecular bone remodels during life in response to loading (Goldstein et al., 1991; Huiskes, 2000; Ma et al., 2002; Giesen et al., 2004; Pontzer et al., 2006; Ruff et al., 2006; van der Meulen et al., 2006; Barak et al., 2011), and the temporomandibular joint is directly loaded by mastication and oral processing of food (Hylander, 1979b; Brehnan et al., 1981; Faulkner et al., 1987; Herring and Liu, 2001). Trabecular bone within the mandibular condyle may thus present epigenetic signals related to the mechanical demands of feeding.

Differences in bone volume and overall structure are key to understanding how trabecular morphology varies in accordance with mechanical usage (Giesen et al., 2001; van Eijden et al., 2006). Trabecular orientation and bone volume fraction explain the majority of variation in the mechanical properties of trabecular bone (Goldstein et al., 1993; Odgaard et al., 1997; Van Rietbergen et al., 1998; Kabel et al., 1999b; Ulrich et al., 1999; Giesen and van Eijden, 2000; Mittra et al., 2005). Measures of orientation and volume fraction are thus well-positioned to quantify morphological responses to masticatory loading.

To test the relationship between jaw form and diet, I performed the first study investigating whether the trabecular bone within the mandibular condyle reflects differences in dietary FMPs, using data on toughness and Young's modulus from wild primate populations in combination with high-resolution X-ray computed tomography (HRXCT). My goal was to quantify how trabecular architecture varies in association with common measures of the mechanical properties of food items.

Hypotheses

Trabecular responses to biomechanical loading are likely best represented by interrelationships among different measures of three-dimensional trabecular architecture (Mittra et al., 2005; Ryan and Shaw, 2012). Trabecular parameters are interdependent; an increase in bone volume fraction, for example, is associated with an increase in connectivity (Hodgskinson and Currey, 1990a, 1990b; Mittra et al., 2005). No one variable accounts for all variation in the elastic modulus of trabecular bone; while bone volume fraction and anisotropy are particularly mechanically relevant, the structure model index (Hildebrand and Rüegsegger, 1997a) is perhaps an equally useful metric in determining trabecular strength, although SMI is highly correlated with BV/TV (Mittra et al., 2005). Connectivity density (Odgaard and Gundersen, 1993) may also influence bone strength (Hodgskinson and Currey, 1990a; Goulet et al., 1994; Kabel et al., 1999a). Other, more descriptive measures, such as trabecular thickness (Hildebrand and Rüegsegger, 1997b), trabecular spacing, and trabecular number, will be quantified here as well to provide a detailed portrait of potential relationships between FMPs and trabecular structure. These latter variables contribute to (Parfitt et al., 1983) and are predicted to covary with bone volume.

Prediction 1. Trabecular bone volume fraction (BV/TV) is higher in primate species with higher values for dietary FMPs. BV/TV quantifies the percentage of the volume of interest that is composed of bone rather than air (Carter and Hayes, 1977; Parfitt et al., 1987; Fajardo et al., 2002; Ryan and Ketcham, 2002a). The need for increased resistance to loading associated with higher values for dietary FMPs should influence BV/TV, which is related to bone elastic modulus (Goldstein et al., 1993; Odgaard et al., 1997; Van

Rietbergen et al., 1998; Kabel et al., 1999b; Ulrich et al., 1999). Trabecular thickness and trabecular number should be associated with higher values for BV/TV, and higher values for trabecular spacing will be associated with lower values for BV/TV.

Prediction 2. Degree of anisotropy (DA) is higher in primate species with higher values for dietary FMPs. Anisotropy indicates trabecular orientation, which in turn is associated with mechanical stress, such that trabecular bone tends to be laid out in the primary direction of force (Galante et al., 1970; Townsend et al., 1975; Odgaard, 1997). More mechanically challenging diets should therefore require more anisotropic, ergo stronger, bone.

Prediction 3. Elongation index is higher in primate species with higher values for dietary FMPs. Like DA, elongation index quantifies the overall structure of trabecular bone.. Higher values for this variable indicate a stronger primary orientation, and lower values indicate more plate-like anisotropy.

Prediction 4. Structure model index (SMI) is lower in primate species with higher values for dietary FMPs. Like elongation index, SMI describes the overall structure of trabecular bone as either plate-like or rod-like. Higher values for SMI indicate rod-like trabeculae. Plate-like trabecular bone is associated with increased elastic modulus, and rod-like trabecular bone is commonly seen in osteoporotic humans (Hildebrand et al., 1999; Giesen et al., 2004). Because plate-like trabeculae are stronger, more mechanically challenging diets should be associated with lower values for SMI.

Prediction 5. Connectivity density (Conn.D) is higher in primate species with higher values for dietary FMPs. As connectivity may contribute to trabecular strength (Goulet et al., 1994; Kabel et al., 1999a), increased loading demands should produce increased

connectivity in the mandibular condyles.

Prediction 6. Toughness has a greater influence on trabecular structure than does Young's modulus. Toughness is associated with increased fiber content (Hill and Lucas, 1996), and fibrous foods require more oral processing (Hylander, 1979c) and/or larger masticatory forces (Hylander, 1979a). Increased toughness should thus directly contribute to strains experienced during chewing.

3.3 Materials and Methods

Sample

The sample consisted of HRXCT scans of nineteen primate mandibles from eleven species (Figure 3.1) (Table 3.1), including both males and females. All specimens were wild-shot adult individuals from the collection at the National Museum of Natural History.

HRXCT is a noninvasive imaging technique that provides internal and external views of skeletal material, and it is widely used for the study of internal bone structure in both extant and fossil skeletal specimens, particularly those too large for μCT (Daegling, 1989, 1993; Daegling and Grine, 1991; Schwartz and Conroy, 1996; Giesen and van Eijden, 2000; Ryan and Ketcham, 2002a, 2002b, 2005; van Ruijven et al., 2002; Fajardo et al., 2002, 2007; Galik et al., 2004; Mittra et al., 2005; Vinyard and Ryan, 2006; Maga et al., 2006; Ryan et al., 2010; Griffin et al., 2010; Zeininger, 2013). The procedures for analyzing scan data are well-established (Spoor et al., 1993; Odgaard, 1997; Fajardo and Müller, 2001; Ketcham and Ryan, 2004; Scherf and Tilgner, 2009), and HRXCT data are thus well-positioned for comparison with previously published results. For these reasons,

HRXCT was selected as the primary means of investigation for this study.

Food mechanical properties

Data on dietary food mechanical properties (Table 3.1) are those presented in Chapter 2. The primate species included in the sample for this paper were selected because of the availability of FMP data. While information as to the exact origin of skeletal specimens was rarely available, every effort was made to select specimens from the same country or region as the populations from which FMP data were collected.

I included measures of both toughness (*R*) and Young's modulus (*E*). Toughness, defined as the energy required to extend a crack (Gordon, 1978; Lucas and Pereira, 1990; Vincent, 1992; Lucas et al., 2000, 2011), was measured either with scissors tests or with wedge tests for thicker items. Young's modulus, or the elastic modulus, is the ratio of stress to strain, and represents an object's ability to resist deformation (Gordon, 1978; Williams et al., 2005). Young's modulus was measured either with bending or with compression tests. Data on toughness were available for all species in the sample. Data on Young's modulus were available for eight species, excluding *Alouatta palliata, Ateles paniscus,* and *Pygathrix nigripes,* for which dietary Young's modulus was not measured.

Three different estimates of toughness and Young's modulus were used for each species: median, maximum, and mean weighted by time spent feeding on different food items. These estimates are described in detail in Chapter 2.

Scanning procedures

All specimens were scanned at the High-Resolution X-ray Computed Tomography

Facility at the University of Texas at Austin (UTCT). Data were produced in the form of a series of individual image slices, each representing a cross-section through the specimen. Specimens were mounted in florist foam and scanned along the coronal plane, moving posterior from the incisors. Some specimens were scanned two at a time, with one specimen inverted and scanned in the reverse direction (i.e. posterior to anterior). These inverted specimens were digitally restored to anatomical position prior to analysis. Some specimens were scanned in a position rotated a few degrees off of center, which may have minimally influenced estimates of elongation index. All specimens were scanned with energy settings of 150kV and 0.24mA with 8000 projections. Nominal resolutions ranged from 0.0623 mm to 0.1784 mm with isotropic voxels. For each mandible, between 610 and 937 slices were collected. Image data were reconstructed as 1024 x 1024 16-bit TIFF images and were converted to 8-bit images for processing and analysis.

Image resolution and downsampling

Measurement of trabecular parameters is dependent on nominal image resolution (Majumdar et al., 1996; Müller et al., 1996; Kothari et al., 1998). The partial volume effect, in which different materials (e.g. bone and air) are imaged in the same voxel, is more likely at lower resolutions relative to the size of trabecular struts, and can skew measurements of trabecular structure. Specimens scanned at disparate resolutions are therefore not necessarily readily comparable. Because of the wide range of image resolutions included in the sample, higher-resolution images were artificially degraded (Müller et al., 1996; Kothari et al., 1998; Tabor, 2004; Sode et al., 2008) for comparison with the remainder of the specimens. It should be noted, however, that image resolution is

not solely contingent on voxel size (Bouxsein et al., 2010). True spatial resolution is also dependent on the settings and strength of the scanner. The machine at UTCT was recently upgraded (Maisano pers. comm.) and the images used in this study are consequently of a higher spatial resolution than images of comparable nominal resolution produced on the previous machine.

A three-dimensional resize operation using bilinear interpolation was performed in Matlab after image segmentation and volume of interest (VOI) selection were complete. Most specimens (n = 11) were scanned at or within six microns of 0.0993 mm. Of the remainder, three were scanned at a lower resolution (0.1784 mm). These lower-resolution mandibles represent the hominoids (*Pongo abelii* and *Pan troglodytes schweinfurthii*). Five specimens were scanned at a resolution of 0.0812mm or higher. These five specimens were artificially degraded to a nominal resolution of 0.0993 mm using a scaling factor to determine the target size for the downsampled VOI (Figure 3.2). I elected not to degrade the entire sample to 0.1784 mm (i.e. the lowest resolution present in the sample) to strike a balance between preserving image resolution and enabling valid comparisons.

Each trabecular variable was thus measured for three sub-samples of HRXCT scans. The first included all specimens in the sample at their original resolution. The second sub-sample included the artificially degraded VOIs in place of the higher-resolution original scans. The third sub-sample excluded the low-resolution hominoids. These sub-samples were used to account for potential resolution effects. If statistical analyses are consistent across all sub-samples, this indicates that resolution effects are not driving significant results. On the other hand, if artificial degradation changes the results,

nominal resolution may be responsible.

Volume of interest selection and segmentation

The left condyle of each specimen was used for analysis. Prior to analysis, all images were processed using Fiji (Schindelin et al., 2012), a version of ImageJ, to enable selection of a VOI, which is necessary for quantification of three-dimensional anisotropy variables. The VOI represents the portion of the scanned specimen that is selected for quantitative analysis (Ketcham and Ryan, 2004). Due to morphological differences between individuals and taxa, systematically choosing a VOI to apply to the entire data sample can be problematic, although doing so is necessary for accurate comparative analysis (Ryan and Ketcham, 2002a). Consequently, there is no universal process for selecting a VOI, and the parameters used vary according to the goals of each study and the limitations of the data set in question.

Two different VOIs were used for this study: one to represent the full volume of the left condyle, from which BV/TV and Conn.D were calculated, and a second cubic volume for analyses that require a symmetrical VOI. When investigating small-bodied animals with low absolute volumes of trabecular bone, utilizing the entire morphological area of interest may be necessary in order to provide enough data for analysis (Lublinsky et al., 2007). Moreover, this form of VOI selection eliminates the sampling problems that can arise when individuals in a data set show wide variation in size. Analyzing the full volume of the mandibular condyles provides the most complete understanding of the three-dimensional trabecular bone structure. However, many measures of trabecular architecture are contingent upon a symmetrical VOI due to software limitations, and the

second cubic VOI was included for this reason.

The first, *full* VOI was selected using external landmarks (Figure 3.3). The mediolateral dimension was defined by the dimensions of the condyle. Three-dimensional reconstruction of the mandibular volume was used to determine the superoinferior and anteroposterior limits of the VOI. The superoinferior dimension was defined as the full interior volume of the condyle extending down the neck of the mandibular ramus until the narrowest point of the neck of the condyle (Figure 3.3A). Using the 3D Viewer plugin (Schmid and Schindelin, 2010) for Fiji, I placed a landmark in this position. I then placed a second landmark at the anterior base of the condylar neck (Figure 3.3B). I rotated the mandible to view both points from a lateral position, and used the rectangular cropping tool to draw a straight line between the two points and crop out all bone below those points (Figure 3.3C). Thus, the base of the VOI is bounded by a (quasi-transverse) plane that runs through this line and is normal to the sagittal plane. This method of VOI selection was chosen because it allowed for consistency across specimens of varied external and internal morphology, and included the full volume of trabecular bone contained within the condyle.

The VOI for each specimen was then segmented to remove the cortical shell from the mandibular condyle (Figure 3.4). Segmentation of cortical and trabecular bone was performed using the Trainable Weka Segmentation plugin (Arganda-Carreras et al., 2011). Trainable Weka Segmentation combines machine learning algorithms with user inputs to classify pixels. The training features selected were the default Gaussian blur, Sobel filter, Hessian, difference of Gaussians, and membrane projections. I additionally selected variance, mean, minimum, maximum, and median, which produced better

results. Classifiers were trained on a stack of four or more slices taken at even intervals through the condyle. Additional slices were added as needed if segmentation proved difficult. Trabecular bone, cortical bone, and background were classified separately.

Early testing indicated that a classifier trained on one specimen often yielded poor results when applied to a different specimen, and so a separate algorithm was trained for each specimen. After training was completed, the classifier was applied to the image stack, creating a stack of segmented ternary gray-scale images. The segmented stack was then thresholded to create a mask and applied to the original images. This step removed the cortical shell and yielded the final volume of interest for analysis. I then cropped each image stack to the maximum extent of the VOI.

While the process described here has not been used for any other studies of trabecular bone structure, fully automated segmentation of cortical and trabecular bone is reported to be comparable to results from manual selection by experienced operators (Buie et al., 2007; Lublinsky et al., 2007).

The second, *cubic* VOI was selected as the largest possible cubic volume taken from within the *full* VOI. Efforts to systematically place the cubic VOI within the center of the condyle were not successful due to morphological variations in the skeletal sample. Consequently, the VOI was placed where the largest possible cube could be selected. This method inherently scaled the dimensions of the VOI to the size of the condyle, which is important as scaling prevents over-sampling from smaller specimens (Fajardo and Müller, 2001; Kivell et al., 2011; Lazenby et al., 2011). The size of the cube scaled with both mandible length (OLS $p < 0.0001$, $R^2 = 0.909$) and the external dimensions of the left condyle as measured with digital calipers (OLS $p < 0.0001$, $R^2 = 0.879$). Each VOI

was visually inspected to insure that at least five trabecular struts were present (Harrigan et al., 1988).

Trabecular bone analysis

All analyses of three-dimensional bone architecture were performed using Quant3D (Ryan and Ketcham, 2002a; Ketcham and Ryan, 2004) and the BoneJ plugin (Doube et al., 2010) for Fiji. The *full* VOI was used to measure bone volume fraction (BV/TV). All other analyses were performed using the *cubic* VOI due to software constraints. For analyses performed with Quant3D, the VOI was defined as the largest enclosed sphere within the *cubic* VOI. Spherical VOIs are less likely to exclude orthogonal features, and are preferable when available (Ketcham and Ryan, 2004). Quant3D was used to measure the degree of anisotropy (DA) and trabecular number (Tb.N). The star volume distribution (SVD) method (Cruz-Orive et al., 1992) used to calculate DA in Quant3D is generally superior to the mean intercept length (MIL) method used by BoneJ (Odgaard, 1997; Ketcham and Ryan, 2004). These parameters were calculated using 2049 uniform orientations, random rotation, and dense vectors. BoneJ was used for trabecular thickness (Tb.Th) (Hildebrand and Rüegsegger, 1997b), trabecular spacing, connectivity density (Conn.D) (Odgaard and Gundersen, 1993), and structure model index (SMI) using the technique of Hildebrand and Rüegsegger (Hildebrand and Rüegsegger, 1997a) with voxel resampling set to one voxel (Tabor, 2011). These structural parameters have been described in detail elsewhere (Parfitt et al., 1987; Odgaard, 1997; Fajardo et al., 2002; Ryan and Ketcham, 2002a; Bouxsein et al., 2010), but are briefly discussed below.

Bone volume fraction (BV/TV), or trabecular volume fraction, which is often used to

examine density, quantifies the percentage of the VOI that is composed of bone rather than air. In order to determine this measure, the number of bone voxels is divided by the total number of voxels contained within the VOI. This provides a general indication of trabecular bone volume fraction at a particular location.

Degree of anisotropy (DA) was calculated here using the star volume distribution (SVD) method. SVD operates by selecting a point within the VOI and extending lines in various directions from that point; each line stops when it encounters air rather than bone (Odgaard, 1997; Ryan and Ketcham, 2002a; Ketcham and Ryan, 2004). The longest of these lines is the intercept. The eigenvectors and eigenvalues produced by the SVD can then be used to determine the degree of anisotropy of the VOI, which is calculated by dividing the primary over the tertiary eigenvalue. A value of 1 indicates a perfectly isotropic structure, and higher values indicate great anisotropy. These eigenvalues are also used to determine the elongation index (E), which is calculated using the primary and secondary eigenvalues. A value of 0 for E indicates perfect plates, and a value of 1 indicates rod-like trabecular struts.

The structure model index (SMI) describes the relative structure of a VOI as being more plate-like or more rod-like. Perfect plates have an SMI of 0, and perfect rods have an SMI of 3 (Hildebrand and Rüegsegger, 1997a). Negative values indicate concave structures. SMI is calculated using the first derivative of the surface based on surface deformation along each face's normal path to determine shape characteristics of the structure.

Connectivity density (Conn.D) conceptualizes trabecular bone as a node-and-branch network, and quantifies the extent to which the VOI is multiply connected (Odgaard and

Gundersen, 1993). The Euler number for the VOI, representing connectivity, is divided by the total area of the VOI to calculate Conn.D.

Trabecular thickness (Tb.Th) is calculated using a sphere-fitting method that determines the diameter of the largest possible sphere that can be fitted within bone voxels in the VOI. Mean Tb.Th is the average of these measurements. Trabecular spacing (Tb.Sp) is essentially the inverse approach: it quantifies the average diameter of spheres that can be fitted within air voxels in the VOI.

Mean trabecular plate number (Tb.N) is another measure associated with quantifying bone density. Tb.N is calculated by placing a linear grid over the image and counting the number of times the grid intersects with bone. This measure is highly dependent on both resolution and appropriate thresholding, as trabecular bone cannot be measured if it cannot be detected by the software. Consequently, Tb.N is often underestimated by analyses performed using computed tomography instead of traditional bone histology (Fajardo et al., 2002), which undermines the usefulness of this measure; however, it is frequently reported in studies on trabecular bone, and as such is included here.

Prior to analysis, all VOIs were thresholded using an automated iterative algorithm (Ridler and Calvard, 1978; Trussell, 1979). Thresholding is the process of determining the boundary levels for distinguishing bone from the surrounding air or marrow, and accurate image thresholding is essential for trabecular analysis (Ding et al., 1999; Fajardo et al., 2002; Hara et al., 2002). The automated iterative algorithm is widely used, and support for this technique has been provided in detail elsewhere (Ryan and Ketcham, 2002a). The asymmetrical shape of the *full* VOIs produced difficulties with automated thresholding: the black background skewed the histogram values and generated

artificially high values for bone volume fraction (see e.g., Link et al., 2003). To solve this problem, I used the *cubic* VOI to determine the threshold histogram values for that specimen. I then opened the full VOI in Fiji and manually set the threshold using the histogram values from Quant3D. This procedure allowed me to apply a valid threshold to the asymmetrical condylar volumes which would otherwise have been difficult to accurately threshold.

Calculating BV/TV required manual correction. Both Quant3D and BoneJ require all slices in an image stack to be the same size. Because the condyle is irregularly shaped, the necessary rectangular or square volume of interest includes background pixels that should not be included in density or connectivity analyses. To solve this problem, I manually adjusted the values for BV/TV by subtracting the area of the background pixels from the total volume.

Statistical analysis

I used phylogenetic generalized least squares (PGLS) analysis (Martins and Hansen, 1997) to account for potential phylogenetic signal in my sample ($\alpha = 0.05$), using the GenBank primate consensus tree from 10kTrees (http://10ktrees.nunn-lab.org) (Arnold et al., 2010) to estimate divergence dates and phylogenetic relationships. *Cebus libidinosus* is not included in the 10kTrees database, and so I used a divergence date of 400,000 years for *C. libidinosus* and *C. apella* (Lynch Alfaro et al., 2012). Bonferroni-Holm correction for multiple comparisons (Holm, 1979) was used to control for family-wise error rate and was applied separately to models including toughness and Young's modulus. All variables were natural logged prior to analysis, and species means were used for each trabecular

variable. Because some values for SMI were negative, thus preventing log transformation, I added a constant so that the smallest value was equal to one. All analyses were performed using the R Statistical Programming Language version 3.1.0 (http://www.R-project.org). Packages APE (Paradis et al., 2004) and caper (Orme et al., 2013) were used for PGLS.

3.4 Results

Degree of anisotropy was positively related to some estimates of toughness and Young's modulus, while most other trabecular variables measured here did not have any consistent relationships with FMPs. Trabecular spacing was positively related to maximum Young's modulus in the raw sample and in the sample including artificially degraded specimens, and trabecular thickness was positively related to all estimates of Young's modulus in the sample excluding hominoids. Trabecular number was negatively related to maximum Young's modulus and to weighted mean and median toughness in the sample including artificially degraded specimens. Connectivity density was negatively related to weighted mean and median toughness in the raw sample.

Trabecular variables are presented in Tables 3.2-3.3, and results of statistical analysis are summarized in Tables 3.4-3.5.

Bone volume fraction

Neither toughness nor Young's modulus showed any relationship with BV/TV.

Trabecular thickness

Trabecular thickness was positively related to all estimates of Young's modulus in the sample excluding hominoids.

Trabecular number

In the sample including artificially degraded specimens, Tb.N was negatively related to weighted mean and median toughness (Table 3.4).

For Young's modulus, Tb.N was negatively related to maximum Young's modulus in the sample including artificially degraded specimens (Table 3.5).

Trabecular spacing

Trabecular spacing had no relationship with toughness.

In the raw sample and in the sample including artificially degraded specimens, Tb.Sp showed a positive relationship with maximum Young's modulus (Table 3.5).

Degree of anisotropy

Degree of anisotropy had a positive relationship with both weighted mean and median toughness (Figure 3.5A) (Table 3.4). However, there was no relationship with maximum toughness. Including artificially degraded specimens increased the strength of these relationships (Figure 3.5B). When hominoids were excluded from the degraded sample, these relationships strengthened further, indicating that the low-resolution hominoid specimens were not responsible for the apparent positive relationship between toughness and DA (Figure 3.5C). A strong phylogenetic signal was present in all of these results. When λ was set to 0, the relationships among DA and toughness were not as

strong in the raw (weighted mean toughness: $p = 0.020$, $R^2 = 0.479$; median toughness: $p = 0.005$, $R^2 = 0.603$) and degraded samples (weighted mean toughness: $p = 0.027$, $R^2 = 0.438$; median toughness: $p = 0.007$, $R^2 = 0.574$), and were not significant in the sample excluding hominoids.

For Young's modulus, DA was positively related to maximum Young's modulus in the raw and artificially degraded samples (Table 3.5).

Elongation index

Elongation index showed no relationship with toughness or Young's modulus.

Connectivity density

Connectivity density was negatively related to weighted mean and median toughness in the raw sample (Table 3.4).

Structure model index

Structure model index had no relationship with toughness or Young's modulus.

3.5 Discussion

Mandibular morphology, both external and internal, is likely subject to a number of evolutionary constraints. Primates use their teeth and jaws to prepare foods for ingestion (Jolly, 1970; Kinzey and Norconk, 1990; Ungar, 1994; Yamashita, 2003; Yamashita et al., 2012), to bite (Agrawal and Lucas, 2003), and to masticate (Hylander, 1979c; Kay, 1985; Ross et al., 2007). Feeding is an incredibly complex behavior; primates peel, puncture,

crack, gouge, gnaw, and wadge their foods, all of which are associated with different loading regimes, and even the placement of a food item along the tooth row alters the resultant muscle activation forces (Hylander, 1979b; Spencer, 1998). The jaw must therefore be capable of withstanding the loading forces associated with consuming foods of a variety of mechanical and geometric properties and with a number of different feeding behaviors.

In addition to these behaviors directly related to feeding, the primate masticatory apparatus is also involved in a range of behaviors unrelated to diet or mastication. These include social behaviors such as threat displays (i.e. gape) (Hylander, 1979a; Smith, 1984) and vocalizations (Riede et al., 2005; Youlatos et al., 2015), Mandibular morphology may be influenced by canine size dimorphism (Lucas, 1981), which is related to predation and male-male competition (Plavcan and van Schaik, 1992; Plavcan, 2001). The mandible is also shaped by its interface with the rest of the skull (Sakka, 1984). Much of the variation in primate jaw form thus likely represents a trade-off between the demands of feeding and the selection pressures presented by social behaviors and various aspects of craniofacial morphology.

Untangling potential relationships between jaw form and diet is consequently a tricky prospect. Previous attempts to link particular diets with specific aspects of jaw morphology (Smith, 1983; Smith et al., 1983; Bouvier, 1986a, 1986b; Daegling, 1992; Daegling and McGraw, 2001; Taylor, 2006a, 2006b) suggest either that no consistent relationship exists or that researchers have thus far focused on portions of the mandible other than those that demonstrate a dietary signal. Alternately, reliance on dietary categories rather than FMPs may have obscured a meaningful relationship.

My results suggest two principal findings: 1. FMPs influence trabecular orientation in the mandibular condyle, and 2. FMPs do not influence trabecular bone volume fraction in the mandibular condyle. The relationship between degree of anisotropy and weighted mean and median toughness may indicate a remodeling response to inter-specific variation in FMPs. Many of the trabecular parameters analyzed in this study are descriptive measures of bone architecture and only minimally contribute to the strength of trabecular bone. Bone volume fraction and anisotropy account for most of the variation in elastic modulus of trabecular bone (Goldstein et al., 1993; Odgaard et al., 1997; Van Rietbergen et al., 1998; Giesen and van Eijden, 2000), and bone density can be impacted by a number of factors other than mechanical demands (Fajardo et al., 2007), including age (Parfitt et al., 1983), hormone levels (Jerome et al., 1994), and dietary quality (Parsons et al., 1997). Anisotropy may therefore be a more accurate indicator of differences in trabecular structure associated with loading and stress. While a relationship between DA and Young's modulus is only seen in the raw sample and the sample including artificially degraded specimens, and only with the maximum estimate of Young's modulus, the relationship between DA and weighted mean and median toughness is consistent across all image samples and does not appear to be dependent image resolution.

That DA is significantly correlated with weighted mean and median but not with maximum toughness suggests that these relationships may be related to repetitive loading of the mandible during mastication. Duration of loading rather than magnitude may present an important adaptive pressure on mandibular morphology (Hylander, 1979c). Some experimental evidence suggests that tough foods necessitate longer chewing bouts

in primates and insects (Williams, 1954; Tanton, 1962; Wright et al., 2008). Average and median dietary toughness, then, may be closely related to average chewing time. If this is the case, the lack of a significant relationship between DA and maximum toughness is not surprising. The toughest foods in a primate's diet are not necessarily those eaten most frequently. The most mechanically challenging foods in a primate's diet may represent rarely consumed fallback foods, which present important adaptive pressures (Lambert et al., 2004; Marshall and Wrangham, 2007) (although some mechanically challenging food are preferentially selected for consumption, e.g. Vogel et al., 2008, 2009, 2014; Chalk, 2011; Daegling et al., 2011). Thus, estimates of average and median toughness are likely more representative of the mechanical challenges met by a primate on a daily basis than is maximum toughness, and thus more accurately represent the habitual diet.

The results of this study suggest that primate trabecular bone may respond to increases in masticatory loading (and specifically dietary toughness) primarily through increased directionality. While bone volume fraction and anisotropy together contribute to trabecular bone strength, the primate masticatory apparatus may rely on a strategy of increasing anisotropy in lieu of increasing bone volume fraction. The mandible, like other bony structures, should have evolved to resist loading forces with minimum bone, although this view of the form-function relationship may be overly simplistic (Huiskes, 2000). Increased anisotropy may thus be an adaptation for efficiency in withstanding the forces associated with mastication. Trabecular bone is not necessarily optimally designed to be both maximally strong and maximally light (Huiskes, 2000), but it must still adequately serve its function.

The strong phylogenetic signal ($\lambda = 1$) in the relationship among DA and estimates of

weighted mean and median toughness suggests that the trends seen here exist primarily within taxa (Figure 3.5), and are not necessarily patterns that are consistent across all primates. This interpretation is consistent with previous research on external jaw morphology, which has found dietary signals within but not consistently between primate taxa (Smith, 1983; Smith et al., 1983; Bouvier, 1986a, 1986b; Taylor, 2005, 2006b). At the same time, OLS analysis of the relationships among DA and toughness yields significant (albeit weaker) results in both the raw (weighted mean toughness: $p = 0.020$, $R^2 = 0.479$; median toughness: $p = 0.005$, $R^2 = 0.603$) and degraded samples (weighted mean toughness: $p = 0.027$, $R^2 = 0.438$; median toughness: $p = 0.007$, $R^2 = 0.574$), suggesting that phylogeny is important but not critical to this morphological signal.

Other variables had few relationships that were dependent on image resolution, and as such cannot be considered particularly meaningful. It may be the case that these results accurately represent the relationship between FMPs and trabecular morphology of the mandibular condyle: namely, that there is not much of a relationship. The loads experienced by the mandibular condyle during biting and chewing may not be of great enough magnitude or duration to produce a bone signal. Alternately, variation in dietary FMPs may not influence feeding in a meaningful way (Ross et al., 2009, 2012; Reed and Ross, 2010; Ross and Iriarte-Diaz, 2014). However, as stated, the strength and consistency of the relationship between DA and toughness suggests that FMPs do influence mandibular morphology and thus likely influence feeding behavior as well.

One factor that deserves further consideration is the degree to which DA is the product of epigenetic remodeling versus phylogenetic adaptation. Little is known about the ontogenetic development of this region in primates. Trabecular ontogeny has been

minimally studied, but existing data from human populations show loss of trabecular bone after birth followed by growth and remodeling with the advent of bipedal locomotion (Ryan and Krovitz, 2006; Gosman and Ketcham, 2009; Abel and Macho, 2011; Raichlen et al., 2015). Thus, both phylogeny and ontogeny likely play a role in trabecular architecture.

Caveats and limitations

Potential problems with the size and composition of the skeletal sample may have obscured a relationship between FMPs and trabecular variables other than DA. First, the mandibular specimens were not taken from the same populations for which FMPs were measured. This was a consequence of the availability of museum specimens. Because of known inter-population variability in diet and feeding behavior (Watts, 1984; Brown and Zunino, 1990; Panger et al., 2002; Russon et al., 2004; Yépez et al., 2005), the mandibles used for this study likely did not experience the exact loading demands reflected by the sampled FMPs. Given this mismatch between mandibles and FMPs, it is possible that a skeletal sample from the same populations for which FMPs were measured would yield a stronger relationship between condylar trabecular architecture and dietary FMPs. Nonetheless, my sample spanned eleven species from nine genera and five families, and I am thus confident that the observed relationships are real. Future systematic sampling of FMPs for more primate species will greatly add to these data.

Second, the nominal resolution of the scans may have played a role in the results. The resolution of the scans was lower than is typical for analyses of trabecular bone. Analysis of trabecular parameters is highly dependent on resolution; at lower resolutions,

trabecular thickness and bone volume fraction increase, and trabecular number, trabecular spacing, and degree of anisotropy decrease (Majumdar et al., 1996; Müller et al., 1996; Kothari et al., 1998; Ketcham and Gosman, 2010). However, comparison of the raw and downsampled results from a slightly larger sample (Chapter 4) than that analyzed here shows correlations between all variables other than SMI (Table 4.3).

Comparisons of μCT scanning with lower-resolution in vivo medical techniques such as magnetic resonance imaging (MRI) and peripheral quantitative computed tomography (pQCT) indicate that it is still possible to extract meaningful architectural information from low-resolution scans. Even at lower resolutions, bone volume fraction (Link et al., 2003; Varga and Zysset, 2009) and connectivity density calculated from MRI scans correlate well with values calculated from μCT images (Pothuaud et al., 2002), and at resolutions at or below 200μ, the mean error of BV/TV and Tb.N is below 10% (Kothari et al., 1998). High-resolution pQCT likewise yields strong correlations with BV/TV, Tb.N, and Tb.Th as measured from μCT scans (Laib and Rüegsegger, 1999). Directionality is also quantifiable at a range of resolutions (Majumdar et al., 1998). Anisotropy calculated using the tensor scale method, which is similar to star volume distribution, shows low variation up to at least 88μ (Saha and Wehrli, 2004). Moreover, even "gold standard" μCT does not perfectly represent the true structure of trabecular bone. Comparison with histological samples demonstrates that, while μCT is a very close approximation of trabecular morphology, error is still present even at resolutions of 14μ (Müller et al., 1998). Consequently, while the results of this study may not be readily comparable with other studies of condylar trabecular bone, the relationships between degree of anisotropy and toughness are most likely not an artifact of image resolution.

3.6 Conclusion

The results presented here suggest a strong relationship between dietary toughness and the orientation of trabecular bone within the mandibular condyle. No correlation was found between FMPs and trabecular density, nor was there any relationship between FMPs and other estimates of fabric density and orientation. These results indicate a remodeling response based on altering the orientation of trabecular struts rather than the density, which may be a more biologically efficient means of adapting to mechanical loading.

I propose two primary directions for future study. First, skeletal collections from long-term field sites with known individuals and known FMPs can be used to more precisely quantify the relationship between FMPs and trabecular morphology. A weakness of the current study is the implicit assumption that all members of a particular primate species consume foods with more or less the same mechanical properties. Examining the internal morphology of the mandibular condyle of specimens whose diets during life are a known quantity will clarify the influence of inter-population variability. Second, controlled feeding experiments in laboratory settings can allow for direct observation of the trabecular response to different diets. Experiments on rabbits demonstrate that FMPs have a strong influence on the ontogenetic development of the masticatory apparatus (Taylor et al., 2006; Ravosa et al., 2007, 2008; Scott et al., 2014); a similar response may exist in primates. If this is indeed the case, degree of anisotropy may eventually be used to infer the dietary FMPs of fossil specimens.

Acknowledgments

Dr. John Mioduszewski performed the artificial image degradation.

Table 3.1. List of specimens included in the sample and values for toughness (*R*) and Young's modulus (*E*) for each species. FMP data are taken from chapter 2.

NMNH catalog #	Species	Sex	Weighted mean *R*	Median *R*	Maximum *R*	Weighted mean *E*	Median *E*	Maximum *E*
543117	*Alouatta palliata*	M	508.481	528.867	1419.477	--	--	--
339925	*Alouatta palliata*	F	508.481	528.867	1419.477	--	--	--
398507	*Alouatta seniculus*	F	830.973	555.196	2558.950	169.072	169.072	169.072
545853	*Ateles paniscus*	M	725.064	659.400	1615.400	--	--	--
545885	*Ateles paniscus*	F	725.064	659.400	1615.400	--	--	--
461384	*Cebus apella*	M	688.712	589.450	2308.600	98.092	111.445	169.072
388197	*Cebus apella*	F	688.712	589.450	2308.600	98.092	111.445	169.072
518414	*Cebus libidinosus*	M	1331.444	1563.514	3907.461	366.924	257.972	3132.555
518418	*Cebus libidinosus*	F	1331.444	1563.514	3907.461	366.924	257.972	3132.555
236971	*Pan troglodytes schweinfurthii*	F	224.185	250.340	4223.000	1.028	0.610	4.270
481792	*Piliocolobus badius*	F	514.451	460.213	1561.610	9.403	8.396	21.850
546265	*Pithecia pithecia*	F	856.724	621.400	2255.500	111.445	111.445	111.445
339658	*Pithecia pithecia*	M	856.724	621.400	2255.500	111.445	111.445	111.445
143588	*Pongo abelii*	M	671.148	477.875	3734.700	4.264	3.434	8.641
143596	*Pongo abelii*	F	671.148	477.875	3734.700	4.264	3.434	8.641

320783	*Pygathrix nigripes*	F	634.612	623.433	1027.767	--	--	--
257998	*Pygathrix nigripes*	F	634.612	623.433	1027.767	--	--	--
307737	*Trachypithecus phayrei*	M	896.053	847.612	5817.506	3.344	3.212	7.890
307736	*Trachypithecus phayrei*	F	896.053	847.612	5817.506	3.344	3.212	7.890

Table 3.2. Results of BoneJ and Quant3D analyses for the sample of raw, undegraded images.

NMNH catalog #	Species	VOI cube (pixels)	BV/TV (%)	Tb.Th (mm)	Tb.N (mm^{-1})	Tb.Sp (mm)	DA	E	Conn.D (mm^{-3})	SMI
543117	*Alouatta palliata*	44	0.428	0.344	2.00669	0.457	3.808	0.450	4.027	-0.028
339925	*Alouatta palliata*	31	0.526	0.357	1.98478	0.395	3.501	0.436	3.604	0.029
398507	*Alouatta seniculus*	31	0.512	0.333	2.33394	0.373	4.076	0.389	5.512	0.253
545853	*Ateles paniscus*	30	0.411	0.333	1.78159	0.518	6.752	0.577	2.534	0.941
545885	*Ateles paniscus*	28	0.473	0.409	1.39258	0.607	4.581	0.708	1.279	0.69
461384	*Cebus apella*	26	0.466	0.295	2.08292	0.311	8.321	0.480	3.321	0.438
388197	*Cebus apella*	26	0.452	0.293	1.91495	0.457	3.487	0.421	3.401	0.805
518414	*Cebus libidinosus*	27	0.424	0.336	1.69539	0.471	12.464	0.198	2.705	0.665
518418	*Cebus libidinosus*	24	0.507	0.326	1.58203	0.506	8.985	0.264	1.764	1.12
236971	*Pan troglodytes schweinfurthii*	28	0.529	0.594	1.28726	0.567	2.326	0.186	1.468	0.727
481792	*Piliocolobus badius*	27	0.662	0.304	0.933787	0.370	6.301	0.498	5.717	1.18
546265	*Pithecia pithecia*	22	0.493	0.274	2.13255	0.529	6.934	0.200	5.437	1.473
339658	*Pithecia pithecia*	28	0.509	0.276	2.18588	0.356	9.023	0.644	6.335	1.279
143588	*Pongo abelii*	36	0.541	0.889	0.80791	0.582	2.681	0.249	0.309	-1.237
143596	*Pongo abelii*	40	0.557	0.726	1.04753	0.798	2.654	0.471	0.568	-0.081
320783	*Pygathrix nigripes*	24	0.433	0.358	1.64882	0.542	9.536	0.503	2.854	1.898

257998	*Pygathrix nigripes*	26	0.557	0.367	1.84704	0.352	10.617	0.624	2.056	0.252
307737	*Trachypithecus phayrei*	30	0.557	0.369	1.81861	0.370	8.558	0.319	2.643	0.271
307736	*Trachypithecus phayrei*	26	0.495	0.325	1.99924	0.356	14.879	0.542	4.438	1.188

Table 3.3. Results of BoneJ and Quant3D analyses for the sample of artificially degraded images.

NMNH catalog #	Species	BV/TV	Tb.Th (mm)	Tb.N (mm^{-1})	Tb.Sp (mm)	DA	E	Conn.D (mm^{-3})	SMI
461384	*Cebus apella*	0.436	0.315	2.07535	0.318	8.185	0.591	3.171	0.581
388197	*Cebus apella*	0.489	0.312	1.9141	0.457	2.821	0.287	3.005	0.897
481792	*Piliocolobus badius*	0.633	0.329	1.9118	0.376	7.279	0.576	4.94	1.212
546265	*Pithecia pithecia*	0.471	0.309	2.12381	0.402	5.777	0.278	5.025	1.689
339658	*Pithecia pithecia*	0.491	0.297	1.99798	0.379	9.538	0.687	5.801	1.451

Table 3.4. Comparison of trabecular variables and measures of toughness (*R*). All measures were logged before analysis. A constant value (1.659) was added to estimates of SMI for the raw and degraded samples so that the smallest value was equal to one. Significant results after performing a Bonferroni-Holm correction for multiple comparisons are indicated in bold.

		Raw sample (df = 1, 9)					Degraded sample (df = 1, 9)					No hominoids (df = 1, 7)				
Dependent variable	Independent variable	*F*	λ	Slope	R^2	*p*	*F*	λ	Slope	R^2	*p*	*F*	λ	Slope	R^2	*p*
BV/TV	weighted mean *R*	0.286	0.399	-0.039	0.031	0.606	0.244	0.509	-0.031	0.026	0.632	0.571	0.377	-0.081	0.075	0.475
BV/TV	median *R*	1.020	0.348	-0.071	0.102	0.339	0.984	0.447	-0.061	0.099	0.347	0.921	0.451	-0.080	0.116	0.369
BV/TV	maximum *R*	0.014	0.583	0.007	0.006	0.909	0.483	1.000	0.019	0.051	0.505	0.371	1.000	0.019	0.050	0.562
Tb.Th	weighted mean *R*	4.789	1.000	0.145	0.347	0.056	1.123	1.000	0.060	0.111	0.317	1.933	0.000	-0.111	0.216	0.207
Tb.Th	median *R*	6.037	1.000	0.112	0.402	0.036	1.357	1.000	0.047	0.131	0.274	0.125	0.275	-0.024	0.018	0.734
Tb.Th	maximum *R*	4.261	1.000	0.152	0.321	0.069	1.149	1.000	0.066	0.113	0.312	1.319	0.401	-0.047	0.159	0.289
Tb.N	weighted mean *R*	0.633	0.269	0.168	0.066	0.447	11.83	1.000	-0.244	0.568	**0.007**	0.349	0.000	-0.086	0.048	0.573
Tb.N	median *R*	0.415	0.317	0.137	0.044	0.536	20.29	1.000	-0.194	0.693	**0.001**	2.777	0.000	-0.175	0.284	0.139
Tb.N	maximum *R*	0.070	0.660	0.042	0.008	0.797	0.172	0.802	-0.049	0.019	0.688	0.052	0.000	0.019	0.007	0.827
Tb.Sp	weighted mean *R*	0.502	0.000	-0.107	0.053	0.497	1.067	0.000	-0.147	0.106	0.329	0.001	0.000	-0.001	0.001	0.994

Tb.Sp	median *R*	0.393	0.000	-0.096	0.042	0.547	0.723	0.000	-0.124	0.074	0.417	0.417	0.000	0.092	0.056	0.539
Tb.Sp	maximum *R*	0.279	0.000	0.068	0.030	0.609		0.000				1.285	0.000	-0.105	0.155	0.294
DA	weighted mean *R*	67.51	1.000	0.845	0.882	**<0.0001**	72.55	1.000	0.932	0.889	**<0.0001**	127.3	1.000	0.969	0.948	**<0.0001**
DA	median *R*	122.2	1.000	0.625	0.931	**<0.0001**	161.8	1.000	0.692	0.947	**<0.0001**	305.5	1.000	0.686	0.978	**<0.0001**
DA	maximum *R*	0.519	0.852	0.186	0.054	0.489	0.321	0.811	0.152	0.034	0.585	2.119	0.554	0.311	0.232	0.189
E	weighted mean *R*	0.541	0.000	0.193	0.057	0.481	0.487	0.000	0.191	0.051	0.503	9.061	0.000	-0.752	0.564	0.019
E	median *R*	0.065	0.000	0.069	0.007	0.804	0.036	0.000	0.053	0.004	0.854	10.94	0.000	-0.647	0.609	0.013
E	maximum *R*	7.597	0.000	-0.461	0.458	0.022	8.017	0.000	-0.486	0.471	0.019	4.755	0.000	-0.361	0.405	0.066
Conn.D	weighted mean *R*	7.337	1.000	-0.533	0.449	**0.024**	5.146	1.000	-0.422	0.364	0.049	0.476	0.000	-0.326	0.064	0.513
Conn.D	median *R*	10.17	1.000	-0.417	0.531	**0.011**	6.901	1.000	-0.332	0.434	0.027	2.777	0.000	-0.570	0.284	0.139
Conn.D	maximum *R*	0.122	0.916	-0.119	0.013	0.735	0.098	0.951	-0.097	0.011	0.761	0.029	0.000	0.047	0.004	0.869
SMI	weighted mean *R*	0.377	0.000	0.142	0.040	0.555	0.249	0.000	0.119	0.027	0.629	1.625	0.000	3.591	0.188	0.243
SMI	median *R*	0.367	0.000	0.142	0.039	0.559	0.258	0.000	0.123	0.028	0.624	0.465	0.000	1.709	0.062	0.517
SMI	maximum	0.556	0.000	0.144	0.058	0.475	0.534	0.000	0.145	0.056	0.484	0.445	0.000	1.147	0.059	0.526


R

Table 3.5. Comparison of trabecular variables and measures of Young's modulus (*E*). All measures were logged before analysis. Significant results after performing a Bonferroni-Holm correction for multiple comparisons are indicated in bold.

		Raw sample (df = 1, 6)					Degraded sample (df = 1, 6)					No hominoids (df = 1, 4)				
Dependent variable	Independent variable	*F*	λ	Slope	R^2	*p*	*F*	λ	Slope	R^2	*p*	*F*	λ	Slope	R^2	*p*
BV/TV	weighted mean *E*	2.750	0.000	-0.029	0.314	0.148	3.871	0.000	-0.029	0.392	0.097	0.289	1.000	0.004	0.068	0.619
BV/TV	median *E*	2.575	0.000	-0.027	0.300	0.159	3.644	0.000	-0.028	0.378	0.105	0.263	1.000	0.004	0.062	0.635
BV/TV	maximum *E*	3.169	0.000	-0.03	0.346	0.125	4.113	0.000	-0.029	0.407	0.089	0.347	1.000	0.006	0.079	0.587
Tb.Th	weighted mean *E*	4.439	0.000	-0.114	0.425	0.079	5.634	0.000	-0.113	0.484	0.055	69.05	1.000	0.022	0.945	**0.001**
Tb.Th	median *E*	5.176	0.000	-0.114	0.463	0.063	6.479	0.000	-0.112	0.519	0.044	68.88	1.000	0.021	0.945	**0.001**
Tb.Th	maximum *E*	3.649	1.000	0.036	0.378	0.105	0.899	1.000	0.015	0.130	0.379	25.07	1.000	0.029	0.862	**0.007**
Tb.N	weighted mean *E*	3.336	0.000	0.099	0.357	0.118	2.827	0.000	0.078	0.320	0.143	0.002	0.000	-0.001	0.0004	0.971
Tb.N	median *E*	3.741	0.000	0.099	0.384	0.101	3.410	0.000	0.079	0.362	0.114	0.029	0.000	-0.005	0.007	0.873
Tb.N	maximum *E*	1.723	0.000	0.078	0.223	0.237	15.83	1.000	-0.064	0.725	**0.007**	0.481	0.000	0.019	0.107	0.526
Tb.Sp	weighted mean *E*	0.809	0.000	-0.037	0.119	0.403	1.596	0.000	-0.048	0.210	0.253	0.191	0.000	0.014	0.046	0.685
Tb.Sp	median *E*	1.097	0.000	-	0.155	0.335	2.070	0.000	-	0.257	0.200	0.241	0.000	0.016	0.057	0.649

				0.040					0.051							
Tb.Sp	maximum *E*	32.61	1.000	0.079	0.845	**0.001**	35.63	1.000	0.077	0.856	**0.001**	0.025	0.000	-0.005	0.006	0.882
DA	weighted mean *E*	1.703	0.000	0.129	0.221	0.239	2.589	0.000	0.153	0.302	0.159	0.006	0.000	-0.008	0.001	0.943
DA	median *E*	1.848	0.000	0.128	0.235	0.223	1.519	0.000	0.119	0.202	0.264	0.008	0.000	0.009	0.002	0.934
DA	maximum *E*	42.56	1.000	0.201	0.876	**<0.001**	55.1	1.000	0.225	0.902	**<0.001**	0.495	0.000	-0.065	0.110	0.520
E	weighted mean *E*	0.151	0.000	0.025	0.025	0.711	0.135	0.000	0.026	0.022	0.726	0.252	0.000	-0.042	0.059	0.642
E	median *E*	0.348	0.000	0.036	0.055	0.577	0.309	0.000	0.037	0.049	0.598	0.298	0.036	-0.046	0.069	0.614
E	maximum *E*	0.036	0.000	-0.012	0.006	0.856	0.041	0.000	-0.014	0.007	0.846	0.495	0.000	-0.065	0.110	0.520
Conn.D	weighted mean *E*	1.543	0.000	0.182	0.205	0.261	1.602	0.000	0.179	0.211	0.253	0.0003	0.000	-0.002	0.0001	0.985
Conn.D	median *E*	1.839	0.000	0.187	0.235	0.224	1.892	0.000	0.183	0.239	0.218	0.009	0.000	-0.009	0.002	0.931
Conn.D	maximum *E*	7.144	1.000	-0.133	0.544	0.037	4.927	1.000	-0.106	0.451	0.068	0.161	0.000	0.035	0.039	0.709
SMI	weighted mean *E*	0.135	0.000	-0.039	0.026	0.728	0.607	0.000	-0.051	0.092	0.466	2.179	0.000	-0.203	0.353	0.214
SMI	median *E*	0.155	0.000	-0.041	0.029	0.710	0.377	0.000	-0.039	0.059	0.562	1.623	0.000	-0.186	0.289	0.272
SMI	maximum	0.024	0.000	-	0.005	0.883	2.541	0.000	-	0.298	0.162	8.513	0.000	-	0.680	0.043

E	0.017	0.089	0.251

Figure 3.1. Phylogenetic tree used for PGLS analyses, showing the species included in this study.

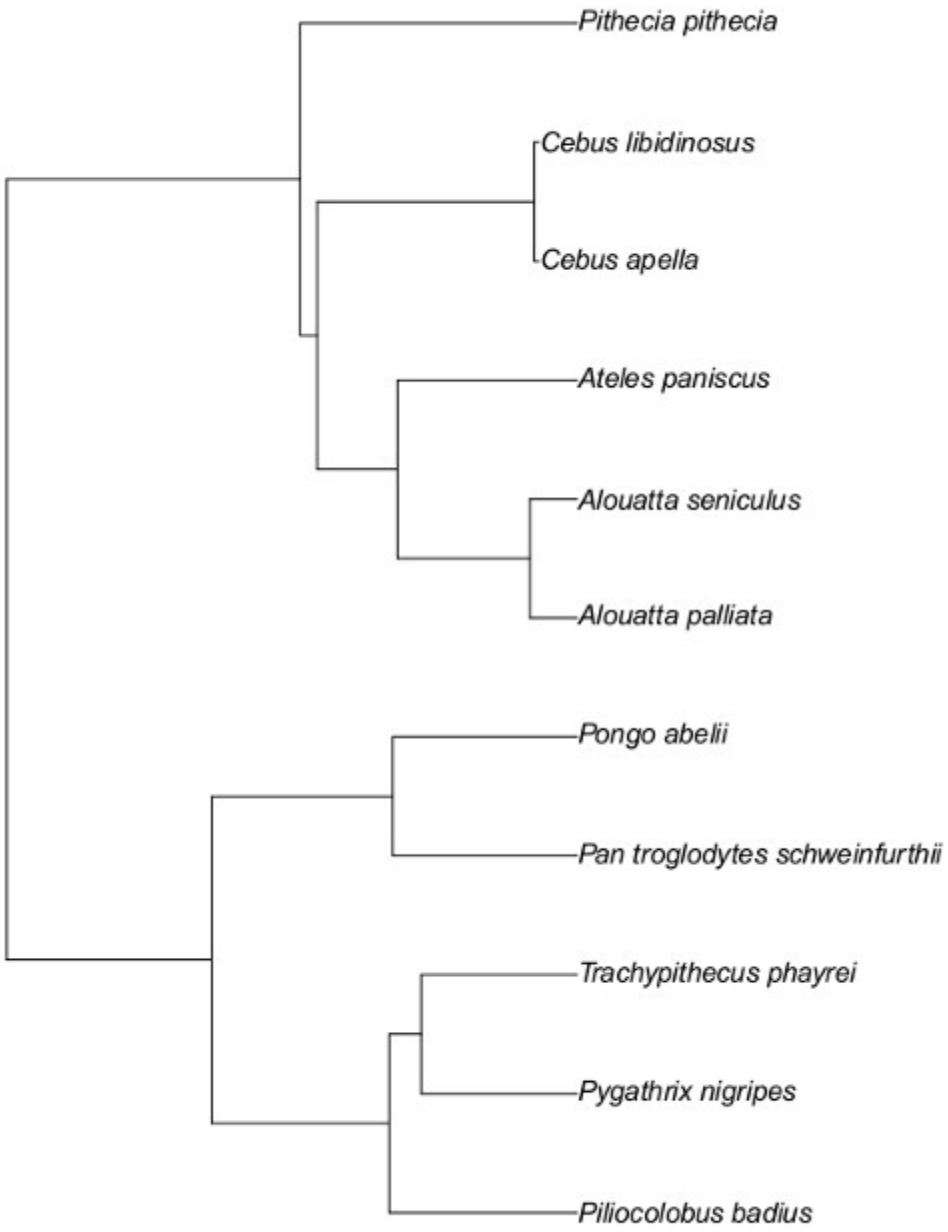

Figure 3.2. Montages of the cubic VOI from one specimen of *Lophocebus albigena* in raw (*A*) and artificially degraded (*B*) form. Both VOIs are magnified to show detail. *B* has fewer slices because the VOI was downsampled in all three dimensions.

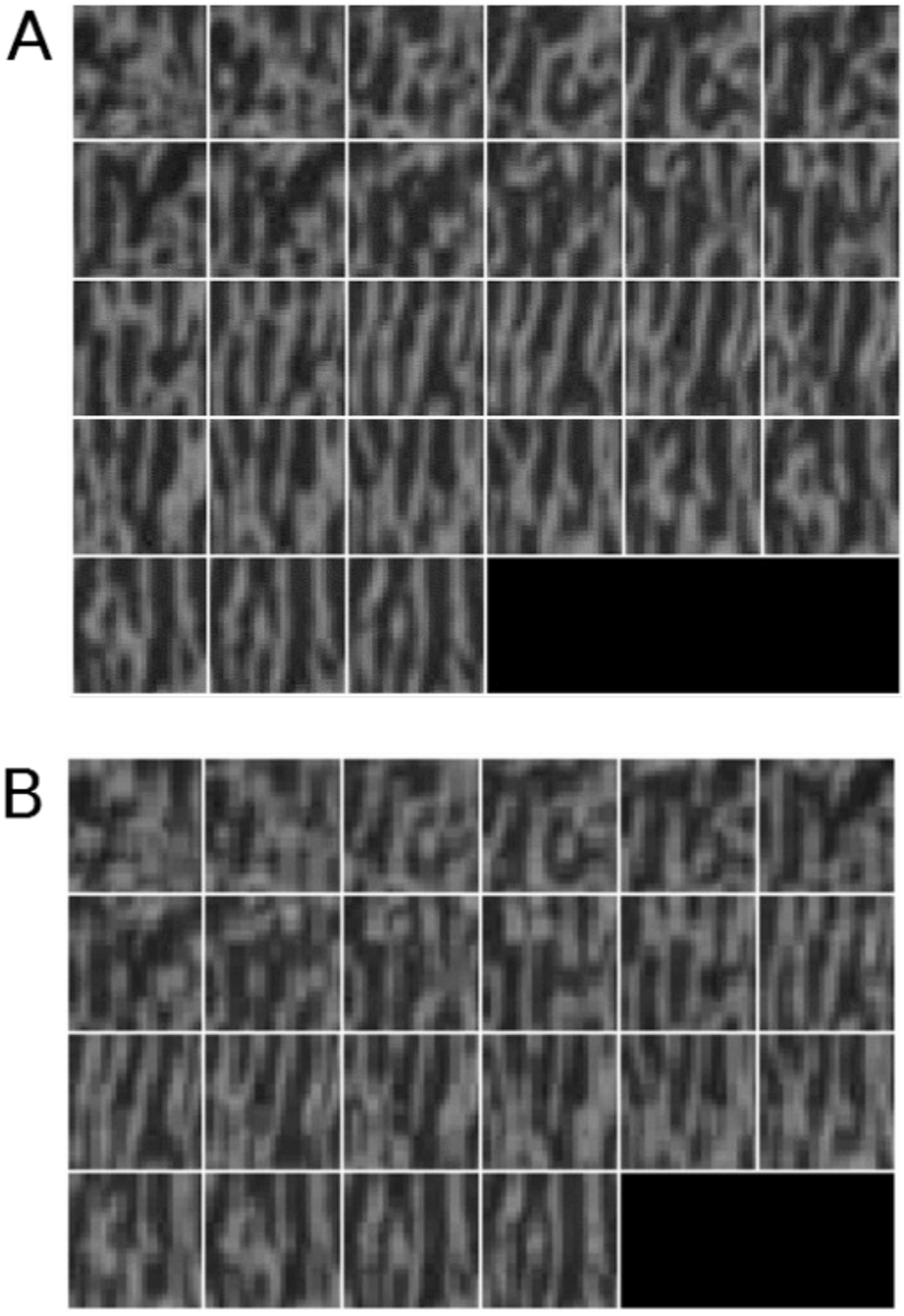

Figure 3.3. Visual representation of the external landmarks used to select the full VOI. A mandible of *Pithecia pithecia* is shown reconstructed in three dimensions. The yellow points in *A* and *B* represent the posterior and anterior landmarks. The area highlighted in *C* represents the region chosen to represent the condyle.

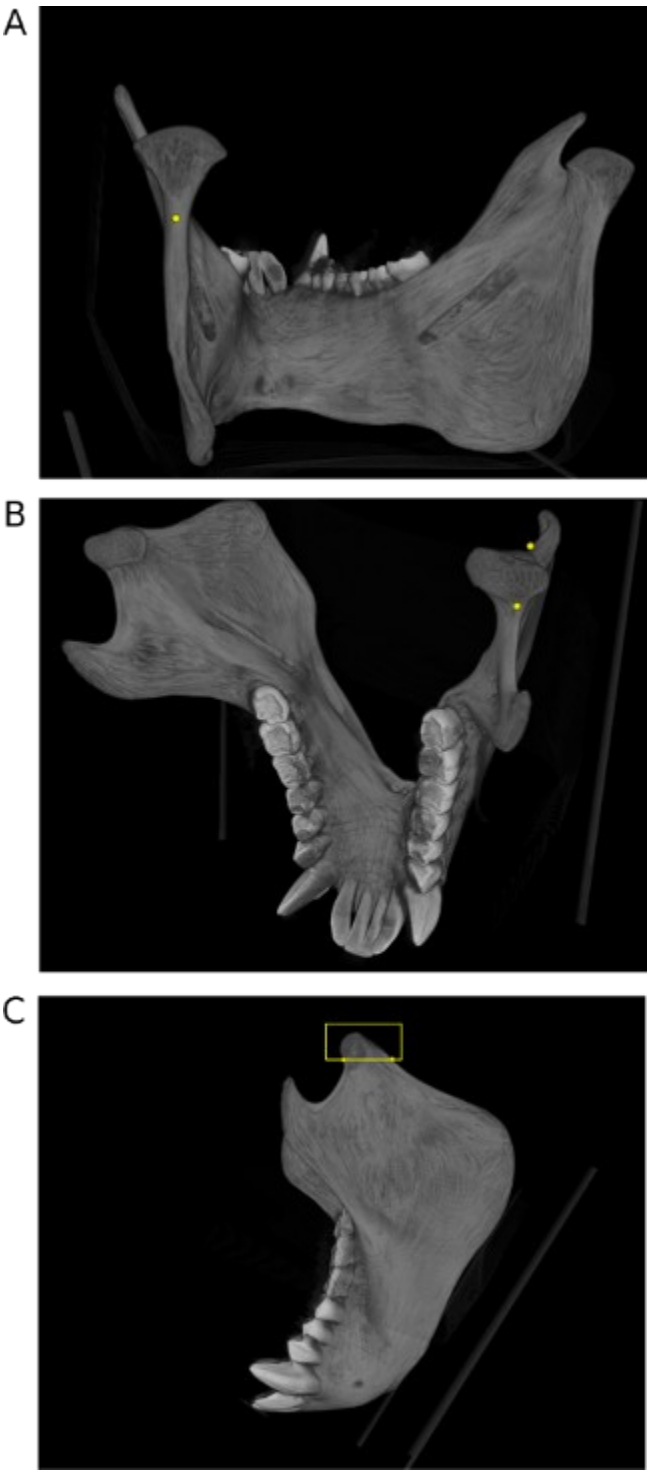

Figure 3.4. Representation of the image segmentation process. *A* is the raw image after the condyle was cropped from the mandible. *B* is the output from Trainable Weka Segmentation, with trabecular bone in black, cortical bone in gray, and background in white. *C* is the mask created by thresholding to remove the cortical bone. In the second row, *C* is applied onto *A* to produce the final segmented image, *D,* which has the cortical bone removed.

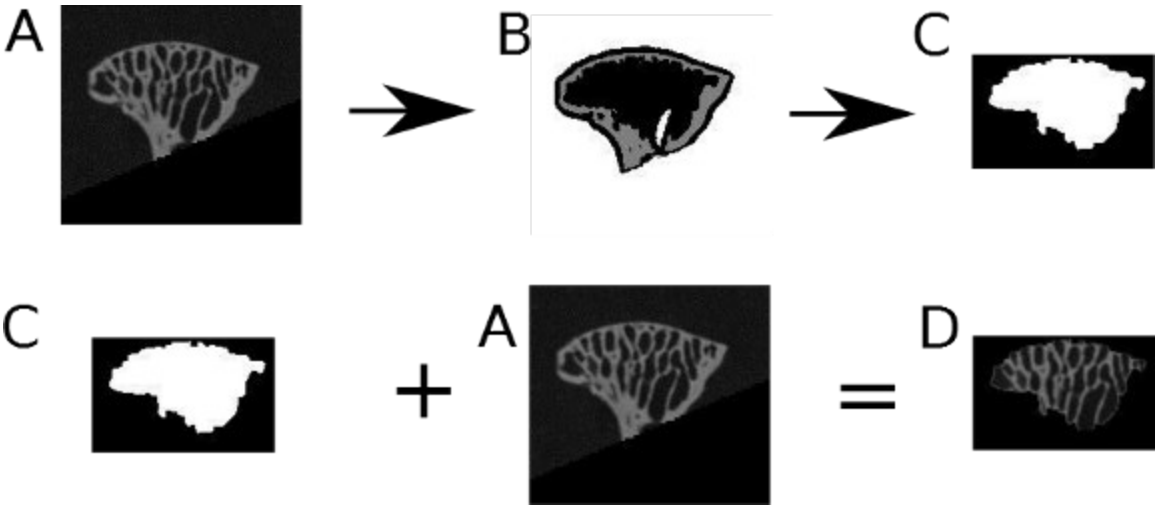

Figure 3.5. OLS regressions of DA and toughness from the raw sample. Species are grouped by taxon, with cercopithecoids represented by teal triangles, hominoids by red triangles, and platyrrhines by purple squares.

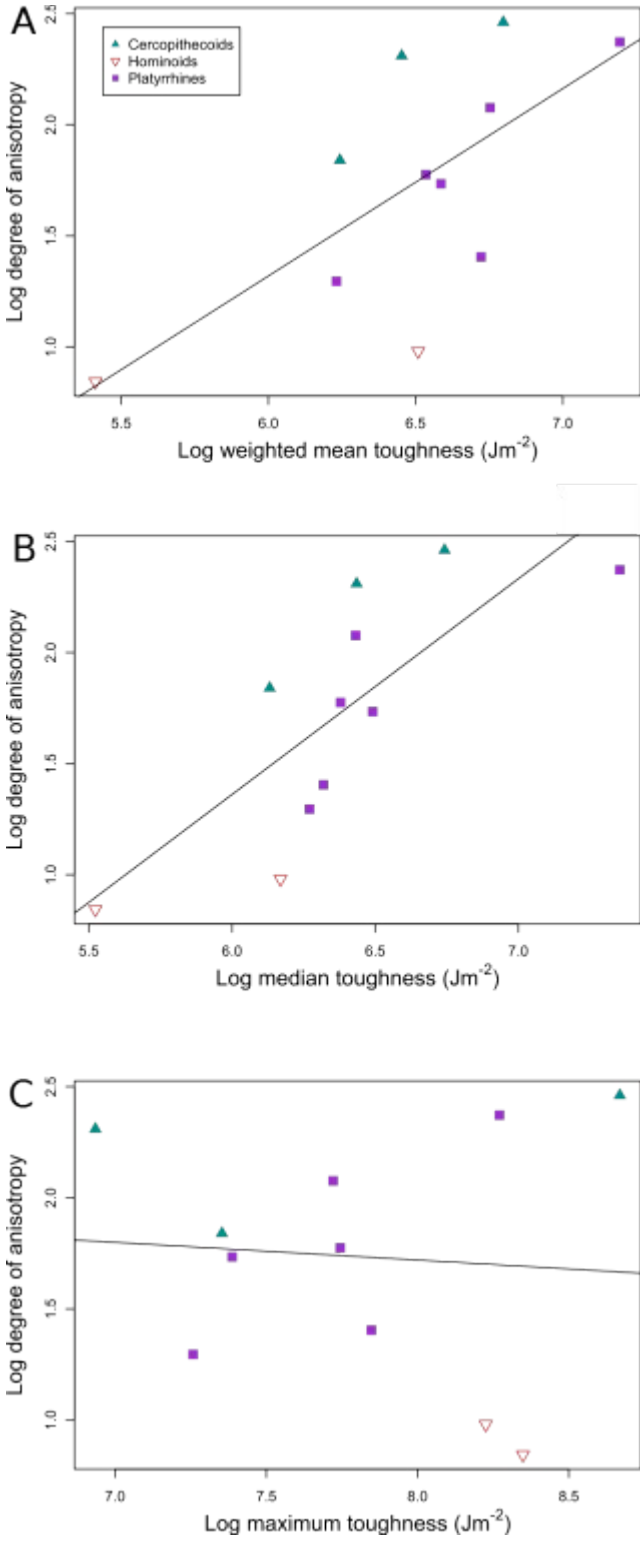

Figure 3.6. OLS regressions of DA and toughness from the sample including artificially degraded specimens.

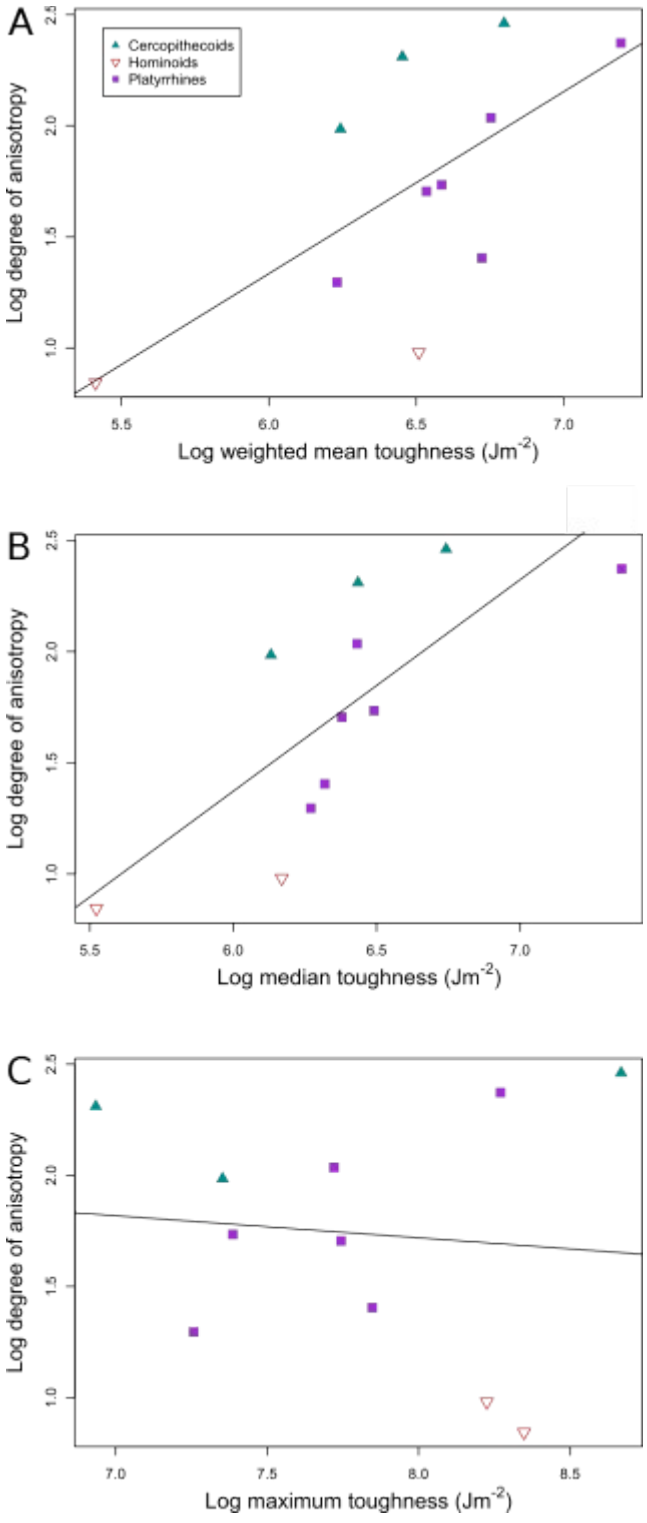

Figure 3.7. OLS regressions of DA and toughness from the sample that both includes artificially degraded specimens and excludes hominoids.

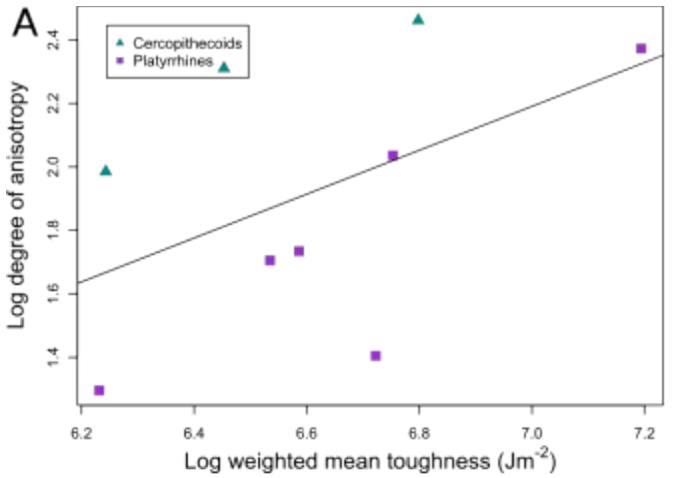

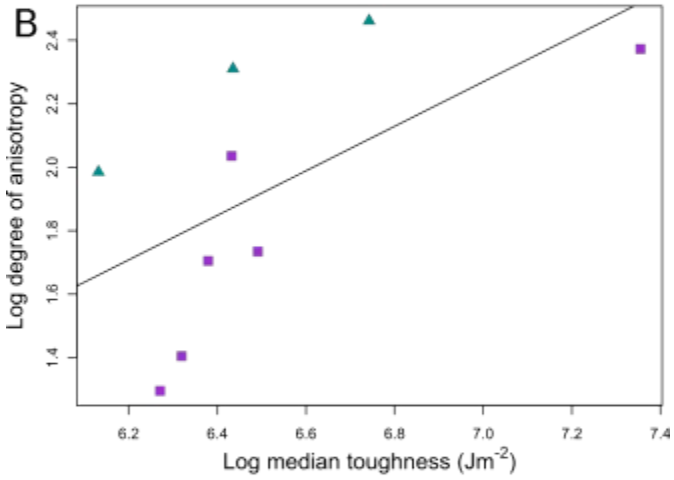

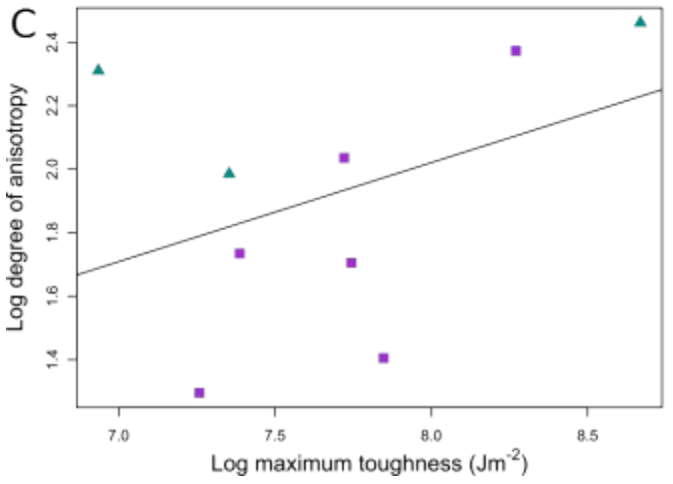

References

Abel, R., Macho, G.A., 2011. Ontogenetic changes in the internal and external morphology of the ilium in modern humans. Journal of Anatomy. 218, 324–335.

Agrawal, K.R., Lucas, P.W., 2003. The mechanics of the first bite. Proceedings of the Royal Society of London: Biology. 270, 1277–1282.

Agrawal, K.R., Lucas, P.W., Bruce, I., Prinz, J., 1998. Food properties that influence neuromuscular activity during human mastication. Journal of Dental Research. 77, 1931–1938.

Agrawal, K.R., Lucas, P.W., Bruce, I.C., 2000. The effects of food fragmentation index on mandibular closing angle in human mastication. Archives of Oral Biology. 45, 577–584.

Arganda-Carreras, I., Cardona, A., Kaynig, V., Schindelin, J., 2011. Trainable Weka Segmentation [WWW Document]. Fiji website. URL http://fiji.sc/Trainable_Weka_Segmentation

Arnold, C., Matthews, L.J., Nunn, C.L., 2010. The 10kTrees website: A new online resource for primate phylogeny. Evolutionary Anthropology: Issues, News, and Reviews. 19, 114–118.

Barak, M.M., Lieberman, D.E., Hublin, J.J., 2011. A Wolff in sheep's clothing: Trabecular bone adaptation in response to changes in joint loading orientation. Bone. 49, 1141–1151.

Berthaume, M.A., 2014. Tooth cusp sharpness as a dietary correlate in great apes. American Journal of Physical Anthropology. 153, 226–235.

Bouvier, M., 1986a. A biomechanical analysis of mandibular scaling in Old World monkeys. American Journal of Physical Anthropology. 69, 473–482.

Bouvier, M., 1986b. Biomechanical scaling of mandibular dimensions in New World Monkeys. International Journal of Primatology. 7, 551–567.

Bouvier, M., Hylander, W.L., 1981. Effect of bone strain on cortical bone structure in macaques (*Macaca mulatta*). Journal of Morphology. 167, 1–12.

Bouvier, M., Hylander, W.L., 1984. The effect of dietary consistency on gross and histologic morphology in the craniofacial region of young rats. American Journal of Anatomy. 170, 117–126.

Bouxsein, M.L., Boyd, S.K., Christiansen, B.A., Guldberg, R.E., Jepsen, K.J., Müller, R., 2010. Guidelines for assessment of bone microstructure in rodents using micro-computed tomography. Journal of Bone and Mineral Research. 25, 1468–1486.

Brehnan, K., Boyd, R.L., Laskin, J., Gibbs, C.H., Mahan, P., 1981. Direct measurement of loads at the temporomandibular joint in Macaca arctoides. Journal of Dental Research. 60, 1820–1824.

Brown, A., Zunino, G., 1990. Dietary variability in Cebus apella in extreme habitats: evidence for adaptability. Folia Primatologica. 54, 187–195.

Buie, H.R., Campbell, G.M., Klinck, R.J., Macneil, J. a, Boyd, S.K., 2007. Automatic segmentation of cortical and trabecular compartments based on a dual threshold technique for in vivo micro-CT bone analysis. Bone. 41, 505–515.

Carter, D.R., Hayes, W.C., 1977. The compressive behavior of bone as a two-phase porous structure. The Journal of Bone and Joint Surgery. 59, 954–962.

Chalk, J., 2011. The Effects of Feeding Strategies and Food Mechanics on the Ontogeny

of Masticatory Function in the *Cebus libidinosus* Cranium. Thesis, George Washington University.
Chen, J., 2009. Food oral processing—A review. Food Hydrocolloids. 23, 1–25.
Constantino, P.J., Lee, J.J.-W., Morris, D., Lucas, P.W., Hartstone-Rose, A., Lee, W.-K., Dominy, N.J., Cunningham, A., Wagner, M., Lawn, B.R., 2011. Adaptation to hard-object feeding in sea otters and hominins. Journal of Human Evolution. 61, 89–96.
Corruccini, R., Beecher, R., 1982. Occlusal variation related to soft diet in a nonhuman primate. Science. 218, 74–6.
Corruccini, R., Beecher, R., 1984. Occlusofacial morphological integration lowered in baboons raised on soft diet. Journal of Craniofacial Genetics and Developmental Biology. 4, 135–142.
Cruz-Orive, L.M., Karlsson, L.M., Larsen, S.E., Wainschtein, F., 1992. Characterizing anisotropy: A new concept. Miron and Microscopica Acta. 23, 75–76.
Daegling, D.J., 1989. Biomechanics of cross-sectional size and shape in the hominoid mandibular corpus. American Journal of Physical Anthropology. 80, 91–106.
Daegling, D.J., 1992. Mandibular morphology and diet in the genus *Cebus*. International Journal of Primatology. 13, 545–570.
Daegling, D.J., 1993. The relationship of in vivo bone strain to mandibular corpus morphology in *Macaca fascicularis*. Journal of Human Evolution. 25, 247–269.
Daegling, D.J., Grine, F.E., 1991. Compact bone distribution and biomechanics of early hominid mandibles. American Journal of Physical Anthropology. 86, 321–339.
Daegling, D.J., Hylander, W.L., 2000. Experimental observation, theoretical models, and biomechanical inference in the study of mandibular form. American Journal of Physical Anthropology. 112, 541–51.
Daegling, D.J., Judex, S., Ozcivici, E., Ravosa, M.J., Taylor, A.B., Grine, F.E., Teaford, M.F., Ungar, P.S., 2013. Viewpoints: Feeding mechanics, diet, and dietary adaptations in early hominins. American Journal of Physical Anthropology. 151, 356–371.
Daegling, D.J., McGraw, W.S., 2001. Feeding, diet, and jaw form in West African Colobus and Procolobus. International Journal of Primatology. 22, 1033–1055.
Daegling, D.J., McGraw, W.S., Ungar, P.S., Pampush, J.D., Vick, A.E., Anderson, E., Bitty, E.A., 2011. Hard-object feeding in sooty mangabeys (*Cercocebus atys*) and interpretation of early hominin feeding ecology. PloS one. 6, e23095.
Demes, B., Creel, N., 1988. Bite force, diet, and cranial morphology of fossil hominids. Journal of Human Evolution. 17, 657–670.
Dias, G.J., Cook, R.B., Mirhosseini, M., 2011. Influence of food consistency on growth and morphology of the mandibular condyle. Clinical Anatomy. 24, 590–598.
Ding, M., Odgaard, A., Hvid, I., 1999. Accuracy of cancellous bone volume fraction measured by micro-CT scanning. Journal of Biomechanics. 32, 323–326.
Doube, M., Kłosowski, M.M., Arganda-Carreras, I., Cordelières, F.P., Dougherty, R.P., Jackson, J.S., Schmid, B., Hutchinson, J.R., Shefelbine, S.J., 2010. BoneJ: Free and extensible bone image analysis in ImageJ. Bone. 47, 1076–9.
Dumont, E.R., 1995. Enamel thickness and dietary adaptations among extant primates and chiroptera. Journal of Mammalogy. 76, 1127–1136.
Fajardo, R.J., Müller, R., 2001. Three-dimensional analysis of nonhuman primate trabecular architecture using micro-computed tomography. American Journal of

Physical Anthropology. 115, 327–36.
Fajardo, R.J., Müller, R., Ketcham, R.A., Colbert, M., Fajardo, R.J., Mu, R., 2007. Nonhuman anthropoid primate femoral neck trabecular architecture and its relationship to locomotor mode. Anatomical Record. 290, 422–36.
Fajardo, R.J., Ryan, T.M., Kappelman, J., Jose, R., 2002. Assessing the accuracy of high-resolution X-ray computed tomography of primate trabecular bone by comparisons with histological sections. American Journal of Physical Anthropology. 118, 1–10.
Faulkner, M., Hatcher, D., Hay, A., 1987. A three-dimensional investigation of temporomandibular joint loading. Journal of Biomechanics. 20, 997–1002.
Galante, J., Rostoker, W., Ray, R., 1970. Physical properties of trabecular bone. Calcified Tissue Research. 5, 236–246.
Galik, K., Senut, B., Pickford, M., Gommery, D., Treil, J., Kuperavage, A., Eckhardt, R., 2004. External and internal morphology of the BAR 1002'00 *Orrorin tugenensis* femur. Science. 305, 1450–1453.
Giesen, E., Ding, M., Dalstra, M., Van Eijden, T., 2001. Mechanical properties of cancellous bone in the human mandibular condyle are anisotropic. Journal of Biomechanics. 34, 799–803.
Giesen, E., Ding, M., Dalstra, M., van Eijden, T., 2004. Changed morphology and mechanical properties of cancellous bone in the mandibular condyles of edentate people. Journal of Dental Research. 83, 255–259.
Giesen, E., van Eijden, T., 2000. The three-dimensional cancellous bone architecture of the human mandibular condyle. Journal of Dental Research. 79, 957–963.
Goldstein, S.A., Goulet, R., McCubbrey, D., 1993. Measurement and significance of three-dimensional architecture to the mechanical integrity of trabecular bone. Calcified Tissue International. 53, S127–S133.
Goldstein, S.A., Matthews, L.S., Kuhn, J.L., Hollister, S.J., 1991. Trabecular bone remodeling: An experimental model. Journal of Biomechanics. 24, 135–150.
Gordon, J., 1978. Structures, or, Why Things Don't Fall Down. Penguin, London.
Gosman, J.H., Ketcham, R.A., 2009. Patterns in ontogeny of human trabecular bone from Sunwatch village in the prehistoric Ohio Valley: General features of microarchitectural change. American Journal of Physical Anthropology. 138, 318–332.
Goulet, R.W., Goldstein, S.A., Ciarelli, M.J., Kuhn, J.L., Brown, M.B., Feldkamp, L.A., 1994. The relationship between the structural and orthogonal compressive properties of trabecular bone. Journal of Biomechanics. 27, 375–389.
Griffin, N.L., D'Août, K., Ryan, T.M., Richmond, B.G., Ketcham, R.A., Postnov, A., Grif, N.L., Août, K.D., 2010. Comparative forefoot trabecular bone architecture in extant hominids. Journal of Human Evolution. 59, 202–13.
Hara, T., Tanck, E., Homminga, J., Huiskes, R., 2002. The influence of microcomputed tomography threshold variations on the assessment of structural and mechanical trabecular bone properties. Bone. 31, 107–109.
Harrigan, T.P., Jasty, M., Mann, R.W., Harris, W.H., 1988. Limitations of the continuum assumption in cancellous bone. Journal of Biomechanics. 21, 269–275.
Herring, S.W., Liu, Z., 2001. Loading of the temporomandibular joint: anatomical and in vivo evidence from the bones. Cells, Tissues, Organs. 169, 193–200.
Hildebrand, T., Laib, A., Müller, R., Dequeker, J., Ruegsegger, P., 1999. Direct three-

dimensional morphometric analysis of human cancellous bone: Microstructural data from spine, femur, iliac crest, and calcaneus. Journal of Bone and Mineral Research. 14, 1167–1174.

Hildebrand, T., Rüegsegger, P., 1997a. Quantification of bone microarchitecture with the Structure Model Index. Computer Methods in Biomechanics and Biomedical Engineering. 1, 15–23.

Hildebrand, T., Rüegsegger, P., 1997b. A new method for the model-independent assessment of thickness in three-dimensional images. Journal of Microscopy. 185, 67–75.

Hill, D.A., Lucas, P.W., 1996. Toughness and fiber content of major leaf foods of Japanese macaques (*Macaca fuscata yakui*) in Yakushima. American Journal of Primatology. 38, 221–231.

Hodgskinson, R., Currey, J.D., 1990a. Effects of structural variation on Young's modulus of non-human cancellous bone. Proceedings of the Institution of Mechanical Engineers. Part H, Journal of engineering in medicine. 204, 43–52.

Hodgskinson, R., Currey, J.D., 1990b. The effect of variation in structure on the Young's modulus of cancellous bone: a comparison of human and non-human material. Proceedings of the Institution of Mechanical Engineers. Part H, Journal of engineering in medicine. 204, 115–121.

Holm, S., 1979. A simple sequentially rejective multiple test procedure. Scandinavian Journal of Statistics. 6, 65–70.

Huiskes, R., 2000. If bone is the answer, then what is the question? Journal of Anatomy. 197, 145–156.

Hylander, W.L., 1979a. Mandibular function in *Galago crassicaudatus* and *Macaca fascicularis*: An in vivo approach to stress analysis of the mandible. Journal of Morphology. 159, 253–296.

Hylander, W.L., 1979b. An experimental analysis of temporomandibular joint reaction force in macaques. American Journal of Physical Anthropology. 51, 433–456.

Hylander, W.L., 1979c. The functional significance of primate mandibular form. Journal of Morphology. 160, 223–239.

Hylander, W.L., 1984. Stress and strain in the mandibular symphysis of primates: A test of competing hypotheses. American Journal of Physical Anthropology. 64, 1–46.

Hylander, W.L., 1985. Mandibular function and biomechanical stress and scaling. American Zoologist. 25, 315–330.

Hylander, W.L., 1988. Implications of in vivo experiments for interpreting the functional significance of "robust"australopithecine jaws. In: Grine, F.E. (Ed.), Evolutionary History of the "Robust" Australopithecines. Transaction, New Brunswick, NJ, pp. 55–80.

Hylander, W.L., Bays, R., 1979. An in vivo strain-gauge analysis of the squamosal-dentary joint reaction force during mastication and incisal biting in Macaca mulatta and Macaca fascicularis. Archives of Oral Biology. 24, 689–697.

Jerome, C., Carlson, C., Register, T., Bain, F., Jayo, M., Weaver, D., Adams, M., 1994. Bone functional changes in intact, ovariectomized, and ovariectomized, hormone-supplemented adult cynomolgus monkeys (*Macaca fasicularis*) evaluated by serum markers and dynamic histomorphometry. Journal of Bone and Mineral Research. 9, 527–540.

Jolly, C.J., 1970. The seed-eaters: A new model of hominid differentiation based on a baboon analogy. Man. 5, 5–26.
Kabel, J., Odgaard, A., Van Rietbergen, B., Huiskes, R., 1999a. Connectivity and the elastic properties of cancellous bone. Bone. 24, 115–120.
Kabel, J., Van Rietbergen, B., Odgaard, A., Huiskes, R., 1999b. Constitutive relationships of fabric, density, and elastic properties in cancellous bone architecture. Bone. 25, 481–486.
Kay, R.F., 1981. The nut-crackers—A new theory of the adaptations of the Ramapithecinae. American Journal of Physical Anthropology. 55, 141–151.
Kay, R.F., 1985. Dental evidence for the diet of *Australopithecus*. Annual Review of Anthropology. 14, 315–341.
Ketcham, R.A., Gosman, J.H., 2010. Accounting for resolution effects in trabecular metrics. American Journal of Physical Anthropology. 141, 141.
Ketcham, R.A., Ryan, T.M., 2004. Quantification and visualization of anisotropy in trabecular bone. Journal of Microscopy. 213, 158–71.
Kinzey, W.G., Norconk, M.A., 1990. Hardness as a basis of fruit choice in two sympatric primates. American Journal of Physical Anthropology. 81, 5–15.
Kivell, T., Skinner, M., Lazenby, R.A., Hublin, J.-J., 2011. Methodological considerations for analyzing trabecular architecture: An example from the primate hand. Journal of Anatomy. 218, 209–225.
Kothari, M., Keaveny, T.M., Lin, J.C., Newitt, D.C., Genant, H.K., Majumdar, S., 1998. Impact of spatial resolution on the prediction of trabecular architecture parameters. Bone. 22, 437– 443.
Laib, A., Rüegsegger, P., 1999. Calibration of trabecular bone structure measurements of in vivo three-dimensional peripheral quantitative computed tomography with 28-microm-resolution microcomputed tomography. Bone. 24, 35–39.
Lambert, J.E., Chapman, C.A., Wrangham, R.W., Conklin-Brittain, N.L., 2004. Hardness of cercopithecine foods: Implications for the critical function of enamel thickness in exploiting fallback foods. American Journal of Physical Anthropology. 125, 363–368.
Lazenby, R.A., Skinner, M.M., Kivell, T.L., Hublin, J.-J., 2011. Scaling VOI size in 3D μCT studies of trabecular bone: a test of the over-sampling hypothesis. American Journal of Physical Anthropology. 144, 196–203.
Link, T.M., Vieth, V., Stehling, C., Lotter, A., Beer, A., Newitt, D., Majumdar, S., 2003. High-resolution MRI vs multislice spiral CT: which technique depicts the trabecular bone structure best? European Radiology. 13, 663–71.
Lublinsky, S., Ozcivici, E., Judex, S., 2007. An automated algorithm to detect the trabecular-cortical bone interface in micro-computed tomographic images. Calcified Tissue International. 81, 285–93.
Lucas, P.W., 1981. An analysis of canine size and jaw shape in some Old and New World non-human primates. Journal of Zoology. 195, 437–448.
Lucas, P.W., 2004. Dental Functional Morphology: How Teeth Work. Cambridge University Press, Cambridge.
Lucas, P.W., Constantino, P.J., Wood, B.A., 2008a. Inferences regarding the diet of extinct hominins: structural and functional trends in dental and mandibular morphology within the hominin clade. Journal of Anatomy. 212, 486–500.

Lucas, P.W., Constantino, P.J., Wood, B.A., Lawn, B., 2008b. Dental enamel as a dietary indicator in mammals. BioEssays : news and reviews in molecular, cellular and developmental biology. 30, 374–85.

Lucas, P.W., Copes, L., Constantino, P.J., Vogel, E.R., Chalk, J., Talebi, M.G., Landis, M., Wagner, M., 2011. Measuring the toughness of primate foods and its ecological value. International Journal of Primatology. 33, 598–610.

Lucas, P.W., Pereira, B., 1990. Estimation of the fracture toughness of leaves. Functional Ecology. 4, 819–822.

Lucas, P.W., Turner, I.M., Dominy, N.J., Yamashita, N., 2000. Mechanical defences to herbivory. Annals of Botany. 86, 913–920.

Lynch Alfaro, J.W., Boubli, J.P., Olson, L.E., Di Fiore, A., Wilson, B., Gutiérrez-Espeleta, G. a., Chiou, K.L., Schulte, M., Neitzel, S., Ross, V., Schwochow, D., Nguyen, M.T.T., Farias, I., Janson, C.H., Alfaro, M.E., 2012. Explosive Pleistocene range expansion leads to widespread Amazonian sympatry between robust and gracile capuchin monkeys. Journal of Biogeography. 39, 272–288.

Ma, B., Sampson, W., Wilson, D., Wiebkin, O., Fazzalari, N., 2002. A histomorphometric study of adaptive responses of cancellous bone in different regions in the sheep mandibular condyle following experimental forward mandibular displacement. Science. 47, 519–527.

Maga, M., Kappelman, J., Ryan, T.M., Ketcham, R. a, 2006. Preliminary observations on the calcaneal trabecular microarchitecture of extant large-bodied hominoids. American Journal of Physical Anthropology. 129, 410–7.

Majumdar, S., Kothari, M., Augat, P., Newitt, D.C., Link, T.M., Lin, J.C., Lang, T., Lu, Y., Genant, H.K., 1998. High-resolution magnetic resonance imaging: Three-dimensional trabecular bone architecture and biomechanical properties. Bone. 22, 445–454.

Majumdar, S., Newitt, D., Mathur, A., Osman, D., Gies, A., Chiu, E., Lotz, J., Kinney, J., Genant, H.K., 1996. Magnetic resonance imaging of trabecular bone structure in the distal radius: Relationship with X-ray tomographic microscopy and biomechanics. Osteoporosis International. 6, 376–385.

Marshall, A.J., Wrangham, R.W., 2007. Evolutionary consequences of fallback foods. International Journal of Primatology. 28, 1219–1235.

Martin, L.B., 1985. Significance of enamel thickness in hominoid evolution. Nature. 314, 260–263.

Martin, L.B., Olejniczak, A.J., Maas, M.C., 2003. Enamel thickness and microstructure in pitheciin primates, with comments on dietary adaptations of the middle Miocene hominoid *Kenyapithecus*. Journal of Human Evolution. 45, 351–367.

Martins, E.P., Hansen, T.F., 1997. Phylogenies and the comparative method: A general approach to incorporating phylogenetic information into the analysis of interspecific data. The American Naturalist. 149, 646.

Meloro, C., Cáceres, N.C., Carotenuto, F., Sponchiado, J., Melo, G.L., Passaro, F., Raiai, P., n.d. Chewing on the trees: Constraints and adaptation in the evolution of the primate mandible. Evolution. 1–29.

Mittra, E., Rubin, C., Qin, Y.-X., 2005. Interrelationship of trabecular mechanical and microstructural properties in sheep trabecular bone. Journal of Biomechanics. 38, 1229–1237.

Müller, R., Koller, B., Hildebrand, T., Laib, A., Gianolini, S., Ruegsegger, P., 1996. Resolution dependency of microstructural properties of cancellous bone based on three-dimensional micro-tomography. Technology and Health Care. 4, 113–119.

Müller, R., Van Campenhout, H., Van Damme, B., Van Der Perre, G., Dequeker, J., Hildebrand, T., Rüegsegger, P., 1998. Morphometric analysis of human bone biopsies: a quantitative structural comparison of histological sections and micro-computed tomography. Bone. 23, 59–66.

Odgaard, A., 1997. Three-dimensional methods for quantification of cancellous bone architecture. Bone. 20, 315–328.

Odgaard, A., Gundersen, H., 1993. Quantification of connectivity in cancellous bone, with special emphasis on 3-D reconstructions. Bone. 14, 173–182.

Odgaard, A., Kubel, J., van Rietbergen, B., Dalstra, M., Huiskes, R., 1997. Fabric and elastic principal directions of cancellous bone are closely related. Journal of Biomechanics. 30, 487–495.

Olejniczak, A.J., 2006. Micro-Computed Tomography of Primate Molars. Thesis, Stony Brook University.

Orme, D., Freckleton, R., Thomas, G., Petzoldt, T., Fritz, S., Isaac, N., Pearse, W., 2013. The caper package: Comparative analysis of phylogenetics and evolution in R. R package version 0.5. 1–36.

Panger, M.A., Perry, S., Rose, L.M., Gros-Louis, J., Vogel, E., Mackinnon, K.C., Baker, M., 2002. Cross-site differences in foraging behavior of white-faced capuchins (Cebus capucinus). American Journal of Physical Anthropology. 119, 52–66.

Paradis, E., Claude, J., Strimmer, K., 2004. APE: Analyses of Phylogenetics and Evolution in R language. Bioinformatics. 20, 289–290.

Parfitt, A., Drezner, M.K., Glorieux, F.H., Kanis, J.A., Malluche, H., Meunier, P.J., Ott, S.M., Recker, R.R., 1987. Bone histomorphometry: standardization of nomenclature, symbols, and units. Journal of Bone and Mineral Research.

Parfitt, A., Mathews, C., Villanueva, A., Kleerekoper, M., Frame, B., Rao, D., 1983. Relationships between surface, volume, and thickness of iliac trabecular bone in aging and osteoporosis: Implications for the microanatomic and cellular mechanisms of bone loss. Journal of Clinical Investigation. 72, 1396–1409.

Parsons, T.J., van Dusseldorp, M., van der Vliet, M., van de Werken, K., Schaafsma, G., van Staveren, W.A., 1997. Reduced bone mass in Dutch adolescents fed a macrobiotic diet in early life. Journal of Bone and Mineral Research. 12, 1486–1494.

Plavcan, J.M., 2001. Sexual dimorphism in primate evolution. American Journal of Physical Anthropology. Suppl 33, 25–53.

Plavcan, J.M., van Schaik, C.P., 1992. Intrasexual competition and canine dimorphism in anthropoid primates. American Journal of Physical Anthropology. 87, 461–477.

Pontzer, H., Lieberman, D.E., Momin, E., Devlin, M.J., Polk, J.D., Hallgrímsson, B., Cooper, D.M.L., 2006. Trabecular bone in the bird knee responds with high sensitivity to changes in load orientation. The Journal of Experimental Biology. 209, 57–65.

Pothuaud, L., Laib, A., Levitz, P., Benhamou, C.L., Majumdar, S., 2002. Three-dimensional-line skeleton graph analysis of high-resolution magnetic resonance images: a validation study from 34-micrometer-resolution microcomputed

tomography. Journal of Bone and Mineral Research. 17, 1883–1895.
Raichlen, D.A., Gordon, A.D., Foster, A.D., Webber, J.T., Sukhdeo, S.M., Scott, R.S., Gosman, J.H., Ryan, T.M., 2015. An ontogenetic framework linking locomotion and trabecular bone architecture with applications for reconstructing hominin life history. Journal of Human Evolution. 81, 1–12.
Ravosa, M.J., 1996. Jaw morphology and function in living and fossil Old World monkeys. International Journal of Primatology. 17, 909–932.
Ravosa, M.J., Kunwar, R., Stock, S.R., Stack, M.S., 2007. Pushing the limit: masticatory stress and adaptive plasticity in mammalian craniomandibular joints. Journal of Experimental Biology. 210, 628–41.
Ravosa, M.J., Lopez, E.K., Menegaz, R.A., Stock, S.R., Stack, M.S., Hamrick, M.W., 2008. Adaptive Plasticity in the Mammalian Masticatory Complex: You Are What, and How, You Eat. In: Vinyard, C., Ravosa, M.J., Wall, C. (Eds.), Primate Craniofacial Function and Biology. Springer US, Boston, MA, pp. 293–328.
Reed, D.A., Ross, C.F., 2010. The influence of food material properties on jaw kinematics in the primate, Cebus. Archives of Oral Biology. 55, 946–962.
Ridler, T., Calvard, S., 1978. Picture thresholding using an iterative selection method. IEEE Transactions on Systems, Man, and Cybernetics. SMC-8, 630–632.
Riede, T., Bronson, E., Hatzikirou, H., Zuberbühler, K., 2005. Vocal production mechanisms in a non-human primate: Morphological data and a model. Journal of Human Evolution. 48, 85–96.
Robinson, J.T., 1954. Prehominid dentition and hominid evolution. Evolution. 8, 324–334.
Rosenberger, A.L., Kinzey, W.G., 1976. Functional patterns of molar occlusion in platyrrhine primates. American Journal of Physical Anthropology. 45, 281–98.
Ross, C.F., Dharia, R., Herring, S.W., Hylander, W.L., Liu, Z.Z., Rafferty, K.L.K., Ravosa, M.J., Williams, S.H., 2007. Modulation of mandibular loading and bite force in mammals during mastication. The Journal of Experimental Biology. 210, 1046–63.
Ross, C.F., Iriarte-Diaz, J., 2014. What does feeding system morphology tell us about feeding? Evolutionary Anthropology. 23, 105–120.
Ross, C.F., Iriarte-Diaz, J., Nunn, C.L., 2012. Innovative approaches to the relationship between diet and mandibular morphology in primates. International Journal of Primatology. 33, 632–660.
Ross, C.F., Washington, R.L., Eckhardt, A., Reed, D.A., Vogel, E.R., Dominy, N.J., Machanda, Z.P., 2009. Ecological consequences of scaling of chew cycle duration and daily feeding time in primates. Journal of Human Evolution. 56, 570–85.
Ruff, C.B., Holt, B., Trinkaus, E., 2006. Who's afraid of the Big Bad Wolff?: "Wolff's Law" and bone functional adaptation. American Journal of Physical Anthropology. 129, 484–498.
Russon, A.E., Wich, S.A., Ancrenaz, M., Kanamori, T., Knott, C.D., Kuze, N., Morrogh-Bernard, H.C., Pratje, P., Ramlee, H., Rodman, P., Sawang, A., Sidiyasa, K., Singleton, I., Schaik, C.P. Van, 2004. Geographic variation in orangutan diets. In: Orangutans: Geographic Variation in Behavioral Ecology and Conservation. pp. 135–156.
Ryan, T.M., Colbert, M., Ketcham, R.A., Vinyard, C.J., 2010. Trabecular bone structure

in the mandibular condyles of gouging and nongouging platyrrhine primates. American Journal of Physical Anthropology. 141, 583–93.
Ryan, T.M., Ketcham, R. a, 2005. Angular orientation of trabecular bone in the femoral head and its relationship to hip joint loads in leaping primates. Journal of Morphology. 265, 249–63.
Ryan, T.M., Ketcham, R.A., 2002a. The three-dimensional structure of trabecular bone in the femoral head of strepsirrhine primates. Journal of Human Evolution. 43, 1–26.
Ryan, T.M., Ketcham, R.A., 2002b. Femoral head trabecular bone structure in two omomyid primates. Journal of Human Evolution. 43, 241–263.
Ryan, T.M., Krovitz, G.E., 2006. Trabecular bone ontogeny in the human proximal femur. Journal of Human Evolution. 51, 591–602.
Ryan, T.M., Shaw, C.N., 2012. Unique suites of trabecular bone features characterize locomotor behavior in human and non-human anthropoid primates. PLoS ONE. 7, e41037.
Saha, P.K., Wehrli, F.W., 2004. A robust method for measuring trabecular bone orientation anisotropy at in vivo resolution using tensor scale. Pattern Recognition. 37, 1935–1944.
Sakka, M., 1984. Cranial morphology and masticatory adaptations. In: Chivers, D.J., Wood, B.A., Bilsborough, A. (Eds.), Food Acquisition and Processing in Primates. Springer, New York, pp. 415–427.
Scherf, H., Tilgner, R., 2009. A new high-resolution computed tomography (CT) segmentation method for trabecular bone architectural analysis. American Journal of Physical Anthropology. 140, 39–51.
Schindelin, J., Arganda-Carreras, I., Frise, E., Kaynig, V., Longair, M., Pietzsch, T., Preibisch, S., Rueden, C., Saalfeld, S., Schmid, B., Tinevez, J.-Y., White, D.J., Hartenstein, V., Eliceiri, K., Tomancak, P., Cardona, A., 2012. Fiji: An open-source platform for biological-image analysis. Nature Methods. 9, 676–82.
Schmid, B., Schindelin, J., 2010. A high-level 3D visualization API for Java and ImageJ. BMC Bioinformatics. 11.
Schwartz, G.T., Conroy, G.C., 1996. Cross-sectional geometric properties of the *Otavipithecus* mandible. American Journal of Physical Anthropology. 99, 613–623.
Scott, J.E., McAbee, K.R., Eastman, M.M., Ravosa, M.J., 2014. Experimental perspective on fallback foods and dietary adaptations in early hominins. Biology Letters.
Smith, R.J., 1983. The mandibular corpus of female primates: Taxonomic, dietary, and allometric correlates of interspecific variations in size and shape. American Journal of Physical Anthropology. 61, 315–330.
Smith, R.J., 1984. Comparative functional morphology of maximum mandibular opening (gape) in primates. In: Chivers, D.J., Wood, B.A., Bilsborough, A. (Eds.), Food Acquisition and Processing in Primates. Springer, New York, p. 231–.
Smith, R.J., Petersen, C.E., Gipe, D.P., 1983. Size and shape of the mandibular condyle in primates. Journal of morphology. 177, 59–68.
Sode, M., Burghardt, A.J., Nissenson, R. a., Majumdar, S., 2008. Resolution dependence of the non-metric trabecular structure indices. Bone. 42, 728–736.
Spencer, M.A., 1998. Force production in the primate masticatory system: electromyographic tests of biomechanical hypotheses. Journal of Human Evolution.

34, 25–54.
Spencer, M.A., Demes, B., 1993. Biomechanical analysis of masticatory system configuration in Neandertals and Inuits. American Journal of Physical Anthropology. 91, 1–20.
Spoor, C.F., Zonneveld, F.W., Macho, G.A., 1993. Linear measurements of cortical bone and dental enamel by computed tomography: Applications and problems. American Journal of Physical Anthropology. 91, 469–484.
Strait, D.S., Grosse, I.A.N.R., Dechow, P.C., Smith, A.L., Wang, Q., Weber, G.W., Neubauer, S., Slice, D.E., Chalk, J., Richmond, B.G., Lucas, P.W., Spencer, M. a, Schrein, C., Wright, B.W., Byron, C., Ross, C.F., 2010. The structural rigidity of the cranium of *Australopithecus africanus*: implications for diet, dietary adaptations, and the allometry of feeding biomechanics. Anatomical Record. 293, 583–93.
Tabor, Z., 2004. Analysis of the influence of image resolution on the discriminating power of trabecular bone architectural parameters. Bone. 34, 170–179.
Tabor, Z., 2011. A novel method of estimating structure model index from gray-level images. Medical Engineering and Physics. 33, 218–225.
Tanton, M., 1962. The effect of leaf "toughness" on the feeding of larvae of the mustard beetle *Phaedon cochleariae Fab*. Entomologia Experimentalis et Applicata. 5, 74–78.
Taylor, A.B., 2005. A comparative analysis of temporomandibular joint morphology in the African apes. Journal of Human Evolution. 48, 555–74.
Taylor, A.B., 2006a. Diet and mandibular morphology in African apes. International Journal of Primatology. 27, 181–201.
Taylor, A.B., 2006b. Feeding behavior, diet, and the functional consequences of jaw form in orangutans, with implications for the evolution of *Pongo*. Journal of Human Evolution. 50, 377–93.
Taylor, A.B., Jones, K.E., Kunwar, R., Ravosa, M.J., 2006. Dietary consistency and plasticity of masseter fiber architecture in postweaning rabbits. The Anatomical Record. 288, 1105–11.
Teaford, M.F., Ungar, P.S., 2009. Diet and the evolution of the earliest human ancestors. Proceedings of the National Academy of Sciences of the United States of America. 97, 13506–13511.
Thexton, A., Hiiemae, K., 1997. The effect of food consistency upon jaw movement in the macaque: A cineradiographic study. Journal of Dental Research. 76, 552.
Townsend, P., Raux, P., Rose, R., Miegel, R., Radin, E., 1975. The distribution and anisotropy of the stiffness of cancellous bone in the human patella. Biomechanics. 8, 363–367.
Trussell, H., 1979. Comments on "Picture thresholding using an iterative selection method." IEEE Transactions on Systems, Man, and Cybernetics. 54, 9472–9472.
Ulrich, D., Van Rietbergen, B., Laib, A., Rüegsegger, P., 1999. The ability of three-dimensional structural indices to reflect mechanical aspects of trabecular bone. Bone. 25, 55–60.
Ungar, P.S., 1994. Patterns of ingestive behavior and anterior tooth use differences in sympatric anthropoid primates. American Journal of Physical Anthropology. 95, 197–219.
Van der Meulen, M.C.H., Morgan, T.G., Yang, X., Baldini, T.H., Myers, E.R., Wright,

T.M., Bostrom, M.P.G., 2006. Cancellous bone adaptation to in vivo loading in a rabbit model. Bone. 38, 871–7.

Van Eijden, T., van Der Helm, P.N., van Ruijven, L., Mulder, L., 2006. Structural and mechanical properties of mandibular condylar bone. Journal of Dental Research. 85, 33–37.

Van Rietbergen, B., Odgaard, A., Kabel, J., Huiskes, R., 1998. Relationships between bone morphology and bone elastic properties can be accurately quantified using high-resolution computer reconstructions. Journal of Orthopaedic Research. 16, 23–28.

Van Ruijven, L.L.J., Giesen, E., van Eijden, T., 2002. Mechanical significance of the trabecular microstructure of the human mandibular condyle. Journal of Dental Research. 81, 706–710.

Varga, P., Zysset, P.K., 2009. Assessment of volume fraction and fabric in the distal radius using HR-pQCT. Bone. 45, 909–917.

Verhaegen, M., 1992. Did robust australopithecines partly feed on hard parts of gramineae? Human Evolution. 7, 63–64.

Vincent, J., 1992. Biomechanics–Materials: A Practical Approach, Oxford University Press, Oxford. Oxford University Press, Oxford.

Vinyard, C.J., Ryan, T.M., 2006. Cross-sectional bone distribution in the mandibles of gouging and non-gouging platyrrhini. International Journal of Primatology. 27, 1461–1490.

Vogel, E.R., Haag, L., Mitra-Setia, T., van Schaik, C.P., Dominy, N.J., 2009. Foraging and ranging behavior during a fallback episode: *Hylobates albibarbis* and *Pongo pygmaeus wurmbii* compared. American Journal of Physical Anthropology. 140, 716–26.

Vogel, E.R., van Woerden, J.T., Lucas, P.W., Utami Atmoko, S.S., van Schaik, C.P., Dominy, N.J., 2008. Functional ecology and evolution of hominoid molar enamel thickness: *Pan troglodytes schweinfurthii* and *Pongo pygmaeus wurmbii*. Journal of Human Evolution. 55, 60–74.

Vogel, E.R., Zulfa, A., Hardus, M.E., Wich, S.A., Dominy, N.J., Taylor, A.B., 2014. Food mechanical properties, feeding ecology, and the mandibular morphology of wild orangutans. Journal of Human Evolution.

Watts, D.P., 1984. Composition and variability of mountain gorilla diets in the central Virungas. American Journal of Primatology. 7, 323–356.

Williams, L., 1954. The feeding habits and food preferences of Acrididae and the factors which determine them. Transactions of the Royal Entomological Society of London. 105, 423–454.

Williams, S.H., Wright, B.W., Truong, V., Daubert, C.R., Vinyard, C.J., 2005. Mechanical properties of foods used in experimental studies of primate masticatory function. American Journal of Primatology. 67, 329–346.

Wright, B.W., Ulibarri, L., O'Brien, J., Sadler, B., Prodhan, R., Covert, H.H., Nadler, T., 2008. It's tough out there: Variation in the toughness of ingested leaves and feeding behavior among four Colobinae in Vietnam. International Journal of Primatology. 29, 1455–1466.

Yamashita, N., 1998. Functional dental correlates of food properties in five Malagasy lemur species. American Journal of Physical Anthropology. 106, 169–88.

Yamashita, N., 2003. Food procurement and tooth use in two sympatric lemur species. American Journal of Physical Anthropology. 121, 125–133.

Yamashita, N., Cuozzo, F.P., Sauther, M.L., 2012. Interpreting food processing through dietary mechanical properties: a Lemur catta case study. American Journal of Physical Anthropology. 148, 205–14.

Yépez, P., De La Torre, S., Snowdon, C.T., 2005. Interpopulation differences in exudate feeding of pygmy marmosets in Ecuadorian Amazonia. American Journal of Primatology. 66, 145–158.

Youlatos, D., Couette, S., Halenar, L.B., 2015. Morphology of howler monkeys: A review and quantitative analyses. In: Kowaleski, M., Garber, P.A., Cortes-Ortiz, L., Urbani, B., Youlatos, D. (Eds.), Howler Monkeys: Adaptive Radiation, Systematics, and Morphology. Springer, New York, pp. 133–176.

Zeininger, A.D., 2013. Ontogeny of Bipedalism: Pedal Mechanics and Trabecular Bone Morphology.

Chapter 4. Feeding time and trabecular structure in the primate mandibular condyle

4.1 Abstract

Repetitive loading of the mandible during mastication may select for morphological features associated with resisting fatigue failure. Data on repetitive loading or number of chewing cycles in extant primates are very limited, but average daily time spent feeding can be used as a rough proxy to explore relationships between feeding behavior and jaw morphology. This study tested the hypothesis that increased time spent feeding is associated with changes in the trabecular structure of the primate mandibular condyle. Image data from high-resolution X-ray computed tomography were collected for a sample of 28 primate mandibles from 16 anthropoid species. Three-dimensional trabecular parameters were calculated using Quant3D and BoneJ, and were then compared to data on feeding time of wild primates drawn from published activity budgets. Results yielded correlations between feeding time and some aspects of trabecular architecture, but these results appeared to be modulated by relationships among trabecular variables, feeding time, and jaw length. When mandible length was incorporated into analyses to control for differences in size, trabecular thickness, trabecular number, and structure model index showed significant relationships with feeding time. These results suggest a limited remodeling response to feeding time.

4.2 Introduction

The relationship between primate jaw form and diet has been extensively studied,

with inconsistent results. Developmental studies of primates and other mammals indicate a link between loading environment and mandibular morphology (Bouvier and Hylander, 1981, 1984; Corruccini and Beecher, 1982, 1984; Ravosa et al., 2007; Dias et al., 2011; Scott et al., 2014), suggesting that jaw form is indeed influenced by factors such as loading magnitude and frequency. Researchers have attempted to link diet with variations in cross-sectional corpus geometry (Daegling and Grine, 1991; Daegling, 1992; Schwartz and Conroy, 1996; Vinyard and Ryan, 2006), dental microwear (Ungar et al., 2008, 2010; Strait et al., 2012), enamel thickness (Olejniczak et al., 2008), and various aspects of external corpus morphology, particularly size and shape (Bouvier, 1986a; Taylor, 2002; Daegling and McGraw, 2007; Koyabu and Endo, 2009).

Many of these investigations have focused on jaw form in light of which types of foods a primate consumes: hard versus soft objects, leaves versus fruit. Recent interest in the study of the mechanical properties of primate diets (Darvell et al., 1996; Lucas et al., 2000; Lambert et al., 2004; Teaford et al., 2006; Dominy et al., 2008; Taylor et al., 2008; Norconk et al., 2009; Yamashita et al., 2009, 2012; Vogel et al., 2014) has offered a potential resolution to the question of the ways in which jaw form is influenced by diet. Mechanical properties are directly related to the processing of food during mastication (Agrawal et al., 1997, 1998; Williams et al., 2005), and the mechanical defenses of food items have been shown to influence mastication and jaw form in a variety of ways. Mechanically challenging foods produce larger jaw muscles and mandibular dimensions (Corruccini and Beecher, 1982; Bouvier and Hylander, 1984; Taylor et al., 2006; Ravosa et al., 2007). Food consistency impacts the amount of strain experienced by the mandible during mastication, such that softer foods create less strain than harder or tougher foods

(Hylander, 1979a), and food consistency is also known to correlate with cortical bone remodeling (Bouvier and Hylander, 1981).

However, while mechanical properties do appear to influence certain aspects of external mandibular morphology (Vogel et al., 2013), their overall impact on jaw form remains ambiguous (Ross et al., 2012). Factors that have little to do with chewing or food properties, such as adaptations for vocalizations (Riede et al., 2005; Youlatos et al., 2015), may have a large influence on mandibular morphology. Differences in corpus size related to allometry—that is, larger-bodied primates often have larger mandibles and more mechanically challenging diets—may account for differences in diet and the related differences in mechanical demands associated with mastication (Ravosa, 2000).

Consequently, specific feeding behaviors may have a greater influence on jaw morphology than do the types of foods consumed or the mechanical properties of those foods: *how* a food is eaten may be equally or more important than its physical properties. Specifically, average daily time spent chewing—or, even more accurately, the total number of chews per days—may generate epigenetic changes in jaw structure that are unrelated to the types of foods consumed and instead result from longer durations of masticatory loading. The repetitive loading cycles related to masticatory processing of tough or fibrous foods could generate an important selective pressure to avoid fatigue failure (Hylander, 1979b).

One possible approach to establishing correlations between feeding behavior and jaw form lies in studying the internal structure of the mandibular condyle of extant primates. The temporomandibular joint is directly loaded during feeding (Hylander, 1979a, 1979c; Brehnan et al., 1981; Mongini et al., 1981; Herring and Liu, 2001), and clinical (Giesen

et al., 2003, 2004) and experimental data (Ravosa et al., 2008; Scott et al., 2014) indicate that this loading influences the morphology of the mandibular condyle, both internally and externally. Because bone remodels during life in response to strain (Bouvier and Hylander, 1981; Rubin and Lanyon, 1984, 1985; Goldstein et al., 1991; Pontzer et al., 2006), an epigenetic signal may be found in the mandibular condyles and prove informative as to the relationship between feeding time and jaw form.

Relatively little research has focused on the morphology of the mandibular condyle. While a number of studies have addressed trabecular bone in the mandibular condyle in humans (Giesen and van Eijden, 2000; Giesen et al., 2001, 2004; van Ruijven et al., 2002, 2005; Renders et al., 2008), only one has investigated the mandibular condyle of non-human primates (Ryan et al., 2010) to test for trabecular signals related to tree-gouging behavior. No research has addressed the potential relationship between trabecular morphology in the mandibular condyle and any aspect of feeding behavior other than tree-gouging. Here, I use high-resolution X-ray computed tomography (HRXCT) to quantify the internal structure of the mandibular condyle and compare different architectural variables to feeding time averages for the species in my sample. Estimates of feeding time drawn from daily activity budgets are at best a rough proxy for time spent chewing, as feeding time estimates often include oral preparation and ingestion and do not account for differences in duration of chewing cycles. However, more detailed data are very limited (Williams et al., 2008; Ross et al., 2009a; b; Vinyard et al., 2012), and a broad, cross-species comparative analysis of chewing time and mandibular morphology is not possible at this time.

4.3 Hypotheses

The three-dimensional trabecular fabric variables included here are those commonly measured and reported in the literature. Bone volume fraction (BV/TV), degree of anisotropy (DA), elongation index (E), connectivity density (Conn.D), and structure model index (SMI) all contribute to the mechanical strength of trabecular bone (Goulet et al., 1994; Kabel et al., 1999; Mittra et al., 2005; Davison et al., 2006), although BV/TV and DA account for the majority of variations in elastic modulus (Galante et al., 1970; Townsend et al., 1975; Goldstein et al., 1993; Odgaard et al., 1997; Van Rietbergen et al., 1998; Ulrich et al., 1999; Giesen and van Eijden, 2000; Giesen et al., 2001; van Eijden et al., 2006). Trabecular thickness (Tb.Th), trabecular number (Tb.N), and trabecular spacing (Tb.Sp) are more descriptive and tend to covary with BV/TV (Mittra et al., 2005; Scherf, 2007; Cotter et al., 2009); thus, I do not present specific predictions about these latter variables. Instead, they are considered in conjunction with BV/TV.

Prediction 1. Bone volume fraction and feeding time. Longer durations of average daily time spent feeding should be correlated with denser trabecular bone in the mandibular condyle. Each chewing cycle consists of jaw occlusion and a single bite stroke, ending when the jaw opens again in preparation for the next cycle; as such, a greater number of chewing cycles entails a longer duration of work for the masticatory muscles, and thus a longer duration of loading for the mandibular condyle. Longer feeding times should thus be associated with mandibular condyles with greater trabecular volume.

Prediction 2. Degree of anisotropy and feeding time. Trabecular bone is oriented in the primary direction of force, and thus repetitive loading should result in more anisotropic

trabecular bone. I therefore predict that species with longer average feeding times will have more anisotropic trabecular bone within the mandibular condyle.

Prediction 3. Elongation index and feeding time. The elongation index provides an overall description of trabecular architecture. Trabecular bone can be rod-like or plate-like, and plates provide greater mechanical strength. Thus, repetitive loading should be associated with more plate-like trabecular bone, and I predict lower values for elongation index, indicating more plate-like trabecular bone.

Prediction 4. Connectivity density and feeding time. As connectivity contributes to trabecular strength, species that spend more time feeding should have higher measures of connectivity density.

Prediction 5. Structure model index and feeding time. Much like elongation index, the structure model index describes trabecular bone as plate-like or rod-like. Values for SMI will thus be lower in species with longer average feeding times, indicating stronger, plate-like trabeculae.

Prediction 6. Body size and trabecular structure. Previous research has demonstrated allometric relationships between body size and trabecular variables (Swartz et al., 1998; Cotter et al., 2009; Doube et al., 2011; Barak et al., 2013; Ryan and Shaw, 2013), such that larger animals tend to have fewer, thicker, more widely spaced, and less connected trabeculae. Postcranial trabecular bone is related to body size because of loading and because of size limits on architecture (i.e. trabecular bone in a small volume is structured differently than in a large volume). The mandibular condyle is loaded by feeding, not by locomotion, but I expect that relationships between feeding time and trabecular variables may be modulated by differences in body size, represented here by jaw length.

4.4 Materials & Methods

Sample

The sample used for this study consisted of HRXCT scans of 28 primate mandibles from 16 species (Table 4.1). The sample incorporated both platyrrhines and catarrhines. All specimens were wild-shot adult individuals, both male and female, from the collection at the National Museum of Natural History. Species included in the sample were selected based on the diversity of their diets and the availability of skeletal specimens and data on time spent feeding.

Scanning procedures

All specimens were scanned at the High-Resolution X-ray Computed Tomography Facility at the University of Texas at Austin. Specimens were scanned with energy settings of 150kV and 0.24mA with 8000 projections. Nominal scanning resolutions ranged from 0.0382 mm to 0.1784 mm with isotropic voxels. Between 661 and 937 slices were collected for each mandible. Images were reconstructed as 1024 x 1024 16-bit TIFF files, and were then converted to 8-bit images prior to analysis.

Because of the wide range of nominal resolutions included in the sample, higher-resolution images were artificially degraded to test for potential partial volume effects. Particularly at low resolutions, the presence of multiple substances (i.e. both air and bone) within one pixel or voxel produces averaging in the CT output (Ketcham and Ryan, 2004). In other words, a black pixel and a white pixel will be averaged together to produce a gray pixel. Results of trabecular analysis are thus highly dependent on nominal image resolution (Majumdar et al., 1996; Müller et al., 1996; Kothari et al., 1998; Peyrin

et al., 1998), and downsampling was thus used to enable comparison of images at disparate resolutions. The methodology used is described in detail in Chapter 3. Here, specimens of *Cebus apella, Cebus capucinus, Piliocolobus badius, Pithecia pithecia,* and *Saimiri sciureus* were downsampled to a nominal resolution of 0.0993 mm.

Three separate sub-samples were thus used for analysis. The first consisted of raw scan data. The second consisted of the sample including artificially degraded specimens. The third included artificially degraded specimens and excluded the hominoids scanned at a lower nominal resolution.

Volume of interest selection and image segmentation

The methods of VOI selection are described in Chapter 3 and will be briefly summarized here. I selected two separate VOIs: one that comprised the full volume of trabecular bone within the left mandibular condyle, and a second cube fitted to the maximum possible dimensions within the left condyle. The cubic VOI was used because both software programs used for analysis require symmetrical VOIs for most analyses. The full VOI was selected using external landmarks to insure systematic selection across individuals with different morphologies.

Segmentation of cortical from trabecular bone was performed using the Trainable Weka Segmentation plugin (Arganda-Carreras et al., 2011) for Fiji (Schindelin et al., 2012). Again, this technique is described in detail in Chapter 3. Trainable Weka Segmentation combines user inputs with machine learning algorithms to automatically classify images. This process enabled removal of the cortical shell from the condyle, which is necessary to insure that no cortical bone is included in image analyses, thereby

skewing results.

Trabecular bone analysis

Each VOI was analyzed for three-dimensional trabecular structure using Quant3D (Ryan and Ketcham, 2002) and the BoneJ plugin (Doube et al., 2010) in Fiji. These programs enable analysis of the most common measures of trabecular architecture, and were developed specifically for the purpose of calculating complex three-dimensional trabecular variables. All VOIs were thresholded with an iterative adaptive algorithm (Ridler and Calvard, 1978; Trussell, 1979) prior to analysis. Quant3D was used to calculate DA, E, and Tb.Th. BoneJ was used for BV/TV, Conn.D, SMI, Tb.Th, and Tb.Sp. Methods of trabecular bone analysis are described in more detail in Chapter 3.

Feeding time

Estimates of average daily time spent feeding were taken from the literature (Table 4.1). Because the skeletal sample was comprised of museum specimens, information on locality was often limited to the name of a country, precluding the use of more specific feeding time data. For this reason, I drew on multiple measures of feeding time for each species, when available, and took the average of these measures to approximate a species average.

I preferentially used annual feeding times that exclude time spent searching for or collecting food. Excluding foraging time underestimates feeding time for primates that eat large quantities of insect matter, which often feed continuously while foraging (e.g., Terborgh, 1983; Robinson, 1986). I elected to use the conservative approach of excluding

foraging time to more closely approximate actual time spent chewing. While many feeding time estimates do include ingestion and/or initial oral preparation, these behaviors load the mandible (Hylander, 1979c), such that estimates of feeding time drawn from activity budgets may more fully represent the cumulative loads generated during feeding than would a stricter (and as of yet unavailable) measure of time spent chewing.

Mandible length

Mandibular length (Table 4.1) was used to represent body size because the length of the mandible scales with body mass (Hylander, 1985; Bouvier, 1986b). In this case, mandible length is a more relevant size variable than is body mass because the mandible does not experience gravitational loads related to locomotion. Mandible length for each specimen was measured using Mitutoyo digital calipers. Measurements were taken as the length from infradentale to the posterior articular surface of the condyle. One specimen (male *Pongo abelii*) was not measured; consequently, this specimen is excluded from analyses including mandibular length.

Statistical analysis

To test for correlations and differences between raw and artificially degraded images, I used OLS regression ($\alpha = 0.05$). The downsampled images used for analysis provide an estimate with simulated partial volume effects. It is important to establish whether significant results are dependent on image resolution. I thus regressed trabecular variables calculated from raw images against those calculated from degraded images to test for

resolution effects.

Phylogenetic generalized least squares (PGLS) analysis was used to test relationships between feeding time and trabecular variables. I also used ordinary least squares (OLS) regressions to test relationships for which PGLS analysis yielded estimates of $\lambda > 0$. Following the method of Ryan and Shaw (2013), I also ran PGLS regressions that tested feeding time against the residuals of mandible length and each trabecular variable. Again, OLS was used to test results with $\lambda > 0$. OLS analysis for results with a phylogenetic signal allowed for interpretation of the influence of phylogeny on significant results.

PGLS analyses used the GenBank consensus tree from the 10kTrees website (http://10ktrees.nunn-lab.org/) (Arnold et al., 2010), which incorporates autosomal and mitochondrial DNA to estimate phylogenetic relationships and divergence dates for primate species. Because some species in the sample are not included in the GenBank database, I relied on published divergence dates for *Cebus apella* and *Cebus libidinosus* (400,000 years; Lynch Alfaro et al., 2012). The phylogenetic tree used for this study is shown in Figure 4.1.

All trabecular variables were natural logged prior to analysis except for tests of image resolution, which were conducted with untransformed values. Due to some negative values for SMI, which prevent log transformation, a constant was added to all values for SMI so that the smallest value was equal to one. Feeding time was logit transformed. Species means were used for all trabecular variables except to calculate the residuals of trabecular variables and mandible length, in which case individual observations were used and the residuals were subsequently averaged. All statistical analyses were performed using the R Statistical Programming Language version 3.1.0

(http://www.R-project.org). PGLS was performed using packages APE (Paradis et al., 2004) and caper (Orme et al., 2013).

4.5 Results

Trabecular variables from the raw and artificially degraded samples are presented in Tables 4.1 and 4.2. Results of regressions of raw and artificially degraded specimens are summarized in Table 4.3 and Figure 4.2. Statistical analyses of trabecular variables and feeding time are summarized in Tables 4.4-4.7.

Effects of image resolution

Estimates of BV/TV from the artificially degraded images were tightly correlated with estimates calculated from the raw scans ($p < 0.0001$, $R^2 = 0.939$) (Figure 4.2A). The intercept was not significantly different from zero, and the slope was not significantly different from one, indicating no bias.

Trabecular thickness also showed high correlation between the raw and degraded samples ($p < 0.0001$, $R^2 = 0.989$) (Figure 4.2B). In general, estimates of Tb.Th from the degraded sample were higher than from the raw sample, indicating some resolution effects; the slope was greater than one and the intercept was greater than zero.

Likewise, estimates of Tb.N from the raw and degraded samples were correlated ($p = 0.002$, $R^2 = 0.829$) (Figure 4.2C). Overall estimates of Tb.N from the degraded sample were slightly higher than from the raw sample, although the intercept was not significantly different from zero.

Raw and degraded values for Tb.Sp were also correlated ($p = 0.008$, $R^2 = 0.717$)

(Figure 4.2D). The intercept was greater than zero and the slope was less than one, and values for the degraded sample were slightly lower than for the raw sample.

Degree of anisotropy showed correlation between the raw and degraded sample (p = 0.014, R^2 = 0.659) (Figure 4.2E). The slope was not significantly different from one and the intercept was not significantly different from zero, although standard error for the intercept was high (1.999).

The raw and degraded samples for elongation index were also correlated (p = 0.035, R^2 = 0.548) (Figure 4.2F). The intercept was not significantly different from zero and the slope was not significantly different from one.

Connectivity density was strongly positively correlated between the raw and degraded samples ($p < 0.0001$, R^2 = 0.940) (Figure 4.2G). The slope was not significantly different from one and the intercept was not significantly different from zero.

Structure model index showed no correlation between the raw and degraded images (p = 0.121, R^2 = 0.352) (Figure 4.2H).

Results of linear regression

Feeding time and BV/TV were positively correlated in the raw sample and the degraded sample without hominoids (Table 4.4). Results from the degraded sample were not significant and showed a phylogenetic signal (λ = 1), and OLS results yielded a positive relationship between feeding time and BV/TV in the degraded sample (Table 4.5).

Feeding time and Tb.Th were positively correlated in the raw sample (Figure 4.3A) (Table 4.4), the sample including artificially degraded specimens (Figure 4.3B), and the

degraded sample without hominoids (Figure 4.3C). The artificially degraded sample showed a phylogenetic signal ($\lambda = 1$), and OLS analysis showed a stronger relationship between Tb.Th and feeding time for the degraded sample ($p < 0.0001$, $R^2 = 0.705$) (Table 5) than did PGLS ($p = 0.002$, $R^2 = 0.498$).

Trabecular number and feeding time were negatively correlated in the degraded sample, the artificially degraded sample, and the sample excluding hominoids (Table 4.4) (Figure 4.4). No phylogenetic signal was present in these relationships.

Feeding time and Tb.Sp were positively correlated in the raw sample and the sample including artificially degraded specimens (Table 4.3). No phylogenetic signal was present ($\lambda = 0$).

Feeding time and Conn.D were negatively correlated in the raw sample and the artificially degraded sample (Table 4.4). No phylogenetic signal was present.

There were no relationships between feeding time and DA, E, or SMI. Phylogenetic signal was present for DA in the raw and degraded samples. When OLS was run for DA, there was still relationship between DA and feeding time (Table 4.5).

Results of linear regression using residual measures

Bone volume fraction was positively related to feeding time only in the sample excluding hominoids (Table 4.6). Feeding time and BV/TV showed phylogenetic signal in the artificially degraded sample ($\lambda = 1$), but OLS analysis yielded no relationship (Table 4.7).

Trabecular thickness and feeding time were positively related in the sample including artificially degraded specimens and the sample excluding hominoids (Table 4.6) (Figure

4.5). Phylogenetic signal was present in the raw and degraded samples, and in the sample excluding hominoids. OLS results showed a positive relationship between Tb.Th and feeding time in all three samples (Table 4.7).

Feeding time and Tb.N were negatively related in the degraded sample and the sample excluding hominoids (Table 4.6). Phylogenetic signal was present in all three samples. OLS analysis eliminated the relationship in the raw sample (Table 4.7), suggesting clade shifts, although no clear trend is visible in the regression (Figure 4.6).

Feeding time and SMI were positively related in the degraded sample and the sample excluding hominoids (Table 4.6). No phylogenetic signal was present.

There were no relationships between feeding time and Tb.Sp, DA, E, or Conn.D. Phylogenetic signal was present in many of these relationships (Table 4.6). OLS analysis did not yield any significant results (Table 4.7).

4.6 Discussion

Effects of image resolution

In general, resolution dependency effects were similar to what has been found in previous studies. Image resolutions that are close to the average thickness of trabeculae (~150 μm) produce partial volume effects (blurring) and thus overestimate some trabecular parameters and underestimate others (see Chapter 3). Estimates of Tb.Th from the degraded sample were higher than those from the raw sample, which is in accordance with what would be expected based on previous results (Müller et al., 1996), although measurement of trabecular variables is contingent on thresholding and different responses to low resolutions have been noted (Majumdar et al., 1996). Similarly, Tb.Sp has been

found to decrease as resolution decreases (Kothari et al., 1998), and the same pattern was present in the current study. In contrast, previous findings that Tb.N is underestimated by lower-resolution scans (Müller et al., 1996) were not supported in the current study, in which values for Tb.N were higher in the degraded sample. BV/TV, DA, E, and Conn.D showed no systematic bias, indicating that these variables were not impacted by nominal resolution in the current study.

The results of this study must be considered in light of the potential resolution dependency of estimates of trabecular parameters. The raw and degraded values for SMI were not correlated, but all other variables were positively correlated (Table 4.3). However, aside from BV/TV, DA, E, and Conn.D, all other trabecular variables showed some influence of nominal resolution. Thus, while the raw sample is preferred for interpretation of relationships between BV/TV, DA, E, and Conn.D and feeding time, the artificially degraded sample excluding hominoids is preferred for all other trabecular variables. In particular, SMI is highly dependent on resolution in the current sample, and results for this variable from the raw sample should not be relied upon.

Thus, interpretation of results depends on the specific variable. As the raw sample is preferred for BV/TV, and PGLS analysis of the raw sample indicated a positive relationship between feeding time and BV/TV, results suggest that BV/TV is sensitive to time spent feeding. Likewise, because the degraded sample excluding hominoids is preferred for Tb.Sp, the lack of a relationship between Tb.Sp and feeding time in that sample will be given priority over the significant relationships from the raw and degraded samples. These results generally suggest some effect of sampling or image resolution on trabecular relationships. More specifically, the low-resolution hominoids may have

skewed the results, suggesting that high-resolution scans are important to accurately understanding the relationship between feeding time and trabecular architecture. These results may also indicate simply that the relationship between most aspects of mandibular condylar trabecular bone and feeding time across primates is weak, and that a relationship can only be seen within certain taxa (although PGLS analysis found no phylogenetic signal with Tb.Sp). It is also important to note that the artificially degraded specimens provide a simulation of specimens scanned at lower resolutions, but the downsampling protocol used certainly introduces some error to the images. Thus, a conservative interpretation of the relationships that are not significant across all sub-samples must consider these results inconclusive.

Even with mixed results, the nature of trabecular relationships with feeding time demonstrates the interdependence of trabecular variables. In the sample with artificially degraded specimens, the variables that contribute to BV/TV—Tb.Th, Tb.N, and Tb.Sp—have different directions: Tb.Th and Tb.Sp are positively correlated with feeding time, but Tb.N is negatively correlated. Thus, as feeding time increases, trabeculae become thicker, more widely spaced, and fewer in number. Conn.D is also negatively correlated with feeding time in the raw and artificially degraded samples. The directions of these relationships are what we would expect based on body size (Doube et al., 2011; Ryan and Shaw, 2013).

Trabecular response to feeding time

Feeding time and Tb.Th were positively correlated, and feeding time and Tb.N were negatively correlated, across all three samples (Table 4.4), suggesting relationships that

are not dependent on nominal image resolution. These results can likely be interpreted as meaningful indicators of trabecular variation in response to feeding time. Tb.N is in part a consequence of Tb.Th—all else being equal, thicker trabeculae are typically fewer in number—and thus it is unsurprising that both of these variables are related to feeding time.

Feeding time likely represents an important constraint on primate behavioral and functional adaptations. Primates must meet their nutritional and caloric needs, but are limited in how much time they can devote to feeding both by the limited numbers of hours in the day and the demands of other behaviors (Dunbar, 1992; Korstjens et al., 2006, 2010; Korstjens and Dunbar, 2007; Dunbar et al., 2009). Tooth and jaw morphology likely experience selection pressures to help primates process their diets more efficiently so as to minimize the time requirements of feeding while maximizing energy intake, although gut adaptations certainly play an important role as well (Milton, 1981, 1984; Milton and McBee, 1983; Lambert, 1998; Mau et al., 2011; Amato et al., 2014).

The correlations seen here between feeding time and trabecular structure in the mandibular condyle suggest a functional relationship between three-dimensional trabecular parameters and average feeding time in primates. Repetitive loading may be necessary to process certain food items, and this type of masticatory loading exposes the mandible to possible fatigue failure (Hylander, 1979b). Changes in trabecular volume and structure may thus provide the load resistance capabilities necessary for the mandibular condyle to withstand greater durations of masticatory loading.

Feeding time, jaw length, and body size

It is important to consider other potential influences on trabecular architecture that may be partially driving the apparent relationship with feeding time. As mentioned, one possibility is a relationship between feeding time and body mass (see Chapter 2). Consequently, it is possible that a scaling relationship between body mass and trabecular architecture is at least partly responsible for the relationships between feeding time and trabecular variables.

Some research has addressed the relationship between body size and three-dimensional trabecular architecture. Some studies of three-dimensional trabecular scaling in mammals showed no relationship between BV/TV and body size (Cotter et al., 2009; Barak et al., 2013), but another found allometry (Doube et al., 2011), and a study of primates showed allometric scaling of BV/TV in the humerus and femur (Ryan and Shaw, 2013). Postcranial data show allometric scaling of Tb.Th (Doube et al., 2011; Ryan and Shaw, 2013) and other structural variables. It is possible that different parts of the body show different scaling, and trabecular bone in the mandibular condyle may show a relationship with body size.

Jaw length was thus included in analyses as a control for body size. When PGLS regressions of feeding time versus the residuals of trabecular variables and mandibular length were performed, the results were quite different from regressions without the residuals. None of the relationships between feeding time and trabecular structure in the raw sample were significant when residuals were incorporated (Table 4.6). The relationships with Tb.Th and Tb.N were maintained in the artificially degraded sample and the sample excluding hominoids, and the strength of the relationships between Tb.Th

and feeding time in those samples increased. Feeding time and SMI were also related in the degraded sample and the degraded sample excluding hominoids.

It thus seems likely that trabecular architecture is impacted by a complex network of relationships among body mass, jaw length, and feeding time. Mandibular length in my sample is correlated with every trabecular variable except for SMI, and it is also related to body mass (OLS $p < 0.0001$, $R^2 = 0.914$) and to feeding time (OLS $p = 0.005$, $R^2 = 0.439$). The relationships between feeding time and trabecular variables demonstrated here may in fact have little to do with feeding time and are instead a product of variations in body size. Although modeling the mandible as a lever is an oversimplification, increases in body size are theoretically linked to increases in force production (Demes and Creel, 1988; Wroe et al., 2005), and thus changes in trabecular structure within the mandibular condyle may be more closely related to maximum loading (associated with jaw length) than to duration of loading (related to feeding).

Complexity of functional relationships

One major difficulty in interpreting functional relationships between diet and jaw form is the multitude of potential confounding factors. Here, specifically, I am considering the possible epigenetic effects of time spent feeding, i.e. the duration of loading. The problem is how to disentangle effects related to feeding (duration) from effects related to food mechanical properties, i.e. the magnitude of loading. Animals likely chew longer on tougher foods (Hylander, 1979a), and morphological responses to repetitive loading may not be easily distinguishable from responses to periodic high loads (Hylander, 1979b), such as those associated with some fallback foods (Lambert et al.,

2004; Lucas et al., 2009; Vogel et al., 2009). Yamashita (2003) argues that "masticatory" toughness (FMPs experienced during chewing) appears to have a greater influence on craniomandibular morphology than does "ingestive" toughness (FMPs experienced during incision and ingestion). Some research has focused on the relationship between FMPs and chewing time (Ross et al., 2009b), but more and better data on feeding and chewing time and FMPs in wild primate populations are needed to establish any consistent, cross-species patterns. Nonetheless, the results presented here show multiple promising relationships between feeding time and trabecular structure in the mandibular condyle, and may yield new information about feeding behavior and daily activity budgets of fossil specimens.

Taken in conjunction with the results from Chapter 3, which showed a positive and phylogenetic relationship between DA and toughness, the relationships shown here suggest different controls on various aspects of trabecular architecture in the mandibular condyle. While DA appears to be determined to some extent by taxonomic relationships, Tb.Th and Tb.N seem to be sensitive to loading regimes during life independent of phylogeny. These density-related variables may thus provide a meaningful cross-primate signal of feeding behavior that is diagnostic even outside the context of phylogenetic analyses.

4.7 Conclusion

The results presented here suggest multiple potential relationships between the trabecular architecture of the mandibular condyle and average daily time spent feeding in extant primates. As feeding time increases, trabecular thickness increases and trabecular

number decreases. These relationships withstand efforts to control for image resolution dependency by artificially degrading higher-resolution specimens. Other aspects of trabecular architecture, including bone volume fraction, trabecular spacing, connectivity density, and structure model index, show some relationship to feeding time, but appear to be influenced to some degree by image resolution. However, body size appears to modulate the relationships between trabecular parameters and feeding time, and when mandible length is included in analyses to control for body size, there are no consistent relationships with feeding time across all three image samples.

Further research into the relationships among feeding time, chewing time, FMPs, and the trabecular architecture of the mandibular condyle may provide further support for the remodeling response suggested by my results. A controlled feeding experiment that regulates time spent chewing would provide direct evidence of the remodeling relationship between repetitive loading and trabecular architecture. More indirectly, careful quantification of time spent chewing among wild primates would generate useful field data for cross-species comparisons. The results of this study represent a promising direction for eventual comparison with fossil specimens.

Table 4.1. Specimen information and feeding time data, along with results of BoneJ and Quant3D analyses for the sample of raw, undegraded images.

Species	Catalog #	Sex	Locality	Feeding time (%)	Mandible length (mm)	BV/TV	Tb.Th (mm)	Tb.N (mm^{-1})	Tb.Sp (mm)	DA	E	Conn.D (mm^{-3})	SMI
Alouatta palliata	543117	M	Panama	14.89 [13–15]	91.85	0.428	0.344	2.001	0.457	3.808	0.450	4.027	-0.028
Alouatta palliata	339925	F	Nicaragua	14.89	76.81	0.526	0.357	1.985	0.395	3.501	0.436	3.604	0.029
Alouatta seniculus	398507	F	Colombia	17.25 [23,24]	77.22	0.512	0.333	2.334	0.373	4.076	0.389	5.512	0.253
Ateles paniscus	545853	M	Brazil	23.95 [25,26]	79.07	0.411	0.333	1.782	0.518	6.752	0.577	2.534	0.941
Ateles paniscus	545885	F	Brazil	23.95	70.34	0.473	0.409	1.393	0.607	4.581	0.708	1.279	0.69
Cebus apella	461384	M	Brazil	16 [21]	58.3	0.466	0.295	2.083	0.311	8.321	0.480	3.321	0.438
Cebus apella	388197	F	Venezuela	16	57.44	0.452	0.293	1.915	0.457	3.487	0.421	3.401	0.805
Cebus capucinus	152130	F	Costa Rica	25.8 [27]	53.32	0.521	0.308	2.021	0.377	7.267	0.585	5.294	1.383
Cebus libidinosus	518414	M	Brazil	18.2 [1]	60.85	0.424	0.336	1.695	0.471	12.464	0.198	2.705	0.665
Cebus libidinosus	518418	F	Brazil	18.2	55.05	0.507	0.326	1.582	0.506	8.985	0.264	1.764	1.12
Colobus polykomos	481786	F	Liberia	28 [2]	77.96	0.578	0.372	1.914	0.384	5.674	0.472	4.057	0.888
Colobus polykomos	477320	F	Cote d'Ivoire	28	77.33	0.487	0.418	1.529	0.476	13.597	0.255	1.44	0.427
Lophocebus albigena	598484	M	Equatorial Guinea	36.42 [3–5]	83.15	0.563	0.422	1.611	0.459	7.334	0.462	2.177	0.621
Lophocebus albigena	598485	F	Equatorial Guinea	36.42	83.51	0.482	0.452	1.199	0.689	6.079	0.308	0.624	0.675

Macaca fascicularis	114506	M	Sumatra	23.57 [6–8]	78.72	0.550	0.328	1.882	0.417	8.466	0.397	4.313	0.754
Macaca fascicularis	114165	F	Sumatra	23.57	73.88	0.635	0.333	2.116	0.320	7.087	0.505	4.834	0.519
Pan troglodytes schweinfurthii	236971	F	Uganda	44.77 [9–11]	123.72	0.529	0.594	1.287	0.567	2.326	0.186	1.468	0.727
Piliocolobus badius	481792	F	Liberia	30.54 [10,12]	66.7	0.662	0.304	0.934	0.370	6.301	0.498	5.717	1.18
Pithecia pithecia	546265	F	Brazil	32.73 [16]	47.78	0.493	0.274	2.133	0.529	6.934	0.200	5.437	1.473
Pithecia pithecia	339658	M	Guyana	32.73	46.55	0.509	0.276	2.186	0.356	9.023	0.644	6.335	1.279
Pongo abelii	143588	M	Sumatra	54.45 [17,18]	--	0.541	0.889	0.808	0.582	2.681	0.249	0.309	-1.237
Pongo abelii	143596	F	Sumatra	54.45	131.96	0.557	0.726	1.048	0.798	2.654	0.471	0.568	-0.081
Pygathrix nigripes	320783	F	Vietnam	27.1 [19]	73.37	0.433	0.358	1.649	0.542	9.536	0.503	2.854	1.898
Pygathrix nigripes	257998	F	Vietnam	27.1	68.1	0.557	0.367	1.847	0.352	10.617	0.624	2.056	0.252
Saimiri sciureus	547905	M	Brazil	12.67 [20,21]	33.94	0.360	0.148	3.663	0.264	8.7016	0.441	20.533	1.278
Saimiri sciureus	547903	F	Brazil	12.67	31.75	0.327	0.152	3.396	0.302	7.595	0.411	23.127	1.123
Trachypithecus phayrei	307737	M	Thailand	25.85 [10,22]	72.43	0.557	0.369	1.819	0.370	8.558	0.319	2.643	0.271
Trachypithecus phayrei	307736	F	Thailand	25.85	69.33	0.495	0.325	1.999	0.356	14.879	0.543	4.438	1.188

1. Sabbatini et al., 2008. 2. Dasilva, 1992. 3. Poulsen et al., 2001. 4. Waser, 1984. 5. Freeland, 1979. 6. Van Schaik et al., 1983. 7. Sussman et al., 2011. 8. Aldrich-Blake, 1980. 9. Lehmann et al., 2008. 10. Chapter 2. 11. Wrangham, 1977. 12. Clutton-Brock, 1974. 13. Milton, 1980. 14. Raguet-

Schofield, 2010. 15. Estrada et al., 1999. 16. Setz et al., 2013. 17. Fox et al., 2004. 18. Morrogh-Bernard et al., 2007. 19. Rawson, 2009. 20. Pinheiro et al., 2013. 21. Terborgh, 1983. 22. Koenig et al., 2004. 23. Gaulin and Gaulin, 1982. 24. Braza et al., 1981. 25. Wallace, 2001. 26. Symington, 1988. 27. Rose, 1998.

Table 4.2. Results of BoneJ and Quant3D analyses for the sample of artificially degraded specimens.

Species	Catalog #	BV/TV	Tb.Th (mm)	Tb.N (mm^{-1})	Tb.Sp (mm)	DA	E	Conn.D (mm^{-3})	SMI
Cebus apella	461384	0.436	0.315	2.075	0.318	8.185	0.591	3.171	0.581
Cebus apella	388197	0.489	0.312	1.914	0.457	2.821	0.287	3.005	0.897
Cebus capucinus	152130	0.469	0.328	1.925	0.379	7.133	0.584	3.274	1.423
Piliocolobus badius	481792	0.633	0.329	1.912	0.376	7.279	0.576	4.94	1.212
Pithecia pithecia	546265	0.471	0.309	2.124	0.402	5.777	0.278	5.025	1.689
Pithecia pithecia	339658	0.491	0.297	1.998	0.379	9.538	0.687	5.801	1.451
Saimiri sciureus	547905	0.325	0.207	3.333	0.281	6.317	0.569	22.156	2.418
Saimiri sciureus	547903	0.290	0.199	3.237	0.301	5.589	0.644	18	2.613

Table 4.3. Comparison of trabecular variables for degraded versus undegraded specimens. Significant results are indicated in bold.

Variable	*F*	df	Slope	Intercept	R^2	*p*
BV/TV	93.200	1, 6	0.997	-0.022	0.939	**<0.0001**
Tb.Th	560.3	1, 6	0.791	0.084	0.989	**<0.0001**
Tb.N	29.11	1, 6	0.636	0.858	0.829	**0.002**
Tb.Sp	15.2	1, 6	0.571	0.149	0.717	**0.008**
DA	11.63	1, 6	0.923	-0.066	0.659	**0.014**
E	7.284	1, 6	0.871	0.127	0.548	**0.036**
Conn.D	94.09	1, 6	0.917	-0.214	0.940	**<0.0001**
SMI	3.257	1, 6	1.215	0.175	0.352	0.121

Table 4.4. PGLS analysis of trabecular parameters and feeding time. All measures were logged before analysis. A constant value (1.659) was added to estimates of SMI for the raw and degraded samples so that the smallest value was equal to one. Significant results are indicated in bold.

	Raw sample (df = 1, 14)					Degraded sample					No hominoids				
Dependent variable	*F*	λ	Slope	R^2	*p*	*F*	λ	Slope	R^2	*p*	*F*	λ	Slope	R^2	*p*
BV/TV	6.05	0.036	0.138	0.302	**0.028**	1.807	1.000	0.093	0.114	0.200	6.980	0.000	0.242	0.368	**0.021**
Tb.Th	23.85	0.000	0.500	0.630	**<0.001**	13.91	1.000	0.338	0.498	**0.002**	7.019	0.000	0.253	0.369	**0.021**
Tb.N	19.24	0.000	-0.447	0.579	**<0.001**	29.88	0.000	-0.401	0.681	**<0.0001**	7.889	0.000	-0.304	0.397	**0.016**
Tb.Sp	15.13	0.000	0.289	0.519	**0.002**	13.09	0.000	0.276	0.483	**0.003**	2.575	0.000	0.185	0.177	0.135
DA	1.608	0.735	-0.308	0.103	0.226	0.917	0.722	-0.235	0.061	0.354	3.742	0.000	0.409	0.238	0.077
E	1.002	0.000	-0.145	0.067	0.334	1.528	0.000	-0.189	0.098	0.237	0.109	0.000	0.063	0.009	0.746
Conn.D	14.51	0.000	-1.073	0.509	**0.002**	16.45	0.000	-1.060	0.540	**0.001**	3.889	0.000	-0.759	0.245	0.072
SMI	2.449	0.000	-0.320	0.149	0.140	0.065	0.000	-0.038	0.005	0.802	1.742	0.000	1.779	0.127	0.212

Table 4.5. OLS comparison of trabecular variables and time spent feeding for PGLS results that showed $\lambda > 0$. All measures were logged before analysis. Significant results are indicated in bold.

	Raw sample (df = 1, 14)				Degraded sample (df = 1, 14)				No hominoids sample (df = 1, 12)			
Dependent variable	*F*	Slope	R^2	*p*	*F*	Slope	R^2	*p*	*F*	Slope	R^2	*p*
BV/TV	6.751	0.143	0.325	**0.021**	6.466	0.157	0.316	**0.023**	--	--	--	--
Tb.Th	--	--	--	--	33.49	0.449	0.705	**<0.0001**	--	--	--	--
Tb.N	--	--	--	--	--	--	--	--	--	--	--	--
Tb.Sp	--	--	--	--	--	--	--	--	--	--	--	--
DA	2.382	-0.327	0.145	0.145	1.398	-0.256	0.091	0.257	--	--	--	--
E	--	--	--	--	--	--	--	--	--	--	--	--
Conn.D	--	--	--	--	--	--	--	--	--	--	--	--
SMI	--	--	--	--	--	--	--	--	--	--	--	--

Table 4.6. PGLS analysis of feeding time and the residuals of mandible length and trabecular parameters. All measures were logged before analysis. Significant results are indicated in bold.

	Raw sample (df = 1, 14)					Degraded sample					No hominoids				
Dependent variable	*F*	λ	Slope	R^2	*p*	*F*	λ	Slope	R^2	*p*	*F*	λ	Slope	R^2	*p*
BV/TV	0.105	0.000	0.008	0.007	0.751	0.468	1.000	0.045	0.032	0.505	5.319	0.000	0.154	0.307	**0.039**
Tb.Th	0.184	0.952	0.029	0.013	0.675	27.69	0.977	0.193	0.664	**0.0001**	21.2	0.932	0.186	0.639	**<0.001**
Tb.N	0.571	1.000	-0.066	0.039	0.463	6.917	0.515	-0.187	0.331	**0.019**	7.164	0.403	-0.251	0.374	**0.020**
Tb.Sp	0.025	0.996	-0.016	0.002	0.876	4.340	0.239	0.157	0.237	0.056	1.621	0.122	0.130	0.119	0.227
DA	1.784	0.000	0.236	0.113	0.203	0.245	0.556	-0.106	0.017	0.629	4.179	0.000	0.424	0.258	0.064
E	0.339	0.000	0.072	0.024	0.569	0.009	0.000	0.015	0.001	0.923	0.237	0.000	0.092	0.019	0.635
Conn.D	0.130	0.991	-0.082	0.009	0.724	4.453	0.781	-0.566	0.241	0.053	4.754	0.721	-0.722	0.284	0.050
SMI	<0.001	0.000	0.001	<0.001	0.995	4.853	0.000	0.175	0.257	**0.045**	14.33	0.000	0.279	0.544	**0.003**

Table 4.7. OLS comparison of time spent feeding and the residuals of trabecular variables and mandible length, for PGLS results with $\lambda > 0$. All measures were logged before analysis. Significant results are indicated in bold.

	Raw sample (df = 1, 14)				Degraded sample (df = 1, 14)				No hominoids sample (df = 1, 12)			
Dependent variable	*F*	Slope	R^2	*p*	*F*	Slope	R^2	*p*	*F*	Slope	R^2	*p*
BV/TV	--	--	--	--	0.225	0.027	0.016	0.642	--	--	--	--
Tb.Th	5.79	0.105	0.293	**0.031**	14.19	0.135	0.503	**0.002**	10.13	0.132	0.458	**0.008**
Tb.N	3.664	-0.130	0.207	0.076	4.888	-0.132	0.259	**0.044**	5.251	-0.198	0.304	**0.041**
Tb.Sp	1.996	0.111	0.125	0.178	2.528	0.109	0.153	0.134	0.946	0.095	0.073	0.349
DA	--	--	--	--	0.038	-0.037	0.003	0.848	--	--	--	--
E	--	--	--	--	--	--	--	--	--	--	--	--
Conn.D	1.163	-0.221	0.077	0.299	1.734	-0.281	0.110	0.209	2.261	-0.468	0.159	0.159
SMI	--	--	--	--	--	--	--	--	--	--	--	--

Figure 4.1. Phylogenetic tree used for PGLS. The consensus tree was taken from the 10kTrees website (Arnold et al., 2010) and pruned to fit the sample.

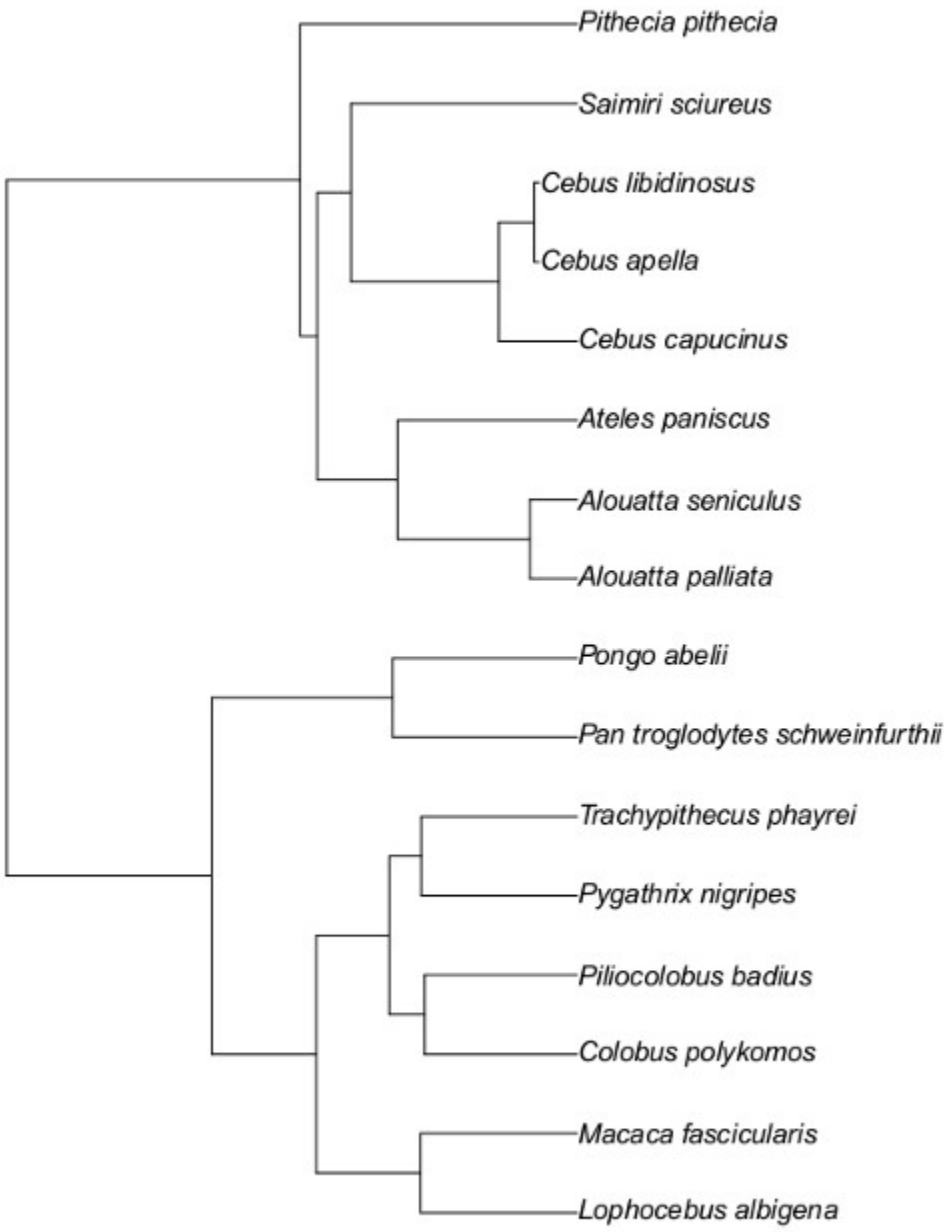

Figure 4.2. Plots of trabecular parameters from raw images (x axis) against parameters from artificially degraded images (y axis). Data points are identified by taxon (shaded teal triangles = cercopithecoids, purple squares = platyrrhines).

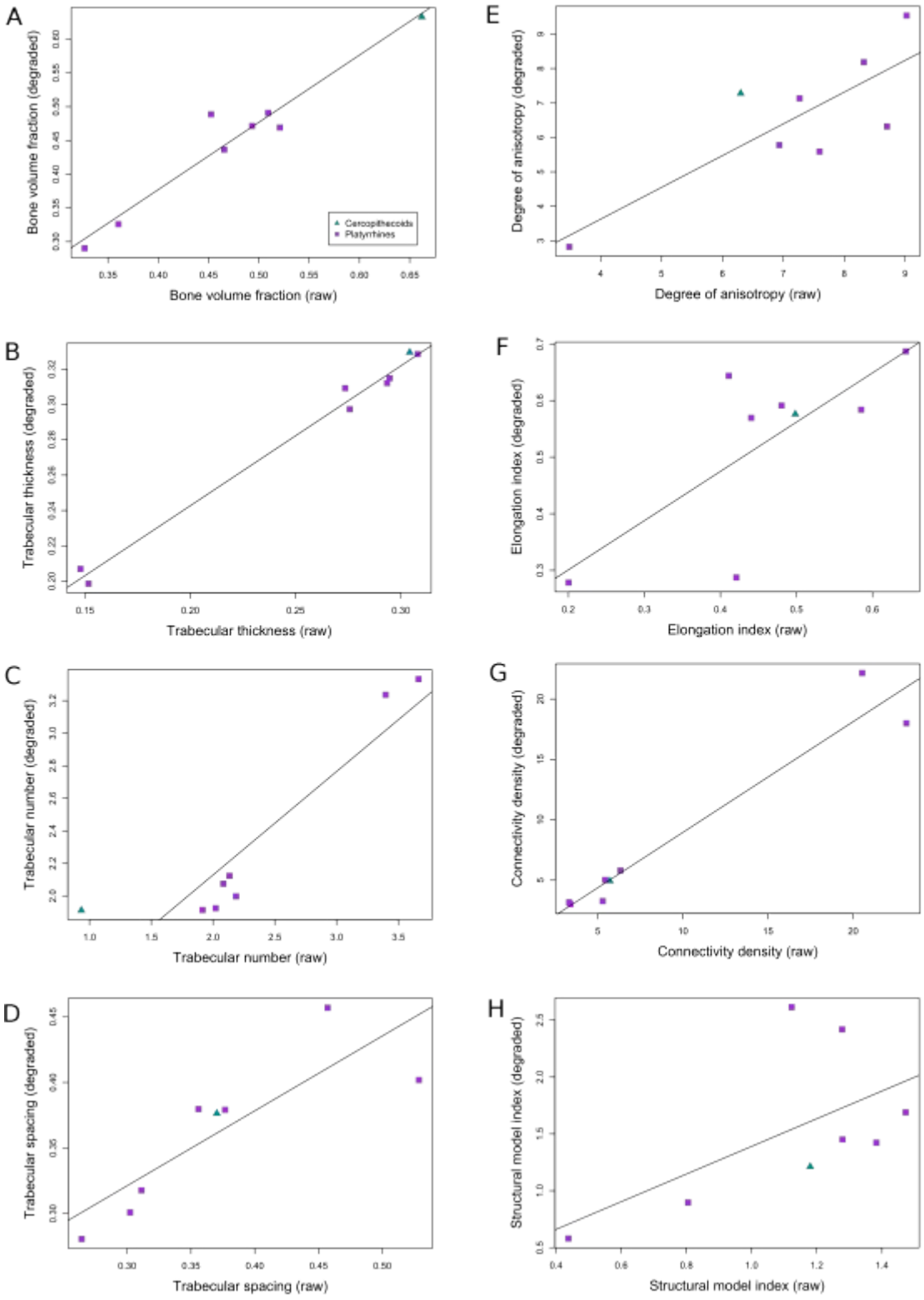

Figure 4.3. Regressions of trabecular thickness and feeding time. The OLS slopes are shown. Species are grouped by taxon, with cercopithecoids represented by teal triangles, hominoids by red triangles, and platyrrhines by purple squares.

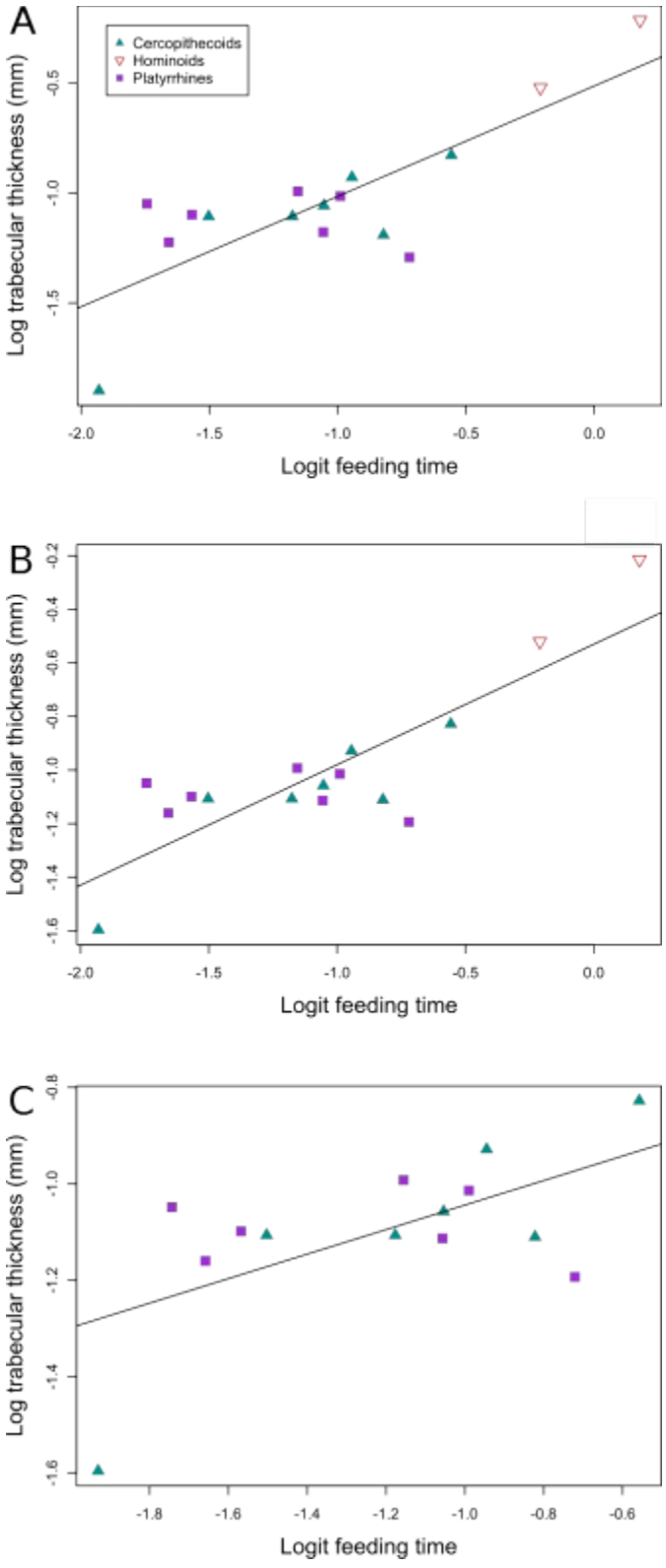

Figure 4.4 Regressions of trabecular number and feeding time. The OLS slopes are shown.

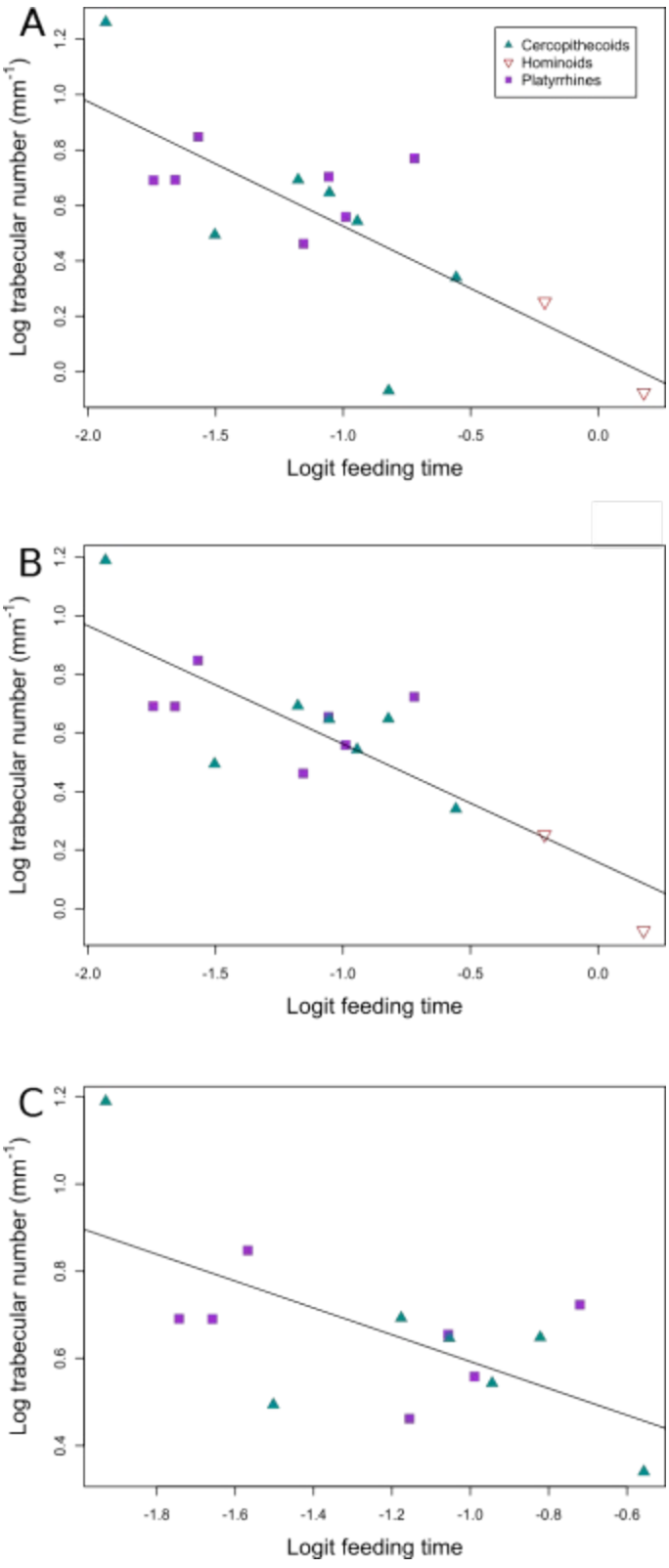

Figure 4.5. Regressions of feeding time and the residuals of trabecular thickness and mandible length. The OLS slopes are shown.

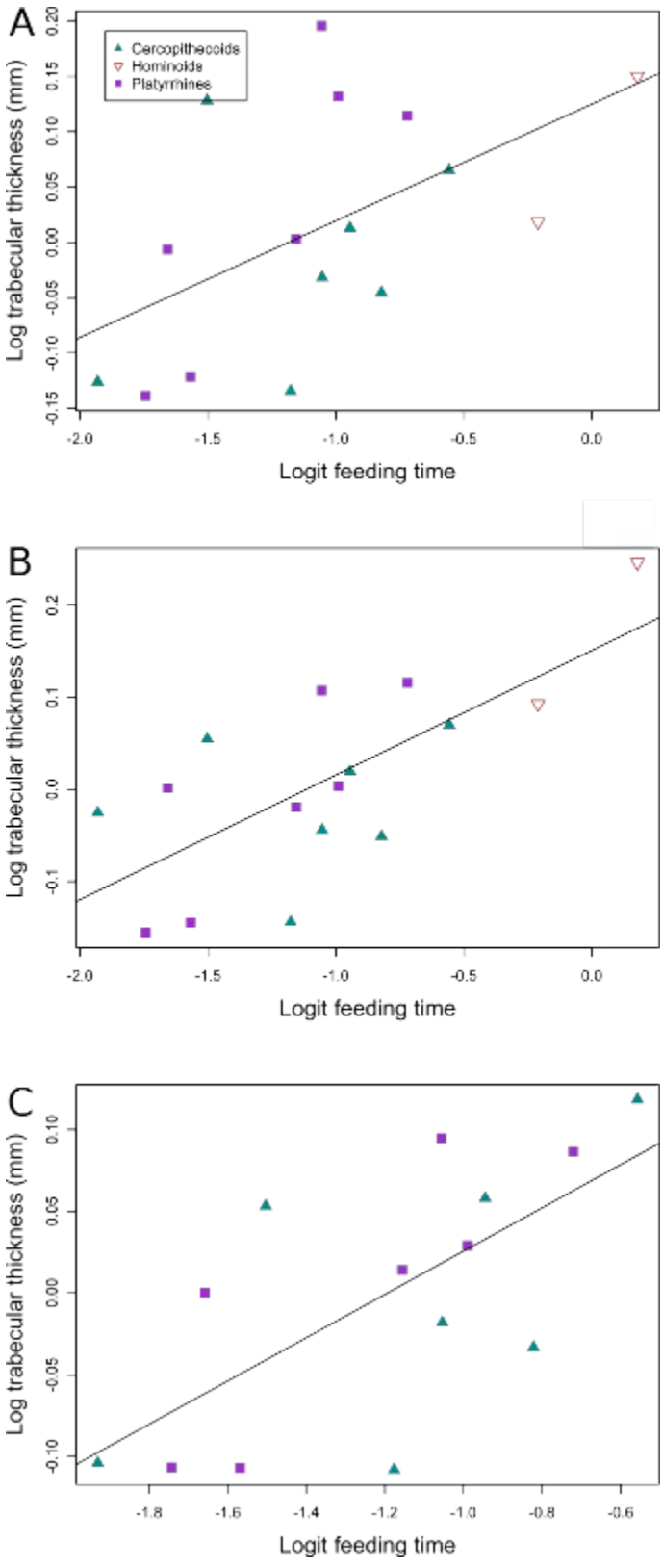

Figure 4.6. Regressions of feeding time and the residuals of trabecular number and mandible length. The OLS slopes are shown.

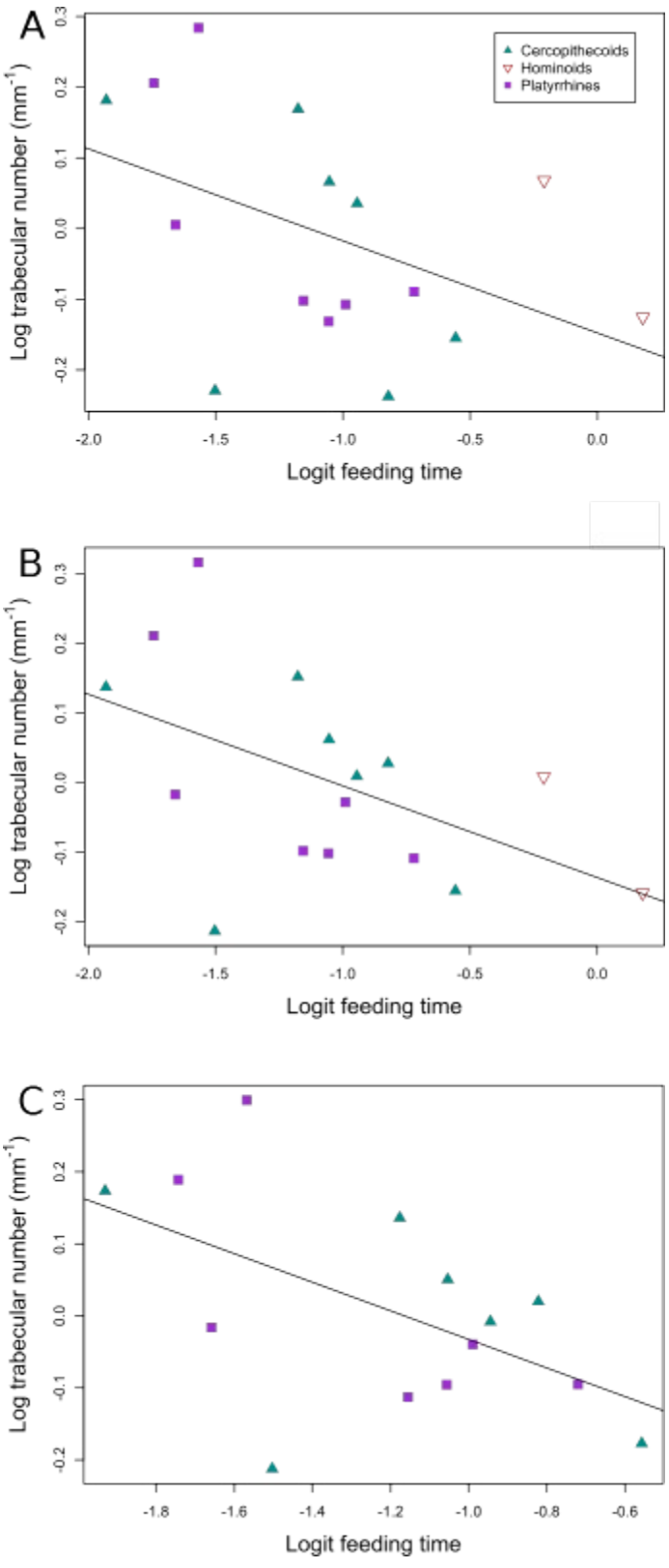

References

Agrawal KR, Lucas PW, Bruce I, Prinz J. 1998. Food properties that influence neuromuscular activity during human mastication. J Dent Res 77:1931–1938.

Agrawal KR, Lucas PW, Prinz J, Bruce I. 1997. Mechanical properties of foods responsible for resisting food breakdown in the human mouth. Arch Oral Biol 42:1–9.

Aldrich-Blake F. 1980. Long-tailed macaques. In: Chivers DJ, editor. Malayan Forest Primates: Ten Years' Study in the Tropical Rainforest. New York: Plenum. p 147–165.

Amato KR, Leigh SR, Kent A, Mackie RI, Yeoman CJ, Stumpf RM, Wilson B a, Nelson KE, White BA, Garber PA. 2014. The role of gut microbes in satisfying the nutritional demands of adult and juvenile wild, black howler monkeys (*Alouatta pigra*). Am J Phys Anthropol 155:652–64.

Arganda-Carreras I, Cardona A, Kaynig V, Schindelin J. 2011. Trainable Weka Segmentation. Fiji website [Internet]. Available from: http://fiji.sc/Trainable_Weka_Segmentation

Arnold C, Matthews LJ, Nunn CL. 2010. The 10kTrees website: A new online resource for primate phylogeny. Evol Anthropol Issues, News, Rev 19:114–118.

Barak MM, Lieberman DE, Hublin JJ. 2013. Of mice, rats and men: Trabecular bone architecture in mammals scales to body mass with negative allometry. J Struct Biol 183:123–131.

Bouvier M, Hylander WL. 1981. Effect of bone strain on cortical bone structure in macaques (*Macaca mulatta*). J Morphol 167:1–12.

Bouvier M, Hylander WL. 1984. The effect of dietary consistency on gross and histologic morphology in the craniofacial region of young rats. Am J Anat 170:117–126.

Bouvier M. 1986a. Biomechanical scaling of mandibular dimensions in New World Monkeys. Int J Primatol 7:551–567.

Bouvier M. 1986b. A biomechanical analysis of mandibular scaling in Old World monkeys. Am J Phys Anthropol 69:473–482.

Braza F, Alvarez F, Azcarate T. 1981. Behaviour of the red howler monkey (Alouatta seniculus) in the Llanos of Venezuela. Primates 22:459–473.

Brehnan K, Boyd RL, Laskin J, Gibbs CH, Mahan P. 1981. Direct measurement of loads at the temporomandibular joint in *Macaca arctoides*. J Dent Res 60:1820–1824.

Clutton-Brock T. 1974. Activity patterns of red colobus (*Colobus badius tephrosceles*). Folia Primatol 21:161–187.

Coiner-Collier. Chapter 2.

Corruccini R, Beecher R. 1982. Occlusal variation related to soft diet in a nonhuman primate. Science (80-) 218:74–6.

Corruccini R, Beecher R. 1984. Occlusofacial morphological integration lowered in baboons raised on soft diet. J Craniofac Genet Dev Biol 4:135–142.

Cotter MM, Simpson SW, Latimer BM, Hernandez CJ. 2009. Trabecular microarchitecture of hominoid thoracic vertebrae. Anat Rec 292:1098–1106.

Daegling DJ, Grine FE. 1991. Compact bone distribution and biomechanics of early hominid mandibles. Am J Phys Anthropol 86:321–339.

Daegling DJ, McGraw WS. 2007. Functional morphology of the mangabey mandibular

corpus: Relationship to dietary specializations and feeding behavior. Am J Phys Anthropol 134:50–62.
Daegling DJ. 1992. Mandibular morphology and diet in the genus *Cebus*. Int J Primatol 13:545–570.
Darvell BW, Lee PKD, Yuen TDB, Lucas PW. 1996. A portable fracture toughness tester for biological materials. Meas Sci Technol 7:954–962.
Dasilva GL. 1992. The western black-and-white colobus as a low-energy strategist: activity budgets, energy expenditure and energy intake. J Anim Ecol 61:79–91.
Davison KS, Siminoski K, Adachi J, Hanley DA, Goltzman D, Hodsman AB, Josse R, Kaiser S, Olszynski WP, Papaioannou A, Ste-Marie LG, Kendler DL, Tenenhouse A, Brown JP. 2006. Bone strength: The whole is greater than the sum of its parts. Semin Arthritis Rheum 36:22–31.
Demes B, Creel N. 1988. Bite force, diet, and cranial morphology of fossil hominids. J Hum Evol 17:657–670.
Dias GJ, Cook RB, Mirhosseini M. 2011. Influence of food consistency on growth and morphology of the mandibular condyle. Clin Anat 24:590–598.
Dominy NJ, Vogel ER, Yeakel JD, Constantino PJ, Lucas PW. 2008. Mechanical properties of plant underground storage organs and implications for dietary models of early hominins. Evol Biol 35:159–175.
Doube M, Kłosowski MM, Arganda-Carreras I, Cordelières FP, Dougherty RP, Jackson JS, Schmid B, Hutchinson JR, Shefelbine SJ. 2010. BoneJ: Free and extensible bone image analysis in ImageJ. Bone 47:1076–9.
Doube M, Klosowski MM, Wiktorowicz-Conroy AM, Hutchinson JR, Shefelbine SJ. 2011. Trabecular bone scales allometrically in mammals and birds. Proc Biol Sci 278:3067–73.
Dunbar R. 1992. Time: A hidden constraint on the behavioural ecology of baboons. Behav Ecol Sociobiol 31:35–49.
Dunbar RIM, Korstjens a. H, Lehmann J. 2009. Time as an ecological constraint. Biol Rev 84:413–429.
Van Eijden T, van Der Helm PN, van Ruijven L, Mulder L. 2006. Structural and mechanical properties of mandibular condylar bone. J Dent Res 85:33–37.
Estrada A, Saui J-S, Martinez TO, Coates-Estrada R, Juan-Solano S. 1999. Feeding and general activity patterns of a howler monkey (*Alouatta palliata*) troop living in a forest fragment at Los Tuxtlas, Mexico. Am J Primatol 48:167–183.
Fox EA, Schaik CP Van, Sitompul A, Wright DN, van Schaik CP. 2004. Intra- and interpopulational differences in orangutan (*Pongo pygmaeus*) activity and diet: Implications for the invention of tool use. Am J Phys Anthropol 125:162–74.
Freeland WJ. 1979. Mangabey (*Cercocebus albigena*) Social organization and population density in relation to food and availability. Folia Primatol 32:108–124.
Galante J, Rostoker W, Ray R. 1970. Physical properties of trabecular bone. Calcif Tissue Res 5:236–246.
Gaulin SJ, Gaulin CK. 1982. Behavioral ecology of *Alouatta seniculus* in Andean cloud forest. Int J Primatol 3:1–32.
Giesen E, Ding M, Dalstra M, Van Eijden T. 2001. Mechanical properties of cancellous bone in the human mandibular condyle are anisotropic. J Biomech 34:799–803.
Giesen E, Ding M, Dalstra M, van Eijden T. 2003. Reduced mechanical load decreases

the density, stiffness, and strength of cancellous bone of the mandibular condyle. Clin Biomech 18:358–363.
Giesen E, Ding M, Dalstra M, van Eijden T. 2004. Changed morphology and mechanical properties of cancellous bone in the mandibular condyles of edentate people. J Dent Res 83:255–259.
Giesen E, van Eijden T. 2000. The three-dimensional cancellous bone architecture of the human mandibular condyle. J Dent Res 79:957–963.
Goldstein SA, Goulet R, McCubbrey D. 1993. Measurement and significance of three-dimensional architecture to the mechanical integrity of trabecular bone. Calcif Tissue Int 53:S127–S133.
Goldstein SA, Matthews LS, Kuhn JL, Hollister SJ. 1991. Trabecular bone remodeling: An experimental model. J Biomech 24:135–150.
Goulet RW, Goldstein SA, Ciarelli MJ, Kuhn JL, Brown MB, Feldkamp LA. 1994. The relationship between the structural and orthogonal compressive properties of trabecular bone. J Biomech 27:375–389.
Herring SW, Liu Z. 2001. Loading of the temporomandibular joint: anatomical and in vivo evidence from the bones. Cells Tissues Organs 169:193–200.
Hylander WL. 1979a. Mandibular function in Galago crassicaudatus and Macaca fascicularis: An in vivo approach to stress analysis of the mandible. J Morphol 159:253–296.
Hylander WL. 1979b. The functional significance of primate mandibular form. J Morphol 160:223–239.
Hylander WL. 1979c. An experimental analysis of temporomandibular joint reaction force in macaques. Am J Phys Anthropol 51:433–456.
Hylander WL. 1985. Mandibular function and biomechanical stress and scaling. Am Zool 25:315–330.
Kabel J, Odgaard A, Van Rietbergen B, Huiskes R. 1999. Connectivity and the elastic properties of cancellous bone. Bone 24:115–120.
Ketcham RA, Ryan TM. 2004. Quantification and visualization of anisotropy in trabecular bone. J Microsc 213:158–71.
Koenig A, Borries C, Suarez S, Kreetiyuotanont, Prabnasuk J. 2004. Socio-ecology of Phayre's leaf monkeys (*Trachypithecus phayrei*) at Phu Khieo Wildlife Sanctuary.
Korstjens AH, Dunbar RIM. 2007. Time constraints limit group sizes and distribution in red and black-and-white colobus. Int J Primatol 28:551–575.
Korstjens AH, Lehmann J, Dunbar RIM. 2010. Resting time as an ecological constraint on primate biogeography. Anim Behav 79:361–374.
Korstjens AH, Verhoeckx IL, Dunbar RI. 2006. Time as a constraint on group size in spider monkeys. Behav Ecol Sociobiol 60:683–694.
Kothari M, Keaveny TM, Lin JC, Newitt DC, Genant HK, Majumdar S. 1998. Impact of spatial resolution on the prediction of trabecular architecture parameters. Bone 22:437– 443.
Koyabu DB, Endo H. 2009. Craniofacial variation and dietary adaptations of African colobines. J Hum Evol 56:525–536.
Lambert JE, Chapman CA, Wrangham RW, Conklin-Brittain NL. 2004. Hardness of cercopithecine foods: Implications for the critical function of enamel thickness in exploiting fallback foods. Am J Phys Anthropol 125:363–368.

Lambert JE. 1998. Primate digestion: Interactions among anatomy, physiology, and feeding ecology. Evol Anthropol Issues, News, Rev 7:8–20.

Lehmann J, Korstjens AH, Dunbar RI. 2008. Time and distribution: A model of ape biogeography. Ethol Ecol Evol 20:337–359.

Lucas PW, Constantino PJ, Chalk J, Ziscovici C, Wright BW, Fragaszy DM, Hill DA, Lee JJ-W, Chai H, Darvell BW, Lee PKD, Yuen TDB, George T. 2009. Indentation as a technique to assess the mechanical properties of fallback foods. Am J Phys Anthropol 140:643–652.

Lucas PW, Turner IM, Dominy NJ, Yamashita N. 2000. Mechanical defences to herbivory. Ann Bot 86:913–920.

Lynch Alfaro JW, Boubli JP, Olson LE, Di Fiore A, Wilson B, Gutiérrez-Espeleta G a., Chiou KL, Schulte M, Neitzel S, Ross V, Schwochow D, Nguyen MTT, Farias I, Janson CH, Alfaro ME. 2012. Explosive Pleistocene range expansion leads to widespread Amazonian sympatry between robust and gracile capuchin monkeys. J Biogeogr 39:272–288.

Majumdar S, Newitt D, Mathur A, Osman D, Gies A, Chiu E, Lotz J, Kinney J, Genant HK. 1996. Magnetic resonance imaging of trabecular bone structure in the distal radius: Relationship with X-ray tomographic microscopy and biomechanics. Osteoporos Int 6:376–385.

Mau M, Johann A, Sliwa A, Hummel J, Südekum K-H. 2011. Morphological and physiological aspects of digestive processes in the graminivorous primate *Theropithecus gelada*-a preliminary study. Am J Primatol 73:449–57.

Milton K, McBee RH. 1983. Rates of fermentative digestion in the howler monkey, *Alouatta paliatta* (Primates: Ceboidea). Comp Biochem Physiol 74A:29–31.

Milton K. 1980. The Foraging Strategy of Howler Monkeys: A Study in Primate Economics. New York, NY: Columbia University Press.

Milton K. 1981. Food choice and digestive strategies of two sympatric primate species. Am Nat 117:496–505.

Milton K. 1984. The role of food-processing factors in primate food choice. In: Rodman P, Cant J, editors. Adaptations for Foraging in Nonhuman Primates.

Mittra E, Rubin C, Qin Y-X. 2005. Interrelationship of trabecular mechanical and microstructural properties in sheep trabecular bone. J Biomech 38:1229–1237.

Mongini F, Preti G, Calderale PM, Barberi G. 1981. Experimental strain analysis on the mandibular condyle under various conditions. Med Biol Eng Comput 19:521–523.

Morrogh-Bernard HC, Husson SJ, Knott CD, Wich SA, Schaik CP Van, Noordwijk MA Van, Lackman-ancrenaz I, Marshall AJ, Kuze N, Sakong R. 2007. Orangutan activity budgets and diet: A comparison between species, populations and habitats. In: Wich SA, Utami Atmoko SS, Mitra Setia T, van Schaik CP, editors. Orangutans: Geographic Variation in Behavioral Ecology and Conservation. Oxford: Oxford University Press. p 119–133.

Müller R, Koller B, Hildebrand T, Laib A, Gianolini S, Ruegsegger P. 1996. Resolution dependency of microstructural properties of cancellous bone based on three-dimensional micro-tomography. Technol Heal Care 4:113–119.

Norconk MA, Wright BW, Conklin-Brittain NL, Vinyard CJ. 2009. Mechanical and nutritional properties of food as factors in platyrrhine dietary adaptations. In: Garber PA, Estrada A, Bicca-Marques JC, Heymann EW, Strier KB, editors. South

American Primates: Comparative Perspectives in the Study of Behavior, Ecology, and Conservation. New York, NY: Springer. p 279–319.
Odgaard A, Kubel J, van Rietbergen B, Dalstra M, Huiskes R. 1997. Fabric and elastic principal directions of cancellous bone are closely related. J Biomech 30:487–495.
Olejniczak AJ, Tafforeau P, Feeney RNM, Martin LB. 2008. Three-dimensional primate molar enamel thickness. J Hum Evol 54:187–95.
Orme D, Freckleton R, Thomas G, Petzoldt T, Fritz S, Isaac N, Pearse W. 2013. The caper package: Comparative analysis of phylogenetics and evolution in R. R Packag version 05:1–36.
Paradis E, Claude J, Strimmer K. 2004. APE: Analyses of Phylogenetics and Evolution in R language. Bioinformatics 20:289–290.
Peyrin F, Salome M, Cloetens P, Laval-Jeantet a M, Ritman E, Rüegsegger P. 1998. Micro-CT examinations of trabecular bone samples at different resolutions: 14, 7 and 2 micron level. Technol Health Care 6:391–401.
Pinheiro T, Ferrari SF, Lopes MA. 2013. Activity budget, diet, and use of space by two groups of squirrel monkeys (*Saimiri sciureus*) in eastern Amazonia. Primates 54:301–308.
Pontzer H, Lieberman DE, Momin E, Devlin MJ, Polk JD, Hallgrímsson B, Cooper DML. 2006. Trabecular bone in the bird knee responds with high sensitivity to changes in load orientation. J Exp Biol 209:57–65.
Poulsen JR, Clark CJ, Smith TB. 2001. Seasonal variation in the feeding ecology of the grey-cheeked mangabey (*Lophocebus albigena*) in Cameroon. Am J Primatol 54:91–105.
Raguet-Schofield M. 2010. The ontogeny of feeding behavior of Nicaraguan mantled howler monkeys (*Alouatta palliata*).
Ravosa MJ, Kunwar R, Stock SR, Stack MS. 2007. Pushing the limit: masticatory stress and adaptive plasticity in mammalian craniomandibular joints. J Exp Biol 210:628–41.
Ravosa MJ, Lopez EK, Menegaz RA, Stock SR, Stack MS, Hamrick MW. 2008. Adaptive Plasticity in the Mammalian Masticatory Complex: You Are What, and How, You Eat. In: Vinyard C, Ravosa MJ, Wall C, editors. Primate Craniofacial Function and Biology. Boston, MA: Springer US. p 293–328.
Ravosa MJ. 2000. Size and scaling in the mandible of living and extinct apes. Folia Primatol 71:305–322.
Rawson BM. 2009. The socio-ecology of the black-shanked douc (*Pygathrix nigripes*) in Mondulkiri Province, Cambodia.
Renders G, Mulder L, Langenbach GEJ, van Ruijven LJ, van Eijden T. 2008. Biomechanical effect of mineral heterogeneity in trabecular bone. J Biomech 41:2793–8.
Ridler T, Calvard S. 1978. Picture thresholding using an iterative selection method. IEEE Trans Syst Man Cybern SMC-8:630–632.
Riede T, Bronson E, Hatzikirou H, Zuberbühler K. 2005. Vocal production mechanisms in a non-human primate: Morphological data and a model. J Hum Evol 48:85–96.
Van Rietbergen B, Odgaard A, Kabel J, Huiskes R. 1998. Relationships between bone morphology and bone elastic properties can be accurately quantified using high-resolution computer reconstructions. J Orthop Res 16:23–28.

Robinson JG. 1986. Seasonal variation in use of time and space by the wedge-capped capuchin monkey, *Cebus olivaceus*: implications for foraging theory. Washington, D.C.: Smithsonian Institution Press.
Rose LM. 1998. Behavioral ecology of white-faced capuchins (*Cebus capucinus*) in Costa Rica.
Ross CF, Iriarte-Diaz J, Nunn CL. 2012. Innovative approaches to the relationship between diet and mandibular morphology in primates. Int J Primatol 33:632–660.
Ross CF, Reed DA, Washington RL, Eckhardt A, Anapol F, Shahnoor N. 2009a. Scaling of chew cycle duration in primates. Am J Phys Anthropol 138:30–44.
Ross CF, Washington RL, Eckhardt A, Reed DA, Vogel ER, Dominy NJ, Machanda ZP. 2009b. Ecological consequences of scaling of chew cycle duration and daily feeding time in primates. J Hum Evol 56:570–85.
Rubin CT, Lanyon LE. 1984. Regulation of bone formation by applied dynamic loads. J Bone Jt Surg 66A:397–402.
Rubin CT, Lanyon LE. 1985. Regulation of bone mass by mechanical strain magnitude. Calcif Tissue Int 37:411–417.
Van Ruijven L, Giesen E, Mulder L, Farella M, van Eijden T, Ruijven LJ Van. 2005. The effect of bone loss on rod-like and plate-like trabeculae in the cancellous bone of the mandibular condyle. Bone 36:1078–85.
Van Ruijven LLJ, Giesen E, van Eijden T. 2002. Mechanical significance of the trabecular microstructure of the human mandibular condyle. J Dent Res 81:706–710.
Ryan TM, Colbert M, Ketcham RA, Vinyard CJ. 2010. Trabecular bone structure in the mandibular condyles of gouging and nongouging platyrrhine primates. Am J Phys Anthropol 141:583–93.
Ryan TM, Ketcham RA. 2002. The three-dimensional structure of trabecular bone in the femoral head of strepsirrhine primates. J Hum Evol 43:1–26.
Ryan TM, Shaw CN. 2013. Trabecular bone microstructure scales allometrically in the primate humerus and femur. Proc R Soc B Biol Sci 280:1–9.
Sabbatini G, Stammati M, Tavares M, Visalberghi E. 2008. Behavioral flexibility of a group of bearded capuchin monkeys (*Cebus libidinosus*) in the National Park of Brasília (Brazil): Consequences of cohabitation with visitors. Brazilian J Biol 68:685–693.
Van Schaik CP, van Noordwijk MA, de Boer RJ, den Tonkelaar I. 1983. The effect of group size on time budgets and social behaviour in wild long-tailed macaques (*Macaca fascicularis*). Behav Ecol Sociobiol 13:173–181.
Scherf H. 2007. Locomotion-related femoral trabecular architectures in Primates.
Schindelin J, Arganda-Carreras I, Frise E, Kaynig V, Longair M, Pietzsch T, Preibisch S, Rueden C, Saalfeld S, Schmid B, Tinevez J-Y, White DJ, Hartenstein V, Eliceiri K, Tomancak P, Cardona A. 2012. Fiji: An open-source platform for biological-image analysis. Nat Methods 9:676–82.
Schwartz GT, Conroy GC. 1996. Cross-sectional geometric properties of the *Otavipithecus* mandible. Am J Phys Anthropol 99:613–623.
Scott JE, McAbee KR, Eastman MM, Ravosa MJ. 2014. Experimental perspective on fallback foods and dietary adaptations in early hominins. Biol Lett.
Setz EZ, Pinto LP, Bowler M, Barnett AA, Vie J-C, Boubli JP, Norconk MA. 2013. Pitheciins: Use of time and space. In: Veiga LM, Barnett AA, Ferrari SF, Norconk

MA, editors. Evolutionary Biology and Conservation of Titis, Sakis, and Uacaris. Cambridge University Press. p 72–83.
Strait DS, Weber GW, Constantino PJ, Lucas PW, Richmond BG, Spencer MA, Dechow PC, Ross CF, Grosse IR, Wright BW, Wood BA, Wang Q, Byron C, Slice DE. 2012. Microwear, mechanics and the feeding adaptations of *Australopithecus africanus*. J Hum Evol 62:165–8.
Sussman RW, Shaffer CA, Guidi L. 2011. *Macaca fascicularis* in Mauritius: Implications for macaque-human interactions and for future research on long-tailed macaques. In: Gumert MD, Fuentes A, Jones-Engel L, editors. Monkeys on the Edge: Ecology and Management of Long-Tailed Macaques and their Interface with Humans. Cambridge University Press. p 207–235.
Swartz SM, Parker a, Huo C. 1998. Theoretical and empirical scaling patterns and topological homology in bone trabeculae. J Exp Biol 201:573–590.
Symington MM. 1988. Demography, ranging patterns, and activity budgets of black spider monkeys (*Ateles paniscus chamek*) in the Manu National Park, Peru. Am J Primatol 15:45–67.
Taylor AB, Jones KE, Kunwar R, Ravosa MJ. 2006. Dietary consistency and plasticity of masseter fiber architecture in postweaning rabbits. Anat Rec 288:1105–11.
Taylor AB, Vogel ER, Dominy NJ. 2008. Food material properties and mandibular load resistance abilities in large-bodied hominoids. J Hum Evol 55:604–16.
Taylor AB. 2002. Masticatory form and function in the African apes. Am J Phys Anthropol 117:133–156.
Teaford MFM, Lucas PPW, Ungar PS, Glander KE. 2006. Mechanical defenses in leaves eaten by Costa Rican howling monkeys (*Alouatta palliata*). Am J Phys Anthropol 129:99–104.
Terborgh J. 1983. Five New World Primates: A Study in Comparative Ecology. Princeton, NJ: Princeton University Press.
Townsend P, Raux P, Rose R, Miegel R, Radin E. 1975. The distribution and anisotropy of the stiffness of cancellous bone in the human patella. Biomechanics 8:363–367.
Trussell H. 1979. Comments on "Picture thresholding using an iterative selection method." IEEE Trans Syst Man Cybern 54:9472–9472.
Ulrich D, Van Rietbergen B, Laib A, Rüegsegger P. 1999. The ability of three-dimensional structural indices to reflect mechanical aspects of trabecular bone. Bone 25:55–60.
Ungar PS, Grine FE, Teaford MF. 2008. Dental microwear and diet of the Plio-Pleistocene hominin Paranthropus boisei. PLoS One 3:e2044.
Ungar PS, Scott RS, Grine FE, Teaford MF. 2010. Molar microwear textures and the diets of *Australopithecus anamensis* and *Australopithecus afarensis*. Philos Trans R Soc Lond B Biol Sci 365:3345–54.
Vinyard CJ, Glander KE, Teaford MF, Thompson CL, Deffenbaugh M, Williams SH. 2012. Methods for studying the ecological physiology of feeding in free-ranging howlers (*Alouatta palliata*) at La Pacifica, Costa Rica. Int J Primatol 33:611–631.
Vinyard CJ, Ryan TM. 2006. Cross-sectional bone distribution in the mandibles of gouging and non-gouging platyrrhini. Int J Primatol 27:1461–1490.
Vogel ER, Coiner-Collier S, Chalk J, Constantino PJ, Glowacka H, Raguet-Schofield M, Talebi MG, Vinyard CJ, Wright BW, Yamashita N, Dominy NJ, Lucas PW, Scott RS.

2013. Do food material properties predict jaw and tooth morphology in primates? Am J Phys Anthropol 150:217.

Vogel ER, Haag L, Mitra-Setia T, van Schaik CP, Dominy NJ. 2009. Foraging and ranging behavior during a fallback episode: *Hylobates albibarbis* and *Pongo pygmaeus wurmbii* compared. Am J Phys Anthropol 140:716–26.

Vogel ER, Zulfa A, Hardus ME, Wich SA, Dominy NJ, Taylor AB. 2014. Food mechanical properties, feeding ecology, and the mandibular morphology of wild orangutans. J Hum Evol.

Wallace RB. 2001. Diurnal activity budgets of black spider monkeys, *Ateles chamek*, in a southern Amazonian tropical forest. Neotrop Primates 9:101–107.

Waser PM. 1984. Ecological differences and behavioral contrasts between two mangabey species. In: Rodman P, Gant JG, editors. Adaptations for Foraging in Nonhuman Primates. New York: Columbia University Press. p 195–214.

Williams SH, Vinyard CJ, Glander KE, Deffenbaugh M, Teaford MF, Thompson CL. 2008. Telemetry system for assessing jaw-muscle function in free-ranging primates. Int J Primatol 29:1441–1453.

Williams SH, Wright BW, Truong V, Daubert CR, Vinyard CJ. 2005. Mechanical properties of foods used in experimental studies of primate masticatory function. Am J Primatol 67:329–346.

Wrangham RW. 1977. Feeding behaviour of chimpanzees in Gombe National Park, Tanzania. In: Clutton-Brock T, editor. Primate Ecology: Studies of Feeding and Ranging Behavior in Lemurs, Monkeys and Apes. London: Academic Press. p 503–538.

Wroe S, McHenry C, Thomason J. 2005. Bite club: Comparative bite force in big biting mammals the the prediction of predatory behaviour in fossil taxa. Proc Biol Sci 272:619–625.

Yamashita N, Cuozzo FP, Sauther ML. 2012. Interpreting food processing through dietary mechanical properties: a *Lemur catta* case study. Am J Phys Anthropol 148:205–14.

Yamashita N, Vinyard CJ, Tan CL. 2009. Food mechanical properties in three sympatric species of *Hapalemur* in Ranomafana National Park, Madagascar. Am J Phys Anthropol 139:368–81.

Yamashita N. 2003. Food procurement and tooth use in two sympatric lemur species. Am J Phys Anthropol 121:125–133.

Youlatos D, Couette S, Halenar LB. 2015. Morphology of howler monkeys: A review and quantitative analyses. In: Kowaleski M, Garber PA, Cortes-Ortiz L, Urbani B, Youlatos D, editors. Howler Monkeys: Adaptive Radiation, Systematics, and Morphology. New York: Springer. p 133–176.

Chapter 5. The general structure of trabecular bone in the mandibular condyle of anthropoid primates

5.1 Introduction

The overall trabecular structure of the mandibular condyle is known from studies on humans (Hongo et al., 1989a, 1989b; Giesen and van Eijden, 2000; van Eijden et al., 2006), pigs (Teng and Herring, 1995; Mulder et al., 2005; Willems et al., 2007), sheep (Cornish et al., 2006), and non-human primates (Ryan et al., 2010). Taken together, the results of these studies demonstrate a pattern of anisotropic, plate-like trabecular struts oriented perpendicular to the articular surface of the condyle. The trabeculae in the mandibular condyle are thus oriented as would be expected for maximum resistance of compressive masticatory forces (Herring and Liu, 2001; van Ruijven et al., 2002).

Because fabric anisotropy and volume fraction explain the majority of variation in the elastic modulus of trabecular bone (Odgaard et al., 1997; Van Rietbergen et al., 1998; Kabel et al., 1999; Giesen et al., 2001), the three-dimensional architecture of the mandibular condyle may be informative as to the loading regimes to which the temporomandibular joint is subjected. Quantifying variation in trabecular architecture may thus provide insight into the functional morphology of the mandibular condyle.

There has been little study of the trabecular structure of the mandibular condyle of non-human primates. The one previous study to address this issue (Ryan et al., 2010) comprised a sample of three New World monkeys. This study tested for effects related to tree-gouging behavior and found no consistent pattern in trabecular architecture. No research has examined trabecular variation across primates. While the trabecular structure

of other skeletal elements, particularly those involved with locomotion, has been extensively studied in non-human primates (Fajardo and Müller, 2001; Fajardo et al., 2002, 2007, 2013; MacLatchy and Müller, 2002; Ketcham and Ryan, 2004; Ryan and Ketcham, 2005; Ryan and van Rietbergen, 2005; Ryan and Krovitz, 2006; Scherf, 2007; Cotter et al., 2009; Ryan and Walker, 2010; Griffin et al., 2010; Kivell et al., 2011; Barak et al., 2013; Ryan and Shaw, 2013), the mandibular condyle experiences different loading regimes (i.e. mastication versus locomotion) and as such may have different trabecular morphology. A general description of the internal structure of the mandibular condyle is thus warranted.

In addition to overall variations in trabecular structure, differences within individuals (side asymmetry) and within taxa may indicate meaningful functional differences. Side asymmetry of the mandibular condyle is of interest because it could indicate bilateral asymmetry in hand usage. Handedness in humans is associated with chewing side preference, although this preference is primarily expressed in the positioning of the initial chew (Hoogmartens and Caubergh, 1987; Nissan and Gross, 2004). However, it has been argued that initial oral preparation and biting may be the primary driver of mandibular morphology in primates that consume hard objects (Yamashita et al., 2009), and thus the first chew may be adequate to present a morphological signature. Some population-wide preferences in hand use exist (e.g. a preference for left-handed reaching in prosimians and cercopithecoids), particularly for more complicated tasks, but the direction of these preferences is not consistent across primates (MacNeilage et al., 1987; Fagot and Vauclair, 1991; McGrew and Marchant, 1997; Papademetriou et al., 2005). However, consistent asymmetries in trabecular structure could indicate chewing side preference and

thus hemispheric laterality in primates.

Here, I present data on trabecular parameters calculated using high-resolution X-ray computed tomography (HRXCT) for a comparative sample of 16 primate species, and provide a general description of primate condylar architecture using trabecular variables commonly presented in the literature. I also test whether there are any indications of side asymmetry in trabecular structure.

The questions investigated here are:

1. What is the general nature of trabecular bone in the primate mandibular condyle? How do these results compare to those of previous studies? I predict a pattern of trabecular architecture generally similar to what has been found previously (i.e. anisotropic, vertically oriented trabeculae).

2. How do these trends vary among different taxa? I examine differences among platyrrhines, cercopithecoids, and hominoids.

3. Is there a consistent pattern of side differences in trabecular architecture across the primates in this sample? That is, does trabecular structure reflect potential chewing side preferences for either the right or left side? If side preferences exist, the right and left condyle should consistently differ.

5.2 Materials and Methods

Sample and data collection procedures

The skeletal sample comprised the mandibles of 28 wild-shot adult individuals from the collection at the National Museum of Natural History (Table 5.1). Both males and females were included in the sample. All specimens were imaged at the High-Resolution

X-Ray Computed Tomography Facility at the University of Texas at Austin. Specimens were mounted in florist foam and scanned roughly perpendicular to the long axis of the mandible. Some specimens were scanned a few degrees off center, precluding accurate analysis of principal trabecular orientation, but I will still present descriptive data on PTO. Some specimens were scanned two at a time, with one mandible inverted and scanned posterior-anterior. These specimens were digitally repositioned prior to analysis. All specimens were scanned with energy settings of 150kV and 0.24mA with 8000 projections. Nominal resolutions ranged from 0.0382 mm to 0.1784 mm with isotropic voxels. For each mandible, between 610 and 937 slices were collected. Image data were reconstructed as 1024 x 1024 16-bit TIFF images and were converted to 8-bit images for processing and analysis.

Volume of interest selection

The volume of interest (VOI) was selected as the largest cubic volume that would fit within the mandibular condyle without including any cortical bone. The procedure is described in detail in Chapter 3 but will be summarized here. First, the maximum extent of the condyle was defined using the 3D Viewer plugin (Schmid and Schindelin, 2010) for ImageJ to designate external landmarks. The mediolateral dimension was defined by the morphology of the condyle. The superoinferior dimension was defined by viewing the mandible posteriorly and placing a point at the narrowest margin of the neck of the condyle along the ascending ramus. The anteroposterior dimension was defined by placing a point at the anterior-most margin of the condyle inferior to the articular surface. I then rotated the mandible to a lateral view and used the rectangular selection tool to

draw a line between the two points, and cropped the condyle above that line. This method enabled systematic isolation of the condylar region among specimens with varying morphologies. Cubic volumes were then selected from within each cropped condyle, which served to scale the VOI to the size of the specimen, thereby preventing over-sampling from smaller specimens (Fajardo and Müller, 2001; Kivell et al., 2011; Lazenby et al., 2011). Cube side lengths ranged from 0.802 mm to 6.422 mm, and scaled with both the length of the mandible (left: OLS p <0.0001, R^2 = 0.909; right: p < 0.0001, R^2 = 0.888) and the external dimensions of the condyle (left: p < 0.0001, R^2 = 0.889, right: p = <0.0001, R^2 = 0.857) as measured with Mitutoyo digital calipers from the skeletal specimens.

Trabecular analyses

Once VOI selection was complete, the threshold for each cube was determined using an iterative adaptive method (Ridler and Calvard, 1978; Trussell, 1979). Thresholding is the process of classifying pixels as either background or bone, and proper thresholding is essential for accurately quantifying variations in trabecular structure (Ding et al., 1999; Fajardo et al., 2002; Hara et al., 2002). Each cube was analyzed using Quant3D (Ryan and Ketcham, 2002; Ketcham and Ryan, 2004) and BoneJ (Doube et al., 2010). Quant3D was used for calculating the degree of anisotropy (DA), elongation index (E), bone volume fraction (BV/TV), and trabecular number (Tb.N). Calculations were performed with settings of 2049 uniform orientations with random rotation and dense vectors. Primary trabecular orientations were taken from the fabric matrix generated by the star volume distribution analysis (Cruz-Orive et al., 1992) used to calculate DA. BoneJ was

used for calculating connectivity density (Conn.D), structure model index (SMI), trabecular thickness (Tb.Th), and trabecular spacing (Tb.Sp). SMI was calculated using the method of Hildebrand and Rüegsegger (1997) with voxel resampling set to one voxel.

Statistical analyses

Pearson's chi-squared tests of goodness of fit were used to test for right-left trabecular asymmetry among species ($\alpha = 0.05$). If there is no consistent morphological signature of chewing side preference, the expectation is that each specimen will show left/right differences (i.e. either the right or the left condyle will have a higher value for each variable), but that the direction of these differences will be randomly distributed across species. Thus, a significant result for a chi-squared test indicates a bias toward either right or left.

I used Kruskal-Wallis one-way analysis of variance tests to examine differences among taxa. Primates were classified as cercopithecoids, hominoids, or platyrrhines for purposes of this analysis, and values for the right and left condyle for each specimen were averaged. When Kruskal-Wallis results yielded significant differences, I used post-hoc pairwise Mann-Whitney tests with Bonferroni-Holm correction to determine which taxa differed from each other.

All analyses were performed using the R Statistical Programming Language version 3.1.0 (http://www.R-project.org).

5.3 Results

Trabecular parameters for the sample are provided in Table 5.1.

Differences across taxa

Taxonomic differences in trabecular structure were found for most trabecular variables (Table 5.2) (Figure 5.1). Hominoids and platyrrhines showed the most difference; post-hoc tests of significant results demonstrated significant differences between hominoids and platyrrhines for all variables. Platyrrhines and cercopithecoids were largely similar, showing a difference only for Tb.Th ($p = 0.029$) (Figure 5.1B). Hominoids and cercopithecoids differed for Tb.Th ($p = 0.011$), Tb.N ($p = 0.022$) (Figure 5.1C), and DA ($p = 0.011$) (Figure 5.1D).

Left/right asymmetry across primates

Results of Pearson's chi-squared analysis yielded no significant results for any trabecular variable (Table 5.3). Side differences are randomly distributed across the specimens in this sample.

Discussion

General structure of the mandibular condyle

In general, the trabecular bone in the mandibular condyles of these primate species is anisotropic, and is oriented in parallel plates that are generally perpendicular to the articular surface of the condyle. This pattern matches what has been found in previous studies of the mandibular condyle (Teng and Herring, 1995; Giesen and van Eijden, 2000; Ryan et al., 2010). Estimates of BV/TV (33.9%-68.75%, mean 43.03%) are comparable to those previously found in three-dimensional studies of primates (Ryan et

al., 2010: 36.4-50.7%, mean 42.2%), higher than those for humans (Giesen and van Eijden, 2000: mean 17%) and pigs (Mulder et al., 2005: 20-38%; Willems et al., 2007), but lower than those for sheep (Cornish et al., 2006: 50-63%). Degree of anisotropy (2.124-51.872, mean 8.259) is similar to previous results for primates (Ryan et al., 2010: mean 7.297) also calculated using the star volume distribution method. Many other studies have used the mean intercept length (MIL) method, limiting the utility of comparisons. MIL results indicate that the pig condyle is less anisotropic than the results here (Willems et al., 2007: mean ~2), as is the human condyle (Giesen and van Eijden, 2000: mean 1.51).

Estimates for Tb.Th were influenced here by the hominoid specimens, which were scanned at low resolutions; the mean Tb.Th for this sample is 0.369 mm, but when the hominoids are excluded, the mean is 0.329 mm. However, this mean is still higher than those previously found in primate (Ryan et al., 2010: 0.104 mm), pig (Willems et al., 2007: 0.2 mm), or human (Giesen and van Eijden, 2000: 0.10 mm) mandibular condyles.

Values for SMI provide a description of the overall structure of the trabecular morphology of the condyle. A few specimens show negative values, indicating convex trabeculae. All other values range from 0.015 to 1.898 (mean 0.755). The trabecular bone of the mandibular condyle is thus more plate-like than rod-like. The mean for SMI is similar to previous results for primates (Ryan et al., 2010: 0.995), pigs (Mulder et al., 2005), and humans (van Ruijven et al., 2005)

Figure 5.2 displays the principal orientation of the trabecular struts within the mandibular condyle, with rose diagrams of the right and left condyles shown separately. As noted previously, not all specimens were scanned at exactly the same orientation, and

so there is some error in this graphical depiction. However, it can still be clearly seen that the trabeculae are on the whole strongly oriented along the superoinferior axis.

The range of values for Conn.D deserves some consideration. Both specimens of *Saimiri sciureus* demonstrated notably higher values for Conn.D than those seen for the other specimens. These are also the two smallest specimens in the sample as determined by mandibular length. Conn.D has been shown to scale negatively with body size in the primate humerus and femur (Ryan and Shaw, 2013), and thus these extreme values are most likely the consequence of small body size. Ryan *et al.* (2010) found similarly high values for Conn.D for this species (mean 26.31).

One other notable outlier is the value of DA for the right condyle of one specimen for *Cebus libidinosus*. The VOI for this specimen contained parallel struts of trabecular bone oriented along an almost perfectly vertical axis (Figure 5.3), which explains the unusually high estimate of DA. The left condyle for the same specimen showed a value for DA more in line with the remaining species in the sample.

Differences among taxa and sides

Taxonomic differences were apparent in trabecular structure. Hominoids and platyrrhines differed in most aspects of trabecular structure, which is unsurprising considering their respective phylogenetic positions. Hominoids and cercopithecoids also differed in Tb.Th, Tb.N, and DA. These latter differences are potentially related to image resolution (see Chapter 4), although it is not unreasonable to expect differences between apes and monkeys. These results suggest some influence of phylogeny or perhaps simply body size on trabecular architecture; this issue is explored in more detail in Chapter 4.

I found no significant patterns in sidedness of trabecular variables across primate species. Chewing and biting load both the contralateral and the ipsilateral condyle (Hylander, 1979, 1985; Spencer and Demes, 1993; Kieser, 1999), and there are no consistent asymmetries in the external morphology of the mandible or the mandibular condyle in the absence of dental or skeletal pathologies (Vig and Hewitt, 1975; Bishara et al., 1994; Saccucci et al., 2012). The internal morphology of the condyle may thus simply reflect the lack of external asymmetry and a more or less even distribution of loading during feeding. While a signal of trabecular asymmetry might indicate hemispheric laterality vis-a-vis chewing side preference, the absence of consistent asymmetry in the condyle should not be taken as evidence of a lack of laterality in primates. The lack of a signal may instead indicate that the initial chew is not sufficient to generate a remodeling response.

Conclusion

The trabecular structure of the mandibular condyle for the current sample is similar to what has been found previously for primates, humans, and other mammals. The trabecular bone within the condyle is anisotropic, plate-like, and oriented vertically within the condyle, such that the struts are roughly perpendicular to the articular surface. These architectural features are likely related to resisting the forces associated with chewing and biting (Giesen et al., 2001; van Ruijven et al., 2002; van Eijden et al., 2006). Trabecular structure varies across primate taxa. Comparisons of the right and left condyle yielded no significant structural asymmetries.

Table 5.1. Results of BoneJ and Quant3D analysis for the right and left condyles of each specimen.

Species	Catalog #	Side	BV/TV	Tb.Th (mm)	Tb.N (mm^{-1})	Tb.Sp (mm)	DA	E	Conn.D (mm^{-3})	SMI
Alouatta palliata	543117	R	0.4828	0.359	1.920	0.496	3.036	0.399	3.418	-0.068
		L	0.4833	0.344	2.007	0.457	3.808	0.450	4.027	-0.028
	339925	R	0.5374	0.370	1.902	0.406	4.486	0.453	3.326	0.159
		L	0.5353	0.357	1.985	0.395	3.501	0.436	3.604	0.029
Alouatta seniculus	398507	R	0.5214	0.340	2.134	0.407	3.438	0.567	4.476	0.125
		L	0.5207	0.333	2.334	0.373	4.076	0.389	5.512	0.253
Ateles paniscus	545853	R	0.3893	0.327	1.705	0.575	11.637	0.625	2.260	0.983
		L	0.4203	0.333	1.782	0.518	6.752	0.577	2.534	0.941
	545885	R	0.4371	0.418	1.378	0.667	3.198	0.454	1.256	1.252
		L	0.4677	0.409	1.393	0.607	4.581	0.708	1.279	0.690
Cebus apella	461384	R	0.5059	0.265	2.348	0.295	9.529	0.559	5.861	0.740
		L	0.5294	0.295	2.083	0.311	8.321	0.480	3.321	0.438
	388197	R	0.4249	0.307	1.877	0.506	4.175	0.252	2.949	0.865

		L	0.4336	0.293	1.915	0.457	3.487	0.421	3.401	0.805
Cebus capucinus	152130	R	0.4632	0.350	1.754	0.461	18.728	0.724	3.529	1.647
		L	0.489	0.308	2.021	0.377	7.267	0.585	5.294	1.383
Cebus libidinosus	518414	R	0.4755	0.334	1.900	0.446	6.016	0.371	3.400	0.817
		L	0.4621	0.336	1.695	0.471	12.464	0.198	2.705	0.665
	518418	R	0.3744	0.331	1.339	0.589	51.873	0.715	1.217	1.342
		L	0.4091	0.326	1.582	0.506	8.985	0.264	1.764	1.120
Colobus polykomos	481786	R	0.5027	0.359	2.038	0.396	7.590	0.586	5.071	0.950
		L	0.5207	0.372	1.914	0.384	5.674	0.472	4.057	0.888
	477320	R	0.5034	0.401	1.521	0.478	12.595	0.379	1.280	0.367
		L	0.5228	0.418	1.529	0.476	13.597	0.255	1.440	0.427
Lophocebus albigena	598484	R	0.5004	0.408	1.593	0.428	6.459	0.575	2.751	0.983
		L	0.5117	0.422	1.611	0.459	7.334	0.462	2.177	0.621
	598485	R	0.4266	0.460	1.140	0.754	4.423	0.269	0.585	0.675
		L	0.4465	0.452	1.199	0.689	6.079	0.308	0.624	0.675
Macaca fascicularis	114506	R	0.4663	0.323	1.883	0.400	10.537	0.211	3.792	0.959

		L	0.4645	0.328	1.882	0.417	8.466	0.397	4.313	0.754
	114165	R	0.5489	0.330	2.167	0.310	5.509	0.291	4.402	0.544
		L	0.5402	0.333	2.116	0.320	7.087	0.505	4.834	0.519
Pan troglodytes schweinfurthii	236971	R	0.5303	0.599	1.341	0.572	3.665	0.166	1.614	0.956
		L	0.5435	0.594	1.287	0.567	2.326	0.186	1.468	0.727
Piliocolobus badius	481792	R	0.5088	0.331	1.990	0.363	7.305	0.503	4.978	0.879
		L	0.4717	0.304	0.934	0.370	6.301	0.498	5.717	1.180
Pithecia pithecia	546265	R	0.3957	0.263	2.081	0.465	5.155	0.515	5.121	1.142
		L	0.422	0.274	2.133	0.529	6.934	0.200	5.437	1.473
	339658	R	0.4388	0.272	2.149	0.375	9.999	0.678	6.094	1.351
		L	0.465	0.276	2.186	0.356	9.023	0.644	6.335	1.279
Pongo abelii	143588	R	0.592	0.711	1.111	0.593	3.574	0.473	0.936	0.015
		L	0.6875	0.889	0.808	0.582	2.681	0.249	0.309	-1.237
	143596	R	0.5325	0.718	1.027	0.779	2.125	0.483	0.642	0.082
		L	0.5383	0.726	1.048	0.798	2.654	0.471	0.568	-0.081
Pygathrix nigripes	320783	R	0.3309	0.340	1.486	0.706	6.076	0.486	2.687	1.857

		L	0.3793	0.358	1.649	0.542	9.536	0.503	2.854	1.898
	257998	R	0.577	0.358	2.076	0.317	8.449	0.498	2.906	0.091
		L	0.5754	0.367	1.847	0.352	10.617	0.624	2.056	0.252
Saimiri sciureus	547905	R	0.4265	0.158	3.863	0.229	12.106	0.363	24.214	1.538
		L	0.3756	0.148	3.663	0.264	8.702	0.441	20.533	1.278
	547903	R	0.3698	0.154	3.371	0.299	11.766	0.546	23.013	1.142
		L	0.3714	0.152	3.396	0.302	7.595	0.411	23.127	1.123
Trachypithecus phayrei	307737	R	0.5353	0.360	1.793	0.372	9.135	0.272	2.53	0.370
		L	0.5426	0.369	1.819	0.370	8.558	0.319	2.643	0.271
	307736	R	0.4833	0.310	2.009	0.356	18.614	0.494	4.669	1.001
		L	0.4867	0.325	1.999	0.356	14.879	0.543	4.438	1.188

Table 5.2. Results of Kruskal-Wallis one-way analysis of variance tests comparing trabecular variables across taxa. Degrees of freedom = 2 for all tests. Post-hoc pairwise Mann-Whitney tests with Bonferroni-Holm correction yielded significant differences between hominoids and platyrrhines for BV/TV, Tb.Th, Tb.N, DA, and Conn.D, and differences between hominoids and cercopithecoids for Tb.Th, Tb.N, and DA. Platyrrhines and cercopithecoids differed only for Tb.Th.

Trabecular variable	chi-square	*p*
BV/TV	8.403	**0.015**
Tb.Th	11.597	**0.003**
Tb.N	9.447	**0.008**
Tb.Sp	5.551	0.062
DA	7.953	**0.019**
E	2.644	0.267
Conn.D	6.674	**0.036**
SMI	3.872	0.144

Table 5.3. Results of Pearson's chi-squared test of goodness of fit. Significant results are in bold. Because of some negative values for SMI, each estimate of SMI was increased by a constant value (2.237, so that the minimum value = 1).

Trabecular variable	χ^2	df	*p*
BV/TV	0.019	27	1.000
Tb.Th	0.027	27	1.000
Tb.N	0.536	27	1.000
Tb.Sp	0.056	27	1.000
DA	37.169	27	0.092
E	0.809	27	1.000
Conn.D	2.524	27	1.000
SMI	0.610	27	1.000

Figure 5.1. Box plots showing variations in trabecular parameters by taxon. Taxa are listed on the x axis (C = cercopithecoids, H= hominoids, P = platyrrhines).

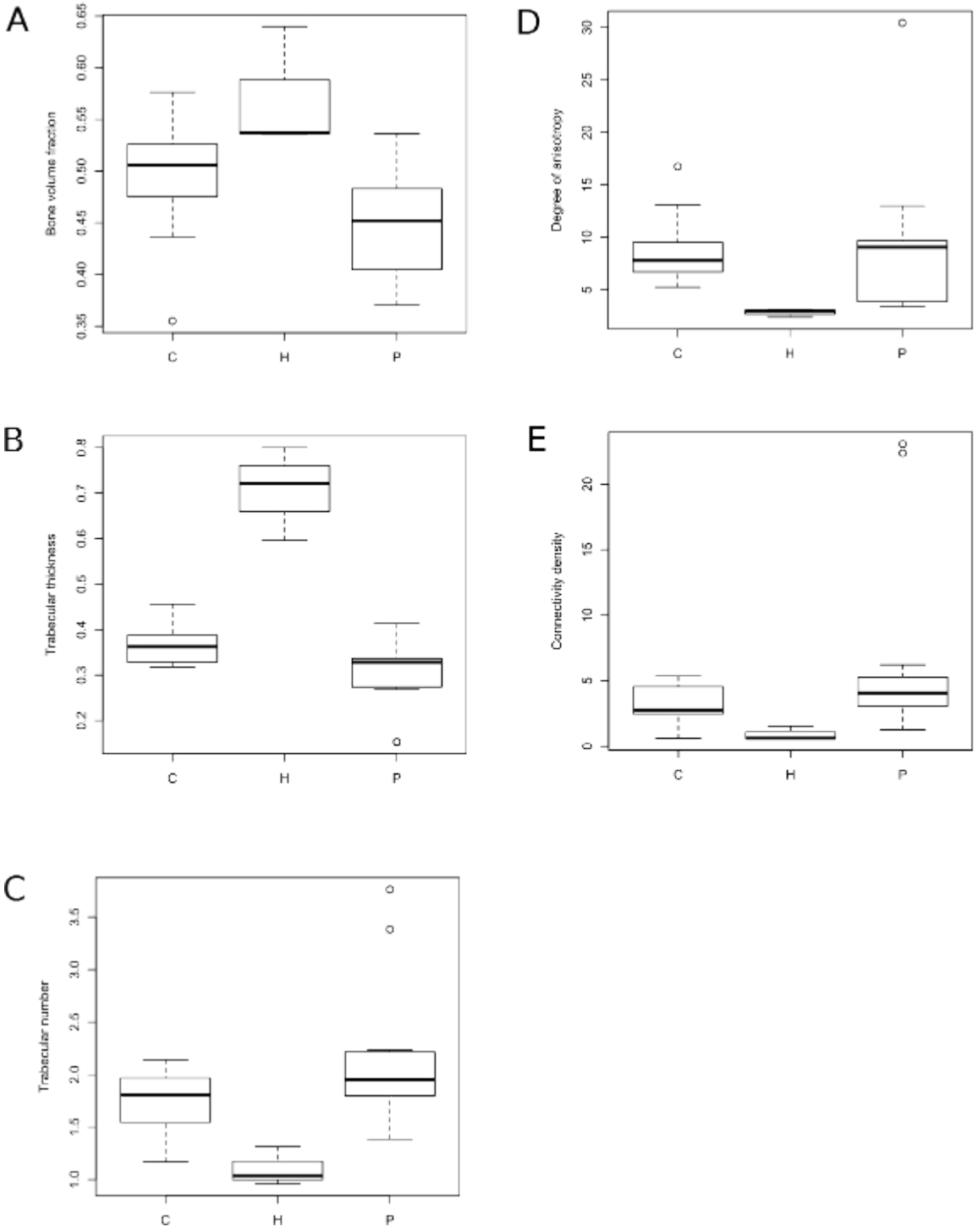

Figure 5.2. Rose diagram stereoplots of the primary trabecular orientations of the mandibular condyle. A is the right condyle; B is the left condyle. Taxa are separated by color: hominoids in red, platyrrhines in purple, and cercopithecoids in blue.

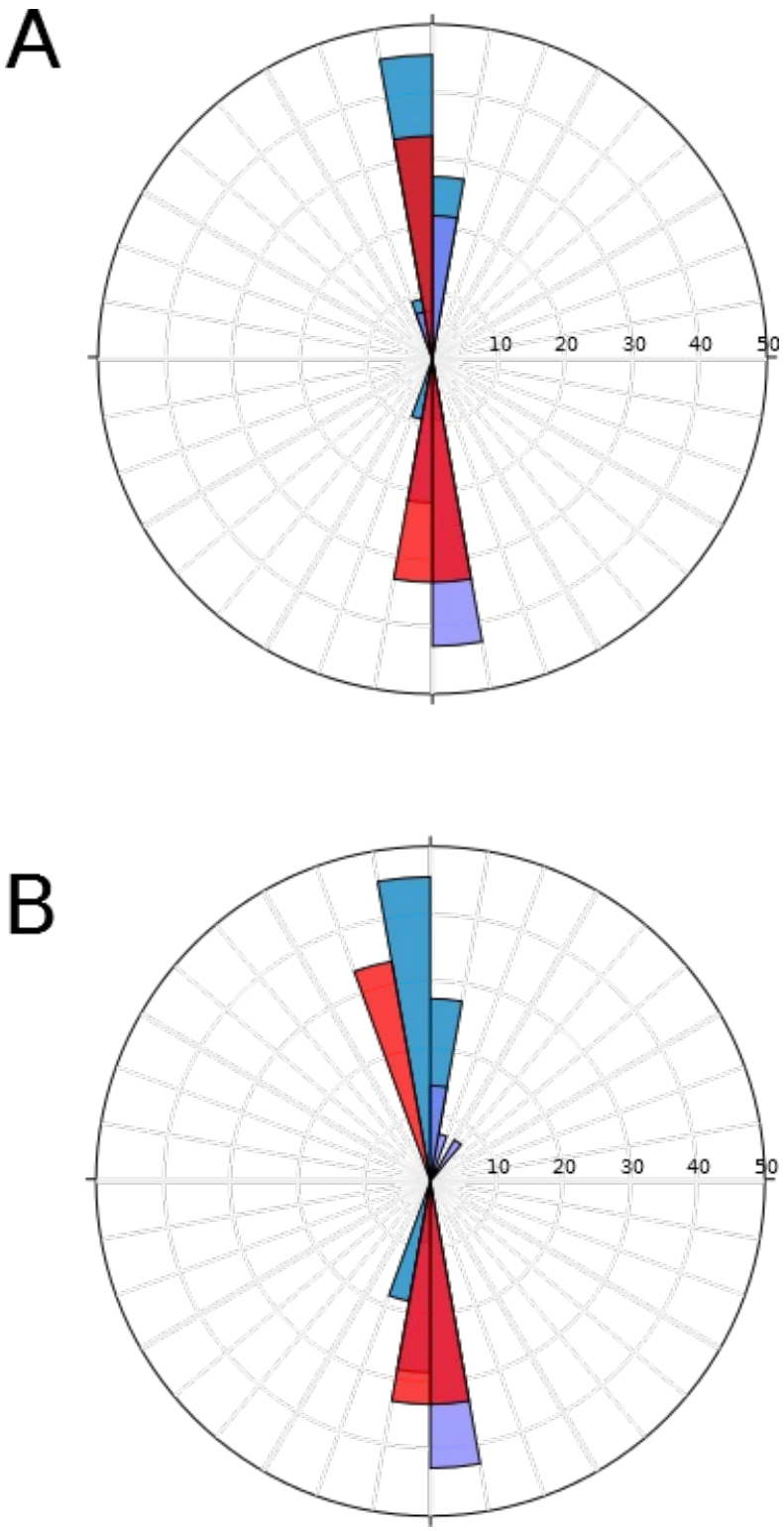

Figure 5.3. Image slices for the VOI for the right condyle of *Cebus libidinosus* 518418. Images have been magnified to show detail.

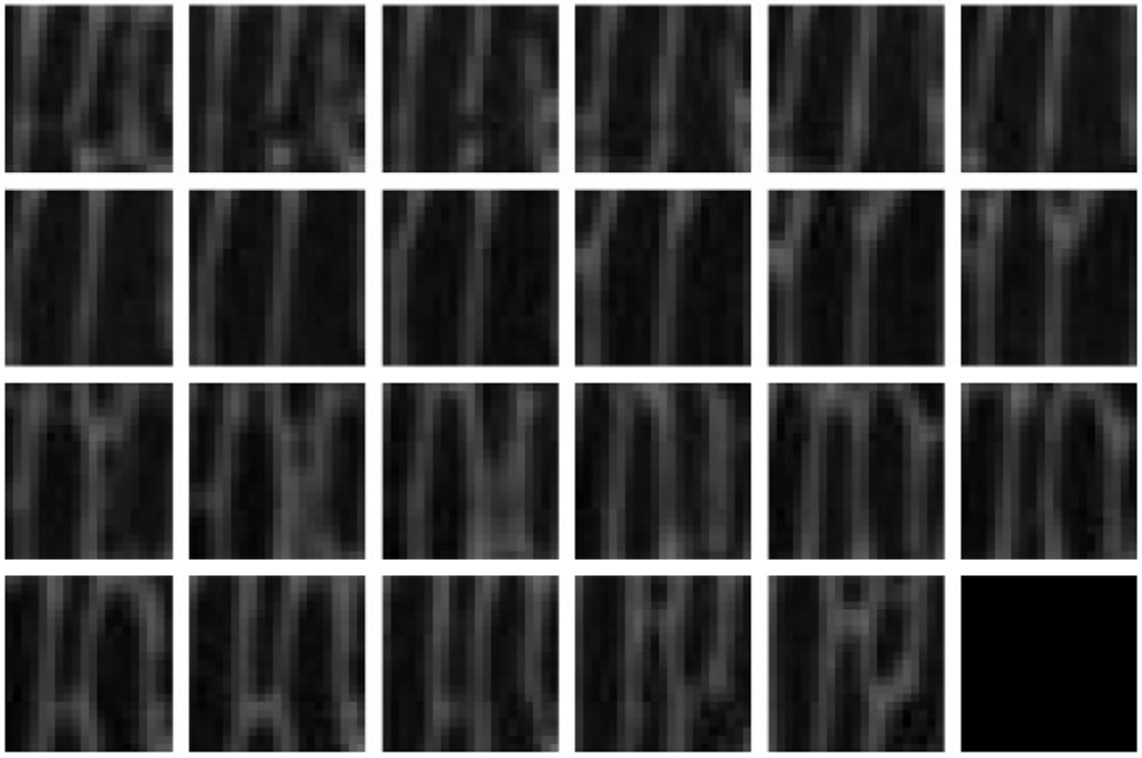

References

Barak, M.M., Lieberman, D.E., Raichlen, D., Pontzer, H., Warrener, A.G., Hublin, J.-J., 2013. Trabecular evidence for a human-like gait in *Australopithecus africanus*. PloS one. 8, e77687.

Bishara, S.E., Burkey, P.S., Kharouf, J.G., 1994. Dental and facial asymmetries: a review. Angle Orthodontist.

Cornish, R.J., Wilson, D.F., Logan, R.M., Wiebkin, O.W., 2006. Trabecular structure of the condyle of the jaw joint in young and mature sheep: A comparative histomorphometric reference. Archives of Oral Biology. 51, 29–36.

Cotter, M.M., Simpson, S.W., Latimer, B.M., Hernandez, C.J., 2009. Trabecular microarchitecture of hominoid thoracic vertebrae. Anatomical Record. 292, 1098–1106.

Cruz-Orive, L.M., Karlsson, L.M., Larsen, S.E., Wainschtein, F., 1992. Characterizing anisotropy: A new concept. Miron and Microscopica Acta. 23, 75–76.

Ding, M., Odgaard, A., Hvid, I., 1999. Accuracy of cancellous bone volume fraction measured by micro-CT scanning. Journal of Biomechanics. 32, 323–326.

Doube, M., Kłosowski, M.M., Arganda-Carreras, I., Cordelières, F.P., Dougherty, R.P., Jackson, J.S., Schmid, B., Hutchinson, J.R., Shefelbine, S.J., 2010. BoneJ: Free and extensible bone image analysis in ImageJ. Bone. 47, 1076–9.

Fagot, J., Vauclair, J., 1991. Manual laterality in nonhuman primates: a distinction between handedness and manual specialization. Psychological Bulletin. 109, 76–89.

Fajardo, R.J., Desilva, J.M., Manoharan, R.K., Schmitz, J.E., MacLatchy, L.M., Bouxsein, M.L., 2013. Lumbar vertebral body bone microstructural scaling in small to medium-sized strepsirhines. Anatomical Record. 296, 210–26.

Fajardo, R.J., Müller, R., 2001. Three-dimensional analysis of nonhuman primate trabecular architecture using micro-computed tomography. American Journal of Physical Anthropology. 115, 327–36.

Fajardo, R.J., Müller, R., Ketcham, R.A., Colbert, M., Fajardo, R.J., Mu, R., 2007. Nonhuman anthropoid primate femoral neck trabecular architecture and its relationship to locomotor mode. Anatomical Record. 290, 422–36.

Fajardo, R.J., Ryan, T.M., Kappelman, J., Jose, R., 2002. Assessing the accuracy of high-resolution X-ray computed tomography of primate trabecular bone by comparisons with histological sections. American Journal of Physical Anthropology. 118, 1–10.

Giesen, E., Ding, M., Dalstra, M., Van Eijden, T., 2001. Mechanical properties of cancellous bone in the human mandibular condyle are anisotropic. Journal of Biomechanics. 34, 799–803.

Giesen, E., van Eijden, T., 2000. The three-dimensional cancellous bone architecture of the human mandibular condyle. Journal of Dental Research. 79, 957–963.

Griffin, N.L., D'Août, K., Ryan, T.M., Richmond, B.G., Ketcham, R.A., Postnov, A., Grif, N.L., Août, K.D., 2010. Comparative forefoot trabecular bone architecture in extant hominids. Journal of Human Evolution. 59, 202–13.

Hara, T., Tanck, E., Homminga, J., Huiskes, R., 2002. The influence of microcomputed tomography threshold variations on the assessment of structural and mechanical trabecular bone properties. Bone. 31, 107–109.

Herring, S.W., Liu, Z., 2001. Loading of the temporomandibular joint: anatomical and in vivo evidence from the bones. Cells, Tissues, Organs. 169, 193–200.

Hildebrand, T., Rüegsegger, P., 1997. Quantification of bone microarchitecture with the Structure Model Index. Computer Methods in Biomechanics and Biomedical Engineering. 1, 15–23.

Hongo, T., Orihara, K., Onoda, Y., Nakajima, K., Ide, Y., 1989a. Quantitative and morphological studies of the trabecular bones in the condyloid processes of the Japanese mandibles; changes due to aging. The Bulletin of Tokyo Dental College. 30, 165–174.

Hongo, T., Yotsuya, H., Shibuya, K., Kawase, M., Ide, Y., 1989b. Quantitative and morphological studies on the trabecular bones in the condyloid processes of the Japanese mandibles--Comparisons between dentulous and edentulous specimens. Bull. Tokyo Dent. Coll. 30, 67–76.

Hoogmartens, M., Caubergh, M.A., 1987. Chewing side preference during the first chewing cycle as a new type of lateral preference in man. Electromyography and Clinical Neurophysiology. 27, 3–6.

Hylander, W.L., 1979. An experimental analysis of temporomandibular joint reaction force in macaques. American Journal of Physical Anthropology. 51, 433–456.

Hylander, W.L., 1985. Mandibular function and biomechanical stress and scaling. American Zoologist. 25, 315–330.

Kabel, J., Van Rietbergen, B., Odgaard, A., Huiskes, R., 1999. Constitutive relationships of fabric, density, and elastic properties in cancellous bone architecture. Bone. 25, 481–486.

Ketcham, R.A., Ryan, T.M., 2004. Quantification and visualization of anisotropy in trabecular bone. Journal of Microscopy. 213, 158–71.

Kieser, J., 1999. Biomechanics of masticatory force production. Journal of Human Evolution. 36, 575–579.

Kivell, T., Skinner, M., Lazenby, R.A., Hublin, J.-J., 2011. Methodological considerations for analyzing trabecular architecture: An example from the primate hand. Journal of Anatomy. 218, 209–225.

Lazenby, R.A., Skinner, M.M., Kivell, T.L., Hublin, J.-J., 2011. Scaling VOI size in 3D μCT studies of trabecular bone: a test of the over-sampling hypothesis. American Journal of Physical Anthropology. 144, 196–203.

MacLatchy, L., Müller, R., 2002. A comparison of the femoral head and neck trabecular architecture of *Galago* and *Perodicticus* using micro-computed tomography (CT). Journal of Human Evolution. 43, 89–105.

MacNeilage, P.F., Studdert-Kennedy, M.G., Lindblom, B., 1987. Primate handedness reconsidered. Behavioral and Brain Sciences. 10, 247.

McGrew, W.C., Marchant, L.F., 1997. On the other hand: Current issues in and meta-analyses of the behavioral laterality of hand function in nonhuman primates. Yearbook of Physical Anthropology. 40, 201–232.

Mulder, L., Koolstra, J.H., Weijs, W. a., Van Eijden, T.M.G.J., 2005. Architecture and mineralization of developing trabecular bone in the pig mandibular condyle. Anatomical Record - Part A Discoveries in Molecular, Cellular, and Evolutionary Biology. 285, 659–667.

Nissan, J., Gross, M., 2004. Chewing side preference as a type of hemispheric laterality. Journal of Oral Rehabilitation. 31, 412–416.

Odgaard, A., Kubel, J., van Rietbergen, B., Dalstra, M., Huiskes, R., 1997. Fabric and

elastic principal directions of cancellous bone are closely related. Journal of Biomechanics. 30, 487–495.
Papademetriou, E., Sheu, C.-F., Michel, G.F., 2005. A meta-analysis of primate hand preferences, particularly for reaching. Journal of Comparative Psychology. 119, 33–48.
Ridler, T., Calvard, S., 1978. Picture thresholding using an iterative selection method. IEEE Transactions on Systems, Man, and Cybernetics. SMC-8, 630–632.
Ryan, T.M., Colbert, M., Ketcham, R.A., Vinyard, C.J., 2010. Trabecular bone structure in the mandibular condyles of gouging and nongouging platyrrhine primates. American Journal of Physical Anthropology. 141, 583–93.
Ryan, T.M., Ketcham, R.A., 2005. Angular orientation of trabecular bone in the femoral head and its relationship to hip joint loads in leaping primates. Journal of Morphology. 265, 249–63.
Ryan, T.M., Ketcham, R.A., 2002. The three-dimensional structure of trabecular bone in the femoral head of strepsirrhine primates. Journal of Human Evolution. 43, 1–26.
Ryan, T.M., Krovitz, G.E., 2006. Trabecular bone ontogeny in the human proximal femur. Journal of Human Evolution. 51, 591–602.
Ryan, T.M., Shaw, C.N., 2013. Trabecular bone microstructure scales allometrically in the primate humerus and femur. Proceedings of the Royal Society B: Biological Sciences. 280, 1–9.
Ryan, T.M., van Rietbergen, B., 2005. Mechanical significance of femoral head trabecular bone structure in *Loris* and *Galago* evaluated using micromechanical finite element models. American Journal of Physical Anthropology. 126, 82–96.
Ryan, T.M., Walker, A., 2010. Trabecular bone structure in the humeral and femoral heads of anthropoid primates. Anatomical Record. 293, 719–29.
Saccucci, M., D'Attilio, M., Rodolfino, D., Festa, F., Polimeni, A., Tecco, S., 2012. Condylar volume and condylar area in class I, class II and class III young adult subjects. Head & face medicine. 8, 34.
Scherf, H., 2007. Locomotion-related femoral trabecular architectures in Primates.
Schmid, B., Schindelin, J., 2010. A high-level 3D visualization API for Java and ImageJ. BMC Bioinformatics. 11.
Spencer, M.A., Demes, B., 1993. Biomechanical analysis of masticatory system configuration in Neandertals and Inuits. American Journal of Physical Anthropology. 91, 1–20.
Teng, S., Herring, S.W., 1995. A stereological study of trabecular architecture in the mandibular condyle of the pig. Archives of Oral Biology. 40, 299–310.
Trussell, H., 1979. Comments on "Picture thresholding using an iterative selection method." IEEE Transactions on Systems, Man, and Cybernetics. 54, 9472–9472.
Van Eijden, T., van Der Helm, P.N., van Ruijven, L., Mulder, L., 2006. Structural and mechanical properties of mandibular condylar bone. Journal of Dental Research. 85, 33–37.
Van Rietbergen, B., Odgaard, A., Kabel, J., Huiskes, R., 1998. Relationships between bone morphology and bone elastic properties can be accurately quantified using high-resolution computer reconstructions. Journal of Orthopaedic Research. 16, 23–28.
Van Ruijven, L., Giesen, E., Mulder, L., Farella, M., van Eijden, T., Ruijven, L.J. Van,

2005. The effect of bone loss on rod-like and plate-like trabeculae in the cancellous bone of the mandibular condyle. Bone. 36, 1078–85.

Van Ruijven, L.L.J., Giesen, E., van Eijden, T., 2002. Mechanical significance of the trabecular microstructure of the human mandibular condyle. Journal of Dental Research. 81, 706–710.

Vig, P.S., Hewitt, A.B., 1975. Asymmetry of the human facial skeleton. The Angle orthodontist.

Willems, N.M.B.K., Mulder, L., Langenbach, G.E.J., Grünheid, T., Zentner, A., van Eijden, T.M.G.J., 2007. Age-related changes in microarchitecture and mineralization of cancellous bone in the porcine mandibular condyle. Journal of Structural Biology. 158, 421–427.

Yamashita, N., Vinyard, C.J., Tan, C.L., 2009. Food mechanical properties in three sympatric species of *Hapalemur* in Ranomafana National Park, Madagascar. American Journal of Physical Anthropology. 139, 368–81.

Chapter 6. Conclusion

6.1 Summary and Conclusions

Current knowledge of the functional relationship between mandibular morphology and primate dietary regimes is insufficient to use skeletal material to diagnose specific diets. While mechanically challenging diets contribute to overall jaw robusticity (Bouvier and Hylander, 1981, 1984; Corruccini and Beecher, 1982, 1984; Yamada and Kimmel, 1991; Teng and Herring, 1995; Ravosa et al., 2007, 2008), the multiplicity of functional responses to descriptive dietary categories (frugivore, folivore) limits the utility of mandibular morphology for application to the fossil record. Cumulative evidence about bone remodeling, masticatory loading, chewing behavior, and food properties suggests a clear, straightforward relationship between jaw form and diet, but at this time it is not possible to use skeletal evidence to infer anything about a primate's diet other than "mechanically challenging" or "not mechanically challenging." Even the difference between hard and tough diets eludes morphologists.

The study of food mechanical properties (FMPs) provides important quantitative data about primate diets that are not encapsulated in descriptive or qualitative assessments, and may serve to provide the long-sought-after functional link between jaw form and diet. Grouping primates by dietary categories (frugivorous, folivorous, omnivorous) does not account for the range of variation within those categories. Primatologists have long been aware of this problem (Kay, 1975; Rosenberger and Kinzey, 1976; Smith, 1983; Lucas et al., 1985; Rosenberger, 1992; Yamashita, 1996, 1998; Wright and Willis, 2012) but have continued to rely on descriptive categories in the

absence of an alternative classification scheme.

Chapter 2 provides the first large, comparative dataset on dietary FMPs among wild primates. Comparing FMPs to different variables related to feeding ecology confirmed what many researchers have long suspected—that there is no relationship between dietary categories and FMPs, and that using dietary quality as a proxy for FMPs is not supported by empirical data—but also demonstrated a complex relationship among FMPs, feeding time, and body mass. FMPs are known to influence primate food choice, and it seems that FMPs also influence other aspects of feeding ecology in ways that have not yet been explored by field researchers. Careful quantification of population-specific data on feeding time, chewing time, oral and manual preparation of food items, and nutritional content would expand our understanding of the importance of FMPs. Recent research on the microbiome has provided further evidence for the complexity of primate feeding ecology (Karasov et al., 2011; Amato et al., 2014a; Amato et al., 2014b), and gut adaptations for food processing may be equally or more important than oral adaptations.

The trabecular structure of the primate mandibular condyle appears to vary in relation to feeding behavior (Chapter 4) and dietary FMPs (Chapter 3). Dietary toughness strongly correlates with trabecular degree of anisotropy, and feeding time is more weakly related to some aspects of trabecular structure, particularly trabecular thickness and trabecular number. Trabecular anisotropy contributes to the mechanical strength of bone (Hodgskinson and Currey, 1990; Goldstein et al., 1993; Odgaard et al., 1997; Van Rietbergen et al., 1998; Kabel et al., 1999), and thus it appears that primates with tougher diets rely on more anisotropic trabecular bone to withstand the loading demands of feeding. Likewise, thicker trabeculae may contribute to resisting the strains associated

with repetitive loading cycles, which reduce the maximal strength limits of bone (Chamay, 1970; Carter and Hayes, 1977; Hylander, 1979).

Interestingly, feeding time and FMPs appear to influence different aspects of trabecular morphology. Tougher foods likely require more chewing (Wright et al., 2008; Chen, 2009), suggesting that both dietary toughness and feeding time should produce a similar morphological signal. That this is not the case indicates that the loading regimes associated with dietary toughness may be different from those associated with increased time spent feeding.

The mandibular condyle is a promising target for additional research on the form-function relationship of diet and craniofacial morphology. A primary goal of comparative research is understanding variation within the fossil record, and reconstructing the behavioral patterns of fossil hominins. Recent research using techniques of microwear (Scott et al., 2005, 2012; Grine et al., 2006; Ungar et al., 2008, 2010; Pontzer et al., 2011) and staple isotope analysis (Lee-Thorp et al., 1994, 2012; Sponheimer and Lee-Thorp, 1999; Sponheimer et al., 2006; Cerling et al., 2011; Wynn et al., 2013) have provided new insight but have not clearly resolved debates about early hominin diets (Smith et al., 2015). Studying the internal structure of the mandible may yield valuable data that will help clarify the nature of hominin dietary adaptations.

6.2 Future Work

Future research is needed to clarify the relationships between trabecular morphology and primate feeding ecology. One possibility is a controlled feeding study to experimentally demonstrate relationships among trabecular bone, FMPs, and time spent

chewing. Controlled feeding experiments using primates (Bouvier and Hylander, 1981, 1984; Corruccini and Beecher, 1982, 1984), pigs (Larsson et al., 2005; Organ et al., 2006; Dias et al., 2011), rats (Beecher and Corruccini, 1981; Bouvier and Hylander, 1984; Yamada and Kimmel, 1991; Mavropoulos et al., 2005; Tanaka et al., 2007), and rabbits (Taylor et al., 2006; Ravosa et al., 2007, 2008) have shown that food consistency contributes to changes in masticatory morphology (both soft and hard tissue) during development. These studies have set a precedent for using non-primate mammals to explore the relationship between feeding and craniofacial morphology. Because pigs have a temporomandibular joint quite similar to that of humans and other primates (Bermejo et al., 1993; Wang et al., 2007), and because their jaws are large enough to facilitate high-resolution scanning, pigs would likely be the best candidate for a feeding study. Experimentally controlling FMPs and/or time spent chewing would enable direct links between feeding ecology and trabecular structure in the mandibular condyle.

Another possibility is utilizing the skeletal collections associated with long-term field research. The Mountain Gorilla Skeletal Project (http://cashp.columbian.gwu.edu/hard-tissue-biology-field-projects), for example, has accumulated a large collection of skeletal specimens from Karisoke, which is the same site at which FMPs for this species were recorded. Imaging these mandibular specimens would provide direct evidence for relationships between FMPs and condylar morphology, and comparison with other skeletal collections would demonstrate variation in trabecular structure in response to variation in FMPs. Moreover, if skeletal material can be associated with individuals who were known during life, it may be possible to track FMP variations within populations and to explore intra-specific trabecular morphology.

Finally, studying the ontogeny of condylar architecture may prove fruitful. Trabecular structure is known to change throughout development in response to locomotor loading (Ryan and Krovitz, 2006; Gosman and Ketcham, 2009; Abel and Macho, 2011; Raichlen et al., 2015); it seems likely, then, that as an organism matures, changes in masticatory loading influence the trabecular structure of the condyle. Harvard's Museum of Comparative Zoology has a large collection of *Macaca fascicularis*, for which FMPs are known, and a microCT scanner. Tracking changes in trabecular structure across different age classes would establish a baseline for ontogenetic shifts in trabecular morphology related to feeding. Because diet is also ontogenetic (Watts, 1985; Raguet-Schofield, 2010; McGraw et al., 2011), it may be necessary to study the ontogeny of several species to parse out trabecular differences related to diet from those related to loading.

References

Abel, R., Macho, G.A., 2011. Ontogenetic changes in the internal and external morphology of the ilium in modern humans. Journal of Anatomy. 218, 324–335.

Amato, K.R., Leigh, S.R., Kent, A., Mackie, R.I., Yeoman, C.J., Stumpf, R.M., Wilson, B.A., Nelson, K.E., White, B.A., Garber, P.A.. 2014a. The role of gut microbes in satisfying the nutritional demands of adult and juvenile wild, black howler monkeys (*Alouatta pigra*). American Journal of Physical Anthropology. 155, 652–64.
2014b. The gut microbiota appears to compensate for seasonal diet variation in the wild black howler monkey (*Alouatta pigra*). Microbial Ecology. 69, 434-443.

Beecher, R., Corruccini, R., 1981. Effects of dietary consistency on craniofacial and occlusal development in the rat. The Angle Orthodontist. 51, 61–69.

Bermejo, A., Gonzalez, O., Gonzalez, J., 1993. The pig as an animal model for experimentation on the temporomandibular articular complex. Oral Surg Oral Med Oral Pathol. 75, 18–23.

Bouvier, M., Hylander, W.L., 1981. Effect of bone strain on cortical bone structure in macaques (*Macaca mulatta*). Journal of Morphology. 167, 1–12.

Bouvier, M., Hylander, W.L., 1984. The effect of dietary consistency on gross and histologic morphology in the craniofacial region of young rats. American Journal of Anatomy. 170, 117–126.

Carter, D.R., Hayes, W.C., 1977. Compact bone fatigue damage--I. Residual strength and stiffness. Journal of Biomechanics. 10, 325–337.

Cerling, T.E., Mbua, E., Kirera, F.M., Manthi, F.K., Grine, F.E., Leakey, M.G., Sponheimer, M., Uno, K.T., Kyalo, F., 2011. Diet of *Paranthropus boisei* in the early Pleistocene of East Africa. Proceedings of the National Academy of Sciences of the United States of America. 108, 9337–41.

Chamay, A., 1970. Mechanical and morphological aspects of experimental overload and fatigue in bone. Journal of Biomechanics. 3, 263–270.

Chen, J., 2009. Food oral processing—A review. Food Hydrocolloids. 23, 1–25.

Corruccini, R., Beecher, R., 1982. Occlusal variation related to soft diet in a nonhuman primate. Science. 218, 74–6.

Corruccini, R., Beecher, R., 1984. Occlusofacial morphological integration lowered in baboons raised on soft diet. Journal of Craniofacial Genetics and Developmental Biology. 4, 135–142.

Dias, G.J., Cook, R.B., Mirhosseini, M., 2011. Influence of food consistency on growth and morphology of the mandibular condyle. Clinical Anatomy. 24, 590–598.

Goldstein, S.A., Goulet, R., McCubbrey, D., 1993. Measurement and significance of three-dimensional architecture to the mechanical integrity of trabecular bone. Calcified Tissue International. 53, S127–S133.

Gosman, J.H., Ketcham, R.A., 2009. Patterns in ontogeny of human trabecular bone from Sunwatch village in the prehistoric Ohio Valley: General features of microarchitectural change. American Journal of Physical Anthropology. 138, 318–332.

Grine, F.E., Ungar, P.S., Teaford, M.F., El-Zaatari, S., 2006. Molar microwear in *Praeanthropus afarensis*: evidence for dietary stasis through time and under diverse paleoecological conditions. Journal of Human Evolution. 51, 297–319.

Hodgskinson, R., Currey, J.D., 1990. Effects of structural variation on Young's modulus of non-human cancellous bone. Proceedings of the Institution of Mechanical Engineers. Part H, Journal of engineering in medicine. 204, 43–52.

Hylander, W.L., 1979. The functional significance of primate mandibular form. Journal of Morphology. 160, 223–239.

Kabel, J., Van Rietbergen, B., Odgaard, A., Huiskes, R., 1999. Constitutive relationships of fabric, density, and elastic properties in cancellous bone architecture. Bone. 25, 481–486.

Karasov, W.H., Martinez del Rio, C., Caviedes-Vidal, E., 2011. Ecological physiology of diet and digestive systems. Annual Review of Physiology. 73, 69-93.

Kay, R.F., 1975. The functional adaptations of primate molar teeth. American Journal of Physical Anthropology. 43, 195–216.

Larsson, E., Øgaard, B., Lindsten, R., Holmgren, N., Brattberg, M., Brattberg, L., 2005. Craniofacial and dentofacial development in pigs fed soft and hard diets. American Journal of Orthodontics and Dentofacial Orthopedics. 128, 731–739.

Lee-Thorp, J.A., Likius, A., Mackaye, H.T., Vignaud, P., Sponheimer, M., Brunet, M., 2012. Isotopic evidence for an early shift to C4 resources by Pliocene hominins in Chad. Proceedings of the National Academy of Sciences. 1–4.

Lee-Thorp, J.A., van Der Merwe, N.J., Brain, C., 1994. Diet of Australopithecus robustus at Swartkrans from stable carbon isotopic analysis. Journal of Human Evolution. 27, 361–372.

Lucas, P.W., Corlett, R., Luke, D., 1985. Plio-Pleistocene hominid diets: An approach combining masticatory and ecological analysis. Journal of Human Evolution. 14, 187–202.

Mavropoulos, A., Ammann, P., Bresin, A., Kiliaridis, S., 2005. Masticatory demands induce region-specific changes in mandibular bone density in growing rats. Angle Orthodontist. 75, 625–630.

McGraw, W.S., Vick, A.E., Daegling, D.J., 2011. Sex and age differences in the diet and ingestive behaviors of sooty mangabeys (*Cercocebus atys*) in the Tai Forest, Ivory Coast. American journal of physical anthropology. 144, 140–53.

Odgaard, A., Kubel, J., van Rietbergen, B., Dalstra, M., Huiskes, R., 1997. Fabric and elastic principal directions of cancellous bone are closely related. Journal of Biomechanics. 30, 487–495.

Organ, J.M., Ruff, C.B., Teaford, M.F., Nisbett, R. a., 2006. Do mandibular cross-sectional properties and dental microwear give similar dietary signals? American Journal of Physical Anthropology. 130, 501–507.

Pontzer, H., Scott, J.R., Lordkipanidze, D., Ungar, P.S., 2011. Dental microwear texture analysis and diet in the Dmanisi hominins. Journal of Human Evolution. 61, 683–687.

Raguet-Schofield, M., 2010. The ontogeny of feeding behavior of Nicaraguan mantled howler monkeys (*Alouatta palliata*). University of Illinois at Urbana-Champaign.

Raichlen, D.A., Gordon, A.D., Foster, A.D., Webber, J.T., Sukhdeo, S.M., Scott, R.S., Gosman, J.H., Ryan, T.M., 2015. An ontogenetic framework linking locomotion and trabecular bone architecture with applications for reconstructing hominin life history. Journal of Human Evolution. 81, 1–12.

Ravosa, M.J., Kunwar, R., Stock, S.R., Stack, M.S., 2007. Pushing the limit: masticatory

stress and adaptive plasticity in mammalian craniomandibular joints. Journal of Experimental Biology. 210, 628–41.
Ravosa, M.J., Lopez, E.K., Menegaz, R.A., Stock, S.R., Stack, M.S., Hamrick, M.W., 2008. Adaptive Plasticity in the Mammalian Masticatory Complex: You Are What, and How, You Eat. In: Vinyard, C., Ravosa, M.J., Wall, C. (Eds.), Primate Craniofacial Function and Biology. Springer US, Boston, MA, pp. 293–328.
Rosenberger, A.L., 1992. Evolution of feeding niches in New World monkeys. American Journal of Physical Anthropology. 88, 525–62.
Rosenberger, A.L., Kinzey, W.G., 1976. Functional patterns of molar occlusion in platyrrhine primates. American Journal of Physical Anthropology. 45, 281–98.
Ryan, T.M., Krovitz, G.E., 2006. Trabecular bone ontogeny in the human proximal femur. Journal of Human Evolution. 51, 591–602.
Scott, R.S., Teaford, M.F., Ungar, P.S., 2012. Dental microwear texture and anthropoid diets. American Journal of Physical Anthropology. 147, 551–79.
Scott, R.S., Ungar, P.S., Bergstrom, T.S., Brown, C. a, Grine, F.E., Teaford, M.F., Walker, A., 2005. Dental microwear texture analysis shows within-species diet variability in fossil hominins. Nature. 436, 693–5.
Smith, A.L., Benazzi, S., Ledogar, J.A., Tamvada, K., Pryor Smith, L.C., Weber, G.W., Spencer, M.A., Lucas, P.W., Michael, S., Shekeban, A., Al-Fadhalah, K., Almusallam, A.S., Dechow, P.C., Grosse, I.R., Ross, C.F., Madden, R.H., Richmond, B.G., Wright, B.W., Wang, Q., Byron, C., Slice, D.E., Wood, S., Dzialo, C., Berthaume, M.A., van Casteren, A., Strait, D.S., 2015. The feeding biomechanics and dietary ecology of *Paranthropus boisei*. The Anatomical Record. 298, 145–67.
Smith, R.J., 1983. The mandibular corpus of female primates: Taxonomic, dietary, and allometric correlates of interspecific variations in size and shape. American Journal of Physical Anthropology. 61, 315–330.
Sponheimer, M., Lee-Thorp, J.A., 1999. Isotopic evidence for the diet of an early hominin, *Australopithecus africanus*. Science. 283, 368–370.
Sponheimer, M., Passey, B.H., de Ruiter, D.J., Guatelli-Steinberg, D., Cerling, T.E., Lee-Thorp, J.A., 2006. Isotopic evidence for dietary variability in the early hominin *Paranthropus robustus*. Science. 314, 980–982.
Tanaka, E., Sano, R., Kawai, N., Langenbach, G.E.J., Brugman, P., Tanne, K., Van Eijden, T.M.G.J., 2007. Effect of food consistency on the degree of mineralization in the rat mandible. Annals of Biomedical Engineering. 35, 1617–1621.
Taylor, A.B., Jones, K.E., Kunwar, R., Ravosa, M.J., 2006. Dietary consistency and plasticity of masseter fiber architecture in postweaning rabbits. The Anatomical Record. 288, 1105–11.
Teng, S., Herring, S.W., 1995. A stereological study of trabecular architecture in the mandibular condyle of the pig. Archives of Oral Biology. 40, 299–310.
Ungar, P.S., Grine, F.E., Teaford, M.F., 2008. Dental microwear and diet of the Plio-Pleistocene hominin Paranthropus boisei. PloS one. 3, e2044.
Ungar, P.S., Scott, R.S., Grine, F.E., Teaford, M.F., 2010. Molar microwear textures and the diets of *Australopithecus anamensis* and *Australopithecus afarensis*. Philosophical Transactions of the Royal Society of London. Series B, Biological sciences. 365, 3345–54.
Van Rietbergen, B., Odgaard, A., Kabel, J., Huiskes, R., 1998. Relationships between

bone morphology and bone elastic properties can be accurately quantified using high-resolution computer reconstructions. Journal of Orthopaedic Research. 16, 23–28.

Wang, S., Liu, Y., Fang, D., Shi, S., 2007. The miniature pig: A useful large animal model for dental and orofacial research. Oral Diseases. 13, 530–537.

Watts, D.P., 1985. Observations on the ontogeny of feeding behavior in mountain gorillas (*Gorilla gorilla beringei*). American Journal of Primatology. 8, 1–10.

Wright, B.W., Ulibarri, L., O'Brien, J., Sadler, B., Prodhan, R., Covert, H.H., Nadler, T., 2008. It's tough out there: Variation in the toughness of ingested leaves and feeding behavior among four Colobinae in Vietnam. International Journal of Primatology. 29, 1455–1466.

Wright, B.W., Willis, M.S., 2012. Relationships between the diet and dentition of Asian leaf monkeys. American Journal of Physical Anthropology. 148, 262–75.

Wynn, J.G., Sponheimer, M., Kimbel, W.H., Alemseged, Z., Reed, K., Bedaso, Z.K., Wilson, J.N., 2013. Diet of *Australopithecus afarensis* from the Pliocene Hadar Formation, Ethiopia. Proceedings of the National Academy of Sciences. 1–6.

Yamada, K., Kimmel, D., 1991. The effect of dietary consistency on bone mass and turnover in the growing rat mandible. Archives of Oral Biology. 36, 129–138.

Yamashita, N., 1996. Seasonally and site specificity of mechanical dietary patterns in two Malagasy lemur families (Lemuridae and Indriidae). International Journal of Primatology. 17, 355–387.

Yamashita, N., 1998. Functional dental correlates of food properties in five Malagasy lemur species. American Journal of Physical Anthropology. 106, 169–88.